UNIVERSITEIT GENT

Tracing hydrological millennial-scale cycles in the late Quaternary of the Cariaco Basin and the southern Gulf of Cádiz using coccoliths and dinoflagellate cysts

Opsporing van hydrologische cycli op millenium-schaal in het late Quartair van het Cariaco Bekken en de zuidelijke Golf van Cádiz met behulp van coccolieten en dinoflagellatencysten

Kenneth Mertens
Promotor: Prof. Dr. Stephen Louwye

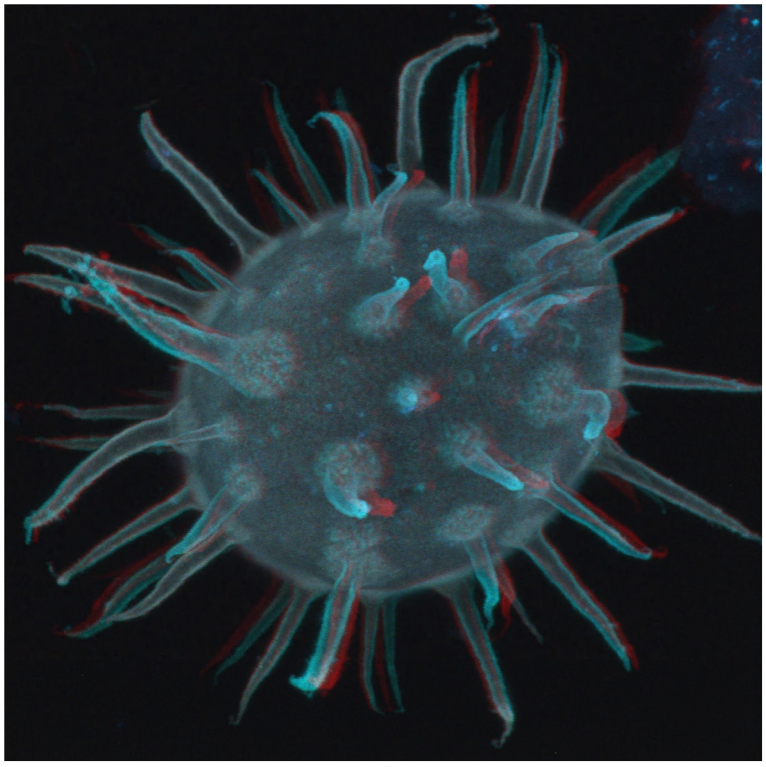

Thesis submitted in fulfillment of the requirements for the degree of Doctor in Sciences, Geology - Proefschrift voorgelegd tot het behalen van de graad van Doctor in de Wetenschappen, Geologie
Academic year 2008-2009
Ghent University – Faculty of Sciences – Department of Geology and Soil Science
Research Unit Palaeontology - Krijgslaan 281 S8 – B-9000 Ghent, Belgium

Faculteit Wetenschappen

Cover illustration:
anaglyph of confocal image of *Lingulodinium machaerophorum*.

Kenneth Mertens carried out the research in the framework of a 4-year research project of the Bijzonder Onderzoeksfonds (BOF) of the UGent.

This research was conducted at the Research Unit Palaeontology, Ghent University (Ghent, Belgium).

To refer to this thesis:
Mertens, K. (2009). Tracing hydrological millennial-scale cycles in the late Quaternary of the Cariaco Basin and the southern Gulf of Cádiz using coccoliths and dinoflagellate cysts, Ph.D. thesis, Ghent University, Belgium.

Acknowledgements

First I would like to thank my promotor Stephen Louwye and co-promotor Jacques Verniers for supporting me throughout these last four years. Things have not always been easy and you must have had your hands in your hair each time I had this new impulsive idea that I wanted to do, which included slicing up varved sediments with lasercutting techniques, using our expensive Zeiss microscope to see what happens when you drop hydrogen peroxide on dinocysts, try to pick thousands of cysts using a micro-injector etc.

I also would like to acknowledge thanks to the other PhD and Postdoc researchers at the Research Unit Palaeontology: Tim De Backer, Pieter Missiaen, Jan Mortier, Bert Van Bocxlaer, Thijs Vandenbroucke, Jan Van Meirhaeghe, Peter Van Roy, Koen Verhoeven, and Thomas 'Ozzy' Verleye. I also want to thank the other collaborators: Cristina Carapito-Krausharr, Achiel Gautier, Frank Gelaude, Dirk Van Damme and Jan Baccaert. Special thanks go to Sabine Van Cauwenberghe and Maarten Verreth for excellent help with processing samples. Also the efficient handling of administrative issues by Nelly Reynaert and Marc Faure is very much appreciated. Kurt Blom is thanked for solving computer problems in a wonderful way. I also want to thank (former) MSc. and BSc. students who were partly involved in my research: Heleen Vanneste, Mieke Thierens, Liesbeth Van Kerckhoven, Laurens Vercruysse, Sharon Schillewaert, Tim Verstraeten and Zoë Verlaak.

I also want to explicitly thank the colleagues at the Renard Center for Marine Geology (RCMG) for the splendid collaboration and for always being welcome: Marc De Batist, Jean-Pierre Henriet, Lieven Naudts, David Van Rooij, Anneleen Foubert, Hans Pirlet, Matthias Baeye, Katrien Heirman, Lies De Mol, Davy De Preiter, Mieke Matthys, Jasper Moernaut, Peter Staelens, Els Verfaillie, Maarten Van Daele, Vera Van Lancker, Wim Versteeg, Koen De Rycker, Dries Boone and Jeroen Vercruysse. Other colleagues from the Geology and soil science department that I wish to thank for the good atmosphere over the years are Cedric Corteel, Peter Van den hautte, Paul De Paepe, Marlina Elburg, Stijn Glorie, Johan De Graeve, Patric Jacobs, Phlorias Mees, Cilia De Reese, Ingrid Smet, Ann Zwertvaegher, Veerle Cnudde, Jan Dewanckele, Elin Van Lierde, Karen Fontijn, Eric Van Ranst, Johan Van de wauw, Peter Finke, Luc Lebbe, Alexander Vanderbohede, Pieter-Jan Wayaert, Kristine Walraevens, Frank Mostaert and Annick Raes (Hydraulic Research Laboratory, Borgerhout).

Similarly, I also want to extend thanks to people from the Protistology and Aquatic Ecology (PAE) group who helped me in numerous ways: Koen Sabbe, Wim Vyverman, Mieke Sterken, Elie Verleyen, Koenraad Vanhoutte, Victor Chepurnov, Koenraad Muylaert, Aaike De Wever, Griet Casteleyn, Nicolas Van Oostende and Jeroen Van Wichelen. A special thanks to Gaetan Borgonie and Marjolein Couvreur from Aquatic Biology department for use of their micro-injector.

For help with the confocal microscopy I wish to explicitly thank people at the Laboratory of General Biochemistry and Physical Pharmacy: Dries Vercauteren, Kevin Braeckmans and Stefaan De Smedt and the Centre for X-ray tomography for help with rendering the 3D images: Manu Dierick, Bert Masschale and Jelle Vlassenbroeck.

For help with alkenone and GDGT analysis I wish to thank the Organic Geochemistry department at Ghent University: Pat Sandra, Tadeusz Gorecki, Frederic Lynen, Sandra Van Vlierberghe and Marc Schelfaut and people at NIOZ: Jaap Sinninghe-Damsté, Marianne Baas, Ellen Hopmans, Stefan Schouten and Marcel Vandermeer and also Belen Martrat (Spanish National Research Council), Sonja Schulte (Institut für Chemie und Biologie des Meeres (ICBM), Oldenburg University) and James Bendle (Bristol Biogeochemistry Research Centre).

I want to thank the dinoflagellate people for all their help in supplying material, data and fruitful discussions: Ana Amorim (Univ. de Lisboa), Hernan Antolinez (Petrobras Columbia), Célia Beaudoin (TOTAL), Juan Blanco (Centro de Investigacións Mariñas), Hulya Caner (Istanbul Univ.), Nathalie Combourieu-Nebout (LSCE), Barrie Dale (University Oslo), Irina Delusina (Davis University), Caroline De Meyere (Univ. de Lausanne), Lucy

Edwards (USGS), Sara Farquhar (Cambridge Univ.), Mariana Filipova (Museum of Natural History, Varna, Bulgaria), Catalina González, Ulrike Holzwarth, Stijn de Schepper, Karin Zonneveld, Gerard Versteegh, Monika Kodrans-Nsiah, Ilham Bouimetarhan (Univ. Bremen), Karen Dybkjaer and Niels E. Poulsen (GEUS), Anne de Vernal, Maryse Henry and Taoufik Radi (GEOTOP-UQAM-McGill), Anna Godhe (Univ. of Gothenburg), Evelyne Goubert (Univ. de Bretagne), Kari Grøsfjeld (Geological survey of Norway), Susanne Feist-Burkhardt and Jonah Chitolie (NHM), Richard Hallett (Reservoirstrat), Rex Harland (DinoData services), Heilmann-Clausen (Aarhus Univ.), Ian Harding and Amr Deaf (SOC), Linda Joyce (ICIT), Ulrich Kotthof (Univ. of Frankfurt), Suzanne Leroy (Brunel University), John Lignum (Kingston Univ.), Laurent Londeix, Jean-Louis Turon and Aurélie Penaud (Univ. Bordeaux), Ivona Marasovic (Institute of Oceanography and Fisheries, Split, Croatia), Kazumi Matsuoka (ECSER), Fabienne Marret (Univ. of Liverpool), Jens Matthiessen (AWI), Francine McCarthy, Martin Head, Jan Hennissen, Manuel Paez and Ida Jansson (Brock University), Marie-Thérèse Morzadec-Kerfourn (Univ. de Rennes), Peta Mudie (Geological survey of Canada), Stefan Nehring (AeT umweltplanung), Yekatherina Novichkova (Shirshov Institute of Oceanology, Russian Academy of Sciences), Yuri Okolodkov (Universidad Veracruzana), Jose Luis Peña-Manjarrez (CICESE), Agneta Persson (Univ. of Gothenburg), Anna Pienkowski (EPE, Alberta), Speranta-Maria Popescu and Florent Dalesme (Univ. de Lyon), Vera Pospelova (Univ. of Victoria), Vandana Prasad (Birbal Institute of Palaeobotany), Michael Prauss (Freie Universität Berlin), Chris Reid (SAHFOS), Sofia Ribeiro and Marianne Ellegaard (University of Copenhagen), Jim Riding and Jane Kyffin Hughes (BGS), André Rochon (ISMER), Francesca Sangiorgi and Natasja Welters (Universiteit Utrecht), Joe Silke (Marine Institute, Ireland), Nathalie Sinclair and Christian Thun (Geoscience Australia), Ali Soliman (Graz Univ.), Nicolas Van Nieuwenhove (ifm-GEOMAR), Stefaan Van Simaeys and Ellen De Man (Exxon), Annemiek Vink (BGR), Jennifer Wolny and Karen Steidinger (Florida Fish and Wildlife Research Institute) and Marty Young (CSIRO).

The coccolith people I wish to thank for similar reasons are: Paul Bown, Jacky Lees and Tom Dunkley Jones (UCL), Karl-Heinz Baumann, Kathe Stolz, Regina Krammer (Univ. Bremen), Jenny Lezius and Hanno Kinkel (IFM-GEOMAR), Harald Andruleit (BGR), Elena Colmenero-Hidalgo (Universidad de Salamanca), Simon Cole (Petrostrat), Bianca de Bernardi (Univ. di Milano), Richard Jordan (Yamagata University) and Jeremy Young and Craig Koch (NHM).

Other researchers that I want to explicitly thank for their collaboration are Jeroen Groeneveld, Jan-Berend Stuut, Claudia Wienberg, Dierk Hebbeln, Ralph Klöcker and Holger Kulhmann (Univ. Bremen), Walter Hale and Chad Broyles (IODP), Jim Broda (WHOI), Gilles Lericolais (IFREMER, France), Jean-Pierre Arrondeau (IAV), Larry Peterson and Matt Lynn (RSMAS/MGG), Warner Brückmann and Silke Schenk (IFM GEOMAR), Rusty Lotti Bond (Lamont Doherty Earth Observatory), Hui-Ling Lin (Sun Yat-Sen University, Taiwan), Gerald Haug (Potsdam Univ.), Jess Tierney (Brown Univ.), Joe Werne (Univ. of Minnesota), Kristina Dahl (Scripps), Philippe Picon (GIPREB), Mylene Aycard (Univ. de Bretagne Sud), Martha McConnell (Univ. of South Carolina), André Catrijsse (VLIZ), Miguel Goni (Univ. of South Carolina), Kris Naessens (INTEC), Richard Telford (Bjerknes Centre for Climate Research), Braddock Linsley (University of New Mexico), Fernando Siringan and Joan Reotita (Univ. of the Philippines) and Katrien Van Landeghem (Univ. of Wales).

I want to dedicate this thesis to my parents Nico Mertens and Gilda Behaeghel for being such wonderful people who enabled me to complete my development in science and as a person. Also, my little brother, Samuel Mertens and his partner from Alaska, Sara Carney, are thanked for being an inspiration throughout the years. Further thanks go to my aunt Martine Behaeghel and her partner Jean-Claude Crispon, little cousin Hans Gruyaert and Lobke D'hespeel, my uncle Johan Mertens and aunt Monique Missault, cousin Kim Mertens and partner Roby Toch, cousin Joke Mertens and Philip Lefever, cousin Tilia Mertens and her partner Stijn Vansteelandt, my grandmother Sissi 't Kindt and her sister Georgette 't Kindt, uncle Joris Mertens and his partner Ilse Vervaeck, my uncle David Mertens and his partner Katja Coene, my aunt Isi Mertens and her partner Ann David. Also I would like to thank my recently acquired family: my parents-in-law André Degezelle and Kristine Vandenbroucke and sister-in-law Tine Degezelle and Alexandre Van Braeckel.

Lastly I want to thank my best friends for moral support throughout the years: Fré Grymonpré, Sven Vanneste and Bjorn Tillaert.

And of course, most thanks go to my partner and soul-mate Leen Degezelle, not only for lay-outing this thesis but moreover for lending me all the necessary support throughout the years. It must be true what is written in your wedding-ring ☺.

Table of contents

Introduction

1. Background

In the nineties, research of the Greenland ice cores in the North Atlantic showed that climatic variations at millennial-scale frequencies occurred much more rapid than previously thought (Bond et al., 1992; 1997; Dansgaard et al., 1993). Cold millennial-scale cycles or stadials (e.g. Heinrich Events) and warm millennial-scale cycles or interstadials were identified in a wide range of locations. The warm interstadials are also called Dansgaard-Oeschger (D/O) events and are the most pronounced climate changes that have occurred during the past 120 kyr. In the Greenland ice cores, D/O events start with a rapid warming by 5–10 °C within at most a few decades, followed by a plateau phase with slow cooling lasting for several centuries, followed by then a more rapid drop back to cold stadial conditions (Figure 1). Alley et al. (2001) have shown that these events appear follow each other every 1500 years, with further preferences around 3000 and 4500 years, which suggests a process of stochastic resonance.

Several ideas, or the combination of these ideas, have been proposed to explain D/O events. The first is the idea of thermohaline circulation bistability (Broecker et al., 1985), which proposes two stable states with active thermohaline circulation during warm phases and a shutdown during stadials. This theory does not explain the observed active circulation during stadials (Sarnthein et al., 1994; Yu et al., 1996) and the shutdown only during or after Heinrich events (Keigwin et al., 1994b; Elliot et al., 2002). The second idea is the so-called "salt oscillator" (Broecker et al., 1990) and is based on the notion that the Atlantic thermohaline circulation balances the net atmospheric freshwater export from the Atlantic basin. A weakening of the circulation would thus lead to a salinity build-up in the Atlantic, strengthening the circulation again. A third idea is that of latitude shifts of the convection between Nordic Seas and the mid-latitude open Atlantic Ocean (Rahmsdorf, 1994). In this mechanism, the rapid warming phase results from a northward intrusion of warm Atlantic waters into the Nordic Seas, the plateau phase is the 'warm

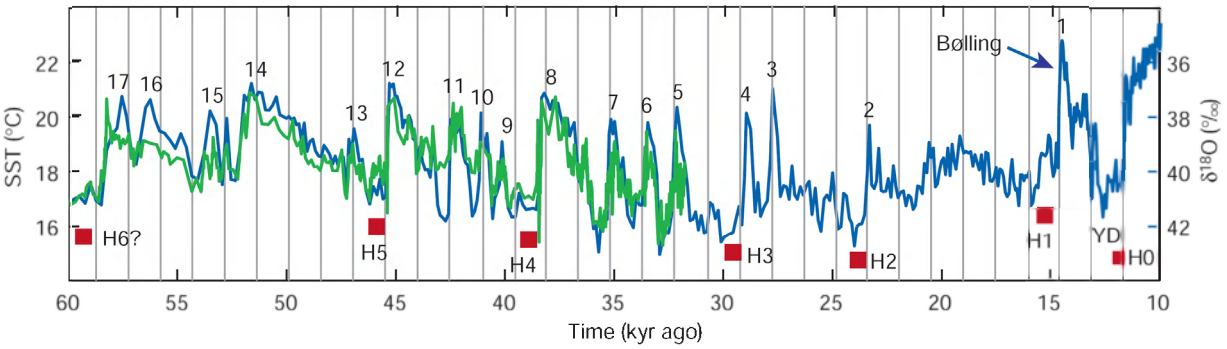

Figure 1 Temperature reconstructions from ocean sediments and Greenland ice. Proxy data from the subtropical Atlantic (green) and from the Greenland ice core (GISP2) show several Dansgaard-Oeschger (D/O) warm events (numbered). The timing of Heinrich events is marked in red. Grey intervals of 1,470 years illustrate the tendency of D/O events to occur with this spacing, or multiples thereof. (Rahmsdorf, 2002).

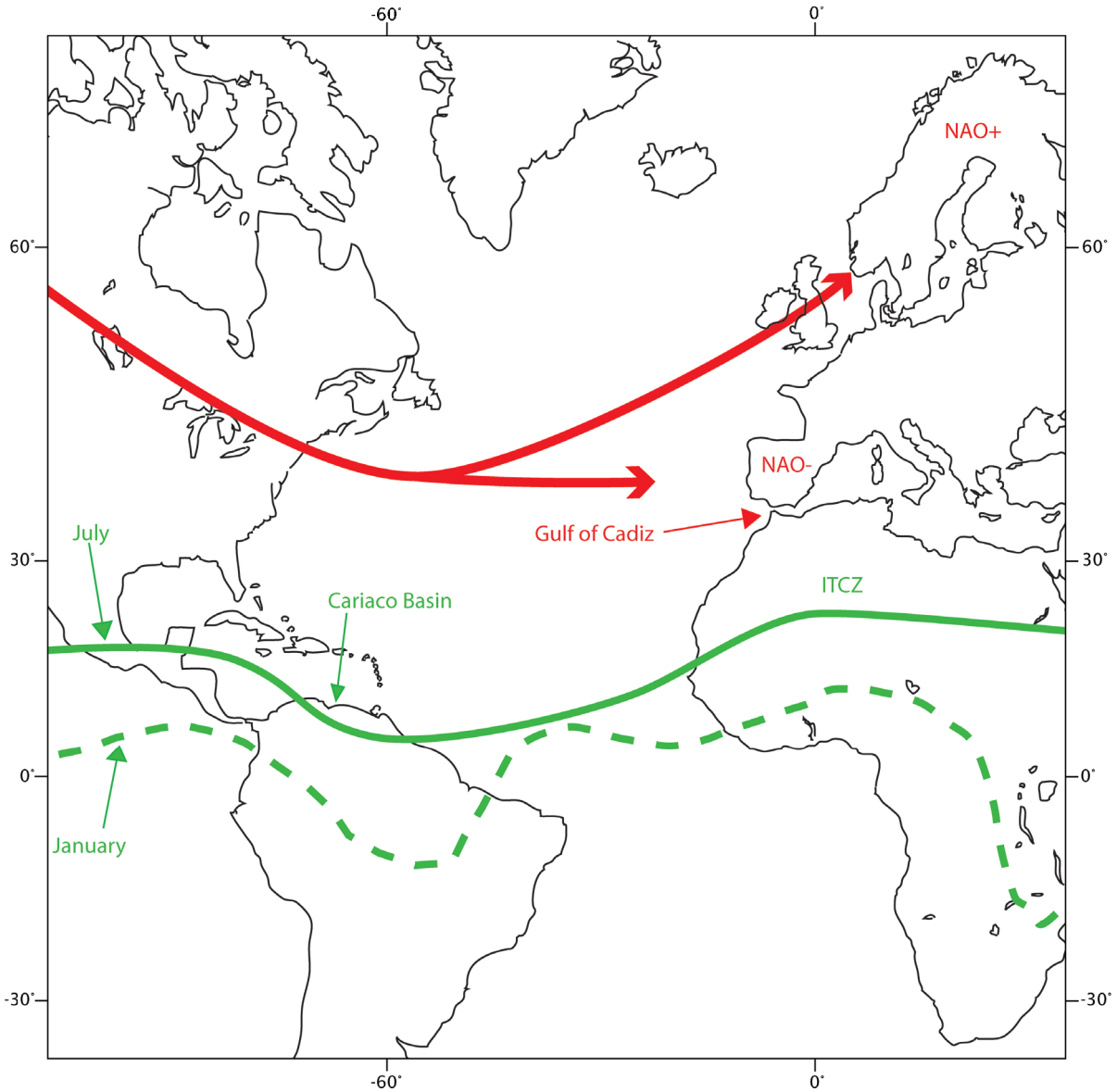

Figure 2 Major fluctuations of the Intertropical Convergence Zone (ITCZ) (green) and the North Atlantic Oscillation (NAO) (red) over the studied areas. In July, the ITCZ shifts north bringing increased rainfall over the Cariaco Basin, whilst in January the ITCZ shifts south and induces increased trade wind activity. During positive NAO years, cool and dry conditions develop over the Gulf of Cádiz, whilst during negative NAO years warm and wet conditions are expressed over the Gulf of Cádiz (modified after Visbeck 2002).

mode' of Atlantic Ocean circulation, which gradually weakens over several centuries, and the final cooling phase marks the end of deepwater formation in the Nordic Seas. The exact nature of the trigger remains unknown.¬¬ Finally, the tropical driver hypothesis (Clement and Cane, 1999; Cane and Clement, 1999) does not involve changes in thermohaline circulation, but suggests that D/O-style temperature shifts in Greenland may be caused by shifts in the atmospheric planetary-wave pattern, controlled remotely from the tropics. This is based on the strong control that tropical sea surface temperatures exert over global atmospheric heat-transport patterns in present climate, but a more specific and quantitative expla-

nation for D/O events building on this idea is yet to emerge.

A second major type of climatic event that occurred mostly in the latter half of the last glacial are Heinrich Events (for a review, see Hemming, 2004). These are characterized by distinct layers (so-called Heinrich layers) deposited by icebergs in North Atlantic sediments, spaced at intervals of 7,000 years with a duration of 500 ± 250 calender years (Hemming, 2004; González et al., 2008). Sediments in these layers are coarse-grained since they are transported out into the ocean by icebergs; hence, are referred to as ice-rafted debris. Heinrich events are massive episodic iceberg discharges from the Laurentide ice sheet through Hudson Strait. Sediment data (e.g. Keigwin et al., 1994a; Elliot et al., 2002) and models (e.g. Manabe and Stouffer, 1995) show that NADW formation ceased or was at least strongly reduced during Heinrich events.

D/O and Heinrich events are not unrelated: each Heinrich event is followed by a particular warm D/O event and successive D/O events get progressively cooler until the next Heinrich events (called a Bond cycle). This could simply be a consequence of the Laurentide ice sheet growing gradually in height between Heinrich events. Also, Heinrich events apparently always occur during cold stadials and not in the warm phase of D/O events. This suggests that ice-sheet instability does not occur at random, but is helped by some climatic trigger – possibly a temperature or sea-level change. This trigger mechanism is still one open a research question.

2. Goal

Research demonstrated whas shown that these rapid oscillationsD/O events have a global signature (e.g. Peterson et al., 2000a; Voelker, 2002), which suggests links between climates of high and low latitudes (Goni et al., 2006; Dean et al., 2007). These links have still not been clearly elucidated, and there is an urgent need to resolve how these regions interact. More recently, research showed that changes within the hydrological cycle, as reflected by changes between precipitation and wind strength, leave a strong paleoclimatological imprint in hemipelagic sediments in lower latitudes, including tropical regions (Clement and Peterson, 2008). These hydrological cycles can be linked to climatological phenomena such as the migrations of the intertropical convergence zone (ITCZ) (Peterson et al., 2000a; Haug et al., 2001) or the North Atlantic Oscillation (NAO) (Moreno et al., 2005). Changes in these phenomena have potential to amplify and perpetuate millennial-scale climate changes through greenhouse gas feedbacks and generation of atmospheric dust (Ivanochko et al., 2005).

Two locations were chosen for a detailed study of hydrological millennial-scale cycles during Late Quaternary times: the Cariaco Basin, an anoxic basin offshore Venezuela and the Southern Gulf of Cádiz, offshore Morrocco (Figure 2). Both sites have similar depths, contain hemipelagic sediments and the paleoclimatological records in both areas can be related to changes of the hydrological cycle (Haug et al., 2001; Peterson et al., 2000a; Marret and Turon, 1994; Moreno et al., 2004). The goal of this study is to improve our knowledge of these hydrological cycles in both study areas (see §2) using a multiproxy approach i.e., with a wide range of study tools (see §3).

3. Study areas and environmental settings

3.1 Cariaco Basin

The Cariaco Basin is a small east-west trending pull-apart basin of Quaternary age (Schubert, 1982) on the continental shelf of Venezuela (Figure 3). The basin actually consists of two sub-basins, each reaching depths of ~1400 m, separated by a central saddle that shoals to ~900 m. The high oxygen demands, created by upwelling-induced surface productivity, and a strong pycnocline which limits vertical exchange, leads to the present-day anoxic and sulphidic conditions below a depth of 300 m (Richards, 1975; Peterson et al., 1991) and deposition of hemipelagic sediments with high sedimentation rates (300 to >1000 m/ma) (Peterson et al., 2000b). The region is influenced by migrations of the intertropical conver-

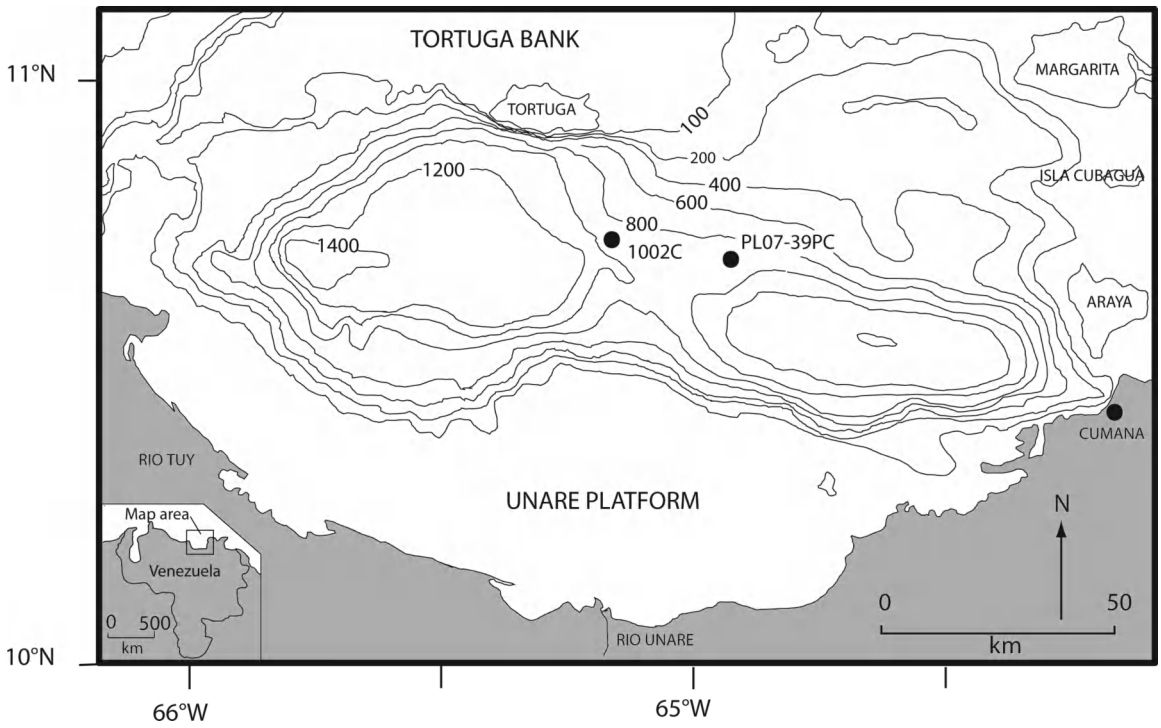

Figure 3 Location of the Cariaco Basin, consisting of two sub-basins separated by a saddle. The studied cores are indicated (ODP Hole 1002C and PL07-39PC).

gence zone (ITCZ), which cause seasonal variations in the strength of the northeastern trade winds (Figure 2) (Muller-Karger and Aparicio-Castro, 1994). During winter and early spring (January to March), the ITCZ is at its southernmost position and strong trade winds blow along the coast of Venezuela, causing upwelling of nutrient-rich water. The phytoplankton exploits this resource and during January and February primary production rates and carbonate and opal fluxes are at a maximum (Peterson et al., 1991). During this period diatoms dominate the phytoplankton (Ferraz-Reyes, 1983). Beginning from about June or July, when the ITCZ migrates north to a position near the Venezuelan coast, the trade winds weaken markedly and primary production rates fall to a minimum (Muller-Karger et al., 2004). As the upwelling subsides, the northward migration of the ITCZ brings its associated rainbelt above the Cariaco Basin, causing increased fluvial discharge from rivers. No large rivers currently discharge into the basin, but in former times fluvial input was more important (Peterson et al., 2000b). During this season, primary production is dominated by cyanobacteria, dinoflagellates (Ferraz-Reyes, 1983) and haptophytes (Goni et al., 2003). As an analogue to the seasonal migrations of the ITCZ, longer term (orbital-scale, millennial-scale) changes in the mean position of the ITCZ have been proposed as a mechanism linking northern high latitude and tropical climates (Peterson and Haug, 2006; Dean, 2006).

3.2 Southern Gulf of Cádiz

The Gulf of Cádiz is located in the NE Atlantic between the Iberian Peninsula and Morocco, west of the narrow Strait of Gibraltar (Figure 4). In the east, the Gulf of Cádiz is connected with the Mediterranean Sea, in the west with the open Atlantic Ocean. Current circulation patterns in the Gulf of Cádiz are characterised by a dynamic oceanographic setting, controlled by exchanges of water masses through the Strait of Gibraltar. The climatological regime in the

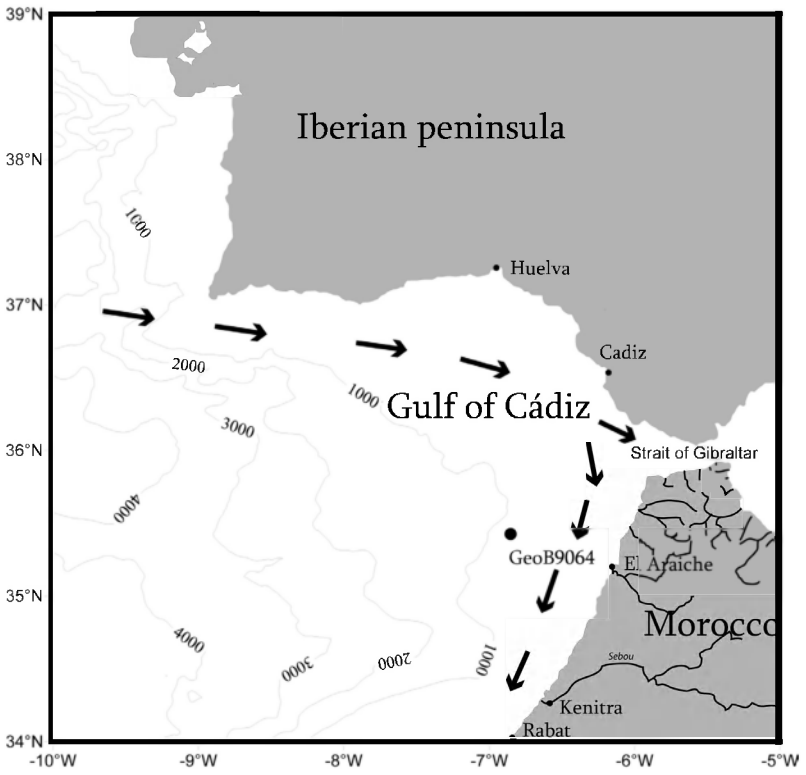

Figure 4 Location of the Gulf of Cadiz connected to the Mediterranean through the narrow Strait of Gibraltar and bounded by Iberian Peninsula and Morocco. GeoB9064: studied core. Arrows mark the flow of the Azores current.

Gulf of Cádiz is typical for the Mediterranean region, and is called the "Mediterranean regime", switching between dry summer and wet winter seasons (Hsu and Wallace, 1976). Over the past decades, changes in this regime in southern Europe can be related to changes in the North Atlantic Oscillation (NAO) (Hurrell, 1995). The NAO is a fluctuation in atmospheric pressure between a subpolar low-pressure center near Iceland and a high-pressure center in the Azores-Gibraltar region; it is most pronounced during winter times. When the NAO is in a positive phase, low-pressure anomalies over the Icelandic region and throughout the Arctic combine with high-pressure anomalies across the subtropical Atlantic to produce stronger than at average westerlies across the midlatitudes. Conversely, when the gradient is reduced or even reversed, with high pressure near to Iceland and low pressure near the Azores, the index is negative.

During a positive NAO, climatic conditions are colder and drier than average due to westerlies blowing over the northwestern Atlantic and Mediterranean regions, while in northern Europe ereas conditions are warmer and wetter than at average. During a negative NAO, the reverse pattern often results in a blocking anticyclone over Iceland or Scandinavia which pulls arctic air down into northern Europe; it results in a warmer temperatures and higher precipitation in the Mediterranean.

The NAO has varied in strength over decades, with persistent positive years in the early 1900s, numerous negative years in the 1960s and 1970s, and a large and persistent strengthening during the 1980s and early 1990s (Hurrell, 1995). These variations are observed over longer time-scales in the Mediterranean: on centennial (Luterbacher and Xoplaki, 2003) to millennial time-scales i.e., D/O cycles (Moreno et al., 2002, 2004, 2005)

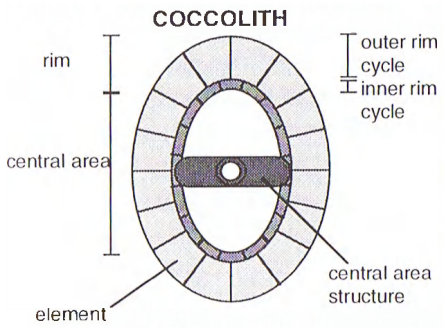

Figure 5 Diagrammatic representation of a heterococcolith (Bown, 1998).

4. Tools

The determination of past sea surface conditions is of primary importance for the reconstruction of climatic changes. Planktonic organisms, such as coccolithophores and dinoflagellates, register these conditions and are thus very sensitive recorders of climate change (e.g. Hays et al., 2005). Their assemblage and morphological changes can be considered as extremely useful for the elucidation of past climate variations in terms of productivity changes and other sea surface conditions such as sea surface temperatures (SST) and sea surface salinities (SSS). Geochemical analysis can be used to make similar, but independent reconstructions. This is important, since different proxies yield inconsistent results and climate models largely rely on accurate estimations of the ocean environmental parameters, such as palaeotemperature. Additionally, sedimentological proxies such as grain size analysis are important to interpret the underlying sedimentological framework; they help for example to trace nutrient sources (river- or upwelling-induced mechanisms).

4.1 Coccoliths

Coccolithophores are small (2-25 µm) unicellular algae that belong to the phylum Haptophyta and the division Prymnesiophyceae (Jordan and Chamberlain, 1997). They constitute one of the major plankton groups and are preserved as coccoliths[1] in marine sediments (Baumann et al., 2005). They are the most important pelagic calcifying organisms in the modern ocean (Baumann et al., 2004). Coccolithophores have recently gained increased attention as they play a unique role in the global carbon cycle, more specifically in the carbon and carbonate pump (Westbroek et al., 1993). Coccoliths can be divided into two main types: holococcoliths consisting of rhombohedral or hexagonal microcrystals identical in size and shape, while heterococcoliths are composed of crystals of different shapes and sizes (Young et al., 1997) (Figure 5). The taxonomy of coccolithophores is based on the morphology of the coccoliths that cover their cells. Modern coccolithophore taxonomy defines approximately 200 species (Young et al., 2003), but the discovery of pseudo-cryptic speciation has challenged species concepts (Sáez et al., 2003; Geisen et al., 2004). Most species produce characteristic holococcoliths during the haploid phase of their life-cycle and heterococcoliths during the diploid phase (Geisen et al., 2004), as evidenced from combination coccospheres (Cros et al., 2000). Although heterococcoliths are more robust than holococcoliths, not all heterococcoliths are regularly recorded in fossil assemblages. Delicate structures such as spines, tubular processes and thin walls are often broken during the sedimentation process. Therefore, placoliths, robust double-shielded interlocking coccoliths composed of wedge-shape elements, are most commonly preserved (Jordan et al., 2002).

Various environmental parameters within the water column affect the coccolithophore communities: water temperature, salinity, macro- and micronutrients, light penetration, turbulence, water depth, toxins and grazing pressure (Jordan, 2002; Baumann et al., 2005). This causes individual species to occur typically in particular biogeographical zones: Subarctic, Temperate, Subtropical, Tropical and Subantarctic (Winter and Siesser, 1994). These biogeographical distribution patterns are reflected in the surface sediments thanks to protected and accelerated sedimentation in faecal pellets or in marine snow

[1] Sometimes the term nannofossils is used. The term nannofossils includes both coccoliths and nannofossils s.s., which may be unrelated but are both composed of calcite. Most Quaternary nannofossils are coccoliths.

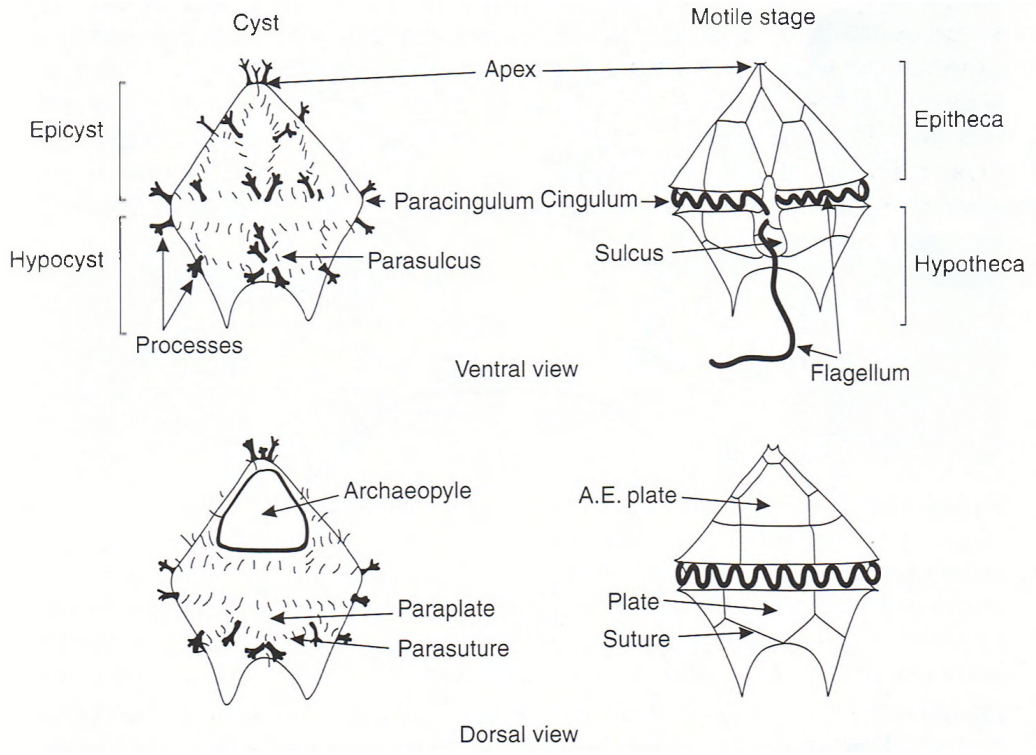

Figure 6 Comparison of basic morphological features of dinoflagellate motiles and cysts (Dale and Dale, 2002).

(Baumann et al., 1999, 2005). The strong link to the environmental parameters causes coccolithophores to react rapidly to climate change, such as the El Niño Southern Oscillation (ENSO) (Ziveri and Thunell, 2000; De Bernardi et al., 2005) which makes them excellent palaeoceanographic tools (e.g. Rogalla and Andruleit, 2005; Álvarez et al., 2004; Krammer et al., 2006; Bollmann and Herrle, 2007). Moreover, coccolithophores have a continuous fossil record from their first occurrence in the Late Triassic to the present day (Bown et al., 2004), making them very useful biostratigraphic tools (Perch-Nielsen, 1985; Bown, 1998).

4.2 Dinoflagellate cysts

Dinoflagellates are eukaryotic, single-celled organisms in which the motile cell possesses two flagella and a unique type of nucleus – the dinokaryon. Based on these characteristics, they are classified in the division Dinoflagellata (Fensome et al., 1993).

Dinoflagellate cysts are the hypnozygotes produced by planktonic dinoflagellates during the sexual phase of the life cycle[2] , and are fossilizable if the wall exists of a resistant substance such as dinosporin[3], calcium carbonate or silica. Cysts are formed within the thecal plates of the motile stage, which sometimes results in the reflection of the morphological features of the motile form[4] (Figure 6). The identification criteria of the cyst are the furrows housing the flagella (cingulum and sulcus), plate patterns, ornamentation and the excystment opening or archaeopyle. The latter is the opening through which the new motile stage exits (Dale and Dale, 2002). Most of the cysts serve as a benthic resting stage of which the cells are filled with food-storage products and are enclosed in

[2] Approximately 10 % of the around 2000 marine dinoflagellate species produce cysts (Dale, 2001).

[3] A macromolecular, highly resistant organic compound forming, or partly forming, the enclosing wall of fossilizable dinoflagellate cysts, comparable to sporopollenin (Fensome et al., 1993).

[4] Difficulties to link dinoflagellates to their cysts results in separate taxonomies.

a protective cell wall (Dale, 2001). After a mandatory resting period, motiles excyst out of the "seed bed" (Anderson and Morel, 1979).

Dinoflagellates have a long ranging geological record. Geochemically detected biomarkers suggest ancestors were already present in the Early Cambrian (Moldowan and Talyzina, 1998). The fossil record is continuous from the Triassic to the present (MacRae et al., 1996). Additionally, the wide geographical distribution and rapid diversification of dinoflagellate cysts enables extensive biostratigraphic zonations (e.g. Stover et al., 1996; De Schepper and Head, 2008), useful amongst others in hydrocarbon exploration.

Dinoflagellates occur in most aqueous environments and exhibit wide diverging feeding strategies including autotrophy, phagotrophy, symbiosis, parasitism and mixotrophy (Fensome et al., 1993), the latter being more frequently observed in cultures (Jeong et al., 2005). Together with other primary producers such as diatoms and coccolithophores, they play an important role in the global carbon cycle (Brasier, 1985). They can form toxic blooms known as 'harmful algal blooms' (HABs)[5] (Anderson, 1997). These HABs often cause large-scale marine mortality and are associated with various types of shellfish poisoning (e.g. Cembella et al., 2002; Landsberg, 2002), with important economic impacts (e.g. Bushaw-Newton and Sellner, 1999). Global climate change may increase the number of HABs (Dale et al., 2006).

Changes in both the assemblage composition and the morphology are related to changes in environmental parameters such as temperature, salinity and nutrient content (Dale, 1996; Dale and Dale, 2002). Despite possible problems with preservation (Zonneveld et al., 2007; 2008) and transport (Dale and Dale, 2002), dinoflagellate cysts are considered to be useful tools for the reconstruction of Late Quaternary palaeoenvironments using a classical approach based on assemblage changes (e.g. Reichart and Brinkhuis, 2003; Pospelova et al., 2006; Kawamura et al., 2006; Mudie et al., 2007; Head, 2007) or via the use of transfer functions (de Vernal et al., 2001; 2005; de Vernal and Marret, 2007). Additionally, dinoflagellate cysts prove to be useful to detect past eutrophication (Dale, 2009).

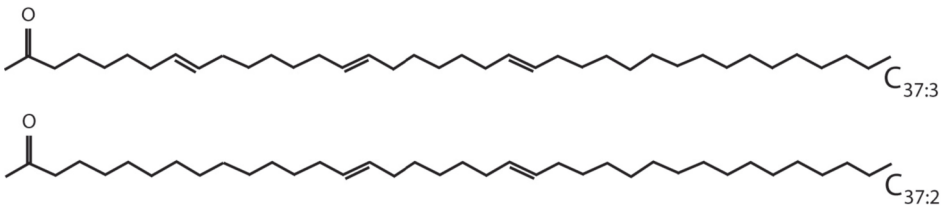

Figure 7 The two most abundant alkenones ($C_{37:2}$ and $C_{37:3}$) used in determination of the water temperature.

4.3 Geochemical analysis

Biomarkers are organic molecules which indicate the presence of living organisms. Two complex molecules, alkenones and Glycerol Dialkyl Glycerol Tetraethers (GDGTs), are applied in proxies.

Alkenones are long-chain (C_{37}-C_{39}) unsaturated ketones (Figure 7), found as highly resistant organic compounds in the membranes of haptophytes. They are well-preserved in the sediments and are used to reconstruct productivity variations (e.g. Schulte and Müller, 2001; Knies, 2005). More extraordinary, the ambient water temperature in which an organism dwelt can be estimated from the ratio of its unsaturated alkenones preserved in the sediments. The Unsaturation Index of "di" versus "tri" unsaturated C_{37} alkenones is defined as follows (Prahl and Wakeham, 1987):

$$U^{K'}_{37}=[C_{37:2}]/[C_{37:2}+C_{37:3}]$$

[5] Sometimes called 'red tides', but Harmful Algal Blooms is preferred since they are always harmful, do not necessarily cause discoloration of the water and are never associated with tides.

The Unsaturation Index can be used to estimate the water temperature according to the global core top calibration of Müller et al.(1998), valid between 60°N and 60°S:

$$T(°C) = \frac{(U^{K'}_{37} - 0.044)}{0.033}$$

The fact that $U^{K'}_{37}$ can be used to reconstruct annual mean temperature is enigmatic, given the strong seasonality in coccolithophore production: coccolithophore production is highest during colder seasons in tropical and subtropical environments, and during warmer seasons in higher latitudes (Bijma et al., 2001). Despite possible drawbacks of the method, such as degradation (Hoefs et al., 1998; Rontani et al., 2008), lateral transport (Mollenhauer et al., 2005; 2008) and problems in certain areas such as the polar oceans (e.g. Sikes and Volkman, 1993), reconstruction of annual sea surface temperatures (SST) is widely applied using this method in late Quaternary research (e.g. Cacho et al., 2001) with relatively high precision (Herbert, 2003).

Besides alkenones, the relative amounts of other lipids in organisms are known to vary with growth temperatures. Membrane lipids, synthesized by Crenarchaea bacteria (GDGTs) occur ubiquitously (Schouten et al., 2000) and are unaffected by water redox conditions (Schouten et al., 2004). Concentrations of these biomarkers are used for the reconstruction of productivity variations (Huguet et al., 2007). GDGTs can contain up to eight cyclopentane rings (DeRosa and Gambacorta, 1988) (Figure 8). From culture studies of the membrane composition of hyperthermophilic archaea it is known that the relative number of cyclopentane moieties increases with growth temperature (Gliozzi et al., 1983; Uda et al., 2001), which probably regulates membrane fluidity (Wuchter et al., 2004). Thus, by measuring the relative amounts of GDGTs present in marine sediments, the temperature can be determined at which Crenarchaeota produced their membranes. This can be expressed as the TetraEther index of tetraethers consisting out of 86 carbon atoms (TEX_{86}) (Schouten et al., 2002):

$$TEX_{86} = \frac{([IV]+[V]+[VI])}{([III]+[IV]+[V]+[VI])}$$

SSTs between 5 and 30°C can then be calculated, according to the following core-top calibration (Kim et al., 2008):

$$T(°C) = -10.78 + 56.2 * TEX_{86} \quad (R^2=0.935)$$

This relationship has been applied mostly for the reconstruction of palaeotemperatures in marine late Quaternary sites (e.g. Huguet et al., 2007), but has also been shown to work for African lakes (Tierney et al., 2008) as well as in the Cretaceous Arctic Ocean (Jenkyns et al., 2004).

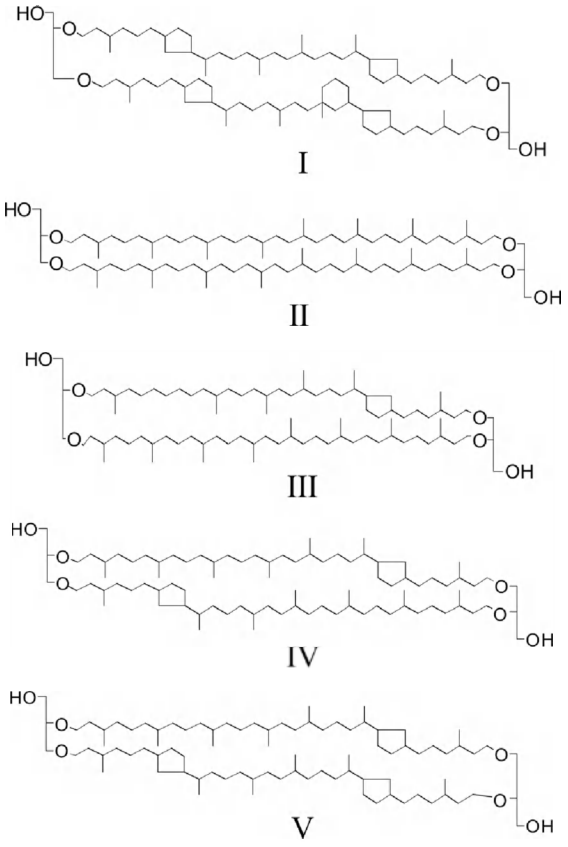

Figure 8 Structures of GDGTs discussed in the text (Schouten et al., 2002).

An inorganic geochemical method is also applied, using Mg/Ca element ratios measured on shells of Foraminifera. This method is based on the thermodynamically different behaviour of trace elements during the calcification of Foraminifera, which is primarily a function of temperature. This enables the relatively new so-called Mg/Ca paleothermometry to reconstruct SSTs (e.g. Mashiotta et al., 1999; Elderfield and Ganssen, 2000; Lea, 2003; Nürnberg and Groeneveld, 2006), although issues of intraspecies and ontogenetic variations (e.g. Nürnberg et al., 1996), preservation (e.g. de Villiers, 2003; Regenberg et al., 2006) and other factors such as sea water carbonate ion concentrations (Russell et al., 2004) should occasionally be taken into account. The exponential dependence of Mg/Ca ratios on temperature within single planktonic foraminiferal species is well-studied and results in species-specific (e.g. Dekens et al., 2002; McConnell and Thunell, 2005) and multi-species calibration curves (e.g. Elderfield and Ganssen, 2000; Anand et al., 2003), with an accuracy of ± 0.2–1.2°C (Elderfield and Ganssen, 2000; Dekens et al., 2002; Anand et al., 2003). The major advantage of this method is that oxygen isotopes ($\delta^{18}O$) can be measured on the same biotic carrier, which ensures the recording of the same seasonality and/or habitat effects. Since oxygen isotopes of planktonic Foraminifera depend both on temperature and both regional and global salinity, the simultaneous analysis of Mg/Ca-ratios allows for the subtraction of the temperature signal from the oxygen isotope signal and subsequently the calculation of salinity variations. This results in reliable palaeosalinity reconstructions (e.g. Schmidt et al., 2004; Nürnberg and Groeneveld, 2006).

4.4 Grain-size analysis

The terrigenous component of marine sediments off continental margins consists of coarse eolian dust (Koopmann, 1981; Moreno et al., 2002; Stuut et al., 2002) and finer river discharged muds (Koopmann, 1981; Sarnthein et al., 1982; Sirocko et al., 1991). In order to differentiate between transport mechanisms for terrigenous sediments, a numerical-statistical algorithm (Weltje, 1997) can be applied to the carbonate-free grain-size distributions. The end-member algorithm attempts to explain observed variations in natural sediments as a result of mixing and has been used successfully to 'unmix' sediments produced by linear mixing. This enables a distinction between wind-blown and fluvially derived sediment fractions and use of their relative proportions as paleoclimate proxies, for the reconstruction of wind strength, aridity (or rainfall) and upwelling variations (Prins and Weltje, 1999; Prins et al., 2000, 2002; Stuut et al., 2002; Frenz et al., 2003).

5. Synopsis

In **Chapter 1**, coccolith assemblages from ODP core 1002C in the Late Quaternary Cariaco Basin are compared with coccolith assemblages from nearby core PL07-39PC, studied by Dr. Matt Lynn. A multi-proxy approach was applied with geochemical data (total organic carbon and carbonate) from Dr. Mylène Aycard, Pteropod data from Dr. Hui-Ling Lin and earlier published data. Changes of the proxies reflect clearly millennial-scale oscillations and suggest a strong link with shifts of the intertropical convergence zone. A new upwelling proxy (GEX) is proposed: the ratio between the two dominant coccolith taxa; it suggests that upwelling induced productivity variations in the anoxic Cariaco basin are tightly linked to preservation of the fragile coccoliths and that terrigenous and marine records show similar fluctuations.

Assemblage changes of coccoliths have proven to be useful paleoceanographic indicators in the northern Gulf of Cadiz by Colmenero-Hidalgo (2002, 2004). A similar approach is therefore applied in **Chapter 2** for core GeoB9064 in the southern Gulf of Cádiz. Morphological variations of *Emiliania huxleyi* have been related to temperature changes and can be used for detection of Heinrich Events (Colmenero-Hidalgo et al., 2004). To frame these climatological variations, paleotemperatures were estimated using $U^{K'}_{37}$ and TEX_{86} sea surface temperature estimates and provide a well-constrained frame for the detection of Heinrich Events. The use of grain-size analysis with end-member modeling, together with data generated from an XRF analysis by Dr. Anneleen Foubert completes the paleoclimate reconstruction. This study generates a detailed characterization of

positive and negative NAO oscillations,.

Assemblage changes of dinoflagellate cysts are frequently based on the calculation of the absolute number of dinoflagellate cysts (or concentrations) in the sample by adding a spike, mostly an exotic spore. Absolute abundances are more reliable as productivity indicators than relative abundances since these could be affected by closed-sum problems or preservation issues (Reichart and Brinkhuis, 2003). Since there was evidence for inconsistencies in the results from different laboratories, a global interlaboratory calibration of this method was carried out in **Chapter 3** where a standard for the method is proposed.

Morphological variations of dinoflagellate cysts are frequently attributed to changes in salinity (Sorrel et al., 2006; Head, 2007). A dinoflagellate cyst that has been thoroughly investigated in this respect is *Lingulodinium machaerophorum* (Kokinos and Anderson, 1995; Mudie et al., 2001; Brenner, 2005). In **Chapter 4**, a global morphological study of this cyst using light and confocal microscopy shows that this variation is much more complex than previously thought. Apparently, the morphological variation is linked to both changes in salinity and temperature, as expressed by a ratio between both (S/T). It appears impossible to extract these parameters separately from the morphological information, which confirmed earlier results from cultures (Hallett, 1999). In **Chapter 5**, it becomes apparent that the cysts can be found only within a restricted range of the S/T ratio, which suggests that the motile is unable to form its cyst outside these limits. This S/T ratio thus generates a convincing explanation for the biogeographical zonation of this dinoflagellate cyst. Furthermore, it is argued that the morphology is the expression of this S/T ratio, whereas the productivity signal is determined by other environmental variables.

In **Chapter 6**, assemblage changes of dinoflagellate cysts and morphological changes of *Lingulodinium machaerophorum* are used to reconstruct productivity and salinity variations in core 1002C from the Late Quaternary Cariaco Basin. This study reveals rapid millennial-scale productivity changes due to shifts in the intertropical convergence zone and an asynchronicity between salinity proxies and hydrological variations.

CHAPTER 1

Coccolithophores as palaeoecological indicators for shifts of the ITCZ in the Cariaco Basin during the late Quaternary

ABSTRACT

Coccoliths were studied from the ODP Hole 1002C and core PL07-39PC in the Cariaco Basin. Increases in *Emiliania huxleyi* are synchronous with decreases of *Gephyrocapsa oceanica* and vice versa. A new index (GEX) based on the relative abundances of these two taxa is proposed, and correlates with various other proxies. It is shown that GEX can serve as upwelling proxy. This confirms that the ITCZ shifted north during the Bølling/Allerød, south during the Younger Dryas and back north during the Preboreal. The upwelling proxy shows few discrepancies with the terrigenous record.

1. Introduction

The equatorial Atlantic plays a key role in global climate changes during the Quaternary. Evidence is increasing that large and rapid climate oscillations occurred at suborbital and millennial frequencies in the North Atlantic during the last glacial (Heinrich events and Dansgaard/Oeschger cycles) (Bond et al., 1992, 1997; Dansgaard et al., 1993). Apparently, these are not restricted to the northern higher latitudes but have a global signature, which is also prominent in the Caribbean Sea (Peterson et al., 2000a; Schmidt et al., 2004). The mechanisms for these pronounced changes in the atmosphere–ocean system are still a matter of debate, partly because of the scarceness of high resolution data from the tropics and the southern hemisphere (Vidal et al., 1999; Vink et al., 2001).

These changes in the climate system are well-reflected in high resolution productivity data (Peterson et al., 2000a; Vink et al., 2001), mainly from shelf areas where 10–15% of the global marine primary production takes place (Muller–Kerger et al., 2005). Pronounced fluctuations of the production are more likely to happen within these borderlands. The Cariaco Basin, located on the Venezuelan margin, is characterized by high productivity, which has caused the basin to become anoxic. In this respect, the basin offers an important opportunity to study changes of productivity.

Coccolithophores are a major plankton group and play an important role in biogeochemical cycles and climate. However, these unicellular algae are not so commonly used for palaeoceanographical and palaeoclimatological studies. This may be partly due to the cosmopolitan range and ubiquitous occurrence of only a few dominant species. Nevertheless, biogeographic distribution patterns of coccoliths in surface sediments reflect the distribution of living coccolithophore species in the overlying watermasses (Baumann et al., 1999). Major ecological factors explaining the spatial and temporal distributions of coccolithophores are discussed in Baumann et al. (2005) and Jordan (2002). The sinking flux of coccolithophores constitutes about 60 % of the total burial flux of $CaCO_3$ to the world's sediments, with a

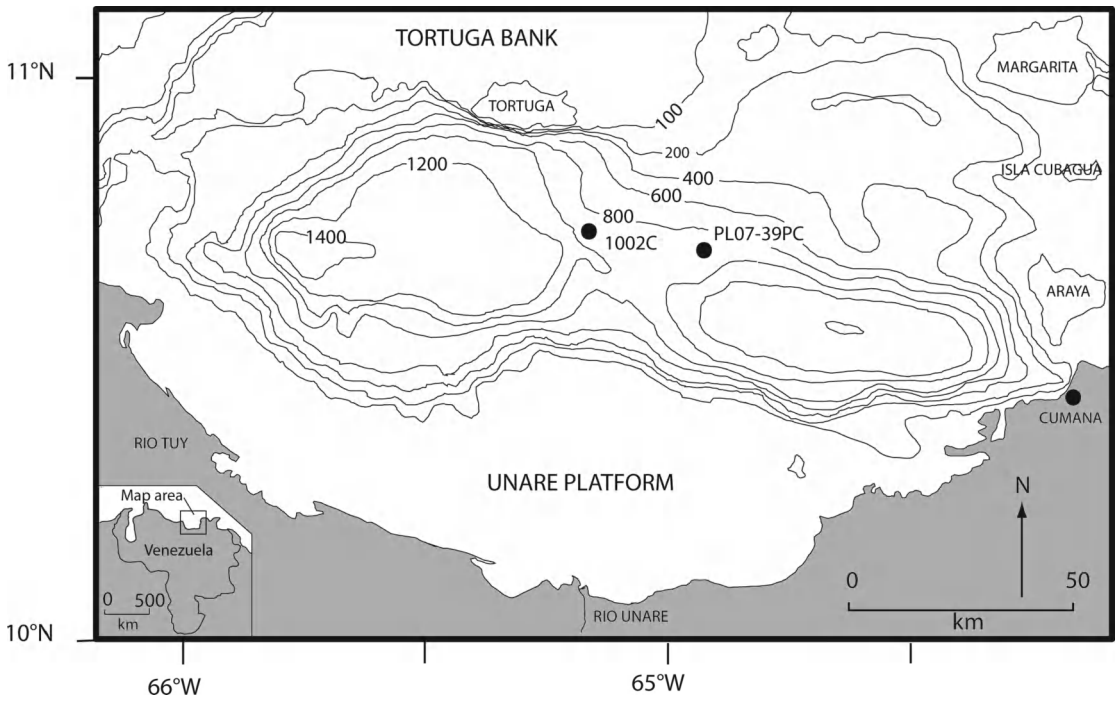

Figure 1 The Cariaco Basin, with location of cores 1002C and PL07–39PC.

regional variability of 20–86% (Honjo, 1996), which makes them an ideal tool for high-resolution productivity study.

Coccolithophores are a major constituent of the phytoplankton blooms which occur during the upwelling season in the Cariaco Basin. This study reports variations in coccolith taxa preserved in sediments of Cariaco Basin and their use for the interpretation of climate and ocean variability in the southern Caribbean region during the latest Quaternary on a millennial timescale, through a high resolution analysis of quantitative coccolith fluctuations in the Cariaco Basin. Using a multiproxy analysis with new data from a geochemical analysis (TOC and carbonate), a pteropod abundance ratio and a palynological analysis, combined with earlier published data (Mg/Ca, alkenones, Mo/Al, XRF), a robust framework for the elucidation of the variations in the coccolith record, is presented.

2. Study area and background

The Cariaco Basin is a small east–west trending Quaternary pull–apart basin on the continental shelf, north of Venezuela (Figure 1). It is composed of two subbasins, separated by a 950 m deep saddle. The western basin has a depth up to 1400 m, whilst the eastern basin has a maximum depth of 1370 m. The basin is isolated in the north from the inlet of deepwater from the Caribbean by a series of sills which form the Tortuga Bank, the deepest connections between the basin and the open Caribbean are at a depth of 146 m, in the northwest. The surrounding topography prohibits inlet of deep water from the Caribbean, causing a 100 year residence time of the bottom waters (Deuser, 1973). The high oxygen demands, created by upwelling–induced surface–productivity, and a strong pycnocline which limits vertical exchange, leads to the present–day anoxic and sulphidic conditions below a depth of

300 m (Richards, 1975; Peterson et al., 1991). The almost complete lack of bioturbation leads to a very complete sedimentary record.

The most important surface waters entering the Caribbean are the North Brazil Current (NBC) and the North Equatorial Current (NEC). These branch off around Lesser Antilles and flow into the Caribbean Basin to form the Caribbean Current. The two upper water masses are the Caribbean Surface Water (CSW) and the Subtropical UnderWater (SUW). The oligotrophic CSW (0–80 m) originates from the NEC and NBC with significant input of low salinity waters of the Amazon and Orinoco rivers in October to November. The eutrophic SUW (at a depth of 80–120 m), comes from the centre of the North Atlantic (the surface waters of the North Atlantic Gyre) and enters the Caribbean between the Lesser Antilles and the Windward Passage between Cuba and Jamaica (Wust, 1964; Nyberg et al., 2002). The SUW forms the permanent thermocline and/or nutricline of the Caribbean. The surface water of the Caribbean is generally characterized by low primary productivity except in coastal regions, for example off the Venezuelan Coast, where due to upwelling, this SUW is shoaling and causes higher productivity (Muller–Karger and Aparicio–Castro, 1994).

The region is influenced by migrations of the Intertropical Convergence Zone (ITCZ) which causes seasonal variations in the strength of the northeast trade winds (Muller–Karger and Aparicio–Castro, 1994). During winter and early spring (January–March), the ITCZ is at its southernmost position and strong trade winds blow along the coast of Venezuela, causing upwelling of nutrient–rich water. The phytoplankton exploits this resource and in January and February primary production rates and carbonate and opal fluxes are at a maximum (Peterson et al., 1991). During this period, diatoms dominate the phytoplankton population (Ferraz–Reyes, 1983). Beginning from about June or July, when the ITCZ migrates north to a position near the Venezuelan coast, the trade winds weaken markedly and primary production rates fall to a minimum (Muller–Karger et al., 2004). As the upwelling subsides, the northward migration of the ITCZ brings its associated rain belt above the Cariaco Basin, and increases fluvial discharge from rivers which affect the southern Caribbean. No large rivers currently discharge into the basin, but in former times fluvial input was more important (Muller–Karger et al., 1989). During this season, the production is dominated by cyanobacteria, dinoflagellates (Ferraz–Reyes, 1983) and also haptophytes (Goni et al., 2003).

The interglacial basin sediments are laminated and reflect migrations of the ITCZ as the high annual sediment flux (20–100 cm kyr^{-1}) forms alternating light and dark laminae. The light laminae are mainly composed of diatoms; they reflect high winter–spring production. The microorganisms appear grouped in aggregates, most likely fecal pellets, surrounded by biogenic silica. The dark laminae have a higher clay and terrigenous material composition, with mainly quartz and feldspars, and this reflects deposition during the summer–autumn rainy season in combination with reduced productivity. Micro–organisms in these laminae are also grouped in aggregates.

3. Materials and methods

ODP Site 1002 (10°42.37'N, 65°10.18'W) is located on the western flank of the central saddle of the Cariaco Basin, at a depth of 893 m (Figure 1). The saddle was chosen because the varves in the subbasins tend to be disrupted by microturbidites. Shipboard Scientific Party (1997) gives the detailed sediment core location and description.

Core PL07-39PC (10°42.00' N, 64°56.50' W) was recovered from a water depth of 790 m on the eastern side of the central saddle that bisects the basin (Figure 1), and is described in Lin et al. (1997).

3.1 Stratigraphy

Hole 1002D is well dated with 65 accelerator mass spectrometry (AMS) ^{14}C dates on planktonic foraminifera, over the studied interval, and was fine–tuned to GISP II $\delta^{18}O$ by matching inflection points and interpolating between them (Hughen et al., 2004). Hole 1002C was then aligned with Hole 1002D by visually matching magnetic susceptibilities records provided by Shipboard Scientific Party (1997).

The studied core sections range in age from the late Pleistocene to the earliest Holocene, covering the Last Glacial Maximum (LGM), Heinrich Event 1, the Bølling–Allerød Warm Period (BA), the Younger Dryas (YD) and the Holocene.

Core PL07-39PC is dated with 29 AMS ^{14}C dates on planktonic foraminifera, has a detailed oxygen isotope record and grayscale correlations (Hughen et al., 1996a,b; Lin et al., 1997).

Sedimentation rates in both cores were calculated by taking the moving average of the two slopes immediately next to the point in the age–depth diagram (Figure 2) and range from about 32 to 170 cm kyr^{-1}. The slower rates are associated with deposition of the faintly laminated upper portion of the core, the highest ones with Heinrich 1 and YD. Mass accumulation rates in Hole 1002C were calculated using dry bulk density measurements based on GRAPE density measurements (Shipboard Scientific Party, 1997) in PL07-39PC (Lynn, 1998). There could be two reasons for discripancies between both cores: one of the cores has been stretched/compressed on certain intervals due to coring or there have been varying inputs of productivity or terrigenous input (both cores are at different sides of the saddle).

Mass accumulation rates (MAR) are much higher during glacial periods and the YD than interglacial ones. MAR during the BA are clearly lower than glacial MAR.

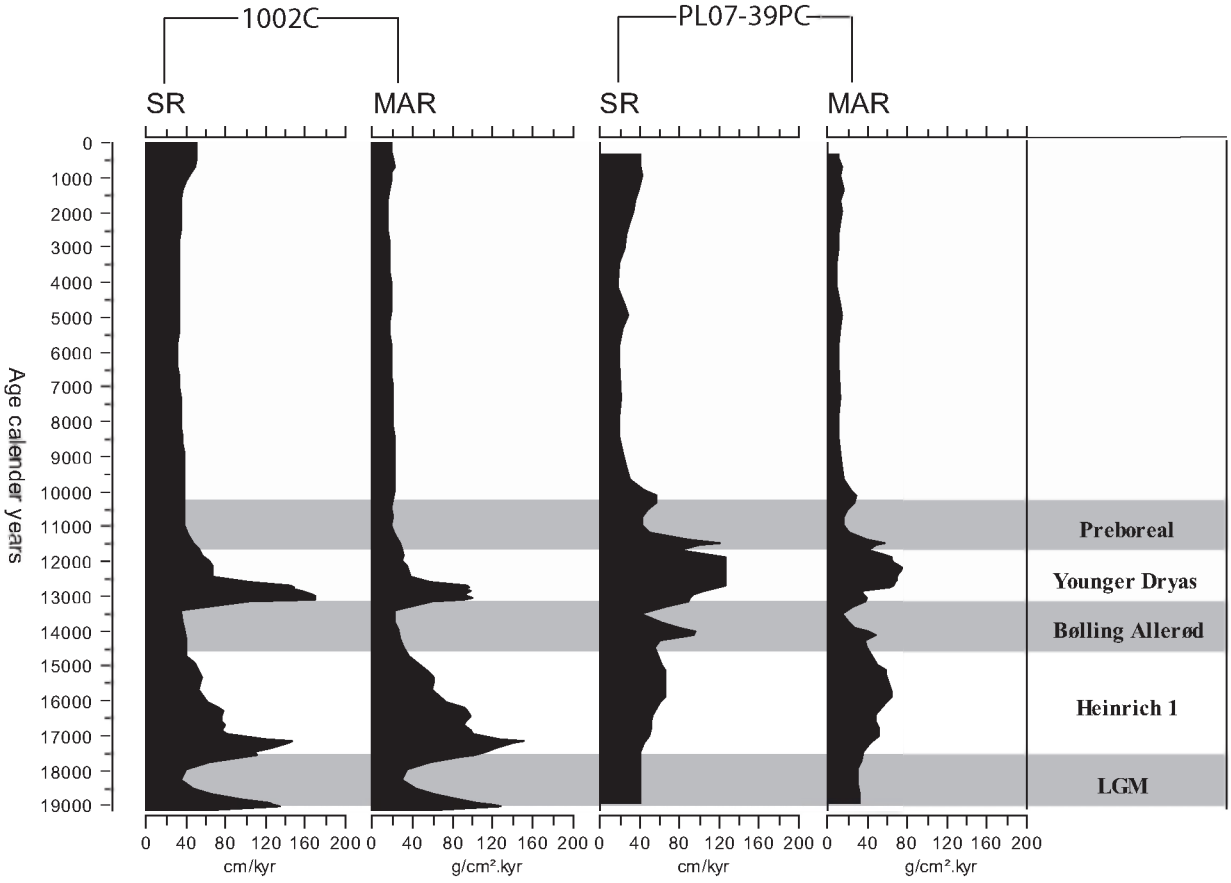

Figure 2 Sedimentation rates and mass accumulation rates in cores 1002C and PL07-39PC.

3.2 Quantification of coccoliths and coccolith carbonate

Samples were taken at 10 cm intervals. Given the range of the sedimentation rates, this sampling interval yields a temporal sampling resolution between about 100 and 300 years. The method of Okada (2000) was used for preparation of the studied 95 samples from Hole 1002C. 400 nannofossils were counted under a JEOL 6400 SEM at a magnification of 2700 x. Absolute abundances were calculated using the formula of Lototskaya (1999):

$$N = \frac{V_1 * S_f * N'}{V_2 * n_s * S' * m_{DBD}}$$

where:

N = absolute abundances of coccoliths g^{-1} dry sediment
V_1 = volume of tapwater used for filtering
S_f = effective filtration area
N' = number of counted coccoliths
V_2 = volume of the solution;
n_s = number of counted square fields
S' = area of the field
m_{DBD} = weight of a bulk sediment sample (in g)

Coccolith accumulation rates can then be calculated as:

$$cocAR = R * DBD * N$$

where

cocAR = total coccolith accumulation rate (coccoliths cm^{-2} kyr^{-1})
R = average sedimentation rate (cm kyr^{-1})
DBD = dry bulk density (g cm^{-3})
N = absolute abundances of coccoliths g^{-1} dry sediment (number g^{-1})

The number of coccoliths were converted into coccolith–carbonate contents on the basis of mean estimates of coccolith masses (Young and Ziveri, 2000). Since the mass of coccolith species varies markedly, size calibrations are necessary (Baumann, 2004) and 50 measurements of the length of the most important taxa were taken as in Baumann et al. (2003). They were converted into mass estimates using the method of Young and Ziveri (2000) (Table 1).

For core PL07-39PC, samples were also taken at 10-cm intervals for this study. Initial sample preparation followed standard micropaleontological techniques. Core samples were washed through a 63 µm sieve, saving one liter of the <63 µm fraction. The <63 µm fraction was allowed to settle for two days or until the water was clear, then excess water was siphoned off. The last 50 ml was left to avoid disturbance of the settled fraction; this remaining water was evaporated off under a heat lamp. The dried fine fraction was then scraped out of the beaker and saved for analysis. Owing to the high proportion of clay material in these samples, coccolith concentration techniques were employed before the samples were counted. This procedure simplified the relative abundance counts but invalidated any later attempt at generating absolute abundance data from the same samples; consequently separate preparations were required to accommodate the absolute abundance study.

Table 1 Lengths and masses of selected species

Species	Length (µm)	Mass (pg)
Gephyrocapsa oceanica	4,78	15,41
Emiliania huxleyi	3,08	1,61
Calcidiscus leptoporus	7,90	109,72
Florisphaera profunda	4,12	8,54
Helicosphaera carteri	7,41	59,82
Umbilicosphaera sibogae	4,89	18,44
Syracosphaera pulchra	5,33	13,00
Umbellosphaera spp.	6,16	10,36

3.3 Total organic carbon and carbonate

TOC was measured by Rock Eval pyrolysis using a Rock Eval IV apparatus. Carbonate% was measured in Hole 1002C by using a manocalcimeter. Details on the methods are described in Aycard et al. (2008).

3.4 Quantification of pteropods and pteropod ratio

After wet sieving at 63 µm, the sample was splitted

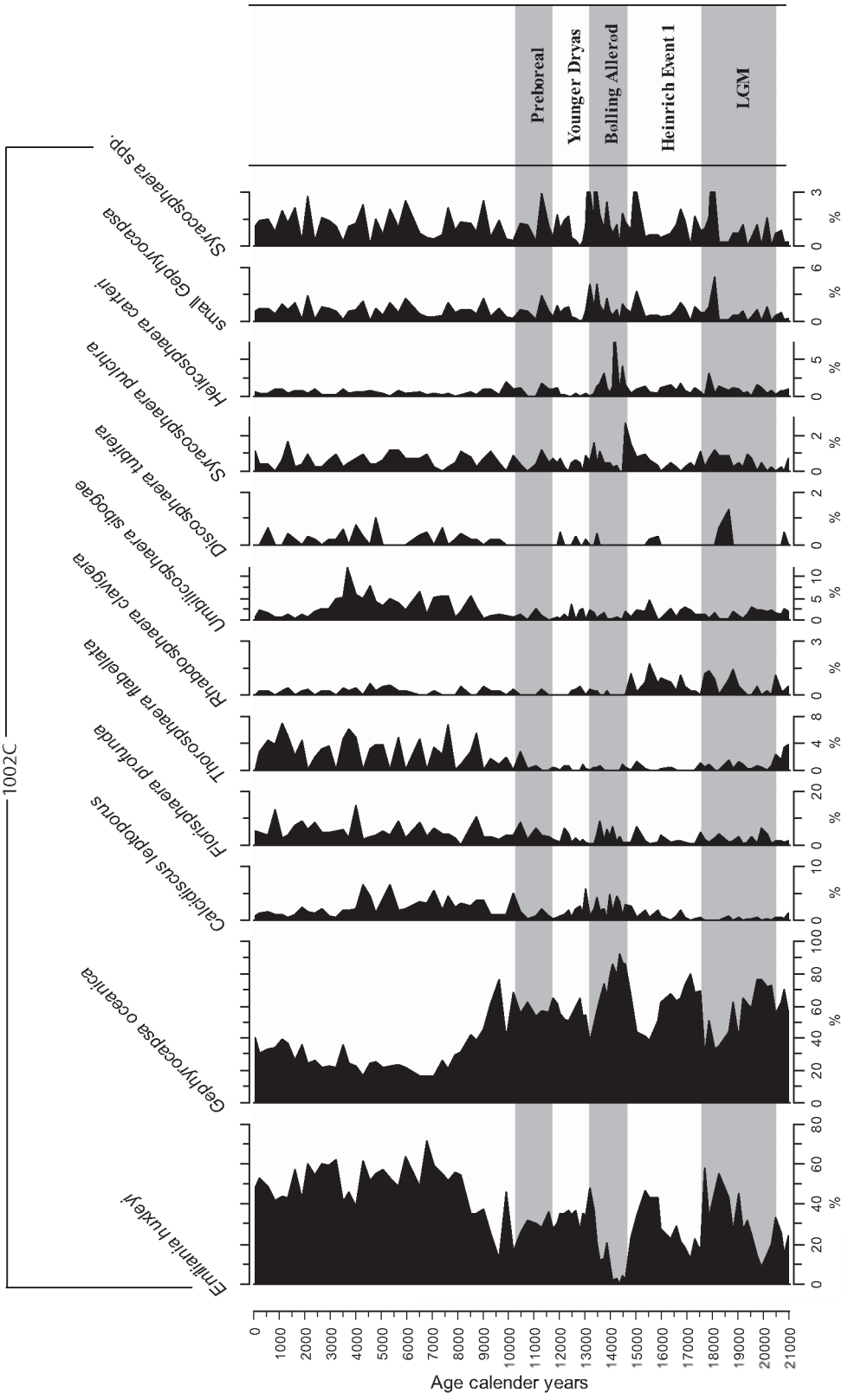

Figure 3 Relative abundances of coccoliths in core 1002C.

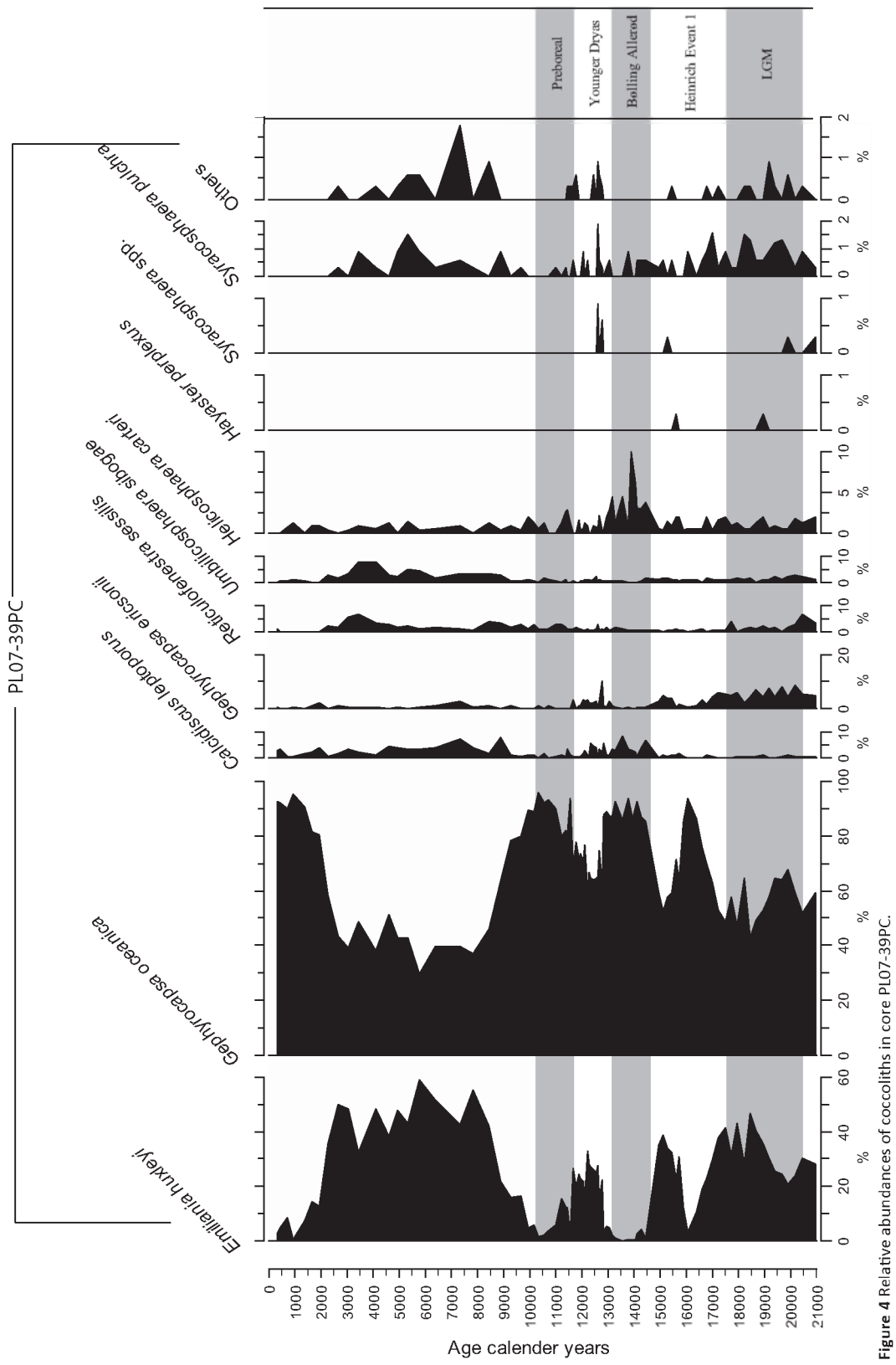

Figure 4 Relative abundances of coccoliths in core PL07-39PC.

multiple times, depending on the abundance of pteropods. The number of pteropods was calculated by multiplying with splitting factor and dividing with dry sample weight. Pteropod abundance ratio was calculated by (# pteropods g^{-1}) / (# pteropods g^{-1} + # planktonic foraminifera g^{-1}).

4. Results

All raw data are included as Supplementary data.

4.1 Coccolith relative abundance data

The assemblages found in the area off Venezuela are typically tropical dominated by placolith–bearing species such as *Emiliania huxleyi, Gephyrocapsa oceanica*, *Umbilicosphaera sibogae* and *Calcidiscus leptoporus* (Figure 3 and 4)

Thirty–nine nannofossil species were identified in core 1002C, but only two species reach relative abundances of more than 15% (Figure 3): *Gephyrocapsa oceanica* (16–92%) and *Emiliania huxleyi* (0–72%). Other important species are *Florisphaera profunda* (up to 15%), *Umbilicosphaera sibogae* (up to 12%), *Helicosphaera carteri* (up to 9%), *Calcidiscus leptoporus* (up to 7%), *Gladiolithus flabellatus* (up to 7%), small *Gephyrocapsa* (up to 7%) and *Acanthoica* spp.(up to 5%). Species with low relative abundances were *Reticulofenestra sessilis* (up to 3%), *Syracosphaera pulchra* (up to 3%), *Rhabdosphaera clavigera* (2%), *Umbellosphaera* spp. (up to 2%), *Calciosolenia* spp. (up to 2%), *Michaelsarsia* spp. (up to 2%), *Reticulofenestra parvula* (up to 1%), *Discosphaera tubifera* (up to 1%), *Hayaster perplexus* (up to 1%), *Algirosphaera robusta* (up to 1%), *Helicosphaera pavimentum* (less than 1%), *Gephyrocapsa caribbeanica* (less than 1%), *Pontosphaera* spp. (less than 1%), *Calciopappus rigidus* (less than 1%), *Syracolithus dalmaticus* (less than 1%), *Ceratolithus cristatus*, now known as alternate life–stage of *Neosphaera coccolithomorpha* (CROS *et al.*, 2000) (less than 1%) and *Coronosphaera mediterranea* (less than 1%). The results for core PL07-39PC are shown in Figure 4 and show very similar changes.

Emiliania huxleyi and *Gephyrocapsa oceanica* are characterised by very rapid abundance changes in the investigated time interval. Increases in relative abundances of *Emiliania huxleyi* are synchronous with decreases of *Gephyrocapsa oceanica* and *vice versa*.

4.2 Coccoliths per gram of sediment and absolute abundance data (coccolith accumulation rates)

The number of coccoliths/g sediment range in 1002C from 3.2×10^8 to 8×10^9 (Figure 6). Boeckel and Baumann (2004) studied the distribution in surface sediments of the south–eastern South Atlantic Ocean and found total coccolith abundances ranging from 0.2 to 39.9 coccoliths x 10^9 g^{-1} sediment. Liths per gram of sediment calculated by Kinkel et al. (2000) from a core in the western equatorial Atlantic range between 10×10^9 and 40×10^9 liths m^{-2} kyr^{-1} (Figure 6). Our estimates fall well within these ranges.

Coccolith accumulation rates were calculated for each species and ranged from 18×10^9 to 49×10^{10} liths m^{-2} kyr^{-1}. Accumulation rates calculated by Kinkel et al. (2000) in a core in the Ceara Rise, western equatorial Atlantic, vary between 8.5×10^9 and 45×10^9 liths m^{-2} kyr^{-1}. The Cariaco Basin thus has in general a greater contribution of coccoliths than the core of Kinkel et al. (2000). This can be expected, since the Cariaco Basin is considered to be a higher productivity area than the western equatorial Atlantic.

The accumulation rates can be converted to fluxes, which allows comparison to fluxes measured in sediment traps. Our fluxes correspond to 4.93×10^8 to 1.34×10^{10} liths m^{-2} d^{-1}. Current coccolith fluxes in the mid–equatorial Atlantic measure up to 6.2×10^7 to 7.8×10^8 liths m^{-2} d^{-1}. in the mid–equatorial Atlantic (Steinmetz, 1991). Haidar and Thierstein (2001) measured an average flux of 1.4×10^9 liths m^{-2} d^{-1}.around Bermuda. Our calculated fluxes are within the same order of magnitude.

4.3 Coccolith carbonate

For core 1002C, the carbonate produced by coccolithophores was calculated using the mass estimates in Table 1 (Figure 5). Averagely 23% of the total carbonate in the sediment is produced by coccolithophores over the last 21 kyr, the remaining

carbonate is attributed to foraminifers and pteropods. The highest percentage of coccolith carbonate are reached during the BA and Preboreal.

Baumann et al. (2003) measure in sediment traps of the South Atlantic region a contribution of coccolith carbonate on average 9,1% to the $CaCO_3$ fluxes. Boeckel and Baumann (2004) studied coccolith distribution in surface sediments of the southeastern South Atlantic Ocean; their mass estimations of the coccolith carbonate reveal coccoliths to be only minor contributors to the carbonate preserved in the surface sediments. The mean computed coccolith carbonate content is 17 wt% equivalent to a mean contribution of 23% to the bulk carbonate. Our estimates are thus comparable.

We have to stress that different methodologies are used in the above mentioned papers, which may cause problems of comparison of absolute quantification (Herrle and Bollmann, 2004). However, the comparison of general trends presents no problem.

4.4 TOC, carbonate and rain ratio

TOC increases during interglacial periods after the anoxic transition, with extreme differences are the much higher TOC in the BA and Preboreal, and a minimum TOC during the YD (Figure 6). Carbonate percentage shows opposite fluctuations to TOC. The rain ratio (TOC/Carbonate) is synchronous to TOC. The average organic carbon accumulation is 0.95 g cm^{-2} kyr^{-1} during the Holocene (after 11.7 cal. kyr BP), and 1,26 g cm^{-2} kyr^{-1} before the Holocene. Goni et al. (2003) measured burial fluxes of about 1–1.2 g cm^{-2} kyr^{-1} in a core on the eastern flank, an average comparable to measured fluxes in both core 1002C and PL07-39PC, and also similar to measurements in the deeper sediment traps (1–1.4 g cm^{-2} kyr^{-1}).

The average carbonate accumulation is 5.15 g $CaCO_3$ cm^{-2} kyr^{-1} during the Holocene, and 9.409

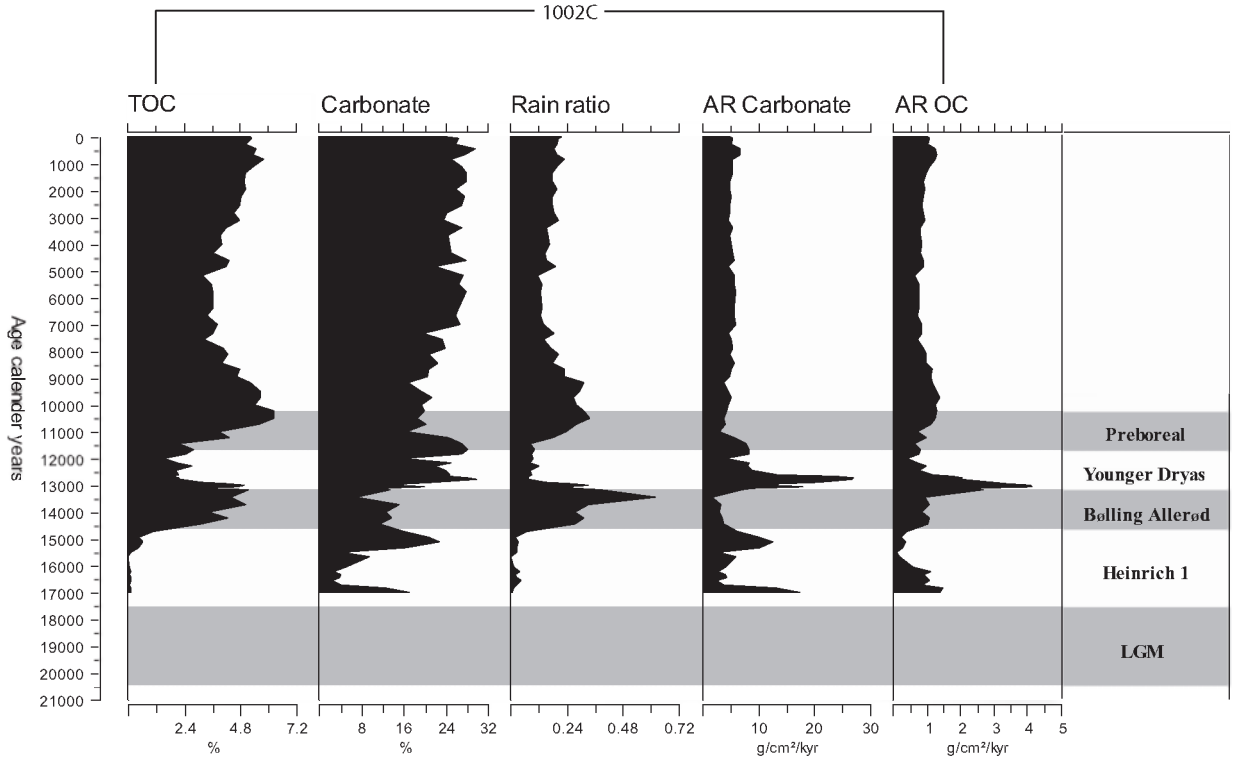

Figure 5 TOC%, carbonate%, rain ratio and accumulation rates for $CaCO_3$ and TOC for core 1002C.

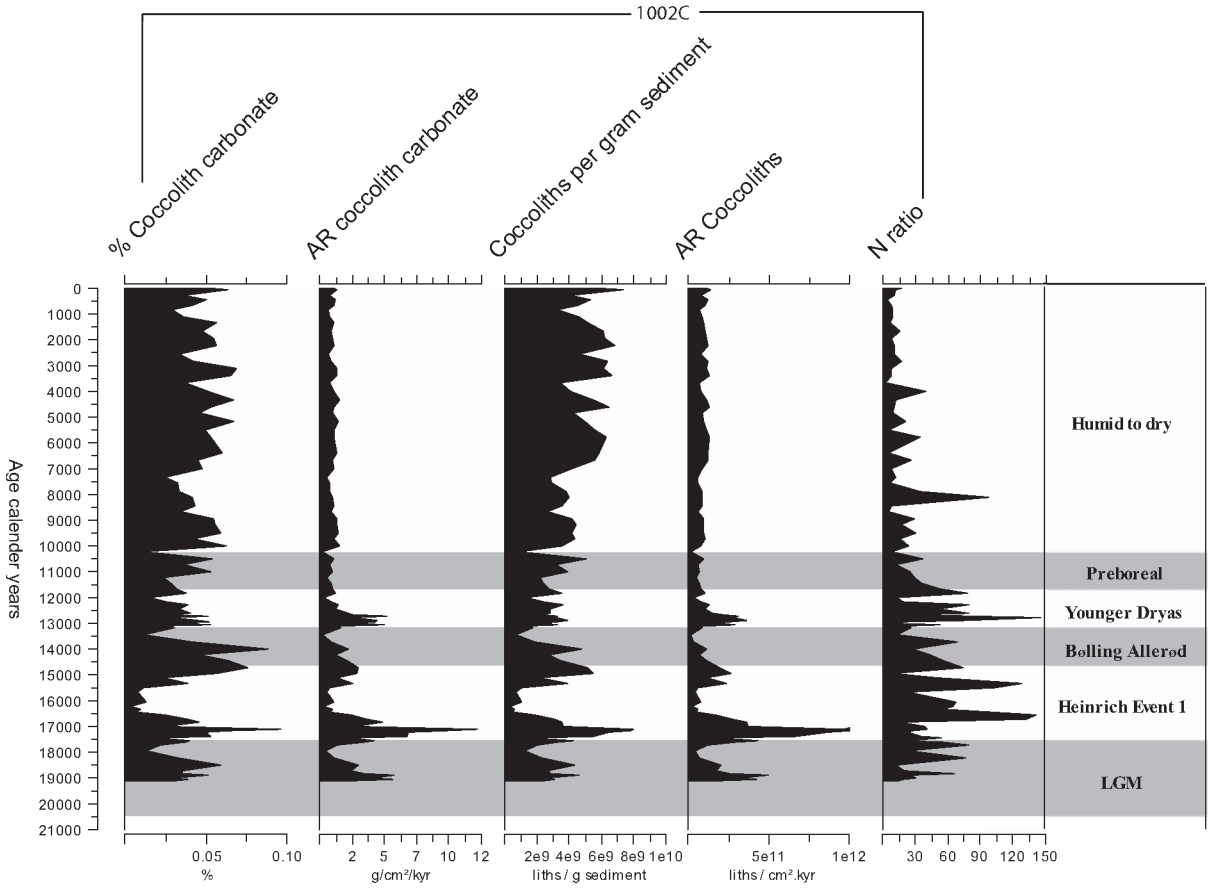

Figure 6 Coccolith carbonate concentrations and accumulations, coccolith concentrations and accumulations and N ratio in core 1002C.

g $CaCO_3$ cm^{-2} kyr^{-1} before the Holocene. There is clearly a decrease in accumulation. Goni et al. (2003) measured burial fluxes of about 3–4 g cm^{-2} kyr^{-1} in a core on the eastern flank. However, our data do not resemble the fluxes measured in deeper sediment traps, only the fluxes in the shallow traps. Such difference has been attributed to various causes; some uncertainty remains about the extent of loss of carbonate through the water column (Smoak et al., 2004).

4.5 Pteropod ratio

The pteropod ratio reaches highest numbers during Heinrich event 1 and Younger Dryas and reaches minima during the Bølling/Allerød and Preboreal (Figure 8).

5. Discussion

Below, the interpretation of the coccolith records will be discussed. This interpretation will be used to link this information to migrations of the ITCZ, leading to a palaeoclimatological reconstruction of the Cariaco Basin.

5.1 Variation between Emiliania huxleyi and Gephyrocapsa oceanica

First and foremost, the variations in relative and absolute abundances of *Emiliania huxleyi* and *Gephyrocapsa oceanica* require an explanation. These bloom–forming species are genetically closely related (Medlin et al., 1996; Fujiwara et al., 2001) and are thought to affect biogeochemical cycles of,

in particular, CO_2 (Tyrrel and Taylor, 1995; Rost and Riebesell, 2004), climate (dimethyl sulphide cloud cover; Malin and Steinke, 2004) and light–scattering albedo (Tyrrell, 1999).

We can express the signal from the two dominant coccolith taxa as GEX (*Gephyrocapsa oceanica* – *Emiliania huxleyi* Index), as an analogue to the CEX of Dittert et al. (1999) (*Calcidiscus leptoporus* – *Emiliania huxleyi* dissolution index), and the CEX' (*Calcidiscus leptoporus* – *Emiliania huxleyi* + *Gephyrocapsa ericsonii* dissolution index) of Boeckel and Baumann (2004), which are analogue indices with different species:

$$GEX = \frac{E.\,huxleyi\%}{(E.\,huxleyi\% + G.\,oceanica\%)}$$

$$CEX = \frac{E.\,huxleyi\%}{(E.\,huxleyi\% + C.\,leptoporus\%)}$$

$$CEX' = \frac{E.\,huxleyi + G.\,ericsonii\%}{(E.\,huxleyi + G.\,ericsonii\% + C.\,leptoporus\%)}$$

We will consider two complementary ways how to explain variations between these two species: one invoking ecological changes and the other dissolution.

5.1.1. Ecology as interpretation

Changes between *E. huxleyi* and *G. oceanica,* as reflected by the GEX ratio, can be linked to changes between an upwelling dominated ecosystem to a river dominated ecosystem. These shifts correspond to an environment with more nutrients, higher SSS and lower SST and reduced water column stability and to an environment with less nutrients, lower SSS and higher SST and higher stratification. Each of these environments can be related to dominance of one of either taxon.

E. huxleyi is often linked with upwelling (Smayda, 1966; Berger, 1976; Stoll et al., 2007). Tyrrell and Merico (2004) postulated that *E. huxleyi* blooms right after the spring diatom bloom when surface irradiances are increasing, and silicate is the limiting factor. The fact that *E. huxleyi* is uninhibited by high light intensities may account for its success at outcompeting other species when it forms gigantic blooms. This same seasonal cycle could be occurring in the Cariaco Basin during the Younger Dryas. Diatom blooms occur during the Younger Dryas, as shown by thick diatom laminations (Peterson et al., 2000b; Piper and Dean, 2002). The increase in the GEX ratio during the Younger Dryas would thus reflect the increase in upwelling, due to the increases of *E. huxleyi*. Coccolith accumulation rates show same trends and major inflection points as the GEX, and would also reflect upwelling conditions (Figure 6).

On the other hand, increases in *G. oceanica* abundances can be related to less saline, warm water, possibly by river runoff. This has been acknowledged in other studies. According to Jordan and Winter (2000) who studied coccolith assemblages off the Coast of Puerto Rico, a nearby region, there can be a relationship between abundances of *Gephyrocapsa oceanica* and inflow of shallow coastal waters. Also Kleijne et al. (1989), Zhang and Siesser (1986) and Knappertbusch (1993) mention blooming of *G. oceanica* at lower salinities than *E. huxleyi.* In the neritic Gulf of Panama it was also found to be the dominant species (Smayda, 1966; Throndsen, 1972). On the other hand, in the oligotrophic Caribbean, it has been only rarely observed (Throndsen, 1972). Weaver and Pujol (1988) mention this species as an indicator of warming and runoff for the Mediterranean. A multiproxy approach of Arabian Sea sediments by Doose-Rolinski et al. (2001) also indicates the ratio between *G. oceanica* and *E. huxleyi* being indicative for warmer and fresher conditions related to higher monsoon activity.

5.1.2 Dissolution as interpretation

In contrast to well–preserved assemblages of planktonic foraminifera, often enriched in delicate forms, even the best preserved recent coccolith assemblages in sediments contain only a small fraction of the taxa found in the water column and are generally dominated by dissolution resistant taxa and as such coccoliths are sensitive indicators of the degree of dissolution (Thierstein, 1980; Roth and Coulbourn, 1982). Coccoliths, therefore, are sensitive indicators of the degree of dissolution in well–pre-

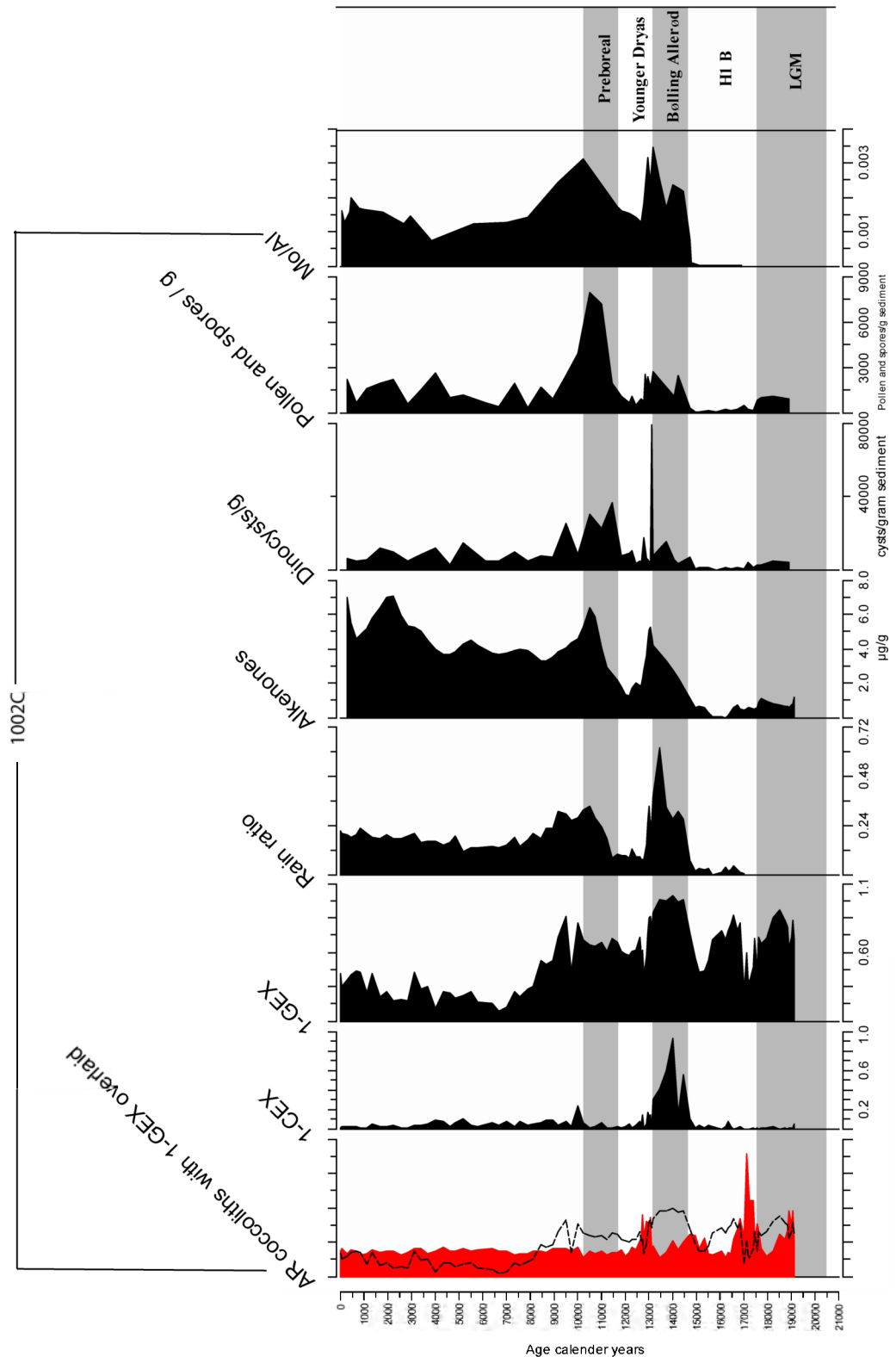

Figure 7 Palaeoecological indicators for core 1002C. GEX and CEX are represented as 1-GEX for better comparison to the other proxies. Also shown are coccolith accumulation rates with 1-GEX overlaid, showing high dissolution concurrent with low accumulation. The alkenone record is from Herbert and Schuffert (2000) and the Mo/Al record is from Lyons et al. (2003).

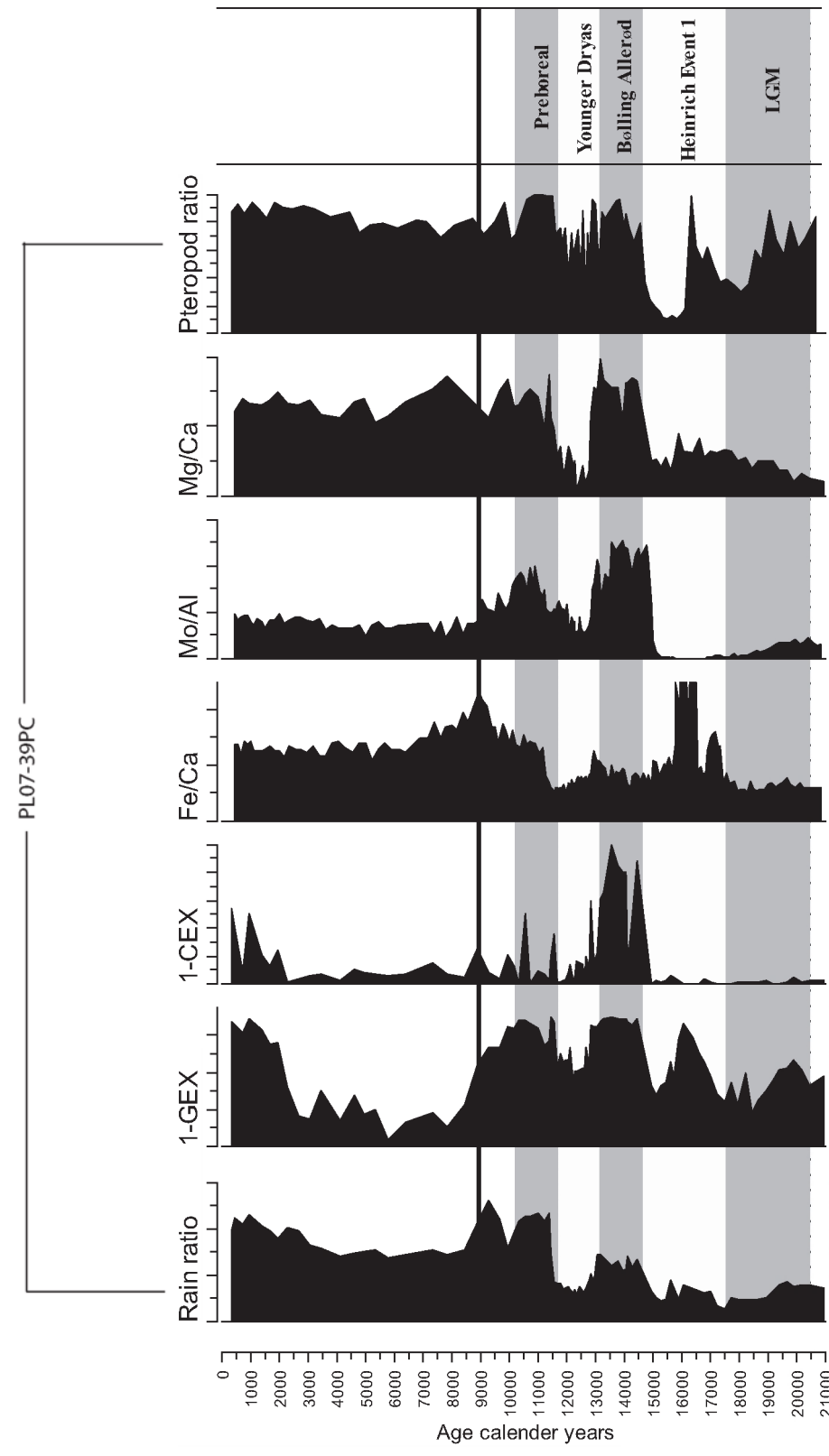

Figuur 8 Palaeoecological indicators for core PL07-39PC. Rain ratio, 1-GEX, 1-CEX, Fe/Ca and Mo/Al (Piper and Dean, 2002), Mg/Ca (Lea et al., 2003) and pteropod ratio (presented in reverse to facilitate comparison). The dark line highlights the lag in the terrigenous record.

served assemblages whereas planktonic foraminifera are sensitive indicators for more dissolved samples (Roth and Berger, 1975).

Carbonate dissolution will have a stronger effect on the delicate *E. huxleyi* than on *G. oceanica*, a fact acknowledged by other studies (e.g. Haidar and Thierstein, 2001). Therefore the GEX will decrease with increasing carbonate dissolution. Selective dissolution of coccolithophores is also reflected in other species such as *G. oceanica*, *C. leptoporus* and *H. carteri* which are dissolution resistant, and *E. huxleyi* and umbelliform species are more delicate. Indeed, clear traces of dissolution are indicated by the CEX–index for example around 14.2 kyr, a period when *G. oceanica* clearly becomes dominant (Figure 7). In our case, CEX is probably not that well applicable since *Calcidiscus leptoporus* abundance is too low to leave a high enough imprint in the fossil record, except for rare occasions when the dissolution is very marked. As far as we can see, extended counting of *C. leptoporus* and *E. huxleyi*, would reveal the same trends as GEX.

This process of dissolution would occur whilst the coccoliths are transported through the watercolumn. Sediment-trap studies in the Cariaco Basin show that major loss of organic carbon and carbonate happens during transport through the water column. About 60 to 70 % of the carbonate is currently lost in the upper 1000 m according to Goni et al. (2003), and 71,5% according to Smoak et al. (2004). Another observation made during the coccolith counts was that in any given sample throughout the section, coccoliths of every species seem to be present with very variable preservation, from pristine to very poorly preserved. This lends support to the idea that varying amounts of dissolution took place during the settling of coccoliths to the seafloor, and less on the seafloor itself, where one would expect a more homogenous effect on the total assemblage. We therefore suggest syndepositional dissolution being the most important process. A possible process that would be occurring would be similar to what Klöcker and Henrich (2006) propose for the Arabian Sea. Low trade-wind activity would cause higher dissolved DIC/low pH anoxic conditions deeper in the basin, and would cause higher carbonate dissolution. High trade-wind activity would result in deep winter mixing, lower DIC/ higher pH conditions deeper in the basin, favouring carbonate preservation. This can again be related to shift between environments (Figure 9).

5.1.3 Multiproxy approach

Different other proxies that have been produced on both cores by other workers, show similar fluctuations to the GEX ratio (Figures 7 and 8). In this paragraph, we want to show that both productivity and preservation can be applied in the interpretation of these records.

The rain ratio, defined as TOC%/$CaCO_3$%, shows similar fluctuations as GEX in both cores (Figure 7 and 8). The rain ratio has previously been considered to be indicative of dissolution (Emerson and Bender, 1981; Jahnke et al., 1994; Dittert et al., 1999). However, this rain ratio can also be related to productivity: higher upwelling rates would then result in higher carbonate production by foraminifera (and coccoliths) and lower input of river related reducing organic matter. On the other hand, these periods with highest accumulations of carbonate are also the periods of lowest dissolution (Bonifay and Giresse, 1992), and this is precisely the case (compare Figure 6 and Figure 7).

We can also note that the aragonitic pteropod abundance index in core PL07-39PC, shows the same trends as our rain ratio and GEX (Figure 8). These higher abundances of pteropods can easily be related with preservation since these aragonite producers dissolve at shallower water depths than calcite due to the higher solubility in seawater (Morse and Arvidson, 2002). The near-absence of pteropods during the BA and Preboreal suggest relatively intense dissolution during these intervals in the Cariaco basin would be difficult to relate to productivity.

A palynological analysis yielded records of dinoflagellate cysts per gram and pollen and spores per gram (unpubl. data), next to alkenone concentrations (Herbert and Schuffert, 2000) (Figure 7). These are all resistant components, which show high concentrations during periods of dissolution. On the other hand, higher pollen and spores concentrations could be related to higher river input, and the higher dinoflagellate cyst abundances could be related to large

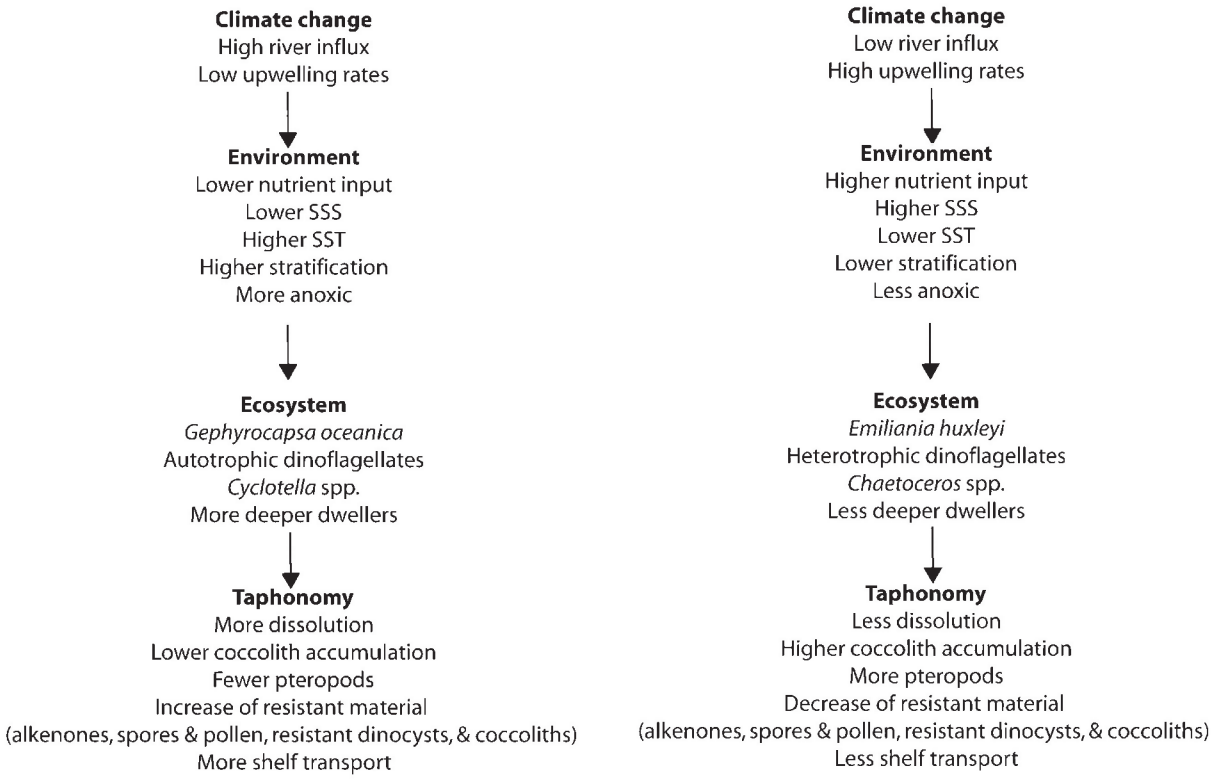

Figure 9 Palaeoecological model explaining variations over the Cariaco Basin.

shifts in the assemblage from an heterotrophic to an autotrophic assemblage, which can be related to changes in the upwelling system. Higher alkenone concentrations can also be related to higher productivity of coccolithophores during these intervals.

We can also note that the change to a *G. oceanica* dominated flora is synchronous to a relative abundance change to centric diatoms, mainly coastal species *Cyclotella* spp., a coastal diatom indicative of low production in warm, stratified, and nutrient-limited waters of the summer and early fall (Barron, et al., 2005). On the other hand, these robust diatoms could also reflect a preservational effect.

Fluctuations of GEX are also synchronous to a Mg/Ca SST reconstruction by Lea et al. (2003) on core PL07-39PC (Figure 8). From an ecological viewpoint, the warming during BA and Preboreal fits well with the relative abundance of *G. oceanica* increasing during these warming events (see 5.1.1). This proxy would be unaffected by dissolution since Mg/Ca ratios decrease with increasing dissolution, and thus Mg/Ca temperatures are lowered.

There is also a good relationship between GEX and the Mo/Al record from PL07-39PC of Piper and Dean (2002) and 1002C of Lyons et al. (2003) (Figure 7 and Figure 8). Higher Mo/Al ratios can be related to elevated anoxic bottom-water conditions (Lyons et al., 2003), which can be related to lower upwelling rates according to our model (Figure 9). This is harder to explain by variations in preservation.

5.1.4. Conclusion

The tentative scheme is summarized in Figure 9. To what extent the fluctuations are caused by dissolution and/or ecology, should be tacklet in future research. However, there is no doubt that productivity and preservation are tightly linked. We assume then that differences in productivity between both

locations could explain dissolution being greater in the PL07–39PC core. Either way, GEX is apparently well-suited as an upwelling proxy.

5.2 Changes in the Lower Photic Zone flora (LPZ)

F. profunda, *T. flabellata* and *H. perplexus* (LPZ) live in well–stratified, low–temperature (<10 °C), nutrient–rich sub–thermocline waters (Okada, 1983). It is generally accepted that these species have an inverse relationship to both productivity and upwelling (Okada and Matsuoka, 1996). Conversely, the surface water can be enriched in nutrients as a result of increased terrigenous materials and shallowing of the thermocline based on changes of the N ratio (abundance of reticulofenestrids (*E. huxleyi* and *Gephyrocapsa* spp. to be little discrepancies.) relative to the LPZ flora) (Flores et al., 2000).

The lower N ratio confirms a higher stratification in the Cariaco Basin during the BA and the Holocene, and a weakening of the stratification (higher N ratio) during the glacial period and YD, where the strong upwelling inhibits photic zone development (Figure 7). These changes in stratification can also be related to the influx of nutrient rich SUW during sea level rise. In the Caribbean, abundance of Lower Photic Zone flora (LPZ) track the presence of the SUW (Kameo, 2002). The lower sea level during the last glacial maximum would have obstructed SUW influx into the basin (Haug et al., 1998) and would have given an additional feedback by delimiting deeper photic zone development. It is clear however, that deeper photic zone development, is not completely dependent of SUW influx since even during the Last Glacial Maximum, when this influx would be non-existent, this deeper photic zone flora is still present (Figure 3).

5.3 Link to migrations of the Intertropical Convergence Zone (ITCZ)

As for an ecological interpretation of the GEX upwelling proxy, any explanation for changes in the upwelling regime on a longer timescale in the Cariaco Basin, would call upon migrations of the ITCZ. When the ITCZ is at a more southern position, the upwelling cycle will be dominant and if the ITCZ is at a more northern position, the river input would be higher. In an ideal model for ITCZ migrations over the Cariaco basin, we would expect to see increases in the upwelling record to go hand in hand with decreases in the terrigenous record and vice versa. As a proxy for terrigenous input we use Fe/Ca (and Ti/Ca which shows similar fluctuations), calculated from data from Piper and Dean (2002), similar to Jennerjahn et al. (2004). This has the advantage that, compared to Ti%, as used by Haug et al. (2001), this corrects for high carbonate inputs, which can be related to marine productivity (carbonate and siliciclastic debris make up major components in the sediment and are inversely related (Piper and Dean, 2002)). So, if we compare the marine upwelling record revealed by GEX (and rain ratio, Mg/Ca), with Fe/Ca (Figure 8), trends are quite similar, except at 9000 year BP, where there seems to be a short lag in the terrigenous record, possibly because of hydrological changes (Jennerjahn et al., 2004), influence by lateral advection (Astor et al., 2003) or eolian transport (Yarincik et al., 2000). Nevertheless, the records suggests synchronous changes in both terrigenous and marine record, linked to migrations of the ITCZ, which enables us to use the GEX as a proxy to trace migrations of the ITCZ.

5.4 Palaeoclimate reconstruction

During the LGM sea level in the Caribbean Sea dropped by about 121 m (Fairbanks, 1989), exposing the Tortuga Bank to the north and restricting influx into the Cariaco basin to a narrow channel to the west of the bank. Because of the relative height of the sill only oligotrophic waters could enter, since SUW influx was obstructed. Thus despite an increase in trade wind intensity during the LGM and Heinrich event 1 (upwelling as shown by GEX), no excessive plankton blooms occurred, the bacterial demand for oxygen was reasonable, the bottom waters were oxic and the accumulating basin sediments are not varved (Peterson et al., 1991, 2000b; Haug et al., 1998; Yarincik et al., 2000).

The interstadial BA would have been characterized by a northern shift of the ITCZ, and thus higher precipitation and lower upwelling (GEX). Higher productivity caused by increased influx of SUW together with

the high river input and less upwelling would cause stratification of the basin (N ratio), and the development of anoxic bottom-water conditions, causing carbonate dissolution (reduction in carbonate accumulation).

During the stadial YD, with its shutdown of NADW formation, a sudden shift of the ITCZ to the south would have occurred, with high upwelling rates (Peterson et al., 1991; Werne et al., 2000). This is confirmed by a high N ratio and GEX. After the YD, a sudden northern shift would induce high river influx during the Preboreal period, which would have been followed by a gradual southern shift of the ITCZ up to the Holocene thermal maximum. After the Holocene thermal maximum, from about 6600 kyr on, the climate would be getting wetter, reflecting a gradual northern shift.

6. Conclusions

Coccoliths are useful paleoecological indicators for migrations of the ITCZ in the Cariaco Basin, as demonstrated by the new GEX index. Both syndepositional dissolution and ecological considerations explain variations in this record. A northern shift of the ITCZ during the BA and Preboreal would alternate southern shifts during the YD and the middle Holocene. There seems to be little discrepancy between the upwelling and terrigenous record.

Additional information

Coccoliths from ODP core 1002C were extracted and counted by Kenneth Mertens at Ghent University, coccoliths from core PL07-39PC were extracted and counted by Matt Lynn at the Rosenstiel School of Marine and Atmospheric Science, Miami (US). The Pteropod ratio was quantified by Hui-Ling Lin Lynn at the Rosenstiel School of Marine and Atmospheric Science, Miami (US). Total organic carbon and carbonate was measured by Mylène Aycard at Université Lille. Interpretations were done by Kenneth Mertens. This chapter has been published in *Journal of Quaternary Science*.

CHAPTER 2

Tracking 40000 years of the North Atlantic Oscillation during the late Quaternary in the southern Gulf of Cádiz using coccoliths, biomarkers and sedimentological proxies

ABSTRACT

A multi-proxy approach based on coccoliths, biomarkers, XRF and grain size data was used for the paleoceanographical analysis of a late Quaternary sequence in the southern Gulf of Cádiz, using gravity core GeoB9064-1. Variations in the records can be related to variations in the North Atlantic Oscillation (NAO). Positive NAO indices are manifested during cold, arid stadials (Heinrich events) and the enhanced aridity results in coarse, hematite rich, carbonate poor deposits. Stronger upwelling results in lower coccolithophore productivity and preservation, with the coccolith assemblages dominated by large *Emiliania huxleyi* (>4 µm). Negative NAO indices are distinct during warm, wet interstadials and result in increased fluvial discharge, as indicated by fine, hematite poor, carbonate rich deposits. The increased fluvial discharge results in enhanced coccolithophore productivity, modulated by precession. *Gephyrocapsa muellerae* dominates the coccolith assemblage during these events. The Ti XRF record displays a strong temperature influence, and spectral analysis of the Ti XRF record reveals two main cycles of 1000 and 580 year cycles, which can be related to NAO variability.

1. Introduction

The Gulf of Cádiz is located in the NE Atlantic between the Iberian Peninsula and Morocco, west of the narrow Strait of Gibraltar (Figure 1). In the east, the Gulf of Cádiz is connected to the Mediterranean Sea, and in the west to the open Atlantic Ocean. Current circulation patterns in the Gulf of Cádiz are characterised by a dynamic oceanographic setting, controlled by exchanges of water masses through the Strait of Gibraltar. The climatological regime in the Gulf of Cádiz is typical for the Mediterranean region and is called the "Mediterranean regime", switching between dry summer and wet winter seasons (Hsu and Wallace, 1976). Over the past decades, changes in this climatological regime in southern Europe can be related to changes in the North Atlantic Oscillation (NAO), with negative NAO indices related to, on average higher atmospheric moisture and warmer temperatures, and positive NAO indices associated with higher aridity and lower temperatures (Hurrell, 1995). These variations are observed over longer periods in the Mediterranean, on centennial (Luterbacher and Xoplaki, 2003) to millennial time-scales (Moreno et al., 2004). In order to further extend the elucidation of this phenomenon, a paleoclimatological reconstruction from the southern Gulf of Cádiz, where paleoclimatological studies are rare (e.g. Marret and Turon, 1994), was undertaken.

Both the terrigenous and biogenic sediment fractions are potential tracers for variations in the NAO index. Terrigenous sediments deposited in the

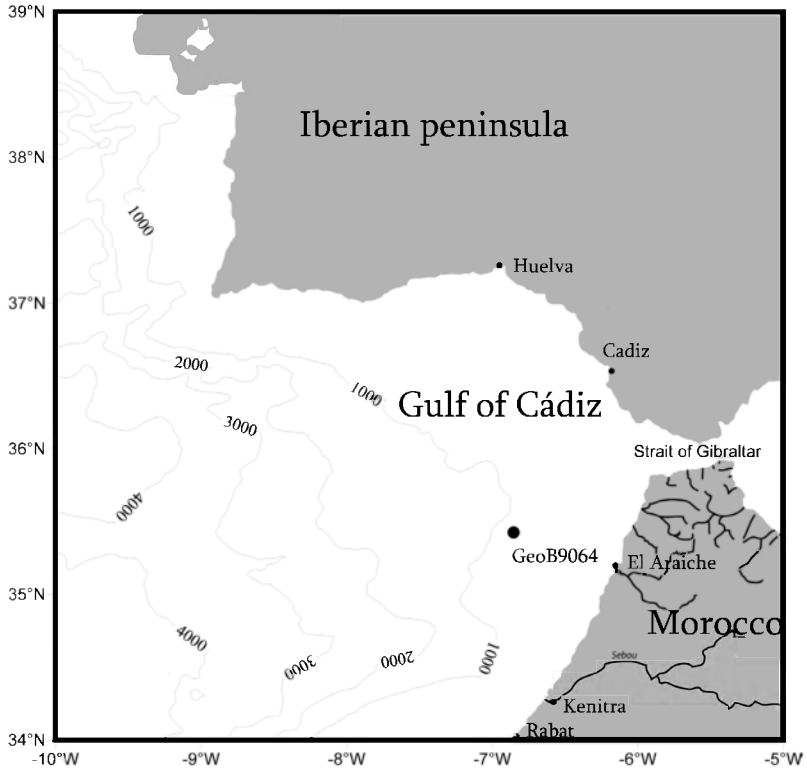

Figure 1 Location of core GeoB9064-1 in the Gulf of Cádiz. Depth contours are every 1000 m. Main rivers in Morocco are drawn. Major coastal cities are marked, together with major Moroccan rivers.

southern Gulf of Cádiz are a mixture of eolian and fluvial components, and have a similar composition as the marine surface sediments off the NW African coast (Holz et al., 2004). The terrigenous sediments are transported from the shelf and are mainly deposited on the slope by low-density turbidity currents and nepheloid sedimentation. These land-derived sediments contain a significant amount of eolian dust due to the proximity of the Saharan desert, and the prevailing strong and stable winds, especially the Levanter and northerly trade winds, which are stronger during summer (Dorman et al., 1995). The rivers draining the Middle Atlas in the Moroccan borderlands are the Sebou and other, smaller rivers (Figure 1). Their plumes spread over a large coastal area (Warrick and Fong, 2004) and the discharge contributes significantly to the deposits. Changes in the NAO disturb the balance between the dry summer season and wet winter season and cause large variations in the amounts of fluvial and eolian sediments transported to the Gulf of Cádiz. Ideal tools to study this terrigenous fraction are XRF (Haug et al., 2001; Kuhlmann et al., 2004) and grain-size analysis (Prins et al., 2000; Stuut et al., 2002; Stuut and Lamy, 2004).

The biogenic fraction of the sediment is restricted to carbonate and organic material: since trade wind related coastal upwelling is restricted to a narrow 5-km band on the shelf (Mittelstaedt, 1991) – a much smaller zone compared to regions in the northern Gulf of Cádiz (Ruiz and Navarro, 2006) and towards the southern Canary Islands (Pelegrí et al., 2005) – there is a general lack of siliceous upwelling indicators such as diatoms in the Gulf of Cádiz (Abrantes, 1988).

Carbonate is produced by coccoliths and foraminifers which are both excellent paleoceanographic tools in the Gulf of Cádiz (Sierro et al., 1999; Colmenero-Hidalgo et al., 2002; 2004; Caralp, 1988; Schönfeld, 2002; Rogerson et al., 2004), and can be used to characterize variations of the NAO along the Iberian margin (Álvarez et al., 2004). The organic matter contains biomarkers such as alkenones and has been used for sea surface temperature (SST) reconstruction (Cacho et al., 2001). Additionally, membrane lipids of Crenarchaeota, i.e. glycerol dialkyl glycerol tetraethers (GDGTs), can be used as independent SST proxy (Schouten et al., 2002; Huguet et al., 2007; Kim et al., 2008).

The aim of this study in the southern Gulf of Cádiz is to

(1) register variations in the terrigenous fraction using XRF and grainsize measurements,
(2) document the variations of the marine productivity by studying relative and absolute abundances of coccolithophores and their biomarkers,
(3) record palaeotemperatures using the $U^{K'}_{37}$ (alkenones), TEX_{86} (GDGTs) indices and morphological data of coccoliths, and
(4) to integrate the micropaleontological, geochemical and sedimentological observations into a model of paleoclimate variations in the southern Gulf of Cádiz linked to variations in the NAO index.

2. Material and methods

Gravity core GeoB9064-1 (35°24,91'N, 6°50,72'W; 702 m water depth, 544 cm recovery) was collected in 2003 during the RV Sonne cruise SO175 to the Gulf of Cádiz (organised by MARUM, Bremen, Germany) (Kopf et al., 2004). The core analysed in this study is located on the Moroccan continental margin, in the El Arraiche mud volcano field in the southern part of the Gulf of Cádiz (Van Rensbergen et al., 2005; Foubert et al., 2008). As the core lies outside the influence of the Mediterranean Outflow plume, which is characterised by strong hydrodynamics (Rogerson et al., 2005), it has the potential to contain a relatively undisturbed palaeoceanographic record compared to cores within or close to the Mediterranean Outflow plume.

2.1 Stable oxygen isotopes and radiocarbon dates

The stable oxygen isotope ($\delta^{18}O$) composition of the planktonic foraminifera *Neogloboquadrina pachyderma* (dextral) was measured with a Finnigan MAT 251 mass spectrometer. Twenty individual tests >150 µm were picked for each measurement. The isotopic composition of the carbonate sample was measured on the CO_2 gas evolved by treatment with phosphoric acid at a constant temperature of 75°C. For all stable oxygen isotope measurements, a working standard (Burgbrohl CO_2 gas) was used, which had been calibrated against PDB by using the NBS 18, 19 and 20 standards. Consequently, all $\delta^{18}O$ data given here are relative to the PDB standard. Analytical standard deviation is about ±0.07 ‰ (Isotope Laboratory, Department of Geosciences, University of Bremen).

Six AMS radiocarbon dates were measured on a mixed assemblage of planktonic foraminifera at Kiel AMS and Poznan Radiocarbon laboratories (Table 1). All dates were converted into calendar years using CalPal with the CalPal-2005-SFCP calibration curve (Weninger et al., 2006). Accumulation rates are calculated by the formula:

$$AR = N * SR * DBD$$

where:
AR = accumulation rate in $kyr^{-1}.cm^{-2}$
SR = sedimentation rate in $cm.kyr^{-1}$
DBD = dry bulk density in $g.cm^{-3}$

The dry bulk density was estimated from wet GRA bulk densities measured on unsplit core sections as they passed through the GRA (gamma-ray attenuation) bulk densiometer using sampling periods and intervals of 2 s and 4 cm, respectively. The gamma-ray source was 137 Cs. The wet GRA bulk densities were compared (calibrated) with bulk densities measured on discrete samples (classical moisture and density measurements (MAD): measuring wet mass, dry mass and dry volume (gas pycnometer) of discrete samples).

Table 1 Radiocarbon dates for sediment core GeoB9064-1 from the Moroccan margin.

Depth (cm)	Lab number	^{14}C age (BP)	STD (yr)	CalAge p (68%) (cal BP (0=AD1950))	STD (yr)
4	Poz-20282	2095	30	2070	50
74	KIA-10065	9665	55	11020	140
169	KIA-13060	12660	80	15000	180
289	KIA-23840	23440	180	28220	220
399	KIA-29420	29020	315	34190	550
524	KIA-35660	35260	625	40720	900

2.2 Grain-size analysis and end-member modelling

In order to separate the terrigenous sediment fraction for grain-size analysis, organic carbon and $CaCO_3$ were carefully removed using respectively H_2O_2 (30% at 85°C) and HCl (10% at 100°C). Microscopic analyses revealed that this method successfully removed all biogenic constituents. Grainsize analyses of the bulk sediments were carried out with a Malvern Instruments Mastersizer 2000 (Malvern laser particle sizer), equipped with a 300-mm focal length lens. A sample of ~500 mg was suspended in demineralized water by stirring. A subsample was taken from this suspension with a 10 ml pipette and introduced into the sample cell of the laser particle sizer. All samples were suspended in the sample cell by stirring and ultrasonic dispersion for 15 s before analysis. The measured size distributions in the range 0.26–2046 µm were analyzed in 66 size classes. The terrigenous sediment fraction from the Southern Gulf of Cádiz is relatively fine-grained (<170 µm), therefore the number of input variables for the end-member model is reduced from 66 to 47 size classes in the range 0.29–170 µm. End-member modelling of compositional data (Weltje, 1997) can be applied to the measured grain-size classes to recognize and separate distinct patterns (end-members) in the grain-size distributions of the terrigenous fraction. To estimate the minimum number of end-members required for a satisfactory approximation of the data, the coefficients of determination were calculated. The coefficient of determination represents the proportion of the variance of each grain-size class that can be reproduced by the approximated data. This proportion is equal to the squared correlation coefficient (R^2) of the input variables and their approximated values (Weltje, 1997; Prins and Weltje, 1999).

2.3 Organic carbon and carbonate analysis

For the analysis of the total organic carbon (TOC) content of the sediments, 25 mg of the sample material was decalcified with 6 N HCl, dried on a hot plate at 80°C and measured in a Heraeus-CHN elementary analyzer. The carbonate contents were calculated from the total carbon (TC) content, measured with the CHN analyzer on untreated samples, as:

$$CaCO_3 = (TC - TOC) * 8.333$$

with a standard deviation of <2% of the measured value for TOC as well as for TC measurements.

2.4 XRF analysis

XRF data were measured directly at the core surface of the working half of the core using the Avaatech XRF core scanner installed at the MARUM at the University of Bremen (Röhl and Abrams, 2000). All XRF scanner measurements were carried out with a X-ray tube voltage of 20 kV which allows the analysis of elements from K through Sr. Element intensities of Fe, Ti and Ca were analysed at 1 cm resolution. A 30 second count time was used for the measurements together with an X-ray current of 0.087 mA. The acquired XRF spectrum for each measurement was processed by the KEVEX™ software Toolbox©. The resulting data are presented as element intensities in counts per second (cps).

Spectral analyses have been carried out using the Blackman-Tukey (BT) Method with a Welch Window (Blackman and Tukey, 1958). It is based on the standard Fourier transform of a truncated and tapered (to suppress spectral leakage) autocovariance function. Linear interpolation of the record was necessary before BT spectral analysis. Significance levels were set at 95% confidence intervals.

2.5 Lipid extraction

Wet sediment samples were freeze-dried for biomarker-analysis to circumvent significant losses (sensu McClymont et al., 2007). After homogenization, the sediments (8-13 g dry weight) were extracted three times for five min. by using a mixture of dichloromethane:methanol (9:1) with a DIONEX accelerated solvent extractor (ASE 200) at a temperature of 100°C and a pressure of $7.6x10^6$ Pa. Extracts were dried over a sodium sulphate column. The total extract was chromatographed in several fractions and activated Al_2O_3 was used as stationary phase. Hexane/DCM (1:1) was used to elute the ketone fraction containing the alkenones. Methanol:dichloromethane (1:1) was used to elute the polar fraction containing the glycerol dialkyl glycerols tetraethers (GDGTs).

2.5.1 Alkenone analysis

Alkenone fractions were manually injected on a Agilent 6890N gas chromatograph equipped with a 50 m CPSil CB column (internal diameter: 0.32 mm, d_f = 0.12 µm). Helium was used as a carrier gas. Initial temperature was 70°C, which was increased at a rate of 20°C/min to a temperature of 200°C and then to 320°C at a rate of 3°C/min. The peak areas of $C_{37:2}$ and $C_{37:3}$ alkenones were determined by GC analysis. The alkenone unsaturation index $U^{K'}_{37}$ was calculated from $U^{K'}_{37} = (C_{37:2})/(C_{37:2} + C_{37:3})$, where $C_{37:2}$ and $C_{37:3}$ are areas of the di- and triunsaturated C_{37} methyl alkenones (cf. Prahl and Wakeham, 1987). The $U^{K'}_{37}$ values were converted into SST values by applying the global core top calibration ($U^{K'}_{37}$ =0.033 x SST + 0.044) of Müller et al. (1998). Saponification of selected alkenone fractions was performed to check if there was co-elution of alkenones with other components, but $U^{K'}_{37}$ remained the same. An internal standard, anteiso C_{22} (concentration 29.8 µg/ml), was added at the appropriate time to determine the concentrations of alkenones.

2.5.2 GDGT analysis

Aliquots of polar fractions were blown dry under a stream of nitrogen, redissolved in hexane/isopropanol (99:1; v/v), and filtered through 0.45 µm PTFE filters. The GDGT analysis was performed by high performance liquid chromatography/atmospheric pressure positive ion chemical ionization mass spectrometry (HPLC/APCI-MS). The conditions for HPLC-MS analysis are as described in Hopmans et al. (2000) and Schouten et al. (2007). Quantification was achieved by integration of the peak areas in the respective [M+H]+ and [M+H]++1 (i.e. protonated molecule and isotope peak) traces of the GDGTs. TEX_{86} values were calculated according to the formula given by Schouten et al. (2002). A known amount of the C_{46} GDGT internal standard was added for the determination of the concentration of GDGTs (cf. Huguet et al., 2006b). In addition, the BIT index (Branched and Isoprenoid Tetraether index) based on the relative abundance of non-isoprenoidal GDGT derived from bacteria in soils, was used for the quantification of the relative fluvial input of terrestrial organic matter (Hopmans et al., 2004).

2.6 Coccoliths

A total of 109 samples at a resolution of 5 cm were studied and cover the entire sequence. The samples were prepared following the methodology of Okada (2000). At least 400 specimens were determined and counted per slide with a JEOL 6400 Scanning Electron Microscope (SEM). *Florisphaera profunda* and *Gladiolithus flabellatus* were not counted due to the difficulties of identification of not very well preserved specimens. Species that could not be determined to genus level were counted as Indeterminate spp. The effects of dissolution may also lead to difficulties distinguishing *E. huxleyi* coccoliths from *G. muellerae* coccoliths, but the use of scanning electron microscopy overcomes this problem (Findlay and Flores, 2000).

Absolute abundances were calculated using the formula of Lototskaya (1999):

where:

$$N = \frac{V_1 * S_f * N'}{V_2 * n_s * S' * m_{DBD}}$$

N = absolute abundances of coccoliths g^{-1} dry sediment

V_1 = volume of tapwater used for filtering

S_f = effective filtration area
N' = number of counted coccoliths
V_2 = volume of the solution;
n_s = number of counted square fields
S' = area of the field
m_{DBD} = welght of a bulk sediment sample (in g)

The number of coccoliths was converted into Coccolith-carbonate contents based on mean estimates of coccolith masses (Young and Ziveri, 2000). Since the mass of coccolith species varies considerably, size calibrations are necessary (Baumann, 2004). Multiple measurements of the length of the most important taxa were analyzed as described by Baumann et al. (2003), and were converted into mass estimates using the method of Young and Ziveri (2000) (Table 2). The amount of carbonate produced by coccolithophores was calculated using the mass estimates in Table 2.

For the biometric analysis, the method described by Colmenero-Hidalgo et al. (2002) was followed. One hundred specimens of *Emiliania huxleyi* were randomly chosen in each sample, and distal shield lengths were measured under SEM, at a magnification of 20000x. The measurements were performed with an accuracy of one tenth of a micrometer.

3 Results

All raw data are included as Supplementary data.

3.1 Chronostratigraphic framework

To construct an age model for core GeoB 9064-1, the stable oxygen isotope and Ti XRF record were tuned to the GISP 2 isotope record and the radiocarbon dates using Analyseries 2.0 (Paillard et al., 1996) (Figure 2). One aberrant age (28220 cal. yrs BP at 289 cm) can be attributed to reworking of foraminifera (e.g. Broecker et al., 2006) and can be related to Heinrich Event 2. This age was therefore discarded. A visual inspection of the foraminifer assemblage confirmed this observation. The age-depth curve can be compared with the age-depth curve from core M39008 situated in the northern Gulf of Cádiz (Cacho et al., 2001) (Figure 2) and sedimentation rates were calculated.

The record ranges from 41300 to 1600 cal. yrs BP and spans the Last Glacial Maximum, Bølling/Allerød (BA), Younger Dryas (YD) and Heinrich event (HE) 1 to 4 (Figure 2). The sedimentation rates vary between 8 and 34 cm/kcal years, and are lower than sedimentation rates of core M39008 (Figure 2). Given the range of sedimentation rates, the coccolith sampling interval yields a temporal sampling resolution between 200 and 800 yrs, whilst the resolution for XRF analysis results in a temporal resolution between 41 and 256 yrs.

3.2 Grainsize analysis

The median grain size varies between 6 and 12 µm (Figure 3). There is relatively fine-grained mud deposition during the Holocene and BA, and relatively coarse-grained during the glacial period, and more particularly during HEs, which confirms observations off Senegal (Mulitza et al., 2008) and off Mauritania (Tjallingii et al., 2008). Coefficients of determination (r^2) can be plotted against grain size for models with 2–10 end-members (Figure 4 B–C). The two end-member model (r^2_{mean}=0.56) shows low r^2 (<0.6) for the size classes 8–16 µm and >56 µm. The three end-member model (r^2=0.77) shows low r^2 for the size range >85 µm only. However, for the choice of the number of end-members, the coarse end (>85 µm) can be ignored because it comprises less than 1.2% weight of the mass of the samples (Figure 4 A). The three end-member model provides the best compromise between the number of end-members and r^2.

The grain-size distributions of the three end-members show that all end-members have a clearly defined dominant mode (Figure 4 D). End-member EM3 has a modal grain size of ~5.8 µm. End-member EM2 has a modal grain size of ~ 16 µm. End-member EM1 has a modal grain size of ~ 25 µm. The downcore record of the relative contributions of the end-members shows that end-member EM1 varies between 0 and 28%, EM2 between 16 and 52% and EM3 between 42 and 84% (Figure 3).

3.3 % Carbonate, % TOC, % Terrigenous and accumulation rates

The TOC content varies between and 0.36 and

Table 2 Specimens measured, lengths, shape factors k_s (Young and Ziveri, 2000), and masses of selected species

Species	Individuals measured	Length (µm)	k_s	Mass (pg)
Emiliania huxleyi	5756	3.65	0.020	2.62
Gephyrocapsa muellerae	5608	3.41	0.050	5.35
Calcidiscus leptoporus	1509	6.95	0.080	72.51
Coccolithus pelagicus	247	10.52	0.060	189.10
Gephyrocapsa oceanica	305	4.93	0.050	16.14
Umbellosphaera spp.	130	5.71	0.015	7.54
Calciosolenia spp.	86	2.75	0.035	1.98
Helicosphaera spp.	432	9.13	0.050	102.85
Syracosphaera pulchra	218	5.79	0.030	15.70

0.68% and the carbonate content varies between 24 and 42% (Figure 5). Since no biogenic silica is present, % Terrigenous can be estimated from % Carbonate and % TOC using the following equation: % Terrigenous = 100% - % Carbonate + % TOC. The terrigenous fraction varies between 58 and 75%. % Carbonate and % TOC show relatively similar fluctuations with decreases during HE and increases during interstadials, whereas % Terrigenous shows opposite fluctuations. Accumulation rates of all three components show similar fluctuations, and accumulation rates of both organic carbon and carbonate show correspondences to their concentrations, whereas for terrigenous accumulations, there are obvious discrepancies with % Terrigenous (Figure 5).

3.4 XRF analysis

The Ca record (cps/total counts) is comparable to the % Carbonate record, and shows a linear relation to % Carbonate (% Carbonate = 83.40 * Ca – 0.945, R^2 = 0.92) (Figures 5 and 6). This is similar for the Fe record, which shows a good correlation to % Terrigenous (% Terrigenous = 90.70 * Fe + 20.34, R^2 = 0.91) (Figure 6). The measured relative iron intensity (counts/s) reflects the original iron deposition, as the X-ray fluorescence analysis detects Fe atoms irrespective of their oxidation state. Moreover, the Ti record shows a nearly identical pattern as the Fe record (Figure 5), so there is no evident indication for diagenetic alteration (Kuhlmann et al., 2004). Ca and Ti records show opposite fluctuations. The Ti record shows distinct maxima during HEs. The Ti record also shows very similar fluctuations as the $U^{K'}_{37}$ SST reconstruction (Figure 5) and a close linear regression ($U^{K'}_{37}$ SST= -803.3 * Ti + 32.61, R^2=0.775) (Figure 6), when removing two outliers. As the continuous Ti-record evidences of no strong diagenetic alteration, this record was used for time series analysis.

3.5 Biomarker analysis

3.5.1 Concentrations and accumulations of alkenones and marine GDGTs, and BIT index

Alkenone concentrations vary between 0.06 and 0.96 µg/g sediment. High values of alkenone concentrations are recorded during the warm interstadials while during cold stadials the concentrations decrease (Figure 7). Minimum alkenone concentrations are recorded during HEs. Marine GDGT concentration varies between 0.2 and 1.1 µg/g. Fluctuations are similar to alkenone concentrations, with decreases during HEs. Accumulation rates of both biomarkers show similar fluctuations as concentrations. The BIT index is always < 0.08 and thus indicates a relatively low amount of terrestrial organic matter (Hopmans et al., 2004).

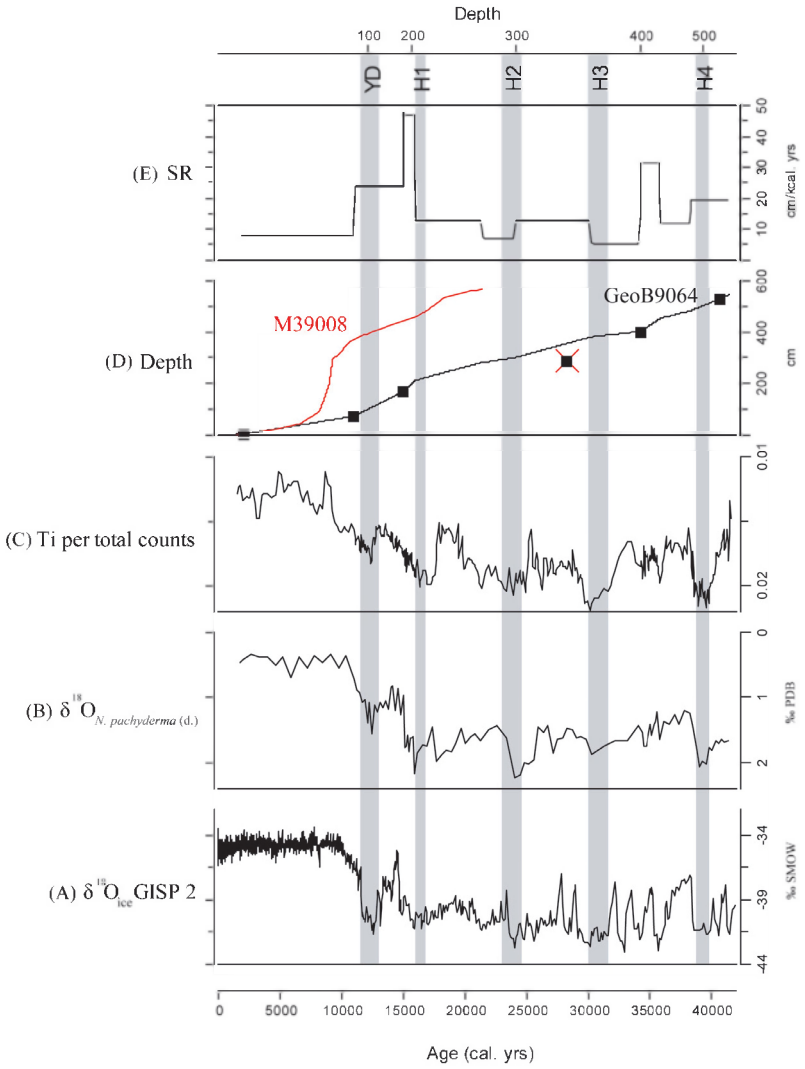

Figure 2 The chronostratigraphy of core GeoB9064-1 established by tying the (b) stable oxygen isotope record measured on *N. pachyderma* (dextral) and (c) Ti XRF counts per total counts to (a) the GISP 2 $\delta^{18}O_{ice}$ record, using the (d) Age-depth curve of core GeoB9064-1 compared with the northern Gulf of Cádiz (M39008) with radiocarbon dates (squares). One date is discarded because of reworking of Foraminifera, and is shown crossed out in the figure. (e) Sedimentation rate (SR) (cm/kcal. years). HEs are shaded.

3.5.2 $U^{K'}_{37}$ and TEX_{86} temperature reconstruction

The obtained $U^{K'}_{37}$ SST curve (Figure 8) shows a relatively similar trend to the stable oxygen isotope data (Figure 6 A, R^2=0.76). Temperatures are relatively stable during the Holocene, while abrupt shifts occurred during the glacial period. SST oscillations during the Holocene are smaller than 2°C (19–21°C) and are close to the present-day annually mean SST of 18.9°C, while reconstructed SSTs of the glacial period range between 11 and 18°C. Termination I starts with a temperature increase of 4°C, is interrupted by a distinct drop of 4°C during the YD, until it reaches a peak of 21°C (10°C total warming). The TEX_{86}-derived SST is slightly higher than those reconstructed with $U^{K'}_{37}$. However both SST records reveal the same temperature trend (R^2=0.73). The TEX_{86}-derived SST shows an even stronger correlation to the

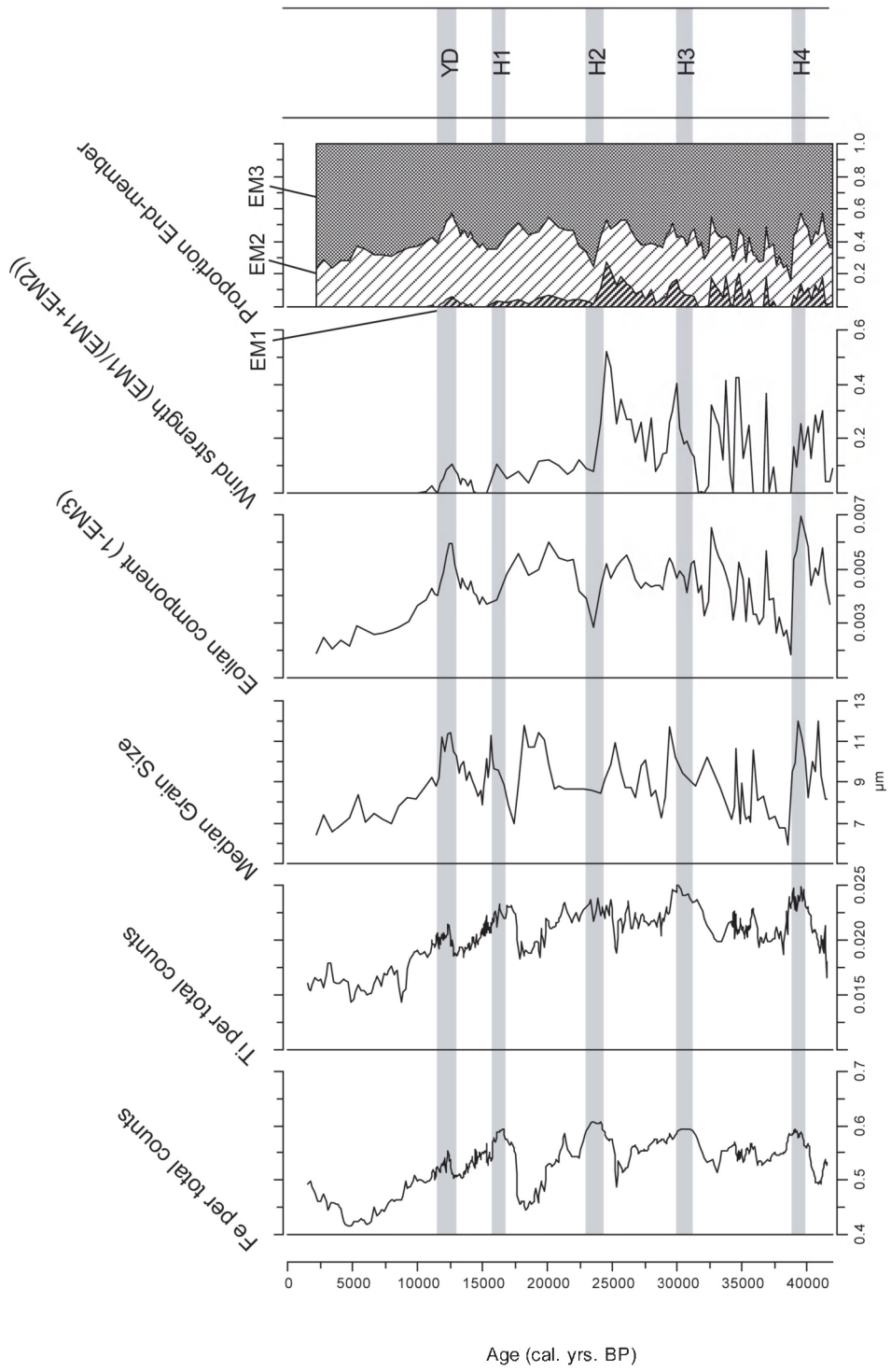

Figure 3 Terrigenous proxies: Fe (XRF), Ti (XRF), median grain size, eolian component and downcore variation of the three end-members.

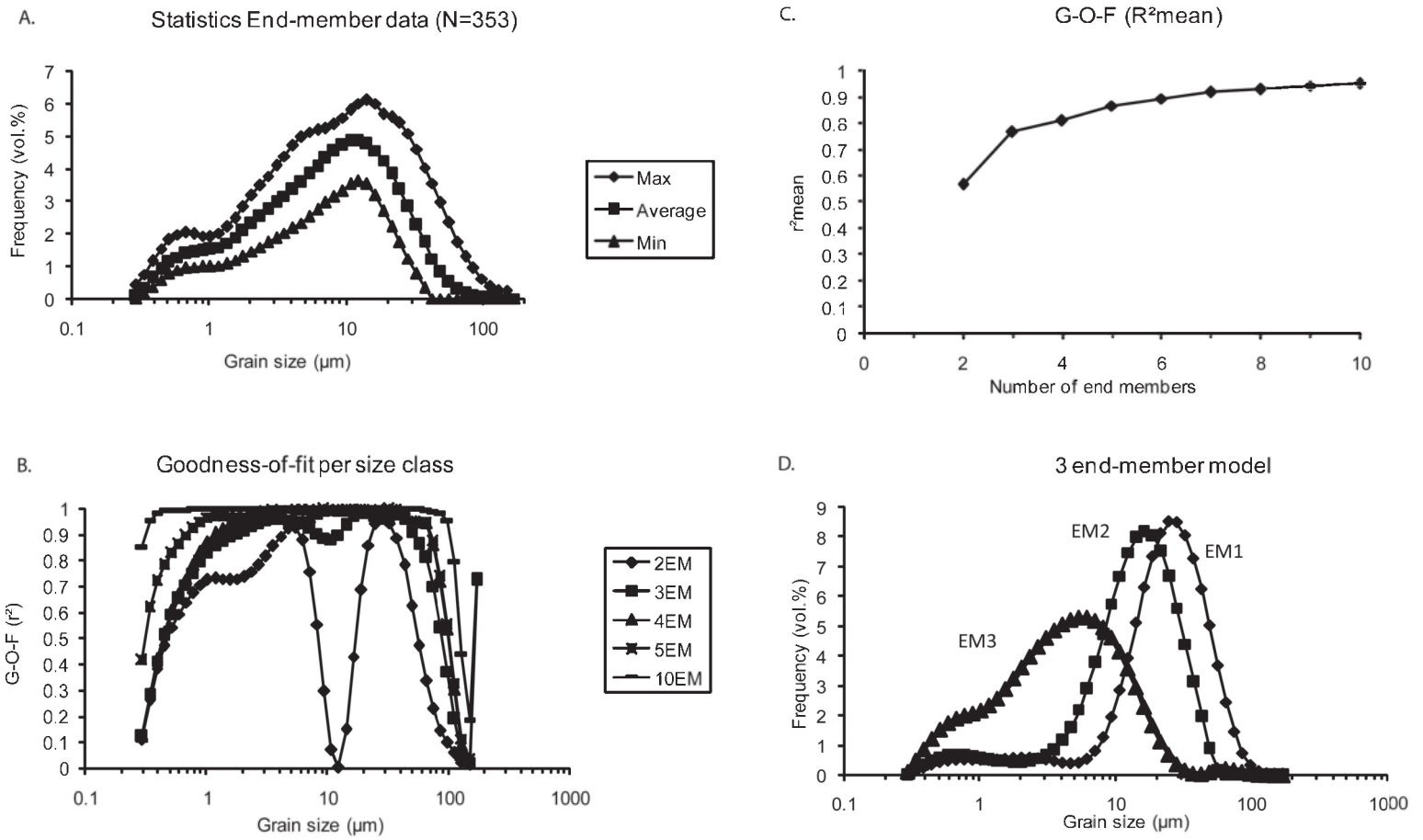

Figure 4 End-member modeling results of core GeoB9064-1. (A) Summary statistics of input data (grainsize distributions); maximum, mean and minimum frequency recorded in each size class. (B) Coefficients of determination (r^2) for each size class of models with 2-10 end-members. (C) Mean coefficient of determination (r^2_{mean}) of all size classes for each end-member model. (D) Modelled end-members of the terrigenous sediment fraction of sediments from the southern Gulf of Cádiz.

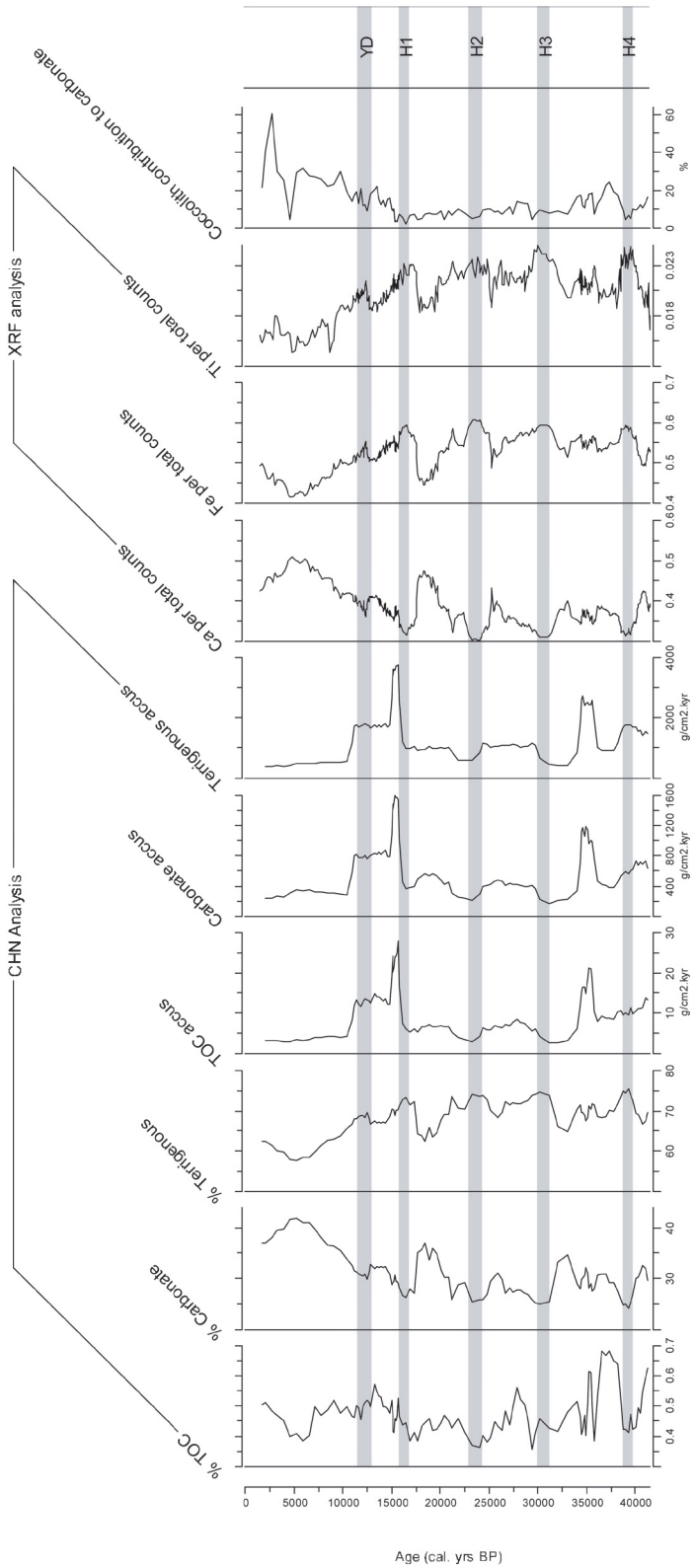

Figure 5 % TOC and % Carbonate as measured by geochemical analysis and Ca, Fe and Ti per total counts as measured by XRF analysis.
% Terrigenous is calculated from % TOC and % Carbonate.

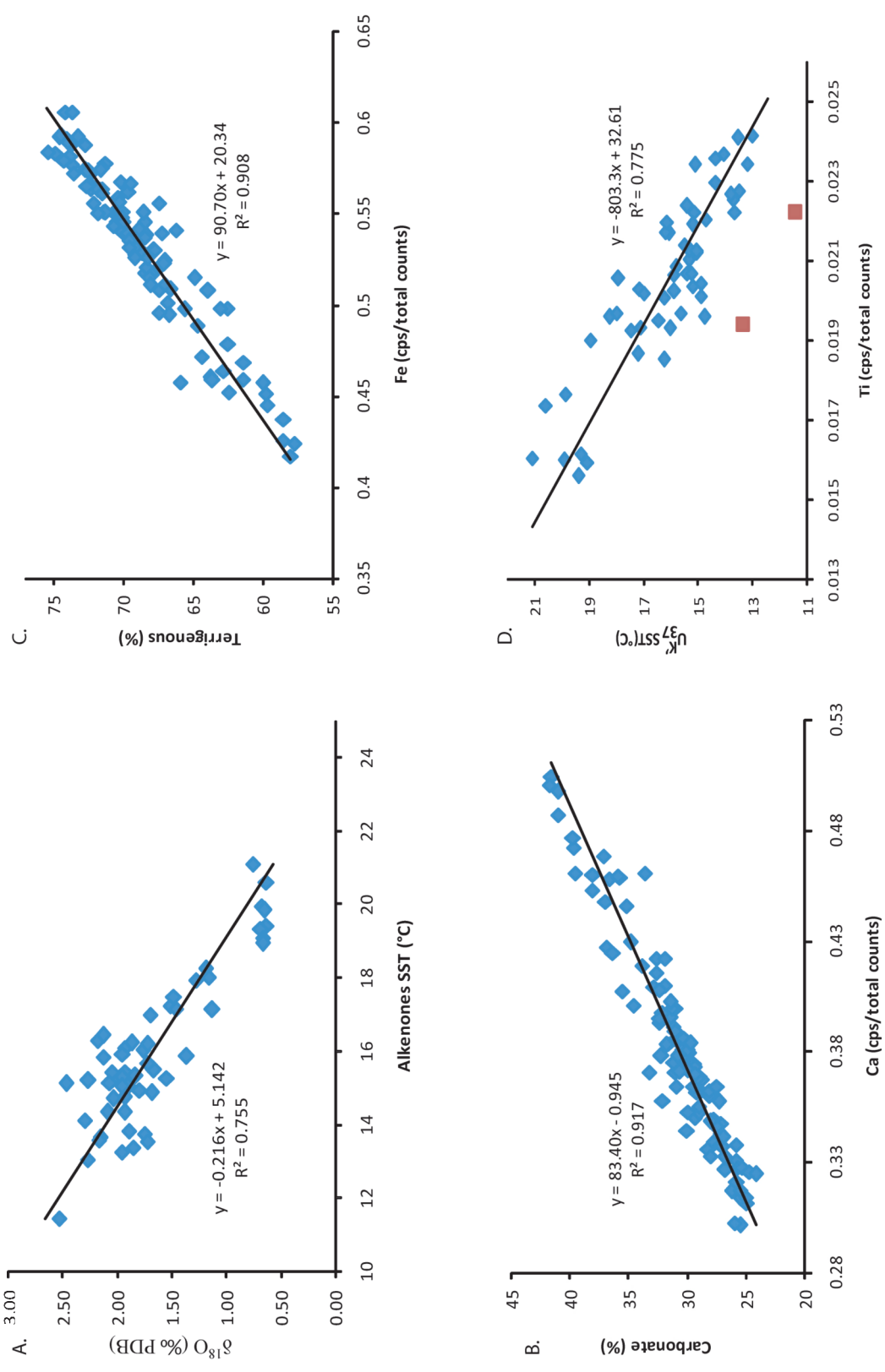

Figure 6 Linear regression between (A) $\delta^{18}O$ (‰ PDB) and $U^{K'}_{37}$ SST (°C), (B) Ca per total counts (XRF) and % Carbonate, (C) Fe per total counts (XRF) and % Terrigenous and (D) Ti per total counts (XRF) and $U^{K'}_{37}$ SST (°C) (the two removed outliers are shown by squares).

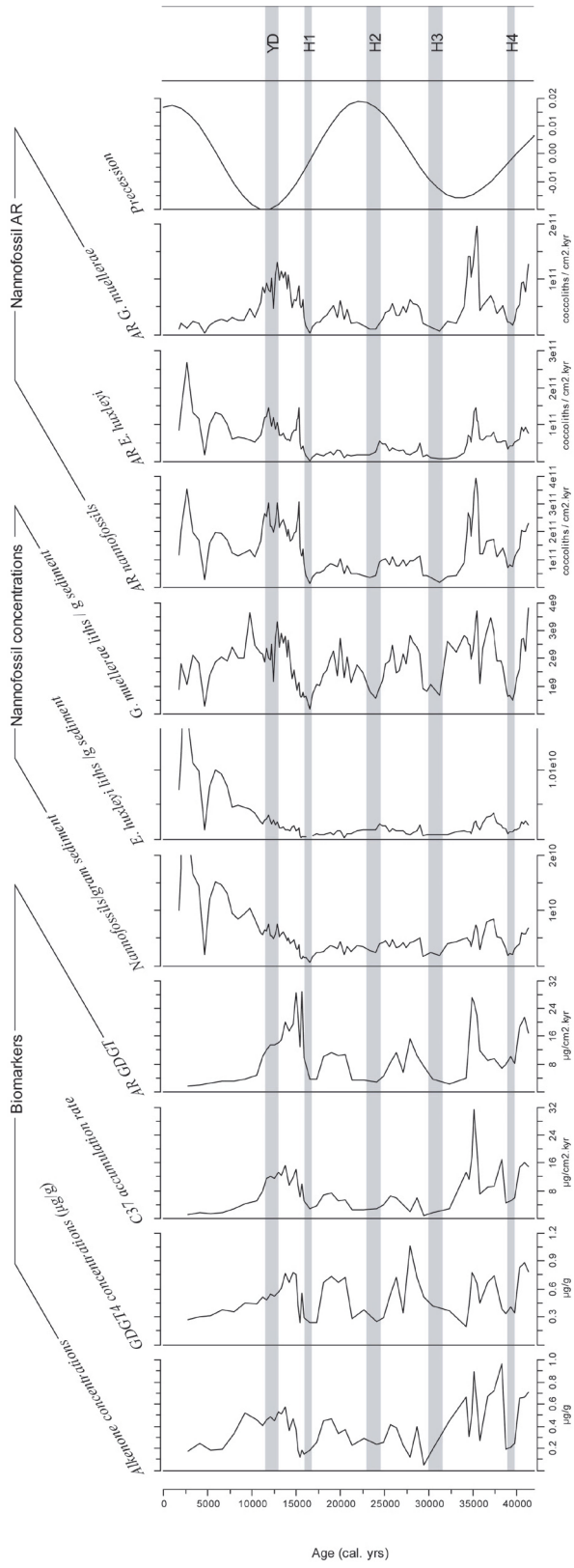

Figure 7 Biomarker concentrations and accumulation rates (AR) and nannofossil concentrations and accumulations. Precession as calculated from Berger and Loutre (1978).

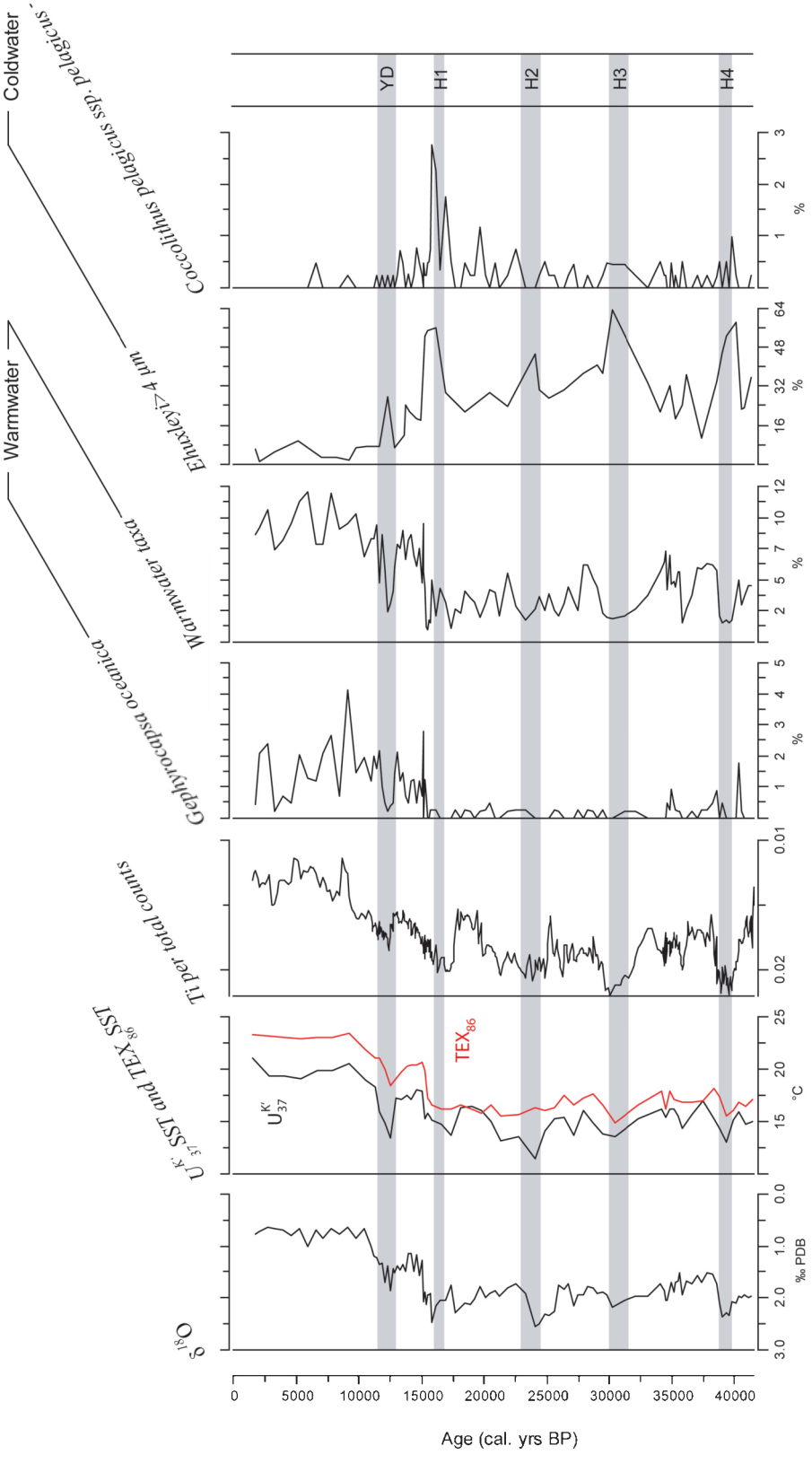

Figure 8 Temperature proxies: stable oxygen isotopes, TEX_{86} SST, $U^{K'}_{37}$ SST, reverse Ti (XRF), relative abundances of *Gephyrocapsa oceanica*, warm-water taxa, *Emiliania huxleyi* (>4 µm) and *Coccolithus pelagicus pelagicus*.

stable oxygen isotope data (R^2=0.83) than alkenone-derived SST. Changes in TEX_{86}-derived SST during the Holocene are smaller than 2°C (21–23°C), while SST of the glacial period range between 15 and 21°C.

3.6 Coccoliths

3.6.1 Coccolith relative abundance data

The assemblages in the area off Northwest Africa are typical for temperate water conditions, dominated by placolith-bearing species such as *Emiliania huxleyi*, *Gephyrocapsa muellerae* and *Calcidiscus leptoporus*. There is a minor contribution of subtropical assemblages which are characterized by *Discosphaera tubifera*, *Rhabdosphaera clavigera*, *Umbellosphaera* spp. and *Syracosphaera* spp.

Thirty-six coccolith species were identified, but only two species reach relative abundances of more than 15 % (Figure 9): *Emiliania huxleyi* (15–76%) and *Gephyrocapsa muellerae* (3–66%). The latter corresponds to the "*Gephyrocapsa* cold" morphotype of Bollmann (1997). Other important species are *Calcidiscus leptoporus* (max. 6%). Species with low relative abundances are *Gephyrocapsa oceanica* (max. 4%), *Umbellosphaera* spp. (max. 3%), *Syracosphaera* spp. (max. 3%), *Helicosphaera wallichi* (max. 3%), *Umbilicosphaera sibogae* (max. 3%), *Coccolithus pelagicus* ssp. *pelagicus* (max. 3%), *Oolithotus antillarum* (max. 3%), *Oolithotus fragilis* (max. 2%), *Gephyrocapsa ericonii* (max. 2%), *Helicosphaera carteri* (max. 2%), *Syracosphaera pulchra* (max. 2%), *Braarudosphaera bigelowii* (max. 1%), *Acanthoica* spp. (max. 1%), *Calciosolenia brasiliensis* (max. 1%), *Umbilicosphaera foliosa* (max. 1%) and *Coccolithus pelagicus* ssp. *braarudii* (max. 1%). Species of relative abundances of less than 1% are *Rhabdosphaera clavigera*, *Syracosphaera anthos*, *Discosphaera tubifera*, *Calciosolenia murrayi*, *Reticulofenestra sessilis*, *Acanthoica biscayensis*, *Syracosphaera lamina*, *Reticulofenestra parvula*, *Helicosphaera pavimentum*, *Coronosphaera mediterranea*, *Hayaster perplexus*, *Pontosphaera* spp., *Pontosphaera syracusana*, *Scyphosphaera apsteinii*, *Syracosphaera ampliora*, *Syracosphaera molischii*, *Pontosphaera discopora*, *Umbilicosphaera hulburtiana*, *Pontosphaera multipora* and *Neosphaera coccolithomorpha*, presently known as alternate life-stage of *Ceratolithus cristatus* (Cros et al., 2000). All the determined species are listed in Appendix I.

On average, 10% of the coccoliths could not be determined to genus level because of dissolution, fragmentation or overgrowth and were counted as indeterminate spp. Coccolith preservation is moderate. Following the classification of Roth (1983), etching and overgrowth varies from minimal to moderate.

The dominant taxa *E. huxleyi* and *G. muellerae* are characterized by very rapid abundance changes in the investigated interval. Increases in relative abundances of *E. huxleyi* are synchronous with decreases of *G. muellerae* and vice versa (Figure 9). The biometric analysis shows that HE are characterized by peaks of large *E. huxleyi* (>4 µm) (Figure 10). *C. leptoporus*, *Umbilicosphaera* spp., *O. fragilis* and *Umbellosphaera* spp. have been grouped as warm water taxa (Colmenero-Hidalgo et al., 2004), as well as *D. tubifera* and *R. clavigera* (Winter et al., 1994). *G. oceanica* has been associated with warming in the Mediterranean (Weaver and Pujol, 1988) and the Arabian Sea (Doose-Rolinski et al., 2001), and shows similar fluctuations as the warm-water taxa (Figure 8). *Coccolithus pelagicus pelagicus* has been associated with cold-water conditions (Parente et al., 2004) and shows a significant peak during H1 (Figure 3). HEs are also characterized by peaks of *Helicosphaera* spp. (Figure 9), indicating cold-water conditions.

About ~1% of the coccoliths are reworked, mainly of Cretaceous age. A maximum of 8% is noted during H1 (Figure 9). The reworked Cretaceous coccoliths indicate erosion and redeposition of material originating from the Moroccan shelf or coastal outcrops and neighbouring mud ridges and mud volcanoes (Ferreira et al., 2008).

3.6.2 Coccolith concentration and accumulation rates

The number of coccoliths per gram sediment ranges from $6.5x10^8$ to $3.0x10^{10}$ and consist mainly of *E. huxleyi* ($9.6x10^7$-$2.3x10^{10}$) and *G. muellerae* coccoliths ($1.8x10^8$-$3.8x10^9$). Colmenero-Hidalgo et al. (2004) studied coccoliths in core M39029-7 in the northern part of the Gulf of Cádiz, and found similar total coccolith abundances, ranging from $1.8x10^8$

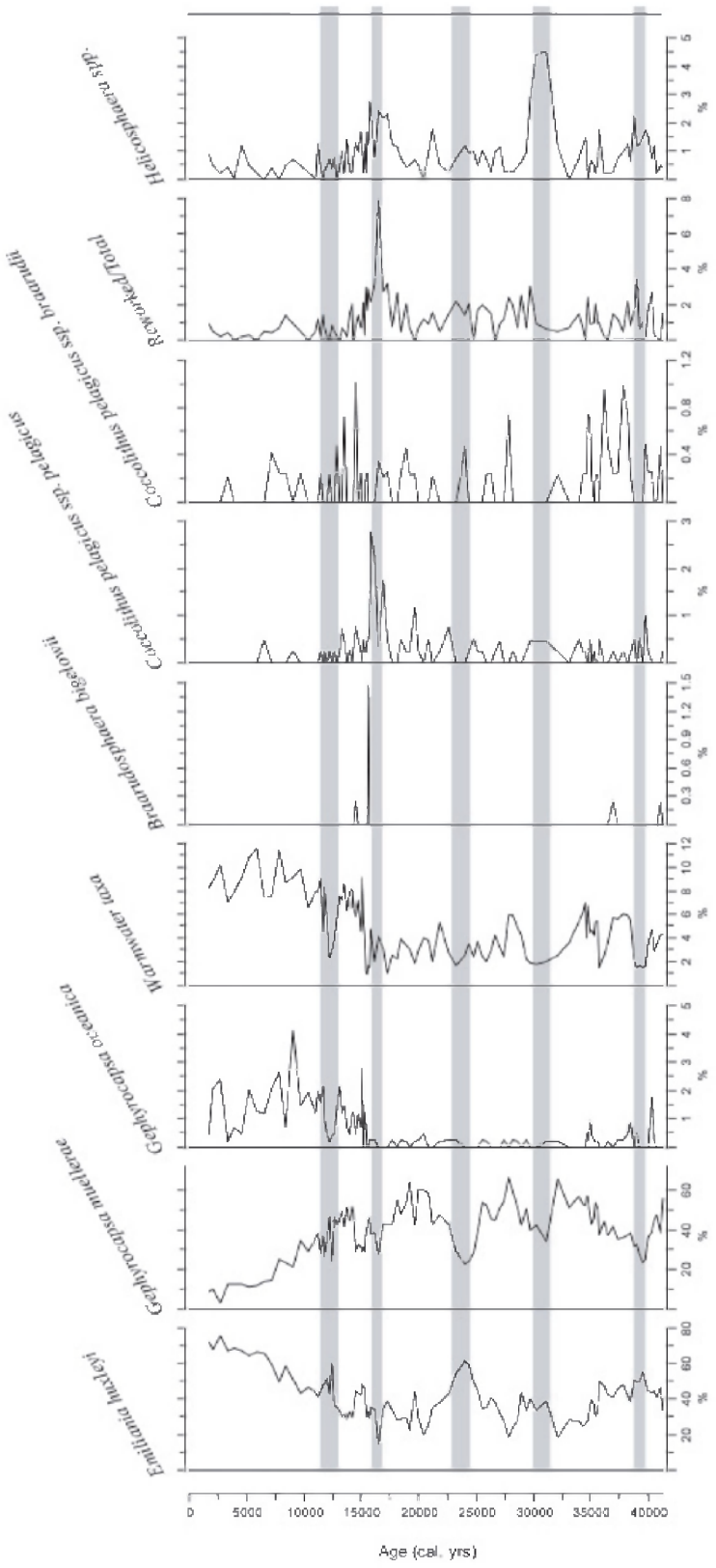

Figure 9 Relative abundances of most important nannofossils recorded in core GeoB9064-1. Also shown are reworked nannofossils per total nannofossils.

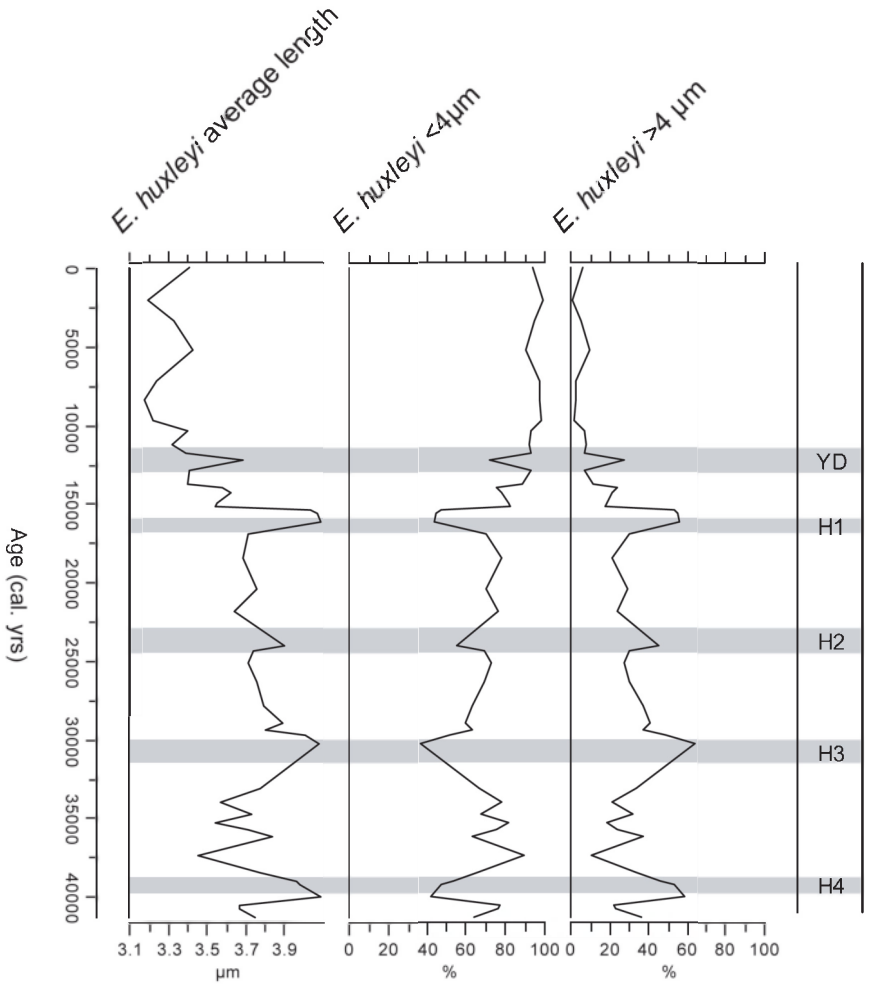

Figure 10 Morphological variations of the length of *E. huxleyi*. Left shows the average length (µm), whilst relative contributions (%) of the warm water associated small (< 4 µm) and cold water associated large (>4 µm) variants is shown on the right.

to $5.9x10^9$. Accumulation rates of coccoliths range between $1.4x10^{10}$ and $3.9x10^{11}$ coccoliths.kyr^{-1}.cm^{-2}, with $2.09x10^9$ to $2.68x10^{11}$ coccoliths of *E. huxleyi* .kyr^{-1}.cm^{-2} and $3.37x10^9$ to $1.97x10^{11}$ coccoliths of *G. muellerae*.kyr^{-1}.cm^{-2}.

The total carbonate produced by coccolithophores over the last 41 kyr is on average 0.044 g/g sediment, which is 14% of the total carbonate budget (Figure 5). This amount gradually decreases to 11% from 41.5 kyr until YD, and reaches an average of 28% in the Holocene. Local minima are observed during the HE. The remaining carbonate can be attributed to Foraminifera.

4. Discussion

4.1 Reconstruction of hydrological variations

Eolian sediments deposited in the deep sea close to the continent are coarser grained than hemipelagic sediments (Koopmann, 1981; Sirocko, 1991; Prins and Weltje, 1999). Terrigenous sediments with mean grain sizes larger than 6 µm are generally attributed to eolian transport, and smaller than 6 µm to hemipelagic transport. This is based on deep-sea sediment studies (Koopmann, 1981; Sarnthein et al.,

1981; Sirocko, 1991; Prins and Weltje, 1999; Prins et al., 2000) as well as sediment-trap studies (Clemens, 1998; Ratmeyer et al., 1999). Consequently, EM1 and EM2 are considered to be of eolian origin, while EM3 is interpreted as a hemipelagic mud settled out of suspension from nepheloid layers. The nepheloid layers that produced EM3 may originate from the ephemeral rivers draining the Middle Atlas Mountains. It is assumed that continental runoff is the main supplier of hemipelagic mud, and that the sediment input by both continental runoff and eolian dust is determined by variations in the hydrology of the area. However, it should be mentioned that local hydrodynamic variations and bottom current variations in the study area might have also an influence on the sorting and the grain size distribution.

The eolian component can thus be expressed as 1-EM3, and shows similarities to the Fe and Ti XRF record (Figure 3). Enhanced heavy minerals, as indicated by Ti contents, are related to arid conditions in Africa (Zabel et al., 2001). Furthermore, enhanced Fe supply is associated with hematite, which is linked with increased eolian input (Rogerson et al., 2006). This suggests relatively arid conditions during the glacial period, more particularly during HEs and YD, and more humid conditions during the Holocene and interstadials (e.g. BA). The coarser median grain size in these periods might have been further boosted by enhanced bottom current activity over the southern Gulf of Cádiz during glacial times (Foubert et al., 2008). Major arid-humid transitions have been documented in African continental records at 15-14.5 kyr BP and 11.5-11 kyr BP by Gasse (2000) and are visible in the Ti record. Increased humidity is also indicated by the peak occurrence of *Braarudosphaera bigelowii* after H1 (Figure 9) which indicates a low salinity event (Bukry, 1974; Siesser et al., 1992), probably caused by a sudden increase in rainfall, and is coincident with a peak in sedimentation rate (Figure 2).

4.2 Productivity reconstruction

Changes in hydrological conditions are also reflected in productivity variations. Warm, humid conditions result in enhanced nutrient supply in the Gulf of Cádiz, which increases primary productivity. These increases in productivity during the humid interstadials are well expressed in the accumulations of *G. muellerae* (Figure 7). *G. muellerae* is nowadays known as a coastal species associated with enhanced nutrient input, e.g in the Alborán Sea (Bárcena et al., 2004) and the South Atlantic (Boeckel et al., 2006; Boeckel and Baumann, 2008). Accumulations of biomarkers (alkenones, GDGTs) and organic carbon show similar fluctuations as accumulations of *G. muellerae* (Figure 7), and can also be related to higher primary productivity during interstadials in the Alborán Sea (Cacho et al., 2000). Since accumulations of terrigenous material and carbonate also show similar fluctuations, these relationships suggest that this enhanced productivity is coupled to enhanced organic carbon preservation through the "mineral ballast" hypothesis (Thunell et al., 2007) and partly explains enhanced preservation during interstadials, although absence of oxygenated bottom waters should also be taken into account (Cacho et al., 2000). Furthermore, pronounced productivity peaks occur during the BA and around 35 kcal. yrs and coincide with precession minima (Figure 7).

Cold, arid conditions are reflected in enhanced upwelling, which is observed in the southern Gulf of Cádiz as filaments south of the Strait of Gibraltar (Vargas et al., 2003). Although a general lack of diatoms is observed in the area downcore (Abrantes, 1988; this study), enhanced abundances of the large variant of *E. huxleyi* (> 4 µm) are associated with intrusion of turbid, cold waters during stadials (HE), which reflect upwelling conditions (Colmenero-Hidalgo et al., 2002), which could be related to migrations of the Azores Front (Rogerson et al., 2004). This is observed downcore in the Gulf of Cádiz (Colmenero-Hidalgo et al., 2004) and is confirmed in this study. Furthermore, for this area enhanced abundances of small *E. huxleyi* (<4 µm) are associated with warm, oligotrophic conditions, since this has been observed elsewhere (Ziveri and Thunell, 2000; Andruleit et al., 2008), also in the oligotrophic Mediterranean (Ziveri et al., 2000). This fits with the observation that relative abundance changes of small *E. huxleyi* are synchronous to oligotrophic warm-water taxa (Figure 9 and 10). Increased degradation can be observed during HEs, reflected in decreased percentages of organic carbon and carbonate and accumu-

lations of *G. muellerae* and biomarkers. Possibly also the shift to the more robust large *E. huxleyi* can be explained partly by effects of carbonate dissolution. *E. huxleyi* has been known to be strongly influenced by carbonate diagenesis in the Mediterranean Sea (Crudeli et al., 2004).

Upwelling is also reflected in the grain size measurements (Figure 3). The ratio of the coarse versus the fine eolian member (EM1/(EM1+EM2)), reflecting the eolian grain size, is interpreted as a measure of the intensity of the northern trade winds, which transport the eolian dust. The eolian component (EM1+EM2) is a measure for the amount of deposited material. These parameters show that trade wind activity was intensified during the stadials linked to increased upwelling. The eolian component shows relatively similar fluctuations to the relative abundances of large *E. huxleyi* (Figure 3 and 10). Also, it can be noted that during H1 and YD there was a large amount of deposited eolian dust, trade wind activity was weaker, compared to previous HEs. This is likely related to the higher sea-level at these times.

Two mechanisms are thus responsible for productivity variations: humid interstadials increase coccolith productivity and preservation, while cold, turbid stadials decrease productivity and preservation. This signal is modulated by the precessional signal: decreased seasonality (precession minima) causes warm, wet, eutrophic conditions and increased seasonality (precession maxima) instigates cold, arid, oligotrophic conditions.

4.3 Temperature reconstructions

$U^{K'}_{37}$ SSTs are similar but slightly lower than alkenone SST reconstructions from core M39008 by Cacho et al. (2001). Differences between TEX_{86} and $U^{K'}_{37}$ SST can be related to subsurface production of GDGT's (Huguet et al., 2007), lateral transport of alkenones (Mollenhauer et al., 2006; 2008), fluvial input of terrestrially derived isoprenoid GDGTs (Weijers et al., 2006) or different growing seasons of the biomarker source organisms (Huguet et al., 2006a). Subsurface production would be reflected as lower temperatures recorded by GDGTs, which is not the case. Lateral transport of alkenones is possible, although it has not been observed in a nearby NW African core (Mollenhauer et al., 2005; 2008). Fluvial input is also possible since the correspondence of $U^{K'}_{37}$ SST to the stable oxygen isotope curve suggests possible influence of salinity on this temperature record (Figure 6 A), although the BIT index is quite low (<0.08). The similar accumulations of both components (Figure 7) suggest no differences in growing season.

The SST trends are also imprinted into changes of relative abundances of warm water coccoliths (G. oceanica and grouped warm-water taxa), next to the cold water indicators, large E. huxleyi (>4 µm) and C. pelagicus pelagicus (Figure 8). The biometric analysis confirms the observations of Colmenero-Hidalgo et al (2004), that HEs are associated with peaks of large E. huxleyi (>4 µm). Furthermore, the significant peak of C. pelagicus pelagicus during H1 coincides with the maximum of reworked coccoliths (Figure 9), and can be associated with intrusions of subpolar water (Narciso et al., 2006).

Also, the linear regression between Ti XRF and $U^{K'}_{37}$ SST suggests a strong relation between temperature fluctuations and changes in the terrigenous record. Time series analysis of the Ti XRF suggest two main cycles of deposition of the eolian component of respectively 1000 and 585 years (Figure 11), which resembles the 1375 and 607 cycles observed by Rogerson et al. (2006) in the northern Gulf of Cádiz.

5. Conclusion - the paleoclimatological model

The proxies enable to construct a paleoclimate model (Figure 12). Variations of the North Atlantic Oscillation (NAO) index can be related to latitudinal shifts of the westerly wind system, causing rapid hydrological variations in the Mediterranean Sea (Sánchez-Goni et al., 2002; Moreno et al., 2004).

Negative NAO indices are related with a higher humidity in the Gulf of Cádiz. During wet periods, higher river induced nutrient influx causes a *G. muellerae* dominated flora with high productivity of coccolithophores, their biomarkers (alkenones), GDGTs, carbonate and organic carbon. A positive feedback by enhanced mineral ballasting and the absence of cold water intrusions cause enhanced

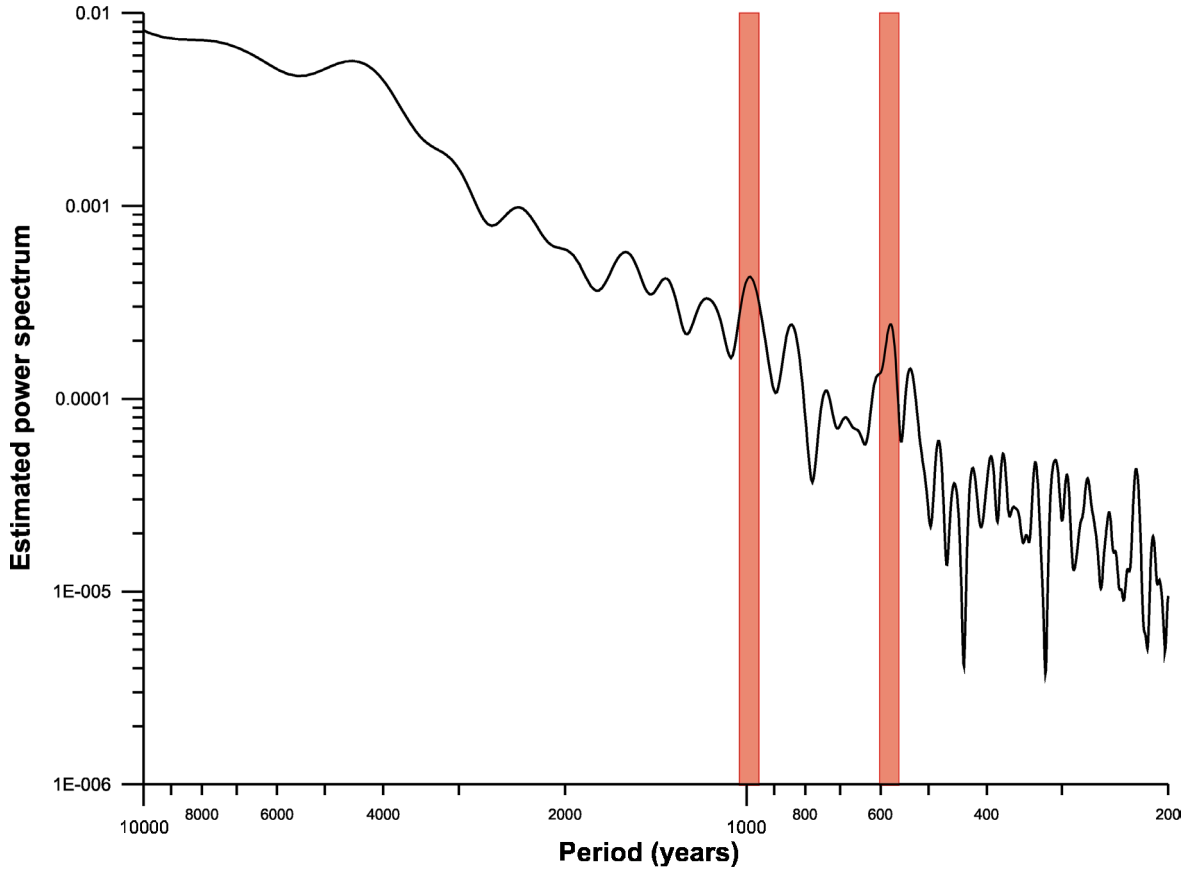

Figure 11 Spectral analysis of Ti XRF record. Two significant cycles of 1000 and 585 years are observed (shown in red). Significance levels were set at 95 % confidence intervals.

preservation. There is a strong precession modulation of the productivity signal, with production maxima during precession minima. These wet interstadial periods coincide with relatively warmer temperatures ($U^{K'}_{37}$ and TEX_{86} SST). The resulting deposits are fine-grained, carbonate rich and hematite poor.

Positive NAO indices can be related to enhanced aridity in the Gulf of Cádiz. Ti XRF and eolian components in core GeoB9064-1 show rapid fluctuations of the aridity record, with more arid glacial conditions and particularly strong trade wind strength and hematite rich layers during HEs (Figure 3). Enhanced upwelling is reflected in a shift to larger forms of *E. huxleyi* and cooler temperatures ($U^{K'}_{37}$ and TEX_{86} SST). Lower accumulations of coccoliths and biomarkers are explained by decreased coccolithophore productivity coupled with increased degradation. The degradation is caused by increased bottom water oxygenation due to intrusion of cold waters coupled with decreased ballasting. Furthermore, the relation between the independent proxies Ti XRF and $U^{K'}_{37}$ SST suggests a rapid transfer between atmospheric and oceanic processes, since climatological fluctuations on the continent and in the ocean are synchronously recorded. Two cycles of 1000 and 585 years are recorded in the Ti XRF signal.

Changes of the NAO oscillation are thus well expressed in the southern Gulf of Cádiz, with pronounced positive phases during stadials and negative phases during interstadials, modulated by precession changes.

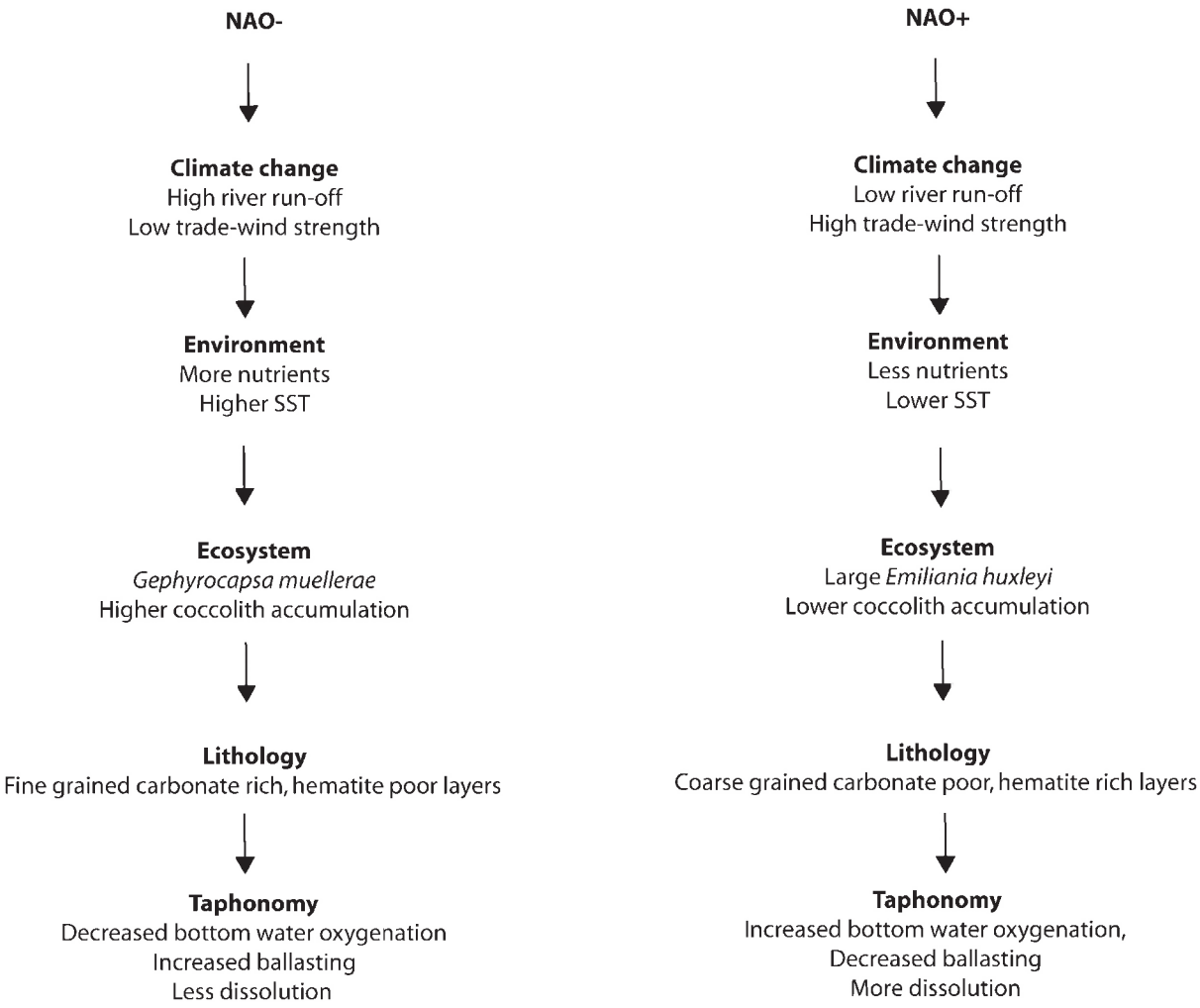

Figure 12 Paleoclimatological model depicting climatic variations recorded in the sediment of the southern Gulf of Cádiz.

Additional information

Coccoliths from core GeoB9064-1 were extracted, counted and measured by Kenneth Mertens and Heleen Vanneste at Ghent University, biomarkers were measured and quantified by Kenneth Mertens at the Royal Netherlands Institute for Sea Research (Texel, The Netherlands). XRF analysis and spectral analysis was done by Anneleen Foubert. Grain-size measurements were done by Kenneth Mertens at Hydraulic Research Laboratory, Borgerhout, end-member modeling of this data was done by Jan-Berend Stuut. Stable oxygen isotopes were measured by Claudia Wienberg at Bremen University, radiocarbon dates were measured by Kiel and Poznan Radiocarbon laboratories. Interpretations were done by Kenneth Mertens. This chapter will be submitted to *Palaeogeography, Palaeoclimatology, Palaeoecology.*

CHAPTER 3

Determining the absolute abundance of dinoflagellate cysts in recent marine sediments: the *Lycopodium* marker-grain method put to the test

ABSTRACT

Absolute abundances (concentrations) of dinoflagellate cysts are often determined through the addition of *Lycopodium clavatum* marker-grains as a spike to a sample before palynological processing. An inter-laboratory calibration exercise was set up in order to test the comparability of results obtained in different laboratories, each using its own preparation method. Each of the 23 laboratories received the same amount of homogenized splits of four Quaternary sediment samples. The samples originate from different localities and consisted of a variety of lithologies. Dinoflagellate cysts were extracted, counted, and relative and absolute abundances calculated. The relative abundances proved to be fairly reproducible, notwithstanding a need for taxonomic calibration. By contrast, excessive loss of *Lycopodium* spores during sample preparation resulted in non-reproducibility of absolute abundances. Use of oxidation, KOH, warm acids, acetolysis, mesh sizes larger than 15 µm and long ultrasonication (>1min) must be avoided to determine reproducible absolute abundances. The results of this work therefore indicate that the dinoflagellate cyst worker should make a choice between using the proposed standard method which circumvents critical steps, adding *Lycopodium* tablets at the end of the preparation or using an alternative method.

1. Introduction

Dinoflagellate cyst concentrations are an important component of paleoceanographical studies (e.g. Pospelova et al., 2006; González et al., 2008b) and can be determined using the volumetric method (e.g. Dale et al., 2002; Holzwarth et al., 2007). In general, dinoflagellate cyst concentrations are calculated by adding a known amount of exotic markers or a "spike" to every sample according to the method described by Stockmarr (1971). The marker commonly used is *Lycopodium clavatum* Linnaeus (Stag's Horn Clubmoss or Ground Pine).

As noted by Lignum et al. (2008), the so-called 'standard' palynological processing methods are still very variable in terms of initial sample sizes, type and concentration of acids, sieve material and mesh size, sonication time and strength, number of decanting cycles and use of heavy liquid separation. This is also apparent in reviews of the preparation techniques for extraction of dinoflagellate cysts given by Wood et al. (1996) and more recently by Riding and Kyffin-Hughes (2004). However, critical evaluation of the effect of different laboratory procedures on the marker grain technique for obtaining dinoflagellate cyst concentration has so far never been attempted.

Although it has been reported that several processing methods such as sonication and chemical treatments can inflict damage on organic-walled microfossils to a certain extent (e.g. Schrank, 1988; Hodgkinson, 1991), the effect on palynomorph concentrations remains unknown.

This study aims to test the reproducibility of the marker-grain method, in order to understand the discrepancies in the results following different preparation techniques. Similar efforts to test the reproducibility of specific laboratory techniques have been done for other microfossil groups: benthic and planktonic foraminifera (Zachariasse et al., 1978), diatoms (Wolfe, 1997), nannofossils (Herrle and Bollman, 2004) and their biomarkers (Rosell-Melé et al., 2001). It is therefore timely to carry out a similar exercise with dinoflagellate cysts.

Surface sediment samples from four localities (North Sea, Celtic Sea, NW Africa and Benguela) were sent to 23 laboratories. The samples were processed using the palynological techniques routinely used in these laboratories. An equal amount of *Lycopodium* tablets, all from the same batch, were added to each sample. The reproducibility of both absolute and relative abundances for dinoflagellate cysts is here put to the test, and has resulted in a proposal of recommendations for a standardized method to determine absolute abundances of Quaternary dinoflagellate cysts with the marker-grain method. Two laboratories used the volumetric method (Dale, 1976) for comparison purposes. This study focuses additionally on whether it is necessary to count 300 or 400 dinoflagellate cysts and on taxonomy, since notable interlaboratorial differences in nomenclature were recorded.

2. Material and methods

Late Quaternary surface sediment samples from four sites with different lithologies were used by the 23 different laboratories involved in the project. The North Sea sample consisted of a homogenized surface sediment taken using a Reineck boxcorer (51.47°N, 3.48°E, 10 m water depth). The Celtic Sea sample was assembled through mixing multi-corer samples from Station 8, collected during several time slots from the Celtic Sea (51.05°N, 5.83°W, 86 m water depth) (Marret and Scourse, 2002). The sample from Northwest Africa was a mixture of multicores GeoB9504-4 (15.87°N, 16.67°W, 43 m water depth) and GeoB9503-3 (16.07°N, 16.65°W, 50 m water depth). The Benguela sample consists of a mixture of sediment samples collected offshore Walvis Bay, at a water depth of about 200 m during Meteor cruise M63/2. Sample details are given in Table 1. Each laboratory was given a number, followed by a letter when the laboratory used more than one processing method. Laboratory identification and numbers were kept anonymous. A brief overview of the methods used is described in section 2.1 to 2.5. A special variation of this method is detailed in section 2.6 and the volumetric method is detailed in section 2.7. Details of the methods used are given in the Supplementary data.

Homogenization was done using the quartile method. The samples were oven dried at a temperature of 58°C for 24 hours. The *Lycopodium* spore tablets used are produced and distributed by the Subdepartment of Quaternary Geology, University of Lund, Sweden (http://www.geol.lu.se/kvg/eng/). Ten *Lycopodium clavatum* tablets of batch 483216 (X = 18.583 per tablet, s = ± 1708), were dispatched with the samples, and a fixed number of tablets was added by each laboratory to each sample.

2.1 Chemical treatment

Hydrochloric acid (HCl) with a concentration of 6.5–36% was added for the removal of carbonate. Some 20 to 300 ml was used depending on the intensity of the reaction. Cold HCl was used in most of the cases, although some laboratories used hot HCl with a temperature ranging between 42 and 80°C. Afterwards, the residue was left to settle (15 min to 42 h). Laboratories that used short settle times at this step, used centrifugation or sieving to concentrate the sample. For centrifugation, the rotation speed used varied between 1900 and 3500 rpm, and lasted between 5 sec to 10 min. Demineralised or distilled water was used for rinsing until pH reached more neutral values of 5 to 7. One to 5 decanting cycles with intervals of 3 to 24 hrs were needed depending on HCl concentrations used. To avoid losing residue

Table 1 Description of the samples.

Sample	Lithology	Dry weight (g)	Number of tablets added	Number of spores added	Stdev spores
North Sea	Fine-medium	10	3	55749	2959
Celtic Sea	Fine silty sand	10	1	18583	1708
NW Africa	Clay	2	2	37166	2416
Benguela	Clay	1	4	74332	3417

during decanting, some laboratories used centrifugation for concentration of the residue. Extensive rinsing is necessary for the removal of Ca^{2+}, to avoid calcium fluoride (CaF_2) precipitation during HF treatment. A few laboratories used KOH for neutralization (laboratory 2: 1% KOH and laboratory 18 b: 10% KOH).

The siliciclastic component of the samples was removed by adding 10 to 250 ml of hydrofluoric acid (HF) with a concentration ranging from 19% to 70%. Commonly a concentration between 40 and 50% was used. All laboratories used cold HF, except laboratories 12 (42°C), 2 (50°C), 6 (60°C), 10 (70°C) and 23 (80°C). Settling times varied between 12 and 144 hrs. A few laboratories repeated the HF treatment up to 3 times before all silicates were removed.

Before neutralisation, about 10 to 300 ml HCl with a concentration of 6.5 to 36 vol% was added for the removal of formed fluorosilicates. Mostly cold HCl was used, although some laboratories used hot HCl with a temperature ranging between 42 and 100°C. The following settling time varied between 15 min to 72 hrs. Again, laboratories that used short settling times, used centrifugation. The sample was subsequently rinsed with distilled water, until pH reached 5–7. The rinsing took 1 to 6 decanting cycles with intervals of 3 to 24 hrs, depending on the concentrations used. Again, to avoid losing residue during decanting, some laboratories used centrifuging for the concentration of the samples. One laboratory used KOH for the neutralisation (laboratory 2: 1%). A few laboratories skipped the second HCl treatment and proceeded directly to the rinsing with distilled water until pH reached values of 5–7. Several of these laboratories used centrifuging and/or sieving for concentration of the samples. During rinsing toxic HF was decanted and removed.

One laboratory (laboratory 22b) oxidised three of the samples (excluding the North-West Africa sample) with Schulze's solution (70% nitric acid saturated with potassium chlorate).

2.2 Mechanical treatment

Heavy liquid separation for the removal of heavy minerals was carried out by a few laboratories. Labs 10 and 16 used sodium polytungstate (SPT) at specific densities to isolate the palynological fractions.

Between 13 and 1800 seconds sonication was used to break down organic matter aggregates by some laboratories. Most laboratories used sonic baths (Branson™, Sonimasse™, Sonicor™, Eurolab™). Laboratory 8 used a standard oscillating sensor.

2.3 Sieving

Some laboratories pre-sieved before the chemical treatment for the elimination of the coarse fraction (mesh size 100, 106, 120, 150 µm) and/or fine fraction (mesh size 10, 11, 15 µm). All the laboratories added the *Lycopodium* tablets before pre-sieving, except laboratory 23.

Sieving after the chemical treatment was used to remove the fine fraction from the residue. Calgon (sodium hexametaphosphate) was used to disaggregate the material in a few cases. The sieve mesh sizes used varied from 6 to 20 µm, and meshes were made of nylon, polyester, polymer or steel. The devices used were hand, mechanical and water pressure pumps. Some laboratories sieved without using a pump.

2.4 Staining and mounting of the slides

Staining with a colouring agent enhances contrast for optical microscopy and can be used for the detection of pre-Quaternary specimens (Stanley, 1966). Safranin-O, Fuchsin or Bismark Brown was used by a few laboratories. Not every laboratory stained the residue. Finally a few drops of a copper sulphate solution, thymol or phenol were often added to the residue for the inhibition of fungal growth.

Slides were mounted on a heated metal plate (65°C) using a pipette, by strewing using a spatula or a mix of both methods. The mounting medium was usually glycerin jelly, but sometimes thymol, Elvacite, Eukitt, UV adhesive, or Canada balsam was used. Although sealing is not *per se* necessary (Poulsen et al., 1990), nail polish or paraffin wax was used to seal the slides to protect the residue from degradation by

dehydration.

2.5 Counting of the palynomorphs and calculation of absolute abundances

Dinoflagellate specimens were counted only when they comprised at least half of a cyst. The same criterion was used for other palynomorphs, also counted by some of the laboratories. Initially 300 dinoflagellate cysts were counted, and subsequently an extra 100 specimens were added. The purpose was to check whether it is necessary to count 300 or 400 dinoflagellate cysts to obtain representative relative and absolute abundances. Indeterminate dinoflagellate cysts were grouped as Indeterminate spp., and were not taken into account for the calculation of the relative abundances, since every observer had a different concept of what counts as an indeterminate dinoflagellate cyst, and this would introduce observer bias into the relative abundances. Raw counts together with a summary of the methodology used are available as Supplementary data.

Absolute abundances of dinoflagellate cysts were calculated following the equation by Benninghoff (1962):

$$c = \frac{d_c \times L_t \times t}{L_c \times w}$$

where:

c = concentration = number of dinoflagellate cysts / gram dried sediment.

d_c = number of counted dinoflagellate cysts

L_t = number of *Lycopodium* spores / tablet

t = number of tablets added to the sample

L_c = number of counted *Lycopodium* spores

w = weight of dried sediment (g)

Maher (1981) devised an algorithm to calculate confidence limits on microfossil concentrations. A slight correction to this algorithm was made, since the current study used sediment weight instead of sediment volume. The confidence limits calculated based on this algorithm have a 0.95 probability (Z = 1.95). It should be noted that these confidence limits are similar to the total error on concentration proposed by Stockmarr (1971); (Appendix II). These confidence limits can then be used in a statistical test to check whether microfossil concentrations are the same in two different samples (Maher, 1981). To investigate the reproducibility of results from the different laboratories, the coefficient of variation (or relative standard deviation) of all counts of a particular sample can be compared. Ideally, the results should fall within the confidence limits of Maher (1981), and thus the coefficient of variation calculated from these confidence limits can be used as a comparison.

2.6 Special methods: the maceration tank method (with HF) and the washing machine method (without HF)

The maceration tank method (Poulsen et al., 1990; Desezar and Poulsen, 1994) was used for HF treatment by laboratory 20a. Other processing steps are similar to those used by the other laboratories and are detailed in Poulsen et al. (1990) and Desezar and Poulsen (1994). Each sample is tightly wrapped in filter cloth (25 cm x 25 cm) with a mesh size of 10 µm, and the filter bags are packed in rubber foam for protection. The samples are placed inside the maceration tank and HF is conducted to the tank in PVC tubes. The samples are treated with cold HF for 7-8 days, after which the HF is drained out through a bottom-stop cock and led via PVC tubes directly to a waste-container for used hydrofluoric acid.

With the washing machine method, used by laboratory 20b, no HF is used. Each sample is tightly wrapped in filter cloth (25 cm x 25 cm) with a mesh size of 10 µm and and the filter bags are packed in rubber foam for protection. The samples are washed in a standard household washing machine with a standard household washing powder, after which carbonates are removed with citric acid at 65°C. Next the samples are again given a normal wash with a standard household washing powder. Finally the remaining minerals are removed by heavy liquid separation. This method removes the amorphous material very efficiently. Furthermore, since HF is not used, siliceous constituents (e.g. diatoms) are not destroyed. Heavy liquid separation with zinc dibromide ($ZnBr_2$) was used at densities of 2.3, 2.0

and 1.8 g/ml to remove heavy minerals. In order to test the influence of the specific density of the $ZnBr_2$, the NW African sample from laboratory 20b, was separated using heavy liquid densities of 1.8, 2.0 and 2.3 g/ml.

2.7 Volumetric method

For comparison with the marker-grain method, the volume aliquot method was performed by laboratories 6 and 8, following Dale (1976). This method was not used for the North Sea sample because of the difficulty associated with counting a fixed volume of this sample with very low abundances.

3. Results

3.1 Relative abundance of dinoflagellate cysts

Quantitative and qualitative disparities between assemblages recorded by the laboratories may be due to the different processing methods. It is obvious that aggressive agents could destroy the more sensitive cysts. To check this dependence of preservation on methodology, it is necessary to group the present species according to their resistance to degradation. It is assumed that both mechanical and chemical degradation have similar effects on an assemblage. The grouping proposed here is similar to the grouping described by Zonneveld et al. (2001). Cysts not referred to by these authors were added to a particular group based on the assumption that comparable morphology (e.g. wall thickness, resistance of structures against folding) is indicative of similar resistance to decay.

Extremely sensitive cysts: cysts of *Alexandrium* spp., *Dalella chathamense*, cysts of *Gymnodinium* spp., *Lejeunecysta* spp., *Polykrikos* spp., round brown cysts (RBC), *Selenopemphix* spp., spiny brown cysts (SBC), *Stelladinium* spp., *Tuberculodinium vancampoae* and *Xandarodinium xanthum*.

Moderately sensitive cysts: *Lingulodinium machaerophorum*, *Operculodinium* spp., *Pyxidininopsis reticulata*, *Quinquecuspis concreta*, *Spiniferites* spp., *Trinovantedinium applanatum* and *Votadinium* spp.

Resistant cysts: *Ataxiodinium choane*, *Bitectatodinium* spp. *Impagidinium* spp., *Nematosphaeropsis labyrinthus*, *Operculodinium israelianum*, *Pentapharsodinium dalei* and *Polysphaeridium zoharyi*.

It is evident from the dataset that some species were not recorded by some observers. One obvious example is *Dubridinium* spp., which was often counted by some laboratories as RBC or not counted at all. To partly reduce this observer bias, we decided to group species into genera or larger groups (Appendix III). Averages of relative abundances were only calculated when at least 300 dinoflagellate cysts were counted. The counts from oxidized samples (laboratory 22b) were also excluded, since all heterotrophic cysts were destroyed. The average results of the four samples are shown in Table 2. Representative cysts from the four samples are shown in Plate I to IV.

3.2 Absolute abundances of dinoflagellate cysts

The cyst concentration (absolute abundance) in the North Sea sample ranges from 570 to 3304 cysts/g, excluding the outliers: laboratory 1a produced a high number (8342 cysts/g) and laboratory 22b a low number (278 cysts/g). The average is 1516 cysts/g with a standard deviation of 698 cysts/g (coefficient of variation, V = 46%). The average coefficient of variation from the confidence limits of Maher (1981) is 20%. The volumetric method was not used for the North Sea sample (Table 3).

The cyst concentration (absolute abundance) in the Celtic Sea sample ranges from 1240 to 5284 cysts/g, excluding the outliers: laboratories 14 and 1a produced high numbers of 75633 and 10961 cysts/g respectively, while laboratory 20a, 2 and 20b give respectively low values of 1053, 731 and 501 cysts/g. The average is 2583 cysts/g, with a standard deviation of 1342 cysts/g (V = 52%). The average coefficient of variation from the confidence limits of Maher (1981) is 25%. Results obtained by the volumetric method

give estimates that are much lower than with the marker grain method. For the Celtic Sea these values (1,160 cysts/g (laboratory 6) and 1167 cysts/g (laboratory 8)) are even below the lowest value obtained by the marker grain method (Table 3).

The cyst concentration (absolute abundance) in the NW Africa sample ranges from 4606 to 38357 cysts per gram, excluding the outliers: labatories 11, 1a and 14 produced very high numbers (168899, 167651 and 129236 cysts/g, respectively). The average is 19441 cysts/g, with a standard deviation of 9148 cysts/g (V = 47%). The average coefficient of variation from the confidence limits of Maher (1981) is 23%. As before, the volumetric method gave lower estimates but within the range of the marker grain method (11,600 cysts/g (laboratory 6) and 9992 cysts/g (laboratory 8)) (Table 3).

The cyst concentration (absolute abundance) in the

Table 2 Average percentages of the four samples for the different taxa.

Species name	North Sea	Celtic Sea	NW Africa	Benguela
Round brown cysts (RBC)	35.8 ± 16.0	10.0 ± 7.7	3.4 ± 2.3	62.7 ± 17.0
Spiny brown cysts (SBC)	15.5 ± 12.5	1.7 ± 3.3	2.3 ± 2.4	8.5 ± 8.5
cysts of *Alexandrium* spp.	0.2 ± 0.3	0.5 ± 0.9	-	0.1 ± 0.5
cysts of *Gymnodinium* spp.	0.3 ± 0.6	0.3 ± 0.6	0.0 ± 0.1	0.0 ± 0.1
Stelladinium spp.	0.3 ± 0.3	0.2 ± 0.2	0.3 ± 0.3	0.1 ± 0.4
Lejeunecysta spp.	9.5 ± 12.0	1.5 ± 1.6	0.4 ± 0.5	1.4 ± 1.6
Selenopemphix spp.	5.5 ± 1.7	4.8 ± 2.1	1.0 ± 0.6	6.5 ± 6.3
Tuberculodinium vancampoae	0.0 ± 0.1	-	0.1 ± 0.3	0.0 ± 0.1
Polykrikos spp.	6.9 ± 3.5	5.7 ± 3.8	1.2 ± 0.8	1.1 ± 0.8
Xandarodinium xanthum	0.2 ± 0.3	0.1 ± 0.1	0.1 ± 0.2	0.0 ± 0.1
Dalella chathamense	-	-	-	0.0 ± 0.1
Extremely sensitive cysts (sum)	74.3 ± 7.4	24.8 ± 11.2	15.4 ± 8.2	80.6 ± 9.9
Lingulodinium machaerophorum	1.5 ± 2.5	0.7 ± 0.9	86.2 ± 4.7	0.2 ± 0.5
Operculodinium spp.	2.8 ± 1.9	12.3 ± 3.7	0.5 ± 0.7	8.4 ± 6.6
Pyxidininopsis reticulata	0.0 ± 0.2	-	-	-
Spiniferites spp.	9.8 ± 3.5	51.8 ± 10.7	3.3 ± 1.1	5.5 ± 3.2
Quinquecuspis concreta	3.3 ± 2.1	2.3 ± 2.0	0.1 ± 0.1	1.0 ± 1.5
Trinovantedinium applanatum	0.2 ± 0.4	1.2 ± 1.0	0.2 ± 0.3	0.3 ± 0.4
Votadinium spp.	5.8 ± 6.6	0.5 ± 0.7	0.0 ± 0.1	0.7 ± 0.7
Moderately sensitive cysts (sum)	23.6 ± 7.2	68.9 ± 10.7	90.3 ± 4.2	16.2 ± 9.7
Nematosphaeropsis labyrinthus	0.0 ± 0.1	0.0 ± 0.1	0.1 ± 0.1	2.1 ± 2.0
Impagidinium spp.	0.3 ± 0.6	0.15 ± 0.3	0.0 ± 0.1	0.0 ± 0.1
Operculodinium israelianum	0.2 ± 0.2	0.0 ± 0.1	0.4 ± 0.7	0.4 ± 0.7
Pentapharsodinium dalei	0.4 ± 0.5	2.6 ± 3.5	0.0 ± 0.1	0.2 ± 0.5
Polysphaeridium zoharyi	0.4 ± 0.6	0.1 ± 0.3	0.1 ± 0.5	0.2 ± 0.7
Ataxiodinium choane	0.0 ± 0.1	0.1 ± 0.1	0.0 ± 0.0	-
Bitectatodinium spp.	0.6 ± 1.1	3.3 ± 2.0	0.1 ± 0.2	0.2 ± 0.6
Resistant cysts (sum)	0.5 ± 0.6	6.2 ± 3.8	0.7 ± 0.9	3.1 ± 2.5

Benguela sample ranges from 30130 to 298972 cysts/gram, excluding the outliers: laboratory 1c produced a high number of 1455988 cysts/g, while laboratories 20b and 8 give values as low as 18472 and 15910 cysts/g, respectively. The average is 144299 cysts/g with a standard deviation of 84159 cysts/g (V = 58%). The average coefficient of variation from the confidence limits of Maher (1981) is 21%. The volumetric method used by laboratory 6 yields 53200 cysts/g (within the range above) and 8492 cysts/g by labo-

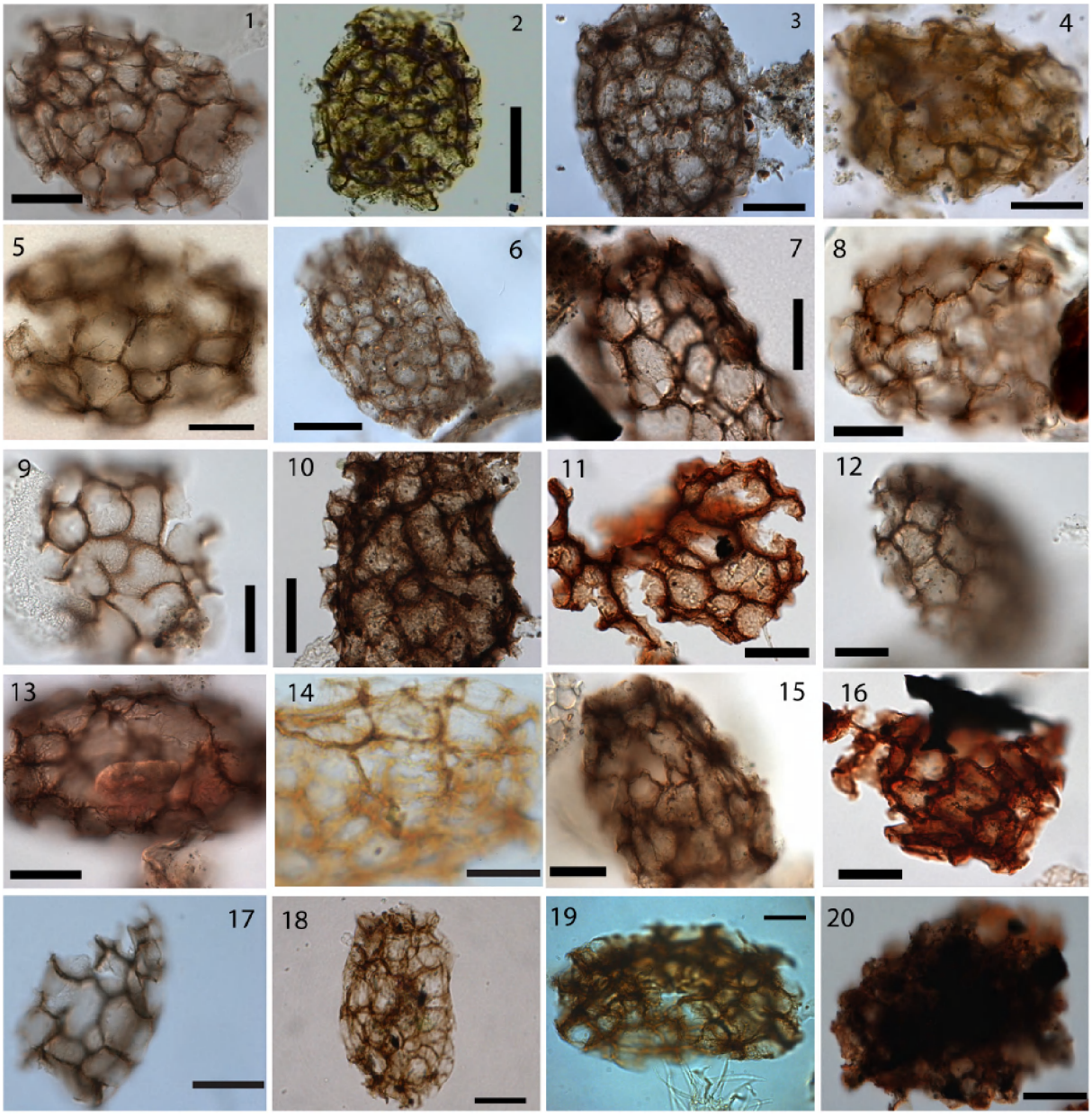

Plate I. Polykrikos schwartzii extracted from the North Sea sample using different methodologies. Labs are sorted from high (upper left corner) to low abundances (lower right corner). (1) Lab 1a. (2) Lab 20a. (3) Lab 13. (4) Lab 12. (5) Lab 19. (6) Lab 2. (7) Lab 11. (8) Lab 21a. (9) Lab 21b. (10) Lab 22a. (11) Lab 10a. (12) Lab 18b. (13) Lab 1b. (14) Lab 16. (15) Lab17. (16) Lab 10b. (17) Lab 18a. (18) Lab 5. (19) Lab 4. (20) Lab 22b, oxidized. All scale bars are 20 µm.

ratory 8. The volumetric estimate by laboratory 8 is considered to be an underestimation caused by the destruction of fragile cysts by sonication (see Discussion); (Table 3).

3.3 Reworked dinoflagellate cysts

About 7% of the recorded dinoflagellate cysts in the North Sea sample were reworked. The pre-Quaternary cysts recorded in the North Sea sample were

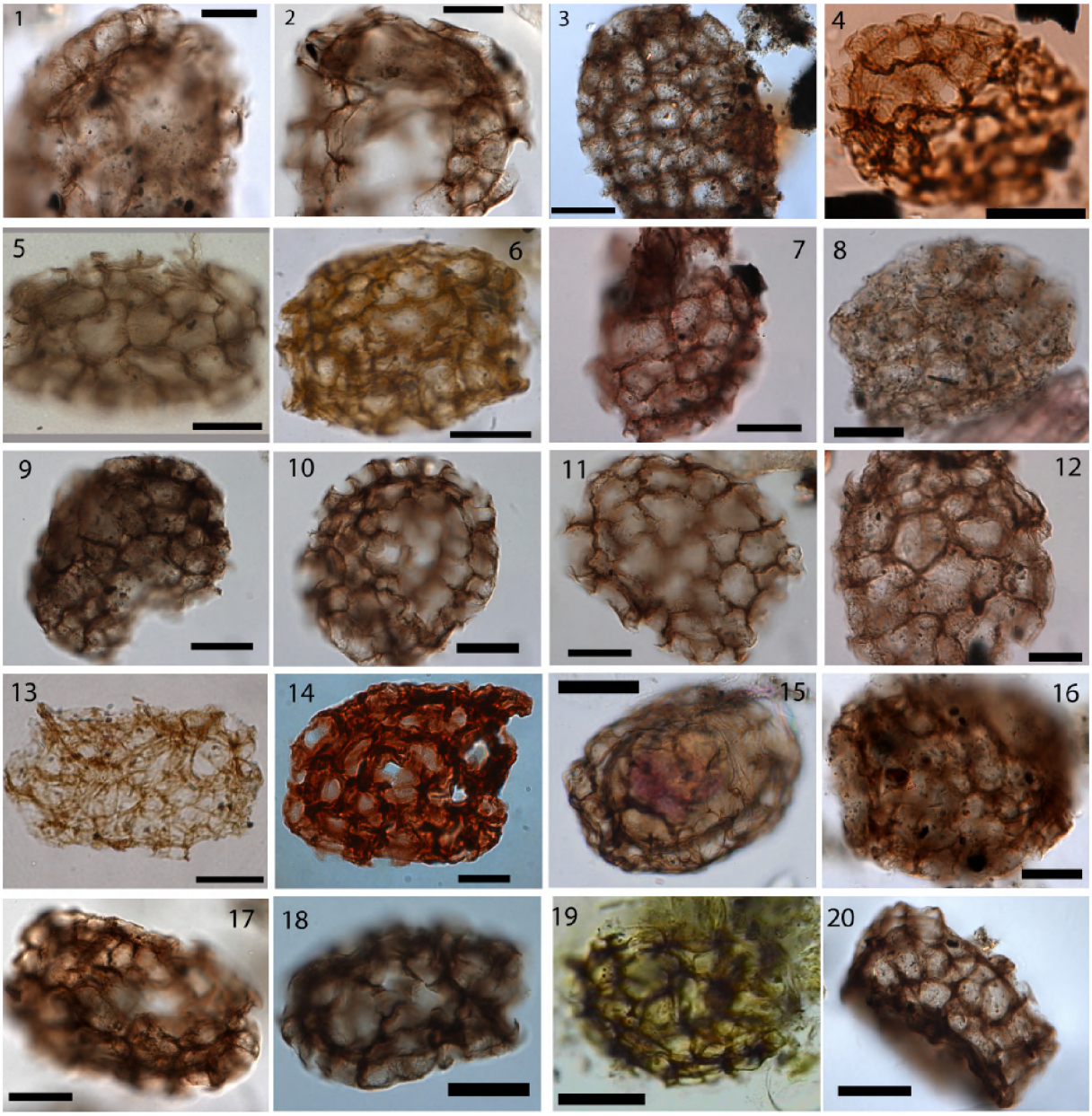

Plate II. Polykrikos schwartzii extracted from the Celtic Sea sample using different methodologies, sorted from high absolute abundances (upper left corner) to low absolute abundances (lower right corner) (1) Lab 14. (2) Lab 1a. (3) Lab 13. (4) Lab 3. (5) Lab 19. (6) Lab 12. (7) Lab 1b. (8) Lab 15b. (9) Lab 1c. (10) Lab 21b. (11) Lab 21a. (12) Lab 11. (13) Lab 5. (14) Lab 4. (15) Lab 16. (16). Lab 23. (17) Lab 17. (18) Lab 18a. (19) Lab 20a. (20) Lab 2. All scale bars are 20 µm.

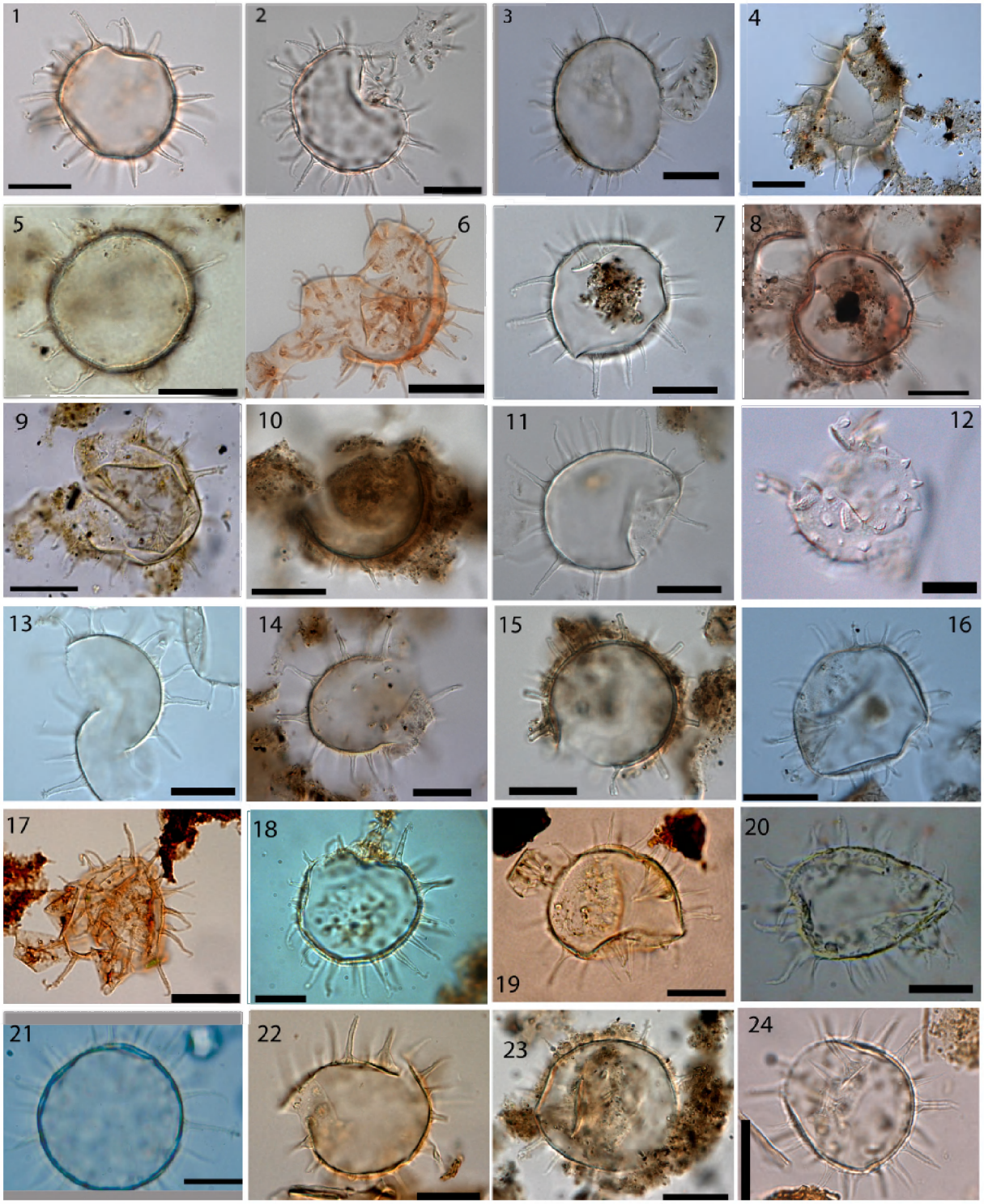

Plate III. *Lingulodinium machaerophorum* extracted from the NW Africa using different methodologies, sorted from high (upper left corner) to low absolute abundances (lower right corner). (1) Lab 11. (2) Lab 1a. (3) Lab 14. (4) Lab 13. (5) Lab 19. (6) Lab 10b. (7) Lab 21a. (8) Lab 1b. (9) Lab 12. (10) Lab 17. (11) Lab 21b. (12) Lab 6. (13) Lab18a. (14) Lab 18b. (15) Lab 1c. (16) Lab 15b. (17) Lab 22a. (18) Lab 4. (19) Lab 5. (20) Lab 20b. (21) Lab 16. (22) Lab 8. (23). Lab 23. (24) Lab 3. All scale bars are 20 µm.

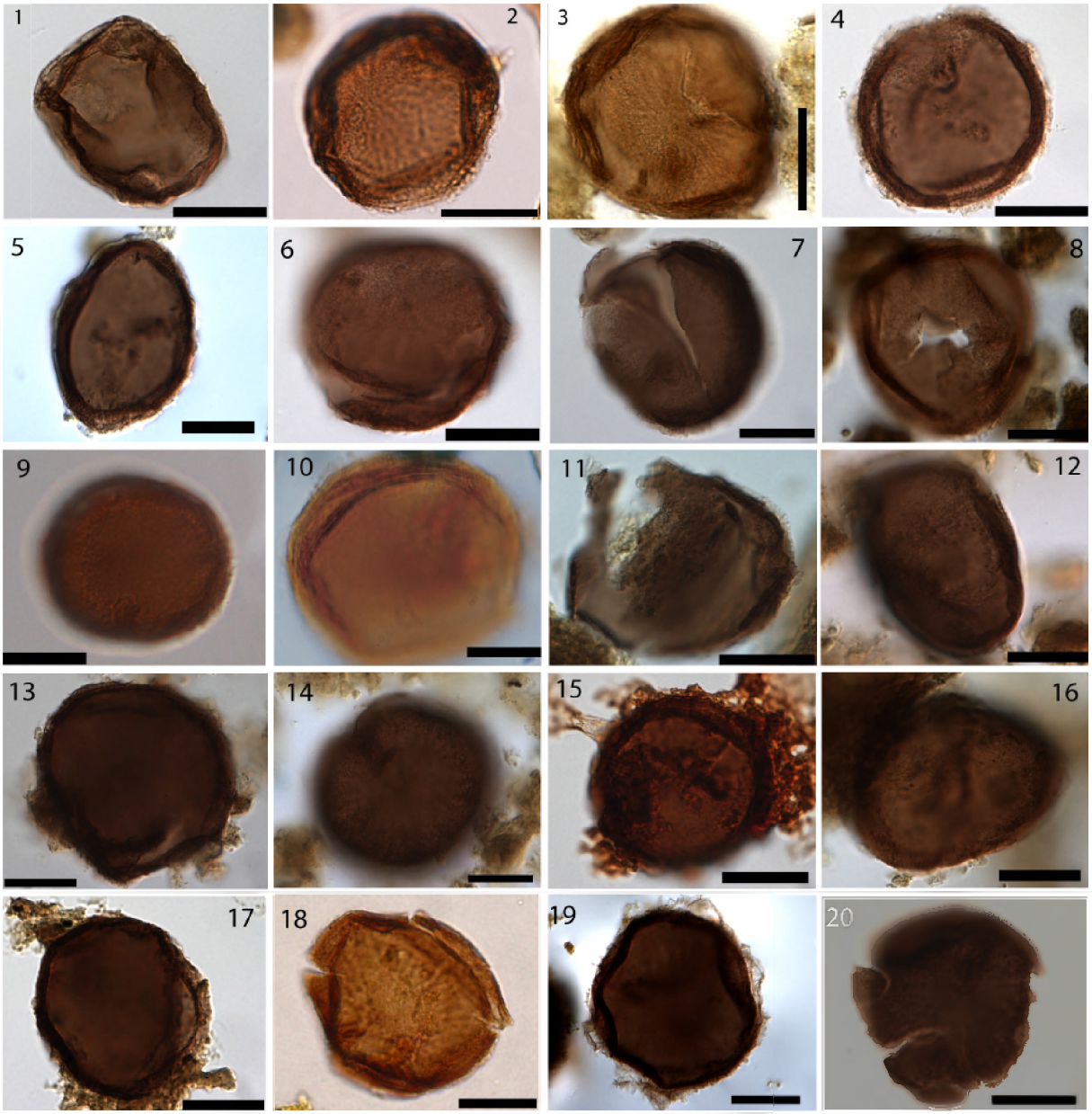

Plate IV. *Dubridinium* spp. extracted from the Benguela sample using different methodologies, sorted from high (upper left corner) to low absolute abundances (lower right corner). (1) Lab 1c. (2) Lab 3. (3) Lab 19. (4) Lab 11. (5) Lab 13. (6) Lab 1a. (7) Lab 21a. (8) Lab 21b. (9) Lab 6. (10) Lab 16. (11) Lab 18a. (12) Lab 18b. (13) Lab 1b. (14) Lab 23. (15) Lab 10b. (16) Lab 17. (17) Lab 10a. (18) Lab 5. (19) Lab 2. (20) Lab 8. Destructive ultrasonication. All scale bars are 20 µm.

Wetzeliella spp. (dominant), *Glaphyrocysta* spp., *Cordosphaeridium* spp., cf. *Oligosphaeridium* spp. and cf. *Cribroperidinium* spp. In terms of absolute abundances, reworking shows the same trends as *in situ* dinoflagellate cyst absolute abundances. Very high absolute abundances were recorded in the sample oxidized by laboratory 22b. This indicates that the robust pre-Quaternary cysts are more resistant to oxidation. Reworking is very low (less than 1%) in the samples from the Celtic Sea, NW Africa and Benguela.

Table 3 Comparison between the marker-grain method and the volumetric method.

Method	Variable / sample	North Sea	Celtic sea	NW Africa	Benguela
Marker grain method	Average (cysts/g)	1516	2583	19441	144299
	St dev (cysts/g)	698	1342	9148	84159
	Coefficient of variation (%)	46	52	47	58
	Coefficient of variation (%) Maher (1981)	20	25	23	21
Volumetric method	Average (cysts/g)	-	1163	10796	53200
	St dev (cysts/g)		5	1137	0
	Coefficient of variation (%)		0	11	0
Difference	Cysts/g	-	1420	8645	91099
	%		55	44	63

3.4 Other palynomorphs

Chlorophycean palynomorphs such as *Cymatiosphaera* sp. (not present in Celtic Sea), *Pediastrum* sp., *Pterospermella* sp. (not present in Benguela), *Tasmanites* sp., *Botryococcus* sp. (not present in Benguela), *Mougeotia* sp. (only North Sea), *Concentricystes circulus* (only NW Africa), *Gelasinicysta* sp. indet. (only NW Africa) are recorded in low numbers in all samples, except the North Sea sample.

Faunal remains such as microforaminiferal linings, scolecodonts, tintinnids, planktonic crustacean eggs and invertebrate mandibles were encountered in almost every sample. Planktonic crustacean eggs are very abundant in the North Sea sample.

Pollen and spores are abundant in the North Sea sample. The assemblage is dominated by pollen (90%). Non-bisaccate pollen include *Quercus*, *Corylus*, *Betula*, *Alnus*, pollen of Poaceae, Cyperaceae and Chenopodiaceae, whereas bisaccate pollen comprise mainly *Pinus* and *Picea*. Some *Cedrus* pollen is recorded. Reworked pollen and spores are present in low numbers.

The Celtic Sea sample is dominated by pollen (94%). Non-bisaccate pollen comprises mainly pollen of Poaceae, *Quercus*, pollen of Ericaceae and Chenopodiaceae. Bisaccate pollen is mainly *Pinus* pollen. Reworked pollen and spores are very rare.

The sample from NW Africa is also dominated by pollen (95%). Non-bisaccate pollen comprise mainly pollen of Poaceae, *Quercus*, pollen of Ericaceae and pollen of Chenopodiaceae. The bisaccate pollen are mainly *Pinus* pollen. Reworked pollen and spores are very rare.

The Benguela assemblage is also dominated by pollen (99%). Non-bisaccate pollen includes mainly pollen of Poaceae, Asteraceae and Caryophyllaceae. Bisaccate pollen is mainly *Pinus* pollen. No reworked pollen and spores were recorded.

Hyphae and fruiting bodies were counted as fungal remains in order to check whether the samples were infected by fungi. No samples showed significant abundances.

The recorded incertae sedis include *Cyclopsiella*, *Halodinium* sp., *Hexasterias problematica* (not present in Northwest Africa), *Micrhystridium* sp. (Celtic Sea and Benguela), *Palaeostomocystis subtilitheca* (North Sea and Celtic Sea), *Radiosperma corbiferum* (Celtic Sea and Benguela) and *Sigmopollis* sp. (NW Africa). These were more abundant in both North Sea and Celtic Sea samples.

Other organisms occurring are the organic linings of calcareous dinoflagellate cysts, thecamoebians (North Sea, Celtic Sea), chrysomonad cysts (North Sea, Celtic Sea) and diatoms. Diatoms can still be present when low concentrations of HF are used, possibly combined with heavy liquid separation, which enhances the abundance of diatoms with low densities (laboratory 1c; 9; 17). laboratory 20b has good recovery of diatoms, since the samples are not treated with HF.

4. Discussion

4.1 Is a 300 or 400 dinoflagellate cyst count sufficient to reach reliable diversities and absolute abundances?

There is no general agreement on the number of cysts which should be counted to obtain reliable data for diversity and absolute abundance studies. Most palynologists usually count 300 cysts per sample, which can provide up to 98% confidence (Germerad et al., 1968). To check whether it is necessary to count 300 or 400 dinoflagellate cysts, results from counting 300 cysts, plus an additional 100 cysts are compared using absolute abundances, species diversity and the Shannon-Wiener Index for all samples (Table 4). The comparison shows that the disparities in the results are insignificant: averages of absolute abundances, species richness and the Shannon-Wiener Index show limited changes compared to the associated standard deviations. The statistical test of Maher (1981) indicates that all absolute abundances derived from the 300 dinoflagellate cyst count statistically produce the same concentration as from the 400 dinoflagellate cyst count. It can thus be concluded that a 300 dinoflagellate cyst count is sufficient for generating reliable diversities and absolute abundance data in Quaternary studies.

4.2 Reproducibility of relative abundances

The standard deviations of the relative abundances observed in the grouping based on cyst preservation are always lower than 11.2%. These relatively small standard deviations suggest that changes in the relative abundance counts are caused by observer bias rather than by differences in methodology. Indeed, the highest standard deviations in the taxonomical groupings are with the taxa RBC, SBC and *Lejeunecysta* s.l. and since it can be assumed that the potential for preservation of these taxa is similar, it is likely that the disparities in the counts are the result of observer bias. The high standard deviation for RBC is probably caused by the high numbers of the morphologically similar *Dubridinium* spp. and the unfamiliarity of many observers with *Dubridinium* spp. Furthermore, an unambiguous definition of a round brown cyst is still lacking. The same is true for the spiny brown cysts, and several poorly defined species fall within this group. All other standard deviations are lower than 10%, which we consider an acceptable range for completely independent dinoflagellate cyst counts. Another possible reason for observer bias could be related to the use of different illumination techniques for routine counting of dinoflagellate cysts. Comparison of the use of phase contrast to interference contrast illumination to count dinoflagellate cysts on the same slides by laboratory 15 revealed that phase contrast emphasizes the transparent cysts (*Spiniferites* s.l., *Operculodinium* s.l., *Nematosphaeropsis labyrinthus*, etc.), whilst interference contrast emphasizes the brown heterotrophic cysts (RBC, SBC, etc.). Despite the observer bias, there is no doubt that dinoflagellate cyst relative abundance counts by one single observer are repeatable.

4.3 Explanation of outliers in absolute abundances

The higher numbers can each be explained by examining specific methodologies employed by particular labs. Labs 1a and 1c lost an excessive amount of *Lycopodium* spores due to the use of sieving at 20 µm as shown by Lignum et al. (2008). Labs 11 and 14 experienced problems with settling after centrifugation and were not confident that the final residues were suitable for quantitative analysis.

The lower numbers by laboratory 22b are due to the use of oxidation, which causes preferential destruction of dinoflagellate cysts. Due to the low amounts of material used in the exercise, the maceration tank and washing machine method (laboratory 20a and laboratory 20b) did not function optimally and yielded atypical results that should not be regarded as representative. This might be due to cysts getting attached to the large filter cloth (25 x 25 cm) used in this technique (see Discussion, assumption eight). Furthermore, one of the samples from NW Africa (laboratory 20b) was separated at specific gravities of 1.8, 2.0 and 2.3 g/ml. At the specific gravities of 1.8 and 2.3 g/ml, there were almost no dinoflagellate cysts in the slides, whereas ten times more dinocysts

Table 4 Comparison between the average results after counting 300 dinoflagellate cysts, and counting 400 dinoflagellate cysts.

Variable / sample	North Sea 300 cysts	North Sea 400 cysts	Celtic sea 300 cysts	Celtic sea 400 cysts	NW Africa 300 cysts	NW Africa 400 cysts	Benguela 300 cysts	Benguela 400 cysts
Average (cysts/g)	1539	1546	2792	2670	33798	33684	141825	142612
Stdev	767	711	1474	1236	43286	42193	87324	88779
Coefficient of variation (%)	50	46	53	46	128	125	62	62
Species richness	22.00	22.85	24.26	25.26	14.75	16.50	19.13	20.22
Stdev	4.67	4.79	5.61	6.02	3.64	4.12	4.94	5.27
Shannon-Wiener index	2.25	2.25	2.29	2.29	0.70	0.72	1.94	1.92
Stdev	0.41	0.41	0.30	0.32	0.22	0.23	0.35	0.33

were noted at the specific gravity of 2.0 g/ml. Further investigation is needed to evaluate the effect of heavy liquid separation at different specific gravities.

For laboratory 8, the use of a sonic oscillator resulted in destruction of sensitive cysts, again yielding lower numbers.

4.4 Reproducibility and accuracy of absolute abundances, excluding the outliers

Total cyst count is less dependent on taxonomical expertise, and thus probably less influenced by observer bias. The different laboratories participating in the current inter-calibration exercise used different processing techniques (see Supplementary data). The reproducibility of estimates of absolute cyst abundances, as expressed as coefficient of variation in Table 2, shows that there are differences among the 23 laboratories: the coefficients of variation are relatively large (46–58%) and nearly twice as high as the coefficients of variations (20–25%) which are calculated from Maher (1981). Our results suggest that the determination of absolute abundances is mainly dependent on processing methodology. In this light the accuracy also needs to be considered: a better understanding of what is causing the variation can only be achieved when correct absolute abundances of dinoflagellate cysts have been determined. To estimate whether the absolute abundances give an accurate picture of the true absolute abundances of the dinoflagellate cysts, results from the marker-grain method are compared with independent methods. When compared to the volumetric method, absolute abundances calculated using the marker-grain method, are 44–63% higher (Table 3). In a similar study, de Vernal et al. (1987), noted systematically higher concentrations from the marker-grain method compared to the results from the volumetric method, and they suggested that significant losses of *Lycopodium* spores (close to 33% on the average) took place during labratory procedures. On the other hand, in a study on Paleogene sediments, Heilmann-Clausen (1985), found marker-grain estimates varying between 70% and 129% of volumetric estimates and on average 2% lower concentration was calculated from the marker-grain method. Our study confirms the observation of de Vernal et al. (1987), and even shows larger deviations. It should also be noted, that counts from strew slides made from unprocessed samples show much lower abundances than the average absolute abundances from the marker grain method. From these observations, it can be concluded that with most preparation techniques there are significant losses of *Lycopodium* spores, and this is most probably the reason for higher absolute abundances using the marker-grain method. Furthermore, there was no evidence of significant loss of dinoflagellate cysts during the laboratory preparations, except when oxidation or very long or destructive sonication was used (see below). Thus, in order to understand what causes the differences in absolute abundances, one needs to consider underlying assumptions. Ten assumptions need to be considered.

1) Drying samples does not cause decay

Although drying is often done in palynological preparation, it should be avoided in organic rich sediments, where drying causes formation of selenite (gypsum, $CaSO_4.2H_2O$), by reaction of calcium carbonate with sulphuric acid, usually derived from pyrite decay. The formation of sulphuric acid significantly affects extremely sensitive dinoflagellate cysts. In this case,

to calculate the weight of the samples, wet volumes should be used, corrected with dry bulk densities. In our samples, gypsum crystals were not observed. The homogenized samples were oven dried before subdivision into smaller batches and dispatching to individual laboratories. This was done to avoid differential drying. However, not all laboratories processed the samples exactly at the same time. Samples were dispatched in March 2007, and were processed within the following year. The possibility exists that samples that were processed at a later stage dried out more. Clustering of amorphous organic matter around the cysts seems to occur in more dried out samples (most obvious around *Lingulodinium machaerophorum* specimens in Plate III), but there were no clear signs that this process caused changes in the assemblage. This assumption is thus acceptable.

2) Samples are homogenous

It needed testing if samples processed in a similar manner yielded reproducible results. All samples were processed twice by laboratory 21 (a and b). with the only difference in preparation the addition of some soap during sieving (Table 5). Following the test by Maher (1981), for every studied sample, the microfossil concentration in the quasi-replicas is the same. It can thus be concluded that the samples are well-mixed and are homogenous. Furthermore, there are few differences between both samples in terms of relative abundances. This assumption is thus acceptable.

3) A single Lycopodium tablet from batch 483216 contains 18583 ± 1708 spores

This reference is given by the supplier (Lund University), and these numbers were calibrated using a Coulter counter. Lignum et al. (2008) also used a Coulter counter for verification and obtained 16971 ± 1251 *Lycopodium* spores. We dissolved one tablet in distilled water and sieved on a 0.25 µm Millipore filter. The filter was cut into two pieces, mounted on a slide and counted under a transmitted light microscope. On this filter, 16993 *Lycopodium* spores were counted, which falls within the range proposed by the supplier and Lignum et al. (2008). A similar exercise has been done for another batch by Stabell and Henningsmoen (1981) which found similar results. This assumption is thus acceptable.

4) There is no degradation of palynomorphs caused by chemical treatment such as oxidation or acid treatments by HF and HCl

Since *Lycopodium* spores are acetolysed during the manufacturing process, they can withstand acetolysis. Effects of chemicals on *Lycopodium* show that only colour changes are caused by acetolysis or HCl treatment (Sengupta, 1975). On the other hand, it has been shown that acetolysis or oxidation selectively destroys the cysts of the Polykrikaceae and Protoperidiniaceae (Reid, 1977; Marret, 1993). KOH treatment causes destruction of the Protoperidiniaceae after five minutes (de Vernal et al., 1996, and Mertens, pers. obs.) and causes swelling of the palynomorphs. Likewise, methods using H_2O_2 (Riding et al., 2007) result in the destruction of protoperidiniacean cysts (Riding, pers. comm., Hopkins and

Table 5 The results of the counts of samples processed and counted by Lab 21, processed with one processing technique. According to the statistical test by Maher (1981), the results are reproducible.

Lab number	*Variable / sample*	*North Sea*	*Celtic sea*	*NW Africa*	*Benguela*
21a	Dinoflagellate cysts/g	1547	2581	27851	172078
	95% confidence limits (Maher, 1981)	1265-1885	2092-3327	21612-32060	138365-206955
21b	Dinoflagellate cysts/g	1447	2723	24929	170888
	95% confidence limits (Maher, 1981)	1166-1785	2117-3354	19294-28216	135585-200884

McCarthy, 2002; Mertens, pers. obs.). This has also been demonstrated for Late Cretaceous peridinioid dinoflagellate cysts (Schrank, 1988). Oxidation with Schulze's solution by laboratory 22b resulted in the near complete destruction of the RBC, SBC and other heterotrophs in all samples, and led to the relative enrichment of resistant pollen and reworked non-peridinioid dinoflagellate cysts. Cold HF and HCl have never been reported to destroy dinoflagellate cysts. However, hot rinses with HCl after the HF treatment were particularly harmful to recent peridinoid cysts (Dale, 1976). Palynomorphs treated with warm HF clearly showed traces of deterioration: destruction of delicate structures with fragmentation along sutures and changes in wall texture with a thickening of the robust structures (Plate I, 11 and 16, Plate III, 6). It can be concluded that this assumption is acceptable when chemical degradation is minimized by using only cold hydrochloric and hydrofluoric acid.

5) Sonication causes no mechanical degradation of the pollen and spores or dinoflagellate cysts

The extensive use of ultrasound will not harm any dinoflagellate cysts according to Funkhouser and Evitt (1959), however, other authors report differential damage (e.g. Hodgkinson, 1991). This has not yet been checked in a quantitative manner for dinoflagellate cysts. The use of a sonic oscillator, although dependent on frequency (Marceau, 1969), is extremely damaging: the sonication by laboratory 8 resulted in the destruction of RBC and SBC in the Benguela sample (Plate IV, 20). Laboratory 18a used an ultrasonic bath for 30 minutes, and this resulted in extensive damage to the cysts. Many cysts were fragmented, often with broken or even lost spines and were often clustered (Plate I, 17, Plate III, 13, Plate IV, 11). In addition microforaminiferal linings were often fragmented. This assumption is thus acceptable when an ultrasonic bath is not used for too long. A limit of 60 seconds is proposed.

6) Centrifugation causes no mechanical degradation of the palynomorphs

No visible signs were noted that this technique causes degradation of the cysts. This assumption is thus acceptable.

7) Sieving causes no loss of palynomorphs

Lignum et al. (2008) demonstrated that sieving should be done with a sieve mesh width smaller than 15 µm. Our results confirm this observation. Laboratories using nylon sieve with widths of 20 µm (laboratory 1a, 1c) showed extremely high absolute abundances. This suggests that significant losses of *Lycopodium* spores occurred during the sieving process, even larger than the 20% that is proposed by Lignum et al. (2008). No significant loss of cysts was documented in this study. It is possible that cysts of *Pentapharsodinium dalei* pass through 20 µm sieves, this species was present in such low abundances in the studied samples to significantly affect relative or absolute abundances. This assumption is thus acceptable when mesh sizes smaller than 15 µm are used.

8) Decantation causes no loss of palynomorphs

An experiment was done to determine how many *Lycopodium* spores were lost during decanting and sieving. One gram of the NW Africa sample together with one *Lycopodium* tablet, was processed with a HCl/HF/HCl cycle, followed by sieving on a nylon mesh of 10 µm. After every decantation, the decanted fluid was filtered through a 0.25 µm Millepore filter. What remained on the filter was counted under a transmitted light microscope. Only *Lycopodium* spores were left on the filters, as well as some amorphous organic matter (Table 6). The number of spores will be dependent of the size of the filter used. Apparently 24% of the *Lycopodium* spores were lost during decanting. This is not surprising, since it is well-known that *Lycopodium* spores float (e.g. Salter et al., 2002). An extra 1.3% was left on the filter and 1% got stuck to handling material (e.g. spatula, tube). In the slides only 43.4% of the *Lycopodium* spores were found. An additional 30.2% spores were unaccounted for, and could have been lost during sieving

and/or could have been obscured by other material in the slides to some extent. Because we did not expect any significant losses to occur during sieving, we did not capture sieved material during this experiment. However, we tested sieving a complete *Lycopodium* tablet on 10 µm and capture on a 0.25 µm sieve. We found losses to be 0.79% when gently pouring the dissolved tablet over the sieve and subsequent washing, 0.97% when using a hand pump to facilitate sieving and 2.01% when using a pipette tip. Lignum et al. (2006) recorded losses up to 5.8 ± 1.2% for 15 µm meshes. It can thus be assumed that only a small part of the missing spores were pushed through the 10 µm nylon sieve. Presumably, spores are often concealed by being obscured by other material, and this plays a more significant role in explaining the missing amount of spores. Also, it is possible that due to the texture of the exines of *Lycopodium* spores, the spores get more easily caught in the sieves than smoother palynomorphs. However, this loss can be easily checked by the observer.

Table 6: Results of an experiment to look into the effects of manipulations on loss of Lycopodium spores. Shown is the number of Lycopodium spores lost during each manipulation. It is supposed that one tablet contains 18583 spores, so the % is calculated by dividing the number of counted spores by 18583 spores.

	Counted *Lycopodium* spores	%
HCl treatment:		
First decantation	916	4.9
Second decantation	267	1.4
Third decantation	2485	13.4
HF/HCl treatment:		
First decantation	6	0.0
Second decantation	143	0.8
Third decantation	650	3.5
Left on filter (not washed off)	242	1.3
Left in tube + stuck on spatula	187	1.0
Found on slides	8067	43.4
Total	12963	69.8
Missing spores	5620	30.2

9) Pre-sieving causes no losses

It is unclear to what extent presieving causes loss of *Lycopodium* spores, although it is evident that it should be avoided in samples from high productivity areas, where high production of amorphous organic matter forms large clusters in the sediment, which can be discarded with the large fraction. However; it can be easily checked whether *Lycopodium* spores were lost. This assumption is thus not acceptable.

10) Heavy liquid separation causes no loss of Lycopodium spores

It has been noted that density separation with heavy liquids can cause incorporation of mineral particles modifying the density of the heavy liquid (de Vernal et al., 1996). Litwin and Traverse (1989) recommend pyrite to be removed prior to density separation. The results of this study do not show any obvious difficulties with this processing step, although for clarity further study is suggested.

From these considerations it can be concluded that a significant amount of *Lycopodium* spores are lost, mainly during decanting and sieving. There is little evidence that there is loss of dinoflagellate cysts during these manipulations.

5 Conclusions and recommendations

• This study was designed as a comparative one, where the degree of variability in preparations could be objectively assessed. The laboratories concerned agreed to take part on the basis that the results would be presented anonymously, in order to ensure maximum participation. The point of this work was to carefully study the techniques used and to encourage best practice in the future. This initial work presents a firm basis for more methodological research.

• The exercise demonstrated that relative abundances are reproducible, but underlined the urgent need for taxonomic intercalibration.

• The study also shows that counting 300 dinoflagellate cysts is sufficient both in terms of diversity and absolute abundances.

• Absolute abundance calculations of dinoflagellate cysts are dependent on processing methodology, since *Lycopodium* spores are being lost during

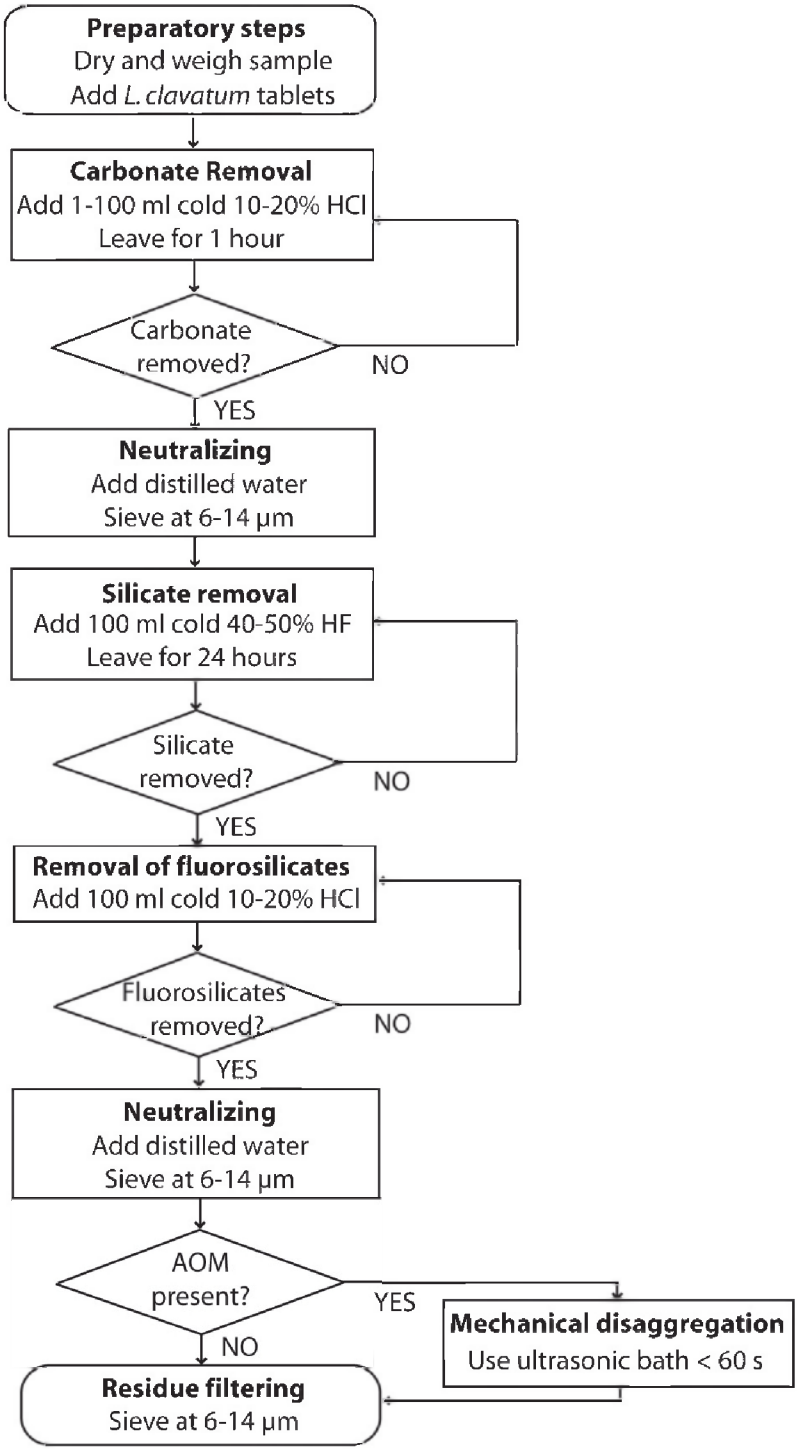

Figure 1 Flow-chart of the proposed standardized method. AOM stands for amorphous organic matter.

different processing steps.

• It is possible that some of the laboratories consistently over- or underestimate concentrations. The addressed problems in methodology might partly explain these outliers. Future work should elucidate possible corrections by detailed investigation of every different processing step.

• At the current state of affairs, there are three possible choices the Quaternary worker can make to calculate reproducible absolute abundances:

1. Standardize methodology for the extraction of dinoflagellate cysts.

Since samples can be reproducible when one fixed methodology is followed (see 4.3), a standard methodology is suggested (Figure 1). We consider that there are critical steps that must be avoided in this standard method when preparing samples for dinoflagellate cyst work: the use of oxidation, KOH, warm acids, acetolysis, mesh sizes larger than 15 µm, decanting (substituted by sieving) and sonication longer than 1 minute. During sieving, care should be taken to avoid *Lycopodium* spores being forced through the sieve. A certain degree of freedom is allowed in the number of HCl and HF cycles, length of ultrasonication (0-60 seconds), duration of sieving and sieve mesh size (6-14 µm), Care should be taken to neutralize HF by diluting at least ten times before sieving. Further studies are required to fine-tune the method by focusing on designated issues.

2. Adding Lycopodium tablets at the end of processing

The marker grain method is based on the assumption that there is no selective loss of fossil and exotic pollen during the procedures. However, this assumption has never been checked. Our study suggests that predominantly *Lycopodium* spores are lost, and that losses of dinoflagellate cysts are negligible. Therefore the addition of *Lycopodium* tablets at the end of the preparation is suggested, thus limiting the loss of *Lycopodium* spores. However, this method is contrary to spiking with an internal standard before the start of preparation.

3. Alternative methods

Alternative methods can be used, but may not yield better results. The use of microbeads was introduced by Ogden (1986), but often results in much higher abundance estimates, apparently because of difficulty in sustaining an even suspension of the particles in the stock solution: the higher specific gravity of microspheres causes them to settle three to four times more rapidly than pollen grains (McCarthy, 1992). Other marker-grain methods, such as the *Eucalyptus globulus* marker-grain method (Matthews, 1969), has also been used (e.g. de Vernal et al., 1987). However, it is not known whether these methods give more reliable results. The aliquot method gives more accurate results than the *Lycopodium* method in our study, but unfortunately not much is known about the precision of this method.

Additional information

Samples were provided by Karin Zonneveld, James Scourse and André Catrijsse, and subsampled by Kenneth Mertens and Koen Verhoeven before sending of to cooperating laboratories. Processing and counting of the samples was done at the cooperating laboratories. Interpretations were done by Kenneth Mertens. This chapter has been accepted for publication in *Review of Paleobotany and Palynology.*

CHAPTER 4

Process length variation in cysts of a dinoflagellate, *Lingulodinium machaerophorum*, in surface sediments: investigating its potential as salinity proxy

ABSTRACT

A biometrical analysis of the dinoflagellate cyst *Lingulodinium machaerophorum* (Deflandre and Cookson 1955) Wall, 1967 in 144 globally distributed surface sediment samples revealed that the average process length is related to summer salinity and temperature at a water depth of 30 m by the equation (salinity/temperature) = (0.078*average process length + 0.534) with $R^2 = 0.69$. This relationship can be used to reconstruct palaeosalinities, albeit with caution. The particular ecological window can be associated with known distributions of the corresponding motile stage *Lingulodinium polyedrum* (Stein) Dodge, 1989. Confocal laser microscopy showed that the average process length is positively related to the average distance between process bases ($R^2 = 0.78$), and negatively related to the number of processes ($R^2 = 0.65$). These results document the existence of two end members in cyst formation: one with many short, densely distributed processes and one with a few, long, widely spaced processes, which can be respectively related to low and high salinity/temperature ratios. Obstruction during formation of the cysts causes anomalous distributions of the processes. From a biological perspective, processes function to facilitate sinking of the cysts through clustering.

1. Introduction

Salinity contributes significantly to the density of seawater, and is an important parameter for tracking changes in ocean circulation and climate variation. Palaeosalinity reconstructions are of critical importance for better understanding of global climate change, since they can be linked to changes of the thermohaline circulation (Schmidt et al., 2004). Quantitative salinity reconstructions have been proposed on the basis of several approaches that use, for example, foraminiferal oxygen isotopes (e.g. Wang et al., 1995), $\delta^{18}O_{seawater}$ based on foraminiferal Mg/Ca ratios and $\delta^{18}O$ (e.g. Schmidt et al., 2004; Nürnberg and Groeneveld, 2006), alkenones (e.g. Rostek et al., 1993), the modern analogue technique applied to dinoflagellate cyst assemblages (e.g. de Vernal and Hillaire-Marcel, 2000) and δD in alkenones (e.g. Schouten et al., 2006; van der Meer et al., 2007; 2008). However, none of these approaches is unequivocal (e.g. alkenones; Bendle et al., 2005).

Some planktonic organisms are known to show morphological variability depending on salinity, e.g. variable noding in the ostracod *Cyprideis torosa*, van Harten (2000) and morphological variation in the coccoliths of *Emiliania huxleyi* (Bollman and Herrle, 2007). A similar dependence has been reported for *Lingulodinium machaerophorum* (Deflandre and Cookson,

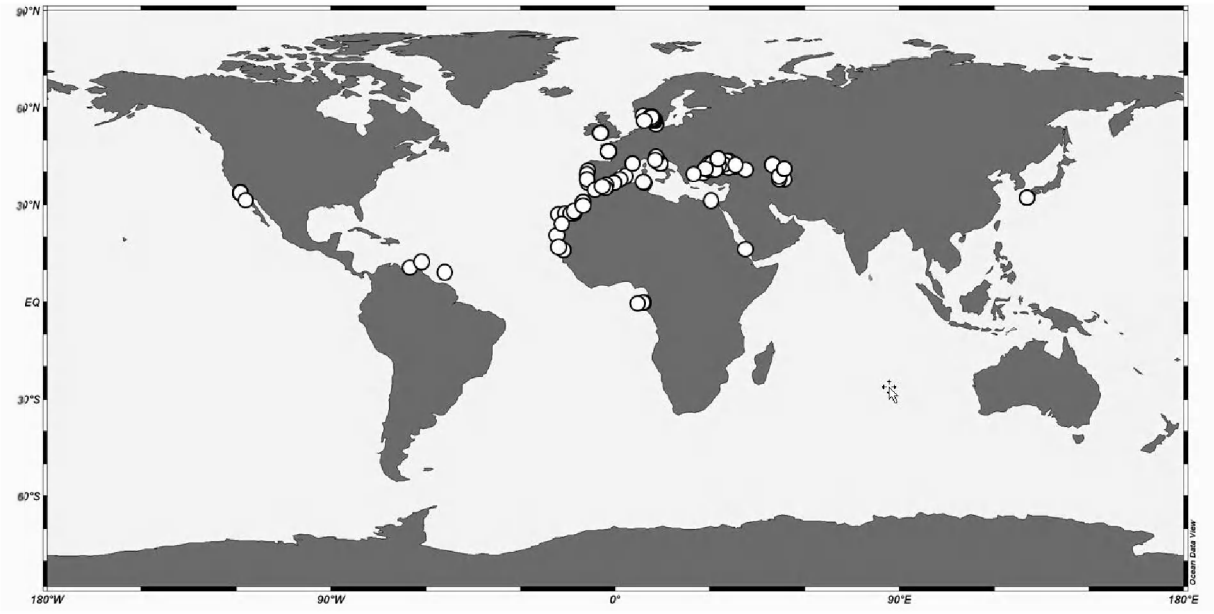

Figure 1 Distribution of the 144 surface samples where *Lingulodinium machaerophorum* process lengths were studied.

1955) Wall, 1967, the cyst of the autotrophic dinoflagellate *Lingulodinium polyedrum* (Stein) Dodge, 1989 which forms extensive harmful algal blooms reported from California (Sweeney, 1975), Scotland (Lewis et al., 1985), British Columbia (Mudie et al., 2002), Morocco (Bennouna et al., 2002), West Iberia (Amorim et al., 2001) and other coastal areas. This species can be considered a model dinoflagellate since it is easily cultured and has been the subject of numerous investigations. An extensive review of these studies was given by Lewis and Hallett (1997).

Process length variation of *Lingulodinium machaerophorum* was initially related to salinity variations in the Black Sea by Wall et al. (1973), and subsequently investigated in other regions (Turon, 1984; Dale, 1996; Matthiessen and Brenner, 1996; Nehring, 1994, 1997; Ellegaard, 2000; Mudie et al., 2001; Brenner, 2005; Sorrel et al., 2006; Marret et al., 2007). Kokinos and Anderson (1995) were the first to demonstrate the occurrence of different biometrical groups in culture experiments. Later culture experiments (Hallett, 1999) revealed a linear relationship between average process length and salinity, but also temperature.

The process length of *L. machaerophorum* as a salinity proxy represents a large potential for palaeoenvironmental studies, since this species occurs in a wide range of marine conditions (Marret and Zonneveld, 2003), and can be traced back to the Late Paleocene (Head et al., 1996). The aim of the present study was to evaluate whether the average process length shows a linear relationship to salinity and/or temperature, and to assess its usability for palaeosalinity reconstruction. To achieve this goal, *L. machaerophorum* cysts were studied from surface sediments collected in numerous coastal areas. Confocal laser microscopy was used for the reconstruction of the complete distribution of the processes on the cyst wall, which has important implications for cyst formation.

2. Material and methods

2.1 Sample preparation and light microscopy

A total of 144 surface sediment samples were

Table 1 Average process length from LM measurements, standard deviation, body diameter and standard deviation, average summer temperature and salinity at 30 meter water depth, ratio between both and density calculated from both. Results are sorted by short to long process length.

Region	# samples	Processes measured	Average process length (µm)	Stdev (µm)	Average body diameter (µm)	Stdev (µm)	Average Summer T_{30m}	Average Summer S_{30m}	S_{30m}/T_{30m}	Density (kg/m³)	Preservation	Reference
Caspian Sea-Aral Sea	13	1320	5.6	3.4	48.1	6.1	15.72	12.72	0.81	1008.87	Bad to good	Marret et al. (2004), Sorrell et al. (2006), Leroy et al. (2006) and Leroy (unpublished data), Leroy et al. (2007)
Etang de Berre	2	300	7.5	2.5	44.9	4.5	19.91	26.10	1.31	1018.14	Average	Leroy (2001) and Robert et al. (2006)
Japan	5	735	8.0	1.9	45.3	3.7	24.54	33.72	1.37	1022.64	Good	Matsuoka (unpublished data)
Caribbean – West Equatorial Atlantic	6	306	13.0	4.4	44.1	6.4	26.19	36.08	1.38	1023.92	Average	Vink et al. (2000), Mertens et al. (2009a) and Vink et al. (2001)
Scandinavian Fjords – Kattegat-Skagerrak	26	2271	13.2	4.2	47.9	6.4	16.55*	24.14*	1.46*	1017.43	Bad to good	Grøsfjeld and Harland (2001), Gundersen (1988), Ellegaard (2000), Christensen et al. (2004) and Persson et al. (2000)
East Equatorial Atlantic – Dakar Coast	7	903	13.2	3.4	46.6	6.2	22.88	35.52	1.55	1024.49	Bad to good	Marret et al. (1994) and Bouimetarhan et al. (unpublished data).
Black Sea and Marmara Sea	35	5195	15.0	4.1	46.3	4.6	12.22	20.08	1.64	1015.14	Good	Verleye et al. (2009), Caner and Algan (2002), Caner (unpublished data), Cagatay et al. (2000), Naudts (unpublished data), Popescu et al. (unpublished), Mudie et al. (2007) and van der Meer et al. (2008)
Portugal - Brittanny	9	1350	16.8	3.6	45.3	5.5	16.53	35.22	2.13	1025.93	Good	Ribeiro et al. (unpublished data), Goubert (unpublished data)
NW Africa	12	1749	18.4	3.8	48.1	6.3	19.47	36.36	1.87	1026.07	Average to good	Holzwarth et al. (unpublished data), Kuhlmann et al. (2004), Richter et al. (2007)
Mediterranean – Red Sea	36	3507	19.6	4.4	45.6	6.1	18.39	37.57	2.04	1027.28	Average to good	Sangiorgi et al. (2005), Londeix (unpublished data), Combourieu-Nebout et al. (1999), Pirlet (unpublished data), Schoell (1974) and Kothoff et al. (2008)
Pacific	9	1224	21.2	4.3	47.7	6.1	14.39	33.45	2.32	1025.04	Good	Pospelova et al. (2008) and Peña-Manjarrez et al. (2005)
Celtic Sea	6	750	21.8	4.1	47.8	5.7	13.50	34.30	2.54	1025.88	Good	Marret and Scourse (2002)

*For this region data from 0 m water depth is used.

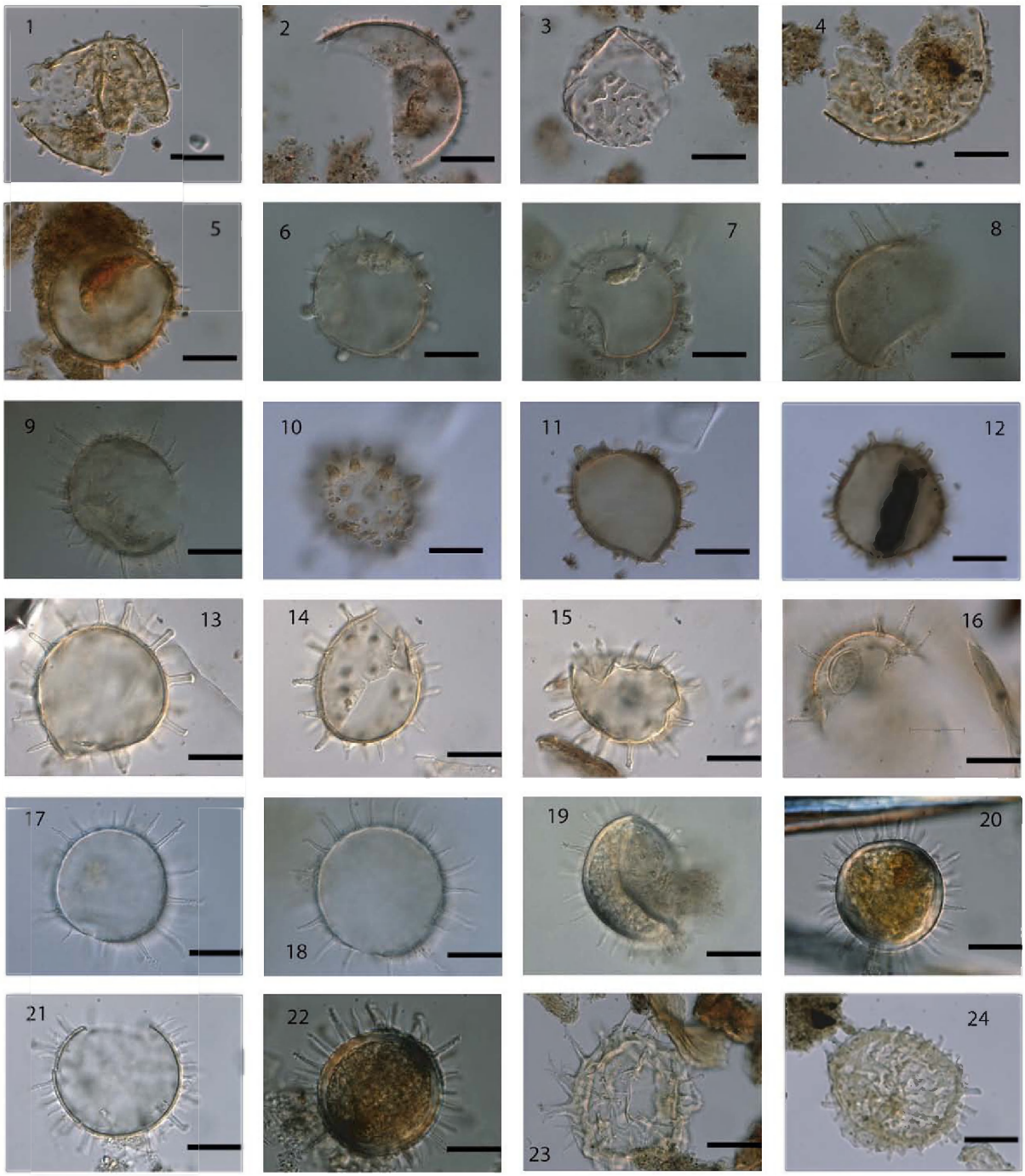

Plate I *Lingulodinium machaerophorum* cysts from Caspian sea (1–5), Aral Sea (6–9), Etang de Berre (10–12). Baltic Sea (13–15) and Scandinavian Fjords (16–24). Specific sample names are 1–4. CPO4. 5.US02. 6–7. AR23. 8–9. AR17. 10–12. Etang de Berre (19). 13. NG6. 14. NG. 7. 15. NG9. 16. Limfjord. Note inclusion of *Nannobarbophora acritarch*. 17. Havstenfjorden 18–19. Guumar Fjord 20–21. G2. 22. K2. 23–24. Risor Site. All scale bars are 20 µm.

studied for biometric measurements of *L. machaerophorum* cysts from the Kattegat–Skagerrak, Celtic Sea, Brittany, Portuguese coast, Etang de Berre (France), Mediterranean Sea, Marmara Sea, Black Sea, Caspian and Aral Seas, northwest African coast, Canary Islands, coast of Dakar, Gulf of Guinea, Caribbean Sea, Santa Monica Bay (California), Todos Santos Bay (Mexico) and Isahaya Bay (Japan) (Figure 1). Most samples were core top samples from areas with relatively high sedimentation rates, and can be considered recent, i.e. representing a few centuries (see Supplementary data). Five samples have a maximum age of a few thousand years, but since process lengths are as long as processes of recent, nearby samples, these were also considered representative. In general, the studied cysts provide us a global view of the biometric variation of cysts formed during the last few centuries by *L. polyedrum*. It is assumed here that the environmental conditions steering the morphological changes within the cysts are similar to recent environmental conditions.

All the cysts were extracted from the sediments according to maceration methods that are described in the literature shown in Table 1. Most methods used standard maceration techniques involving hydrochloric acid and hydrofluoric acid, sieving and/or ultrasonication. Regardless of the method used, the cysts all appeared similar in terms of preservation (Plates I–IV).

All measurements were made using a Zeiss Axioskop 2 and an Olympus BH-2 light microscope, equipped with an AxioCam RC5 digital camera (Axiovision v. 4.6 software) and Color View II (Cell F Software Imaging System) respectively, and 100x oil immersion objectives. All measurements were performed by Kenneth Mertens, except for the samples from Portugal, which were measured by Sofia Ribeiro (Department of Biology, University of Copenhagen). Observer bias did not influence the measurements.

For each sample, the length of the three longest visible processes and the largest body diameter were measured of 50 cysts for each sample. Measuring 50 cysts gave reproducible results: in sample GeoB7625-2 from the Black Sea, three process lengths per cyst for 50 cysts were measured, and was then repeated on 50 different cysts, showing no significant differences ($\bar{x}$ = 13.50 µm ± 2.99 µm and $\bar{x}$ = 13.21 µm ± 2.62 µm, t-test: p = 0.37). The length of each process was measured from the middle of the process base to the process tip. The absolute error in process measurement was 0.4 µm. Within each cyst, three processes could always be found within the focal plane of the light microscope, and for this reason this number seemed a reasonable choice. Three reasons can be advanced for choosing the longest processes. Firstly, the longest processes reflect unobstructed growth of the cyst (see below). Secondly, the longest processes allowed to document the largest variation, and this enhanced the accuracy of the proxy. Thirdly, since only a few processes were parallel to the focal plane of the microscope, it was imperative to make a consistent choice. Sometimes fewer than 50 cysts were measured, if more were not available. Fragments representing less than half of a cyst were not measured, nor were cysts with mostly broken processes.

2.2 Salinity and temperature data

The biometric measurements on cysts from the different study areas were compared to both seasonal and annual temperature and salinity at different depths – henceforth noted as T_{0m}, T_{10m}, ... and S_{0m}, S_{10m}, ... , using the gridded ¼ degree World Ocean Atlas 2001 (Stephens et al., 2002; Boyer et al., 2002) and the Ocean Data View software (Schlitzer, R., http://odv.awi.de, 2008). For the Scandinavian Fjords, in situ data were available from the Water Quality Association of the Bohus Coast (http://www.bvvf.com).

2.3 Confocal laser microscopy

Confocal microscopy was performed using a Nikon C1 confocal microscope with a laser wavelength of 488 nm and laser intensity of 10.3%. No colouring was necessary since the cysts were sufficiently autofluorescent. The Z-stack step size was 0.25 µm with a Pixel dwell time of 10.8 µs. The objective used was a 60x/1.40/0.13 Plan-Apochromat lens with oil immersion. After correcting the z-axis for differences in refractive index between the immersion oil and glycerine jelly (here a factor of 78% of correction was used), images were rendered to triangulated

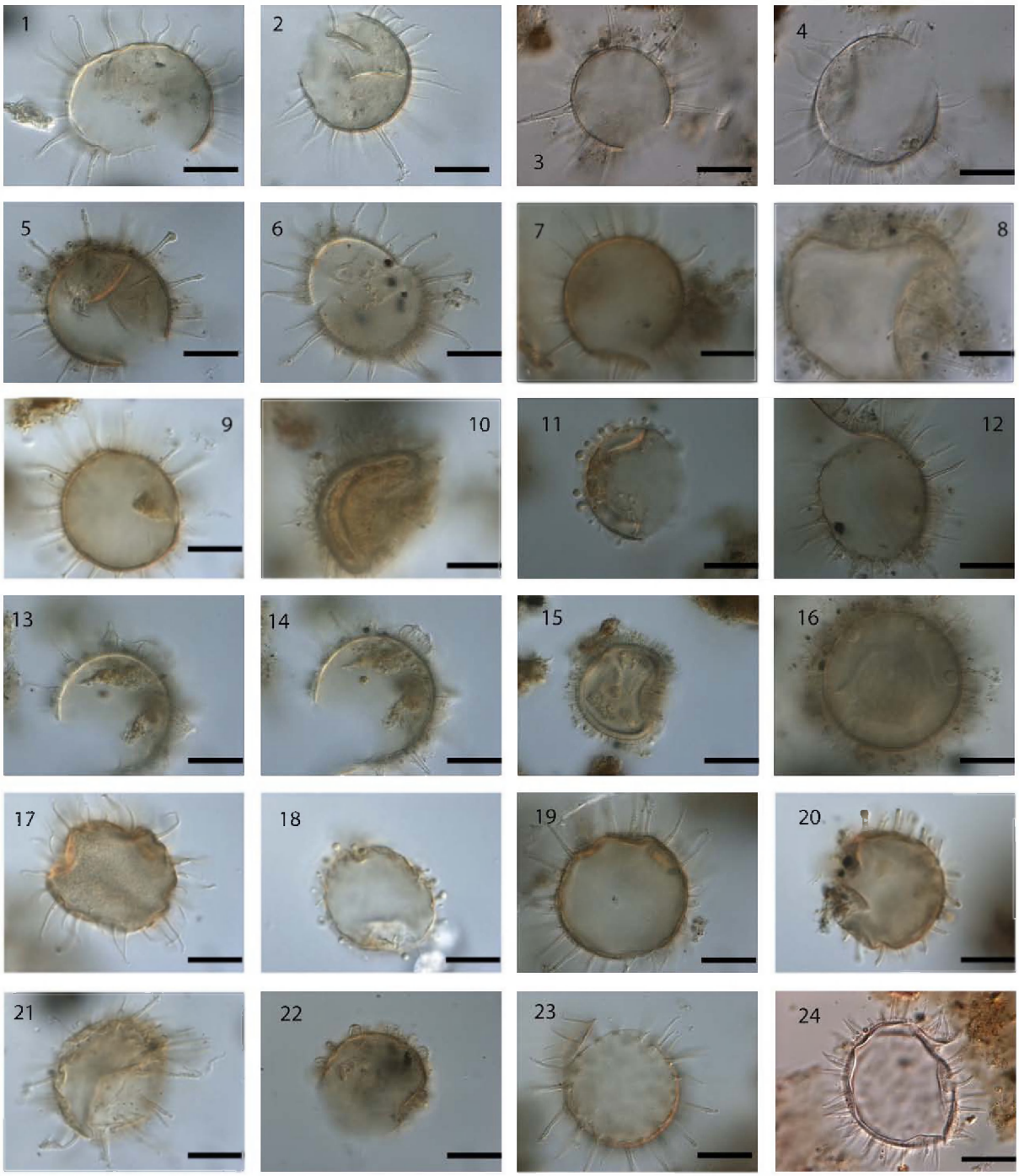

Plate II *Lingulodinium machaerophorum* cysts from Marmara Sea (1-4) and Black Sea (5-24). Note the wide range of morphotypes occurring in these samples. Specific sample names are: 1-2. Dm13 3-4. Dm5. 5-6. Knorr134.72. 7. Knorr 134.51. 8. GGC18. Swollen cyst due to use of acetolysis. 9-10. Knorr 134.35.11-12.Knorr 134.2. 13-15. B2KS33 0-1. Note merged processes in 13 and 14. 16. B2 KS01 0-1. Note globules at basis of processes. 17-18. All 1464.19. All 1443. 20-21. All1438. 22. All 434. Note merged processes. 23. All145.1. 24. GeoB7625. Coloured with Safranin-O. All scale bars are 20 µm.

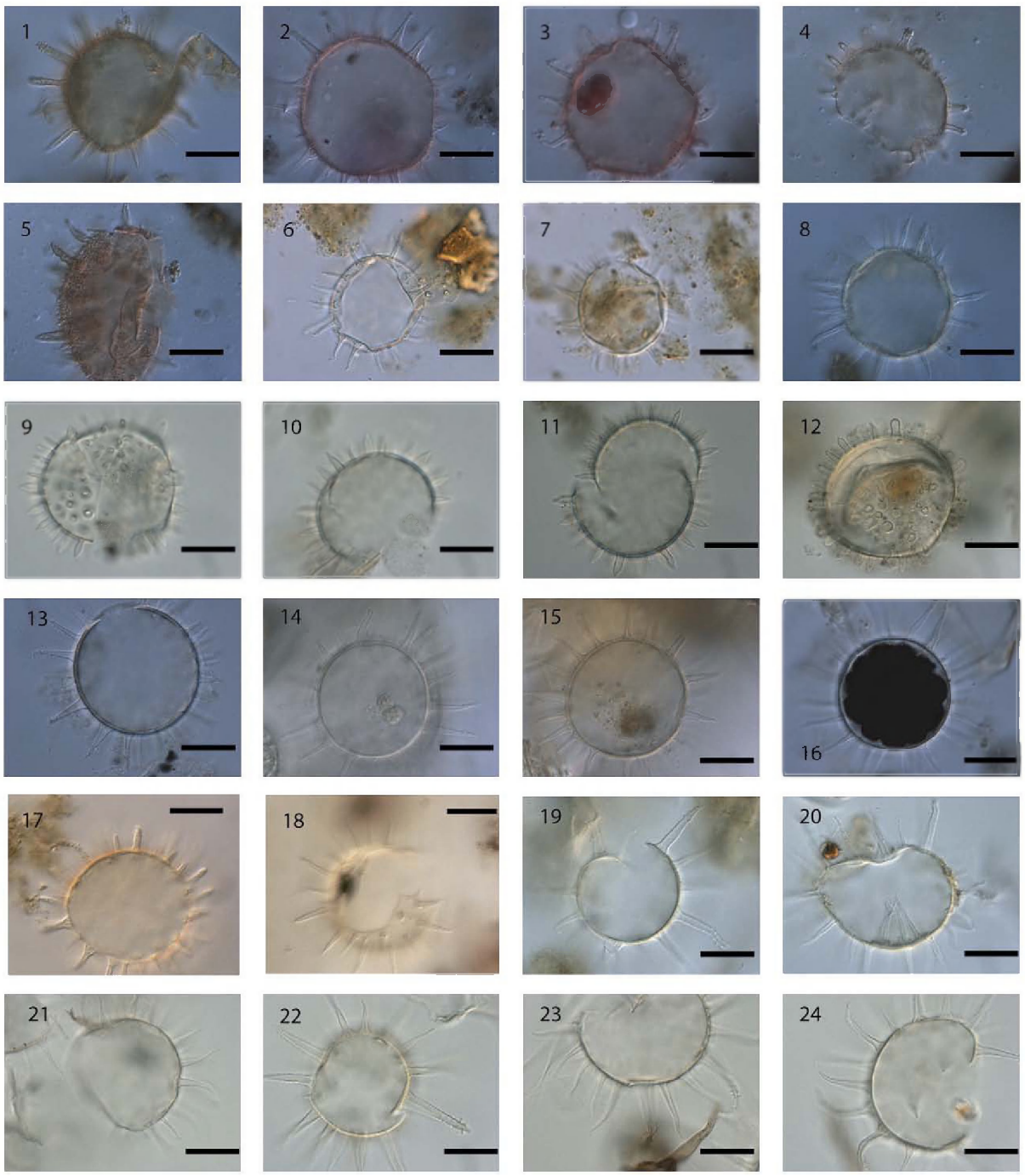

Plate III *Lingulodinium machaerophorum* cysts from East Equatorial Atlantic (1-7), West Equatorial Atlantic (8), Japan (9-12), Brittanny (13-16), Portugal (17-18) and NW Africa (19-24). Specific sample names are: 1. 6437-1. 2-3. 6847-2. 4-5. 6875-1. 6-7. GeoB9503, Dakar. 8. M35003-4. 9-10. AB22. 11. AB40. 12. ISA2. 13. BV1. 14-15. BV3. 16. BV5. 17-18. Tejo. 19-20. GeoB4024-1. 21. GeoB5539-2. 22-24. GeoB5548. All scale bars are 20 µm.

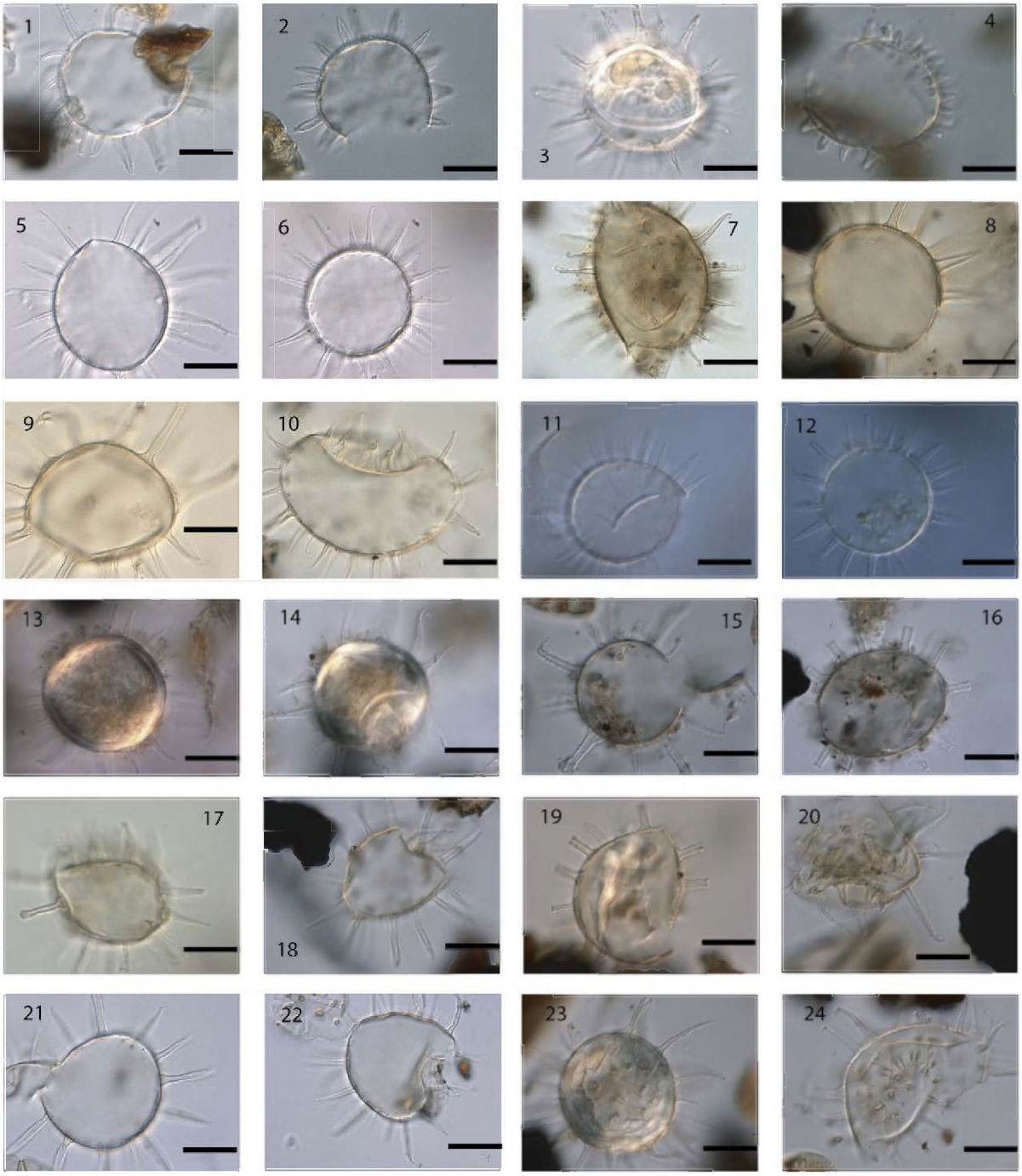

Plate IV *Lingulodinium machaerophorum* cysts from Mediterranean (1-11), Red Sea (12), Celtic Sea (13-16) and Pacific Ocean(17-24). Note the widely distributed very long processes in Celtic Sea and Pacific Ocean samples. Specific sample names are: 1. North Adriatic AN71. 2-4. North Adriatic AN71. 5-6. Nile Delta. 7. 273.4. 8. 515.3. 9. 516.6. 10. 521.3. 11-12. Red Sea VA01-200P. 13-14. Station9 6.99. 15. Station 9 5.00. 16. Station 9 2.99 with truncated processes. 17. Todos Santos Bay (Mexico). 18-19. Santa Monica Bay, UVic07-896 18 with truncated processes. 20. UVic07-897. 21-22. UVic07-898. 22 with truncated processes. 23-24. UVic07-902. All scale bars are 20 µm.

surfaces (.stl files) with Volume Graphics VGStudioMax© software. These were imported in Autodesk 3DsMax©, where XYZ coordinates of the base and top of the processes were recorded. From these coordinates Euclidean distances were calculated, enabling the calculation of the process length and the distances between the processes. Distances to the two closest processes of each process were calculated, and by averaging these numbers, the average distance between processes was calculated. A more detailed description of the methodology is given at http://www.paleo.ugent.be/Confocal.htm.

3. Results

3.1 Preservation issues

To establish the validity of the measurements, preservation needs to be taken into account. Two types of degradation were considered: mechanical and chemical. Three categories were used to describe the mechanical degradation of the cysts: bad (most cysts were fragmented or torn, and processes were broken), average (about half of the cysts were fragmented or torn, and few processes were broken, and good (few cysts were torn or fragmented, and were often still encysted) (see Table 1).

The differences in mechanical breakdown were, from our experience, largely caused by post-processing treatments such as sonication. Prolonged sonication, however, does not significantly change process length variation. The sample from Gullmar Fjord (average process length of 14.6 µm, standard deviation SD 4.0) was sonicated in an ultrasonic bath for two minutes and the results were not significantly different from samples that were not sonicated (average process length of 14.3 µm, SD 4.1, t-test: $p = 0.38$).

Chemical breakdown, on the other hand, could be caused by oxidation or acid treatment. *L. machaerophorum* is moderately sensitive to changes in oxygen availability (Zonneveld et al., 2001). Cysts from samples treated with acetolysis were clearly swollen (Plate II.8). Most interestingly, both processes and cyst body swell proportionately. These samples were not used for analysis. Similar results were noted after treatment with KOH. These maceration methods are not suitable for biometric studies. Cysts extracted using warm HF showed traces of degradation (see

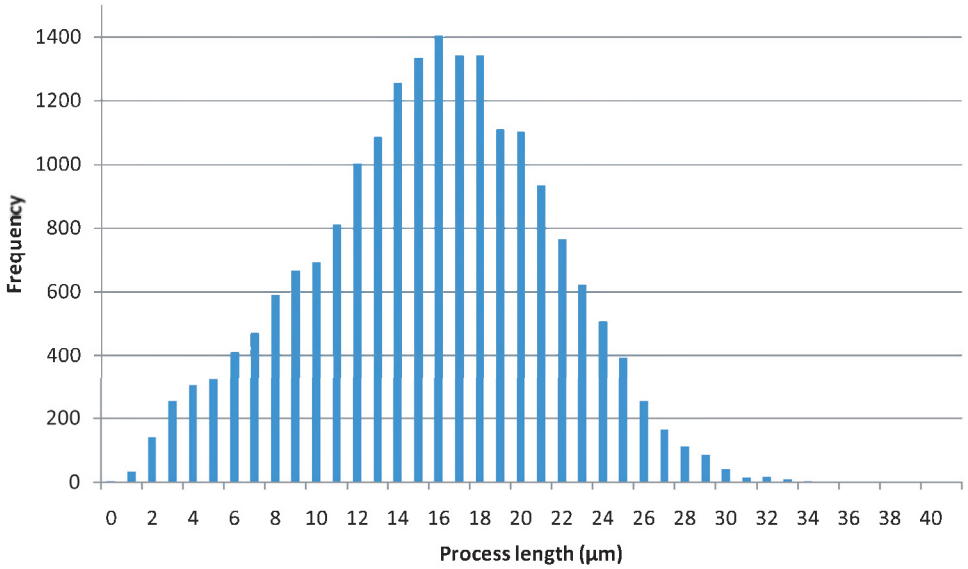

Figure 2 Size-frequency spectrum of 19,611 process length measurements.

Plate I.23; Plate II.24), but process length did not change.

3.2 Overall cyst biometrics for the multi-regional dataset

The 19,611 process length measurements resulted in a global average of 15.5 µm with a standard deviation of 5.8 µm, and a range from 0 to 41 µm (Figure 2). Most cysts encountered were comparable to the forms described by Kokinos and Anderson (1995), and bald cysts were rare. The range found is clearly broader than the 2 to 21 µm range postulated by Reid in 1974. The skewness of the distribution was -0.12, since there is some tailing at the left side of the size frequency curve (Figure 2). The asymmetric distribution was due to the fact that standard deviation increased with average process length. This could be explained partly by the methodological approach - errors on the larger measurements were larger, since larger processes were more often curved or tilted - and by the more common occurrence of cysts with relatively shorter processes in samples that mostly contain cysts with longer processes (also evident in regional size-spectra, Figure 4).

The 6,537 body diameter measurements resulted in an average body diameter of 46.6 µm with a standard deviation of 5.8 µm, over a range from 26 to 77 µm. This was again a broader range than the 31 to 54 µm given by Deflandre and Cookson (1955) and Wall and Dale (1968). This discrepancy could be explained partly by cysts sometimes being compressed or torn, yielding an anomalously long body diameter. This mechanical deformation of the cyst explains also a positive skewness of the size-frequency spectrum (Figure 3).

The averaged data of *L. machaerophorum* cysts in every region is given in Table 1, sorted from low to high average process length. Individual size-frequency spectra are shown in Figure 4 and the cysts are shown in Plate I.4. All measurements are available as Supplementary data.

3.3 Comparison of process length with salinity and temperature

Data from the Scandinavian Fjords and the Kattegat–Skagerrak were excluded from all relations since they significantly increased the scatter on all regressions. The reason is given in the Discussion (section 4.3).

The relation of the average process length of *L. machaerophorum* with only the salinity data, fitted best with the winter S_{0m} (R^2 = 0.54). When

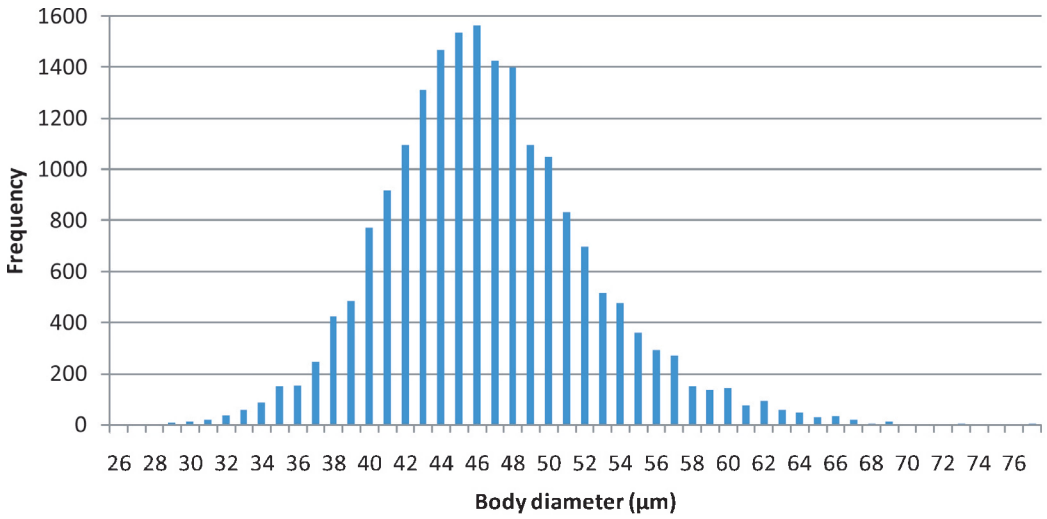

Figure 3 Size-frequency spectrum of 6211 body diameter measurements.

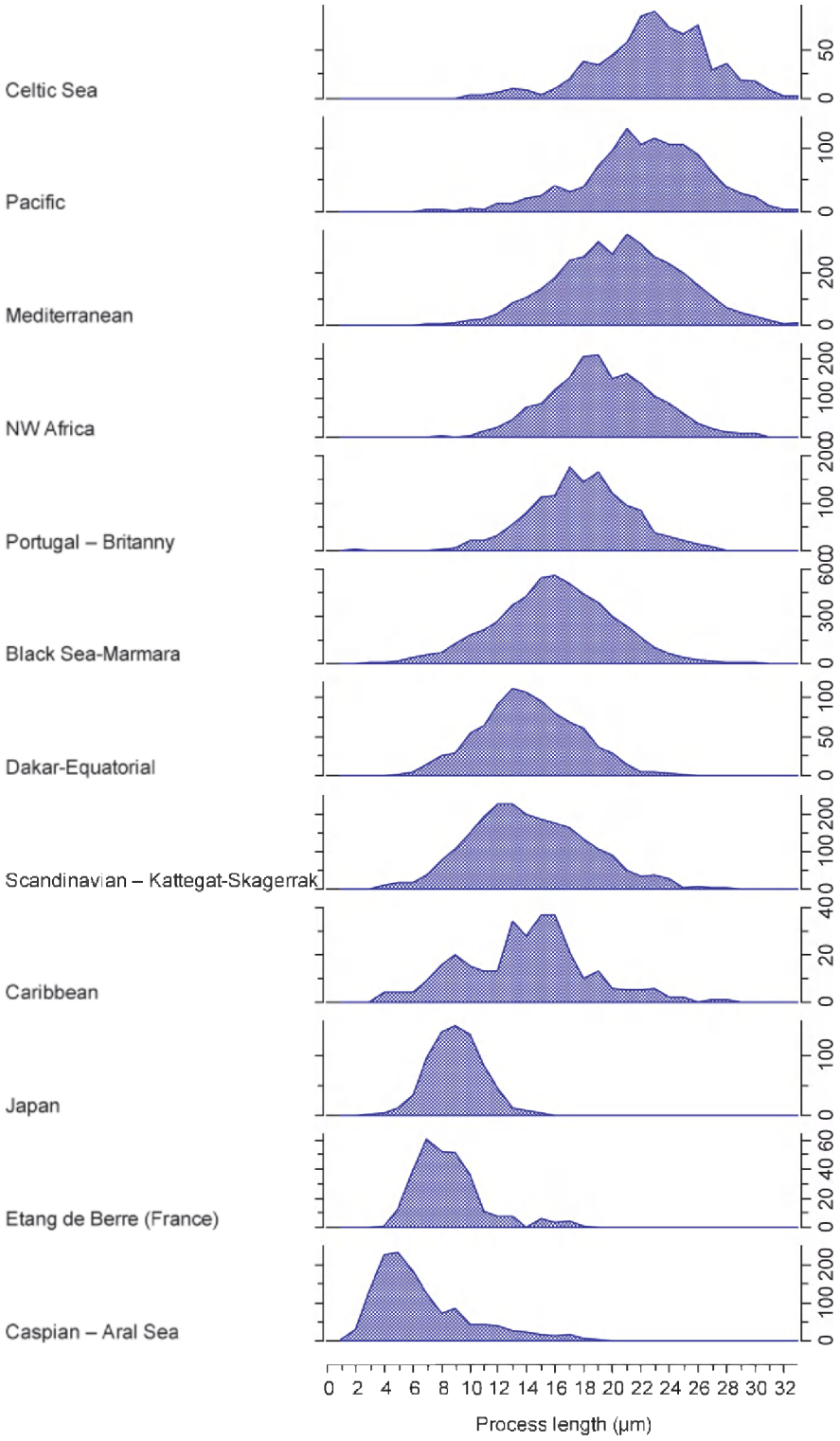

Figure 4 Size-frequency spectra of regional process measurements, sorted from top (long average processes) to bottom (short average processes).

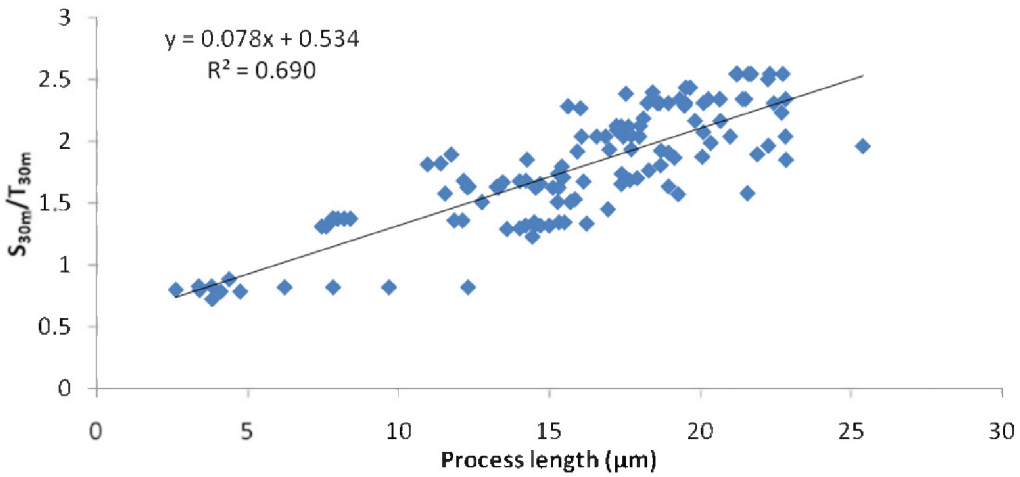

Figure 5 Regression between average process length and summer S30 m/T30 m for the 144 surface samples.

compared to temperature data alone, the best relationship was with the winter T_{50m} (R^2 = 0.06). A much stronger relationship could be found with salinity divided by temperature at a water depth of 30 m from July to September (summer). This relationship is expressed as (S_{30m}/T_{30m}) = (0.078*average process length + 0.534), and has a R^2 = 0.69 (Figure 5) and the standard error is 0.31 psu/°C. Since seawater density is dependent on salinity and temperature, it could be expected that density would have a similar relationship with process length. However, the regression with water density at 30 m water depth shows a stronger relation to process length (R^2 = 0.50) than with salinity alone (R^2 = 0.42 with summer S_{30m}), but not better than with S_{30m}/T_{30m}.

An overview of the results in the studied areas is given in Table 1. Next to average process length, salinity, temperature and S_{30m}/T_{30m}, seawater density data are given, and illustrate that this parameter does not show a better fit than the S_{30m}/T_{30m} ratio. The regression between this averaged data from each region is (S_{30m}/T_{30m}) = (0.085*average process length + 0.468), R^2 = 0.89 (Figure 6).

3.3.1 Process length in relation to body diameter

No relation between the process length and cyst body diameter was found (R^2 = 0.002). This was expected since culture experiments also revealed no relation between the body diameter and the salinity (Hallet, 1999). Furthermore, no significant relation was found between body diameter with the ratio between salinity and temperature at different depths. Variations in cyst body diameter are probably caused mainly by germination of the cyst or compression.

3.3.2 Process length in relation to relative cyst abundance

Mudie et al. (2001) found a correlation of R^2 = 0.71 between the relative abundance of *L. machaerophorum* and increasing salinity between 16 and 21.5 psu for Holocene assemblages in Marmara Sea core M9. To check this relationship in our dataset, the relative abundances of *L. machaerophorum* were determined in 92 surface samples. No significant linear relation between relative abundances in the assemblages and either the process length or the body diameter was found. No significant relationship between relative abundance and temperature or salinity data was found. This is not surprising since the relationship between relative abundances and environmental pa-

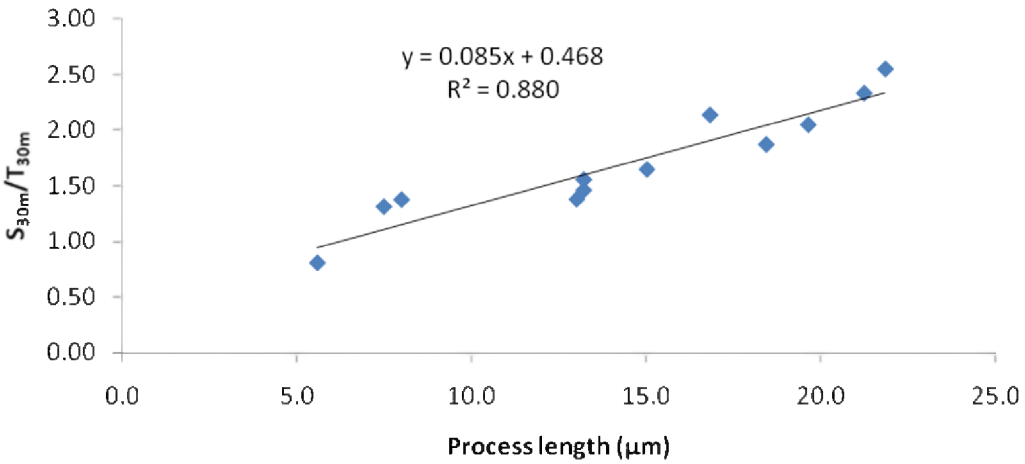

Figure 6 Regression between average process length and summer S30 m/T30 m averaged for every region separately.

rameters is not linear, but unimodal (Dale, 1996), and several other factors play a role in determining the relative abundances on such a global scale, mostly relative abundances of other species (closed-sum problems).

3.4 Confocal laser microscopy

All processes on 20 cysts from the North Adriatic Sea (samples AN71 and AN6b) and one from the Gulf of Cádiz (sample GeoB9064) were measured, resulting in 1460 process measurements. The average distances between the processes were also calculated. A summary of the results is given in Table 2. Process length ranged from 0 to 31 µm, which differs from the 1,983 process lengths from the North Adriatic Sea samples measured with transmitted light microscopy (6 to 34 µm). The shift in the frequency size spectra was obviously due to the fact that only the longest processes were measured (Figure 7). Most remarkable was the large peak around 3 µm for the confocal measurements. Apparently, a large number of shorter processes were present on most of these cysts.

It is noteworthy that the number of processes was significantly inversely related to the average process length (R^2 = 0.65) (Figure 8) and the average process length was significantly related to the average distance between the processes (R^2 = 0.78) (Figure 9). The lower R^2 can be explained by the incompleteness of the cysts: all cysts were germinated and thus lacking opercular plates, which can number between one and five or more in the case of epicystal archeopyles (Evitt, 1985). This implies that a large number of processes can be missing, and it would be subjective to attempt a correction for the missing processes. It was not possible to use encysted specimens since the strong autofluorescence of the endospore of these specimens obscured many of the least autofluorescent processes. No significant relation was found between the body diameter and the average process length (R^2 = 0.04), which supports the observation with transmitted light microscopy.

4. Discussion

4.1 Process length correlated to summer S_{30m}/T_{30m}: is it realistic?

The quasi unimodal size frequency spectrum of both process length and cyst body diameter (Figure 2-3), plus the correlation between the average process

Table 2 Average process length, standard deviation, number of processes measured and average distance between process bases from confocal microscopy in full measurements

Cyst number	Sample	Average length (µm)	Stdev length (µm)	# Processes measured	Body diameter (µm)	Average distance (µm)
2	AN71	9.82	5.78	79	44.53	4.35
4	AN71	7.26	5.72	89	39.84	3.76
5	AN71	15.87	5.06	50	56.89	5.79
7	AN71	9.80	6.36	72	45.11	4.68
9	AN71	17.79	6.41	62	43.25	6.78
10	AN71	10.32	6.49	67	39.95	4.55
11	AN71	12.25	1.90	56	43.26	6.21
12	AN71	6.85	4.82	107	39.34	3.98
13	AN71	11.50	7.26	89	43.32	4.76
14	AN71	15.88	7.27	61	51.76	6.90
15	AN71	13.20	6.19	28*	40.54	5.67
16	AN71	15.43	4.19	59	41.93	5.61
17	AN71	12.44	5.43	71	44.69	4.95
2	AN6B	11.79	6.09	71	36.38	4.40
4	AN6B	9.86	5.47	103	45.60	4.88
5	AN6B	9.14	7.13	102	42.87	4.05
6	AN6B	12.17	4.72	76	47.13	4.71
8	AN6B	12.53	4.53	58	57.84	5.66
9	AN6B	13.07	3.50	51	40.77	5.40
10	AN6B	10.30	4.68	76	41.20	4.44
1	GeoB9064	18.16	6.76	33	36.10	6.24
Average		**12.16**	**5.51**	**69.52**	**43.92**	**5.13**
Stdev		**3.11**	**1.33**	**21.06**	**5.68**	**0.91**

* This number was not used in the regression with process length, since less than half of this cyst was preserved.

length and the summer S_{30m}/T_{30m}, strongly confirm that all recorded cysts are ecophenotypes of a single species. It is furthermore not surprising that the most significant relation was found with the summer S_{30m}/T_{30m} depth. These three extra parameters – seasonality, temperature and depth – are discussed below.

Late summer–early autumn is generally the time of maximum stratification of the surface waters. Reduced salinity would enhance the water column stability with the generation of a pycnocline, and lowered water column turbulence, conditions that favour growth of *Lingulodinium polyedrum* (Thomas and Gibson, 1990). In most upwelling regions, this would coincide with periods of upwelling relaxation (Blasco, 1977). Late summer-early autumn is the time of the exponential growth phase of *Lingulodinium polyedrum*, which coincides with peak production of *Lingulodinium machaerophorum* cysts, at least in Loch Creran, northwest Scotland (Lewis et al., 1985), and in Todos Santos Bay, Mexico (Peña-Manjarrez et al., 2005). Culturing suggests that the cyst production is triggered by nutrient depletion, and influenced by temperature (Lewis and Hallett, 1997).

The relationship found between process length and both temperature and salinity is not surprising since the formation of processes can be considered a biochemical process (Hallett, 1999), dependent on both temperature (negative relation) and salinity (positive relation). The culture experiments by Hallett (1999) confirm a positive relation to salinity and a negative relation to temperature.

Moreover, the cysts are probably formed deeper

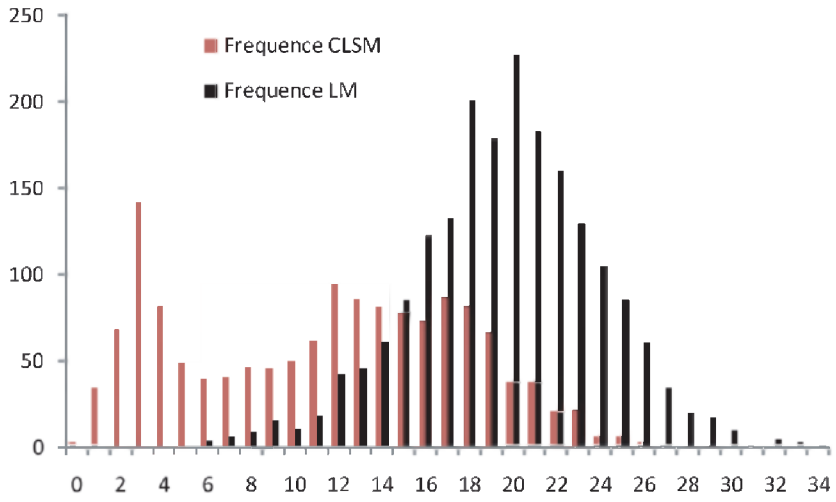

Figure 7 Comparison between the size-frequency spectra from 1460 confocal measurements (CLSM) from the North Adriatic Sea (samples AN71 and AN6b) and from the Gulf of Cádiz and 1983 light microscope (LM) measurements from the North Adriatic.

in the water column, which would explain the fit to a 30 meter depth. It is well known that *Lingulodinium polyedrum* migrates deep in the water column (Lewis and Hallett, 1997). A similar vertically migrating dinoflagellate, *Peridiniella catenata,* also forms cysts deeper in the water column, mostly at 30-40 m depth (Spilling et al., 2006). These cysts are probably formed within a range of water depths, and with 30 m depth reflecting an average depth.

The ranges of temperature (9–31°C) and salinity (12.4–42.1 psu) at 30 meters represent the window in which cyst formation takes place. Cultures show that *Lingulodinium polyedrum* forms cysts at salinities ranging from 10 to 40 psu (Hallett, 1999), which fits with the results obtained in this study. The relation to deeper salinity and temperature data suggests that cyst formation more often than not takes place deeper in the water column, where salinities may be higher and temperatures lower, which suggests that caution is needed before linking *Lingulodinium machaerophorum* cyst abundances directly to near surface data. This could explain the occurrence of cysts of *Lingulodinium polyedrum* in regions with surface salinities as low as 5 psu (e.g. McMinn, 1990, 1991; Dale, 1996; Persson et al., 2000).

No better relation was found with density despite its dependence on salinity and temperature. Apparently, density as calculated from salinity and temperature, and pressure (water depth) by Fofonoff and Millard (1983) is much more determined by salinity, and less by temperature, whereas we assume that measured average process length is influenced by a combination of these parameters.

4.2 Transport issues

Lingulodinium polyedrum occurs in estuaries, coastal embayments and neritic environments of temperate to subtropical regions (Lewis and Hallett, 1997). However, transport of the cysts into other areas by currents must be considered, and the records of *L. machaerophorum* in oceanic environments have been attributed to reworking or long-distance transport (Wall et al., 1977). A classic example is the upwelling area off northwest Africa where the cyst has been recorded over a much wider area than the thecate stage (Dodge and Harland, 1991). In this study, it was assumed that long-distance transport was not an important factor, since the transported cysts would be transported from areas with minor salinity and temperature differences, which would, according to the equation (see 2.3), be reflected in

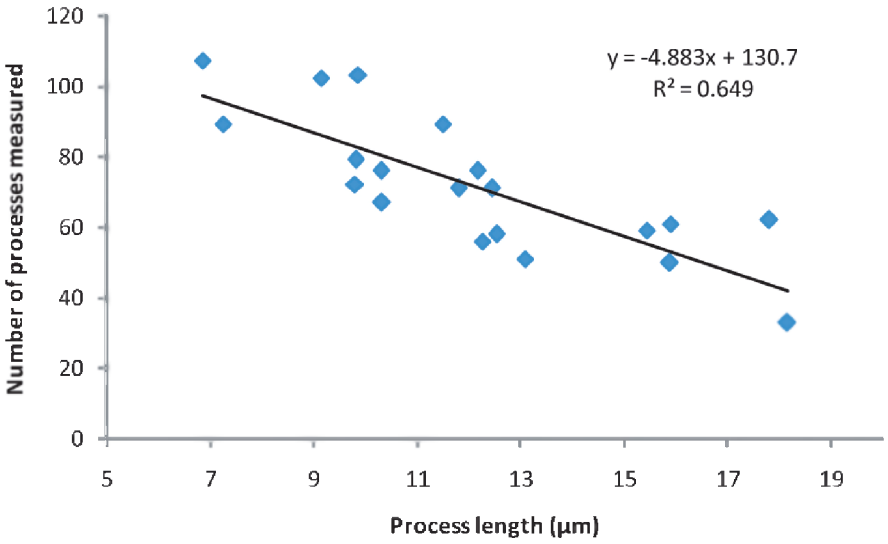

Figure 8 Regression between average process length and the number of processes for the cysts measured with confocal microscopy.

negligible changes in process length.

4.3 The problematic Kattegat–Skagerrak and Scandinavian Fjord samples

It is noteworthy that the inclusion of the Kattegat–Skagerrak and Scandinavian samples increased the scatter of the regression significantly. Two causes can be suggested. Firstly, since most samples plotted above the regression line, the average process length could be anomalously short. Most probably this is not linked to a preservation issue, since the average preservation was average to good (except for the Risör site), and broken processes were rare. All recovered cysts are from the uppermost section of box cores, and are thus recently formed. One possible explanation is that these specimens are genetically different which could result in slightly different morphologies. However, there is no *a priori* reason why this should be so, and this conflicts with the unimodal size-frequency distribution of process length.

Secondly, the used summer S_{30m}/T_{30m} data could be incorrect, and this can be attributed to several causes. On one hand, the cyst production could have taken place at different water depths. When surface data (S_{0m}/T_{0m}) for the Kattegat-Skagerrak and Scandinavian samples is included in the global dataset of summer S_{30m}/T_{30m}, the relation between average process length is more significant ($R^2 = 0.61$). On the other hand, the timing of cyst production might be different. *L. polyedrum* blooms in fjords are probably short-lived, followed by a long resting period (Godhe and McQuoid, 2003). As for the Kattegat–Skagerrak, salinity-driven stratification, with higher salinity bottom waters and low salinity surface waters, could result in a very particular environment. In this way, the cysts are formed probably under specific salinity and temperature conditions, which could explain the increase in scatter.

4.4 Confocal measurements and implications for cyst formation

The results of this study lead to enhanced insight into the process of cyst formation of *L. machaerophorum.* Before discussing the implications of our study in detail we summarise the state of the art knowledge on cyst formation as described by Lewis and Hallett (1997) and Kokinos and Anderson (1995). The studies of these authors indicate that at the start of the cyst formation process, the motile planozygote ceases swimming, ejects its flagella, and

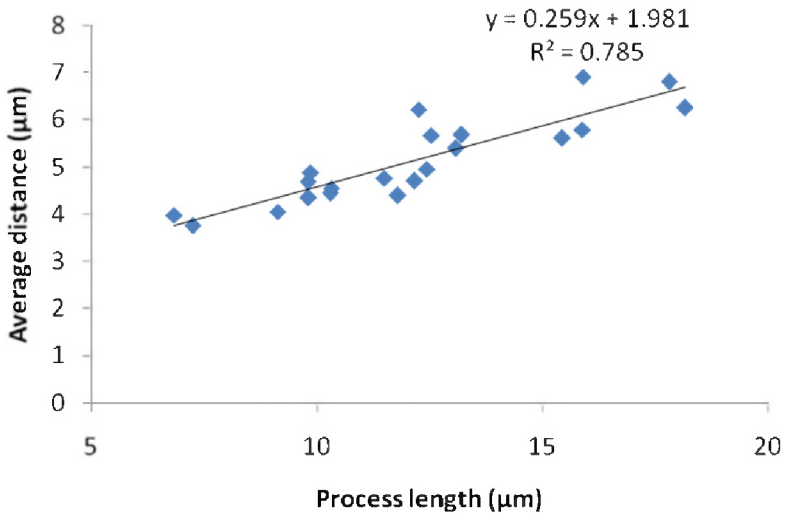

Figure 9 Regression between average process length and the average distance between process bases for the cysts measured with confocal microscopy.

the outer membrane swells. Then, the thecal plates of the planozygote dissociate and are pulled away from the cytoplasm by the ballooning of the outer membrane and underneath this, the formation of the cyst wall occurs. A layer of globules (each ~5 µm across) surrounds the cytoplasm and the spines grow outwards taking the globules with them. These terminal globules collapse to form spine tips and variations in this process confer the variable process morphology observed. Probably, membrane expansion is activated by osmosis (Kokinos, 1994), which causes a pressure gradient. According to Hallett (1999) the outer membrane always reaches full expansion, both for short and long process-bearing individuals. Measurements with confocal laser microscopy clearly show that a positive relation exists between the process length and the distance between processes, and a negative relation between the processes length and the number of processes.

These findings lead towards three implications. Firstly, the amount of dinosporin necessary for constructing the processes would be constant, at least for the studied cysts from the Mediterranean Sea. However, one needs to assume that the amount of dinosporin is proportionate to the number of processes, multiplied by the average process length. This entails that that the amount of dinosporin needed for formation of the periphragm is constant, which is reasonable since the body diameter is independent of process length. Secondly, the good correlation between the average distance and the process length, together with the observation that globules are all forming simultaneously (Hallett, pers. comm.), suggests that the process length is predetermined. Thirdly, these observations suggest the existence of two end members: one with many closely spaced short processes, and one with a few, more widely spaced, long processes (Figure 10). This gradient in biometrical groups can also be visually observed in transmitted light microscopy (Plate I to IV) and the suggested formation process for the two end members is illustrated in Figure 11.

In order to reconcile these observations with observations from cultures, the physico-chemical properties of dinosporin have to be considered. According to Kokinos (1994), dinosporin consists of a complex aromatic biopolymer, possibly made of tocopherols. However, upon re-analysis, De Leeuw et al. (2005) showed the tocopherol link to be untrue. It can now be speculated that a certain fixed amount of this precursor monomer (probably a sugar, Versteegh, pers. comm.) for dinosporin is distributed across the

sphere, in such a way that a minimum of energy is necessary for this process. This can occur through a process of flocculation (Hemsley et al., 2004), and is dependent on both temperature and salinity. Fewer but larger colloids of the monomer will be formed when S_{30m}/T_{30m} is higher and these will coalesce on the cytoplasmic membrane. When many small colloids are formed, it might occur that two or more colloids merge, and form one larger process (Plates II.13, II.15 and II.22). This theory can also explain the rare occurrence of crests on cyst species such as *Operculodinium centrocarpum*, where crests are formed when processes are closely spaced. In the next step, the visco-elastic dinosporin is synthesized on the globules, and stretches out in a radial direction. This stretching is clearly visible in the striations at the base of the processes. Another result of this stretching is the formation of tiny spinules at the distal tip. These are more apparent on the longer processes, and could be the result of a fractal process: what happens at a larger scale, namely the stretching of the processes, is repeated here at a smaller scale in the stretching of the spinules. However, it is unlikely that the stretching is solely caused by membrane expansion. Hallett (1999) indicated that the outer membrane expansion is independent of the definitive process length. Thus the stretching is most probably caused by the combination of outer membrane expansion and a chemical process, similar to the swelling of cysts caused by acetolysis or KOH (see 2.1).

Two types of cysts deserve special attention. Clavate or bulbous process bearing cysts (Plate I.6; Plate II.11, II.20) were frequently encountered in surface sediments from low salinity environments (Black Sea, Caspian Sea, Aral Sea and the Kattegat–Skagerrak). They were frequently encountered in culture by Kokinos and Anderson (1995), but rarely by Hallett (1999). These only seem to differ from normal processes, in that the globules were not able to detach from these processes. This is supported by the fact that the length of normal processes on cysts bearing clavate processes is the same as for clavate processes.

The second type of cysts deserving attention are the bald or spheromorphic cyst. Lewis and Hallett (1997) observed that these cysts are not artefacts of laboratory culturing, since cysts devoid of processes occur in the natural environment of Loch Creran in northwest Scotland. Moreover, Persson (unpubl. experiment, 1996) noted in culturing experiments, that these cysts are viable, and thus cannot be regarded as malformations. Apart from the Aral Sea, very few bald cysts were recorded in surface sediments. It appears that on these cysts, process development did not take place. It can be speculated that this could be caused by a very early rupture of the outer membrane or the inability of the precursor monomer to flocculate at a very reduced S_{30m}/T_{30m}.

4.5 Process distribution

The process distribution on *Lingulodinium machaerophorum* has been considered intratabular to non-tabular (Wall and Dale, 1968), although some authors noted alignment in the cingular area (Evitt and Davidson, 1964, Wall et al., 1973). Marret et al. (2004) showed a remarkable reticulate pattern in the ventral area on cysts with very short processes from the Caspian Sea, suggestive of a tabular distribution. Our findings indicate a regular and equidistant distribution of the processes, with evidence of a tabulation pattern lacking.

The process length distribution is not uniform. In cultures, cysts are formed at the bottom of the observation chambers, resulting in an asymmetrical distribution of the processes on the cysts, where shorter processes are formed at the obstructed side, and longer processes at the unobstructed side (Kokinos and Anderson, 1995; Hallett, 1999). When assuming that a constant amount of dinosporin is distributed over the cyst body, aberrantly long processes would form at the unobstructed side, and aberrantly short processes at the obstructed side. Our observations confirm this phenomenon: cysts from shallow areas show a similar asymmetry. The frequent occurrence of short processes on cysts from shallow areas in the Mediterranean Sea can be explained in a similar way (Figure 7). If one measures the longest processes on these cysts, values will be slightly larger than expected from our equation. This obstruction factor needs to be incorporated into our conceptual model (Figure 10). It is furthermore noticeable that many of the non-shallow cysts show this asymmetry to a certain

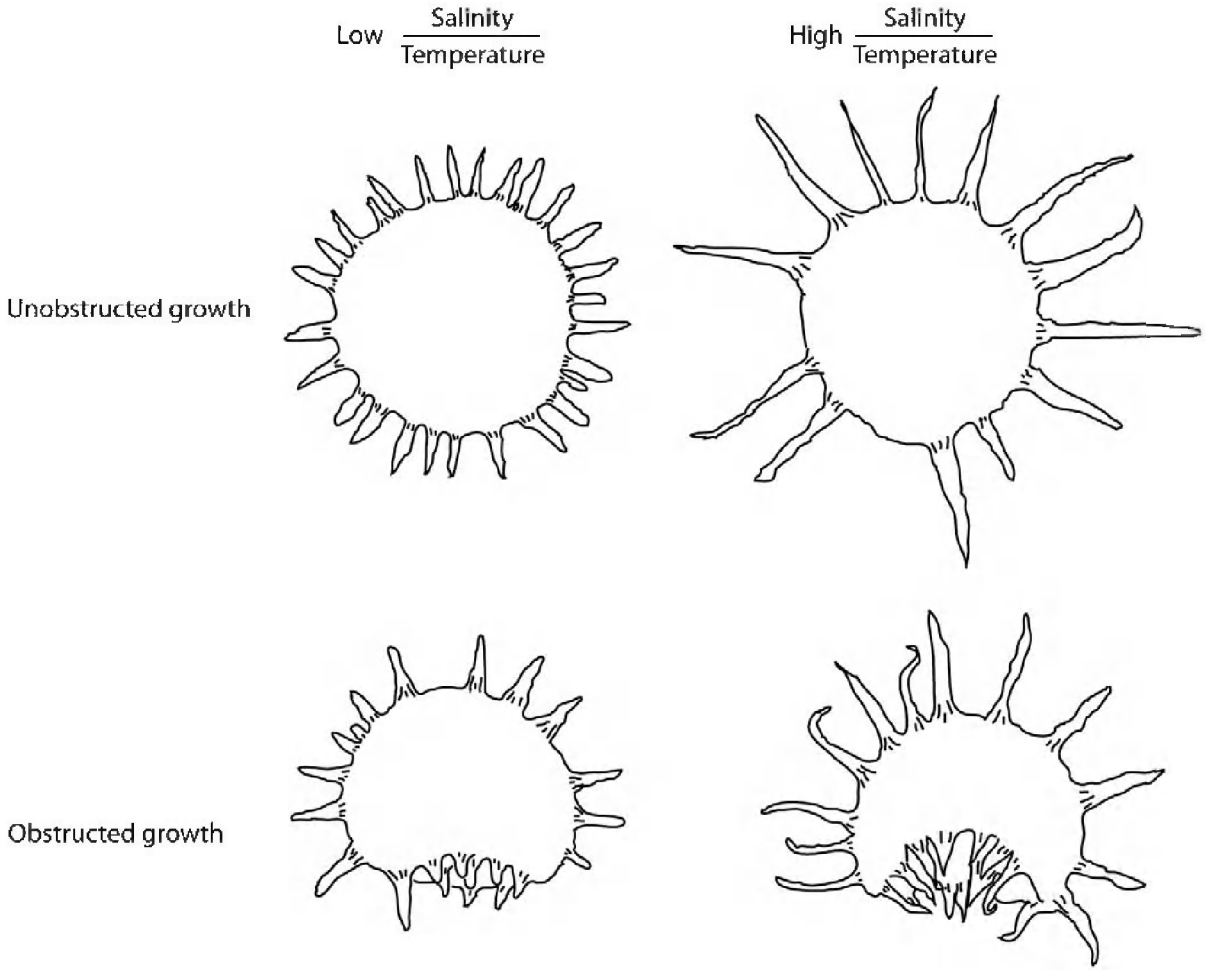

Figure 10 Conceptual model for process formation.

degree (Plate I.4), suggesting that this obstruction could be occurring more generally. The frequent occurrence of short processes along the cingulum could also be explained in a similar way, if the cysts were to be formed in a preferred orientation, with the obstructed side along the archeopyle.

4.6 Biological function of morphological changes?

The final consideration deals with the biological function of the processes. Possible functions of spines on resting stages have been proposed by Belmonte et al. (1997), and include flotation, clustering and enhanced sinking, passive defence, sensory activity and/or chemical exchanges and dispersal. Since the link between process length and S_{30m}/T_{30m} exists and density is also dependent on S_{30m}/T_{30m}, it is obvious that either flotation or clustering and enhanced sinking will be the most important biological function of morphological changes of the processes. Longer processes increase the drag coefficient of the cyst and thus increase floating ability according to Stokes' law, but also increase cluster ability. However, the longest processes occur in high water density (high S_{30m}/T_{30m}) environments, where floatation would be easier, which is counterintuitive. It seems more logical, then, that longer processes are

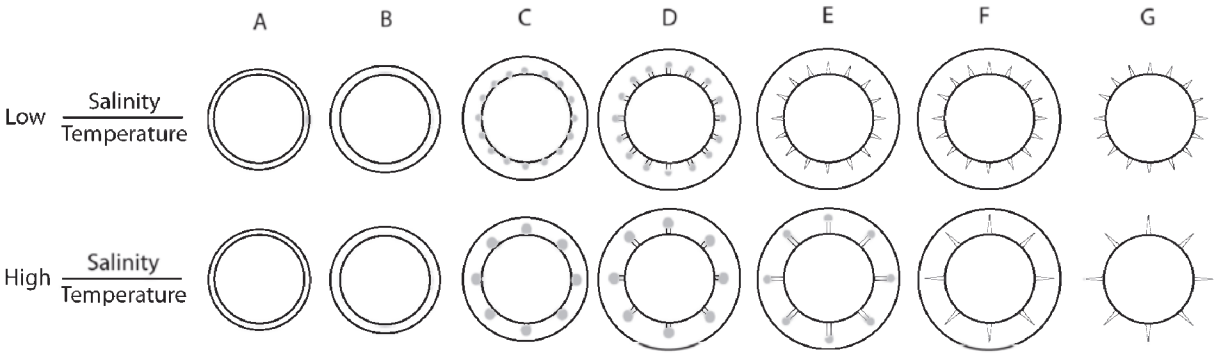

Figure 11 Suggested formation process for the two end members based on observation and documentation by Kokinos and Anderson (1995) and Hallett (1999), and theoretical consideration by Hemsley et al. (2004). Monomer is shown in grey, membranes and polymerised coat in black. (A–B) The outer membrane starts to expand, a fixed amount of monomer is formed and starts to coalesce on the cytoplasmic membrane. (C) Depending on environmental parameters (salinity and temperature), a lot of small or a few large colloids of the monomer are formed. (D) Visco-elastic dinosporin is synthesized on the globules and stretches in a radial direction. (E) Membrane expansion often comes to a stop before radial stretching ends. (F) Formation of longer process takes longer than shorter process formation. (G) Membrane rupture occurs.

developed to facilitate sinking (through clustering) in environments with high water density.

5. Conclusions

- A total of 19,611 measurements of *Lingulodinium machaerophorum* from 144 globally distributed surface samples showed a relationship between process length and both summer salinity and temperature at 30 m water depth, as given by the following equation: (S30m/T30m) = (0.078*average process length + 0.534) with R^2 = 0.69. For salinity the range covered is at least 12.5 to 42 psu, and for temperature 9 to 31°C. To establish the accuracy of this salinity proxy, future culture studies will hopefully further constrain this relationship.
- Confocal microscopy shows that distances between processes are strongly related to average process length, and that the number of processes is inversely related to average process length. This suggests a two end-member model, one with numerous short, closely spaced processes and one with relatively few, widely spaced, long processes.
- Processes of *Lingulodinium machaerophorum* are hypothesized to biologically function mainly as a clustering device to enhance sinking rates.

Additional information

Dinoflagellate cysts were extracted by the respective collaborators. Measurements from all samples were done by Kenneth Mertens, except those from Portugal which were measured by Sofia Ribeiro. Confocal images were recorded by Kenneth Mertens, with assistance of Dries Vercauteren. The raw confocal images were rendered into measurable triangulated surfaces using VGStudioMax software by Kenneth Mertens at the Centre for X-ray Tomography (UGCT). Interpretations were done by Kenneth Mertens. This chapter has been published in *Marine Micropaleontology*.

CHAPTER 5

What drives the distribution of cysts of *Lingulodinium polyedrum*?

ABSTRACT

The biogeographic distribution of *Lingulodinium machaerophorum* - cyst of the corresponding red tide forming motile dinoflagellate *Lingulodinium polyedrum* - is delineated by the ratio between summer salinity and temperature (S/T). The confinement to this ratio can be related to a physicochemical process which determines the morphological variation of the cyst and inhibits formation of the cyst outside the range of tolerable S/T ranges. This finding has far reaching implications for studies on harmful algal blooms, paleoclimate reconstructions using dinoflagellate cysts, interpretation of evolutionary trends and palaeobiogeographical zonations and possibly also of other plankton groups.

Plankton is known to be sensitive a recorder of climate change since it reacts rapidly to small changes in environmental conditions such as temperature and salinity (Hays et al., 2005). Dinoflagellate cysts are the cysts of unicellular plankton and as such show large changes in both assemblages and morphology related to climatological changes (Dale and Dale, 2002). In this way, they are considered to be useful palaeoceanographical tools to reconstruct late Quaternary palaeoproductivity (e.g. Reichart and Brinkhuis, 2003; Pospelova et al., 2006; González et al., 2008b).

The species *Lingulodinium polyedrum* forms red tides in bays, estuaries and river outlets (Lewis and Hallett, 1997) and has occasionally been associated with upwelling conditions (e.g. Blasco, 1975). The production of yessotoxins (YTX) by *Lingulodinium polyedrum* can cause human health problems (Kudela and Cochlan, 2000). The blooms occur in spring to summer and are associated with higher nutrient levels, supplied from a variety of sources, including coastal runoff, upwelling or anthropogenic inputs (Lewis and Hallett, 1997) in stratified conditions (Lewis et al., 1985). The late summer production of the cyst, *Lingulodinium machaerophorum* is likely triggered by nutrient depletion (Blanco 1995), and results in "seed beds", from where the motiles excyst after a mandatory dormancy period (Anderson and Morel, 1979). *Lingulodinium machaerophorum* is well-preserved in the sediments since it can be considered as moderately resistant to oxygenation (Zonneveld et al., 2008), and grazing (Persson and Rosenberg, 2003). The absence of the cysts in certain areas where larger river systems occur (e.g. NE Pacific, (Radi and de Vernal, 2004) and White Sea (Novichkova and Polyakova, 2007)) is often explained by colder seawater temperatures in these areas, which delineate biogeographical zones (Dale, 1996). However, temperature alone cannot explain the occurrence of the cysts in areas with similar temperature ranges but lower salinities such as Kiel Bight (Nehring, 1997) or Scandinavian Fjords (Persson et al., 2000; Grøsfjeld, and Harland, 2001). Its more common presence has indeed often been related to reduced salinities in a.o., the British Coast (Reid, 1972) and the Gulf of Guinea (Marret, 1994). Also the disappearance of *Lingulodinium machaerophorum* cysts in the Black Sea before 9.3 kyr BP, when the Black Sea was still a brackish lake (Mudie et al., 2001), suggests that salinity must be another key factor in determining the presence of cysts of *Lingulodinium polyedrum*. An explanation for these observations is here attempted.

Cultures by Hallett (1999) first showed that process length of the cysts is correlated positively with salinity, but as well negatively with tempera-

ture, suggesting that none of these parameters can separately explain cyst morphology. These observations were confirmed in a study on *Lingulodinium machaerophorum* cysts extracted from recent surface sediments, which shows that process length is related to a ratio between salinity and temperature (S/T) (Mertens et al., 2009b). Apparently similar cysts can be formed under different salinity – temperature conditions, providing a constant S/T ratio.

In a newly composed database of 4842 samples from published and unpublished data (Appendix IV), cysts are found within certain limits of the summer[1] S/T ratio, ranging between 0.7 and 2.55°C/psu. The explanation for the biogeographical delineation supplied by the S/T ratio (Figure 1) is preferred to summer temperature (Figure 2) because of two reasons. Firstly, it explains the absence of *Lingulodinium machaeorophorum* in areas with large salinity variations but similar temperatures to other regions where it is present, e.g. compare the Baltic Sea with the British coasts (Figure 3 and 4). Secondly, it provides an explanation why the cysts are sometimes not present: outside these limits, which correspond to morphological end-members (Mertens et al., 2009b), cysts cannot be formed due to physicochemical constraints of the building blocks of the cysts (Hemsley et al., 2000). Exceptional occurrences can be related to reduced salinities caused by increased rainfall, e.g. along some of the British coasts (Reid, 1972) or increased meltwater discharge, e.g. Scandinavian Fjords (Persson et al., 2000) or can be reworked as previously suggested (Mertens et al., 2009b). The S/T ratio has predictory value for the presence and morphology of the cysts in the sediments (Figure 5). It will be of crucial interest to refine the limits of cyst presence, *in casu* for the northern hemisphere in Norway, northeast Canada, Northern Japan and Britain and for the southern hemisphere New Zealand, Argentinia and South Africa.

In terms of paleoecological reconstruction, this implies that the presence of *Lingulodinium machaerophorum* only yields information about the range of the S/T ratio, although its morphology has potential to reconstruct the S/T ratio (Mertens et al., 2009b). This model can be applied for other dinoflagellate cyst species, which all show particular geographical distributions closely linked to strict limits of salinity and temperature (Marret and Zonneveld, 2003). Species with larger niches, as expressed by a larger range in the S/T ratio, such as *Operculodinium centrocarpum* can be considered cosmopolitan, whereas others which occupy a limited niche, such as *Polysphaeridium zoharyi,* are specialists. The S/T ratio can be related to a particular water mass, and this explains why dinoflagellate cyst assemblages have been used in this way in paleoclimate reconstruction (de Vernal and Marret 2007).

If environmental conditions are met to allow cyst formation, i.e. fall within the limits of the S/T ratio, how many cysts are formed – and thus the relative abundance - will be determined by the magnitude of the bloom, which on its turn is dependent on cell growth. Cultures show that multiple factors determine cell growth such as salinity and temperature (Brand, 1984; Matsuyama et al., 2003), turbulence (Sullivan et al., 2003) and higher nutrient levels (Eppley and Harrison, 1975). Positive feedbacks to these processes could be given by increased cyst germination at prolonged light exposure (Anderson et al., 1987) and higher temperatures and salinities (Blanco, 1990). It is possible that the motile growth is also restricted by the S/T ratio, although there are observations in the high arctic, where cysts have not been found (see Okolodkov 2005 for a review).

The suggestion that *Lingulodinium polyedrum* would be unable to form cysts outside its S/T range, and is thus unable to produce "seed beds", has multiple implications. The tight link between the essential environmental seawater parameters will enable detailed biogeographic zonations for dinoflagellate cysts and possibly other plankton groups. Paleoclimate reconstruction with dinoflagellate cysts, which have shown significant results e.g. with the modern analogue technique (de Vernal et al., 2005), can be fine-tuned using this new ecological model. Transport of dinoflagellate cysts, a heavily debated issue (Telford, 2006), has potential to be resolved with the S/T ratio. Also for evolutionary studies and extinctions this has some implications. It can also be predicted that global warming will result in more and larger harmful algal blooms (HABs), due to expansion of biogeographic ranges, as previously suggested (Dale et al., 2006), and observed (Edwards et al., 2006).

[1] Summer is chosen since this is the season of production of the cysts.

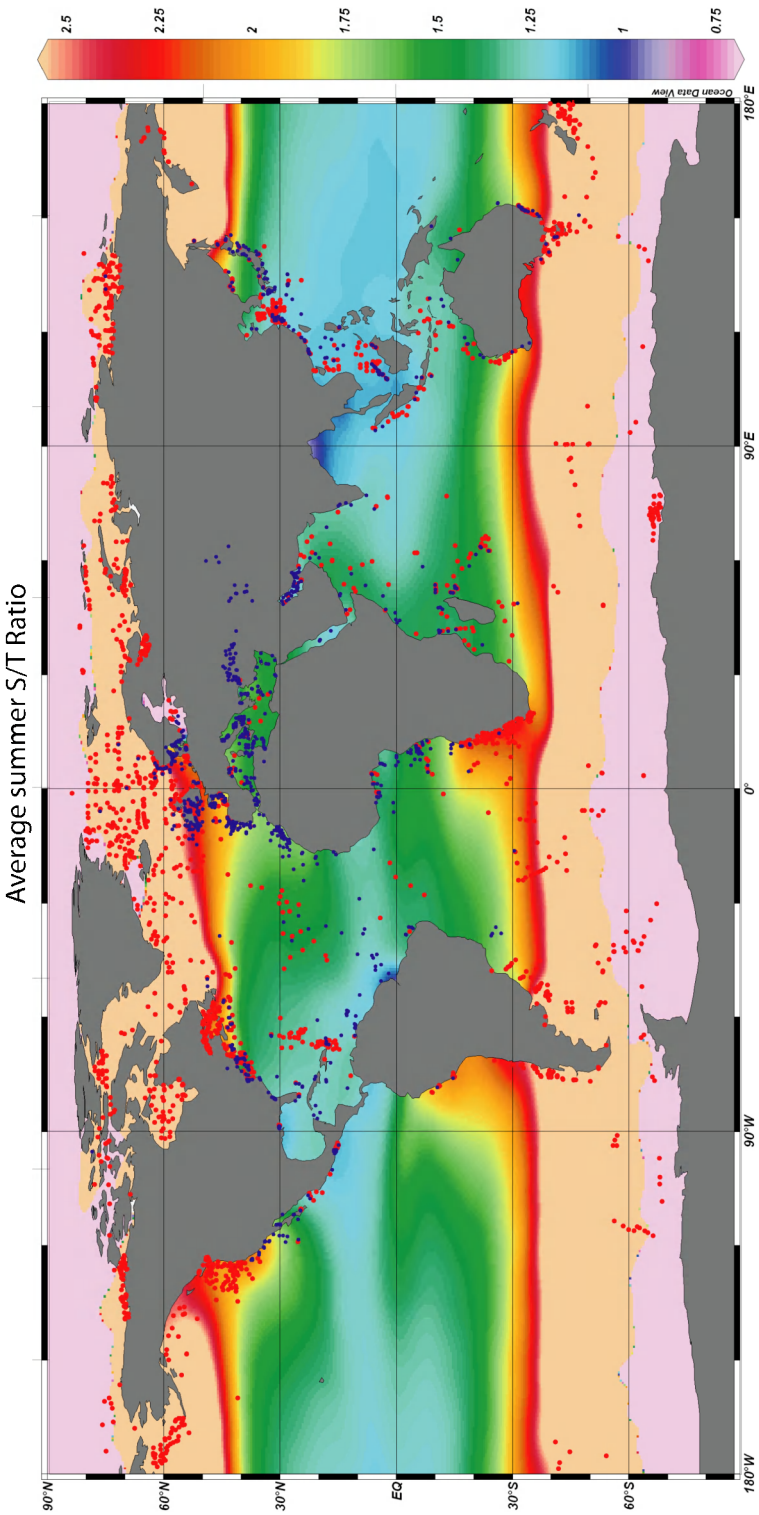

Figure 1 Presence (blue) and absence (red) of *Linguladinium machaerophorum* in samples from a global database mapped on average summer S/T ratios. The suggested tolerable range of the summer S/T ratio ranges from 0.7 to 2.55.

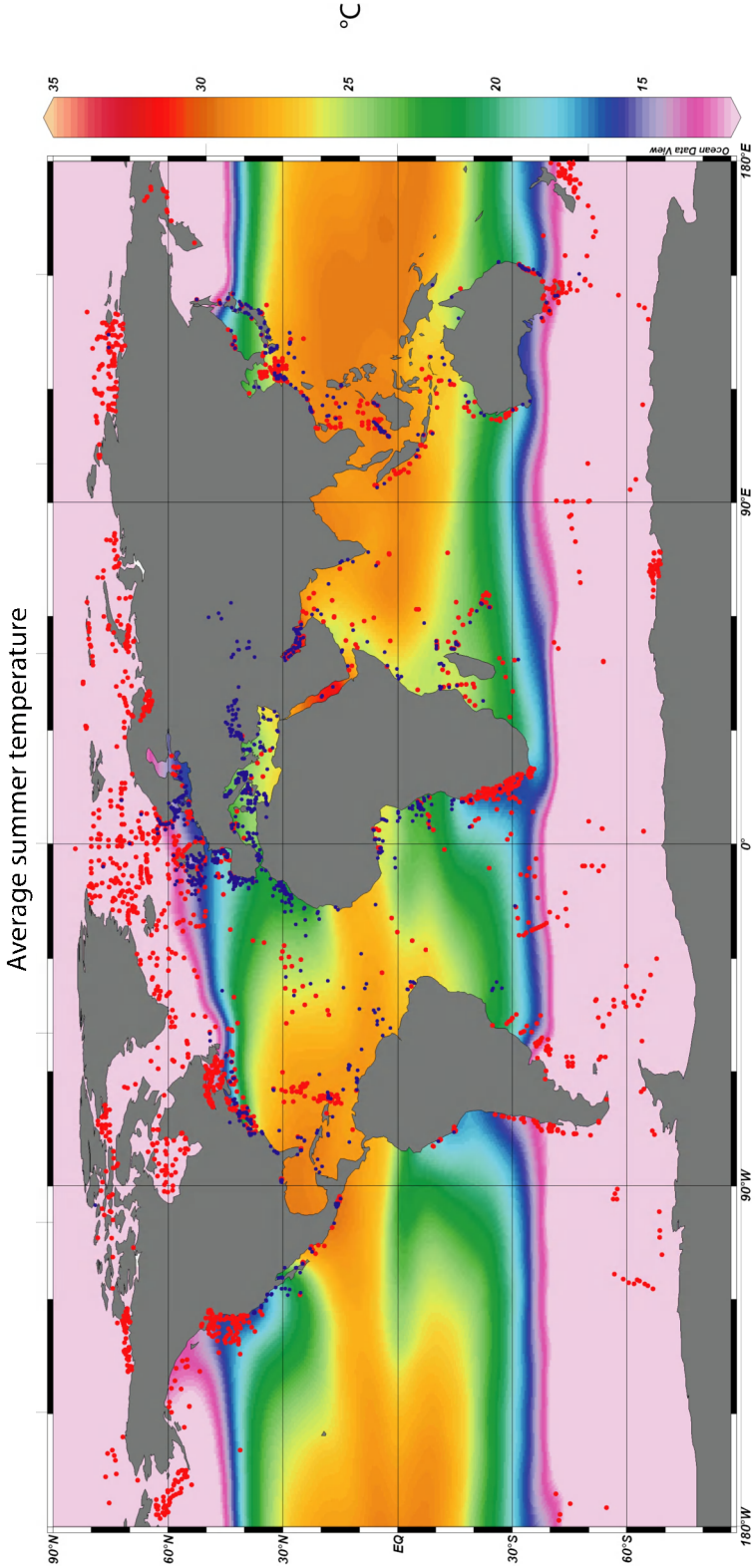

Figure 2 Presence (blue) and absence (red) of *Lingulodinium machaerophorum* in samples from a global database mapped on average summer temperatures. The suggested tolerable range of the summer temperature ranges from 12-35°C.

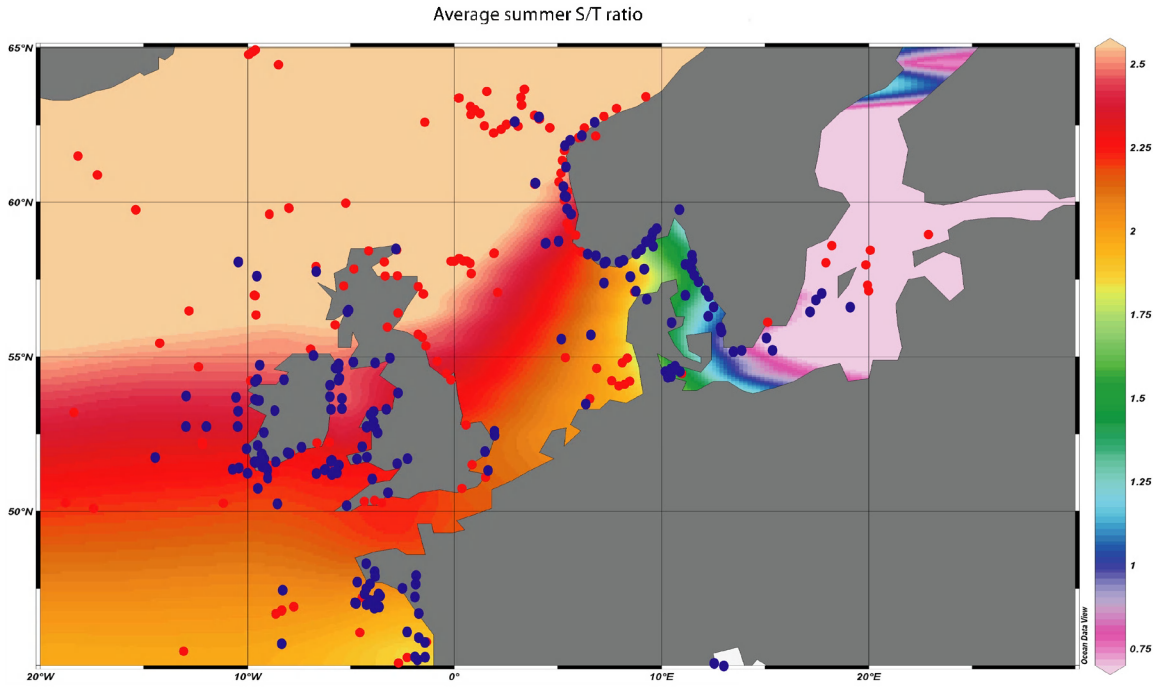

Figure 3 Presence (blue) and absence (red) of *Lingulodinium machaerophorum* in samples from a global database mapped on average summer S/T ratios, zoomed in on Northern Europe. The samples in the Baltic Sea can be considered reworked (Mertens et al., 2009b).

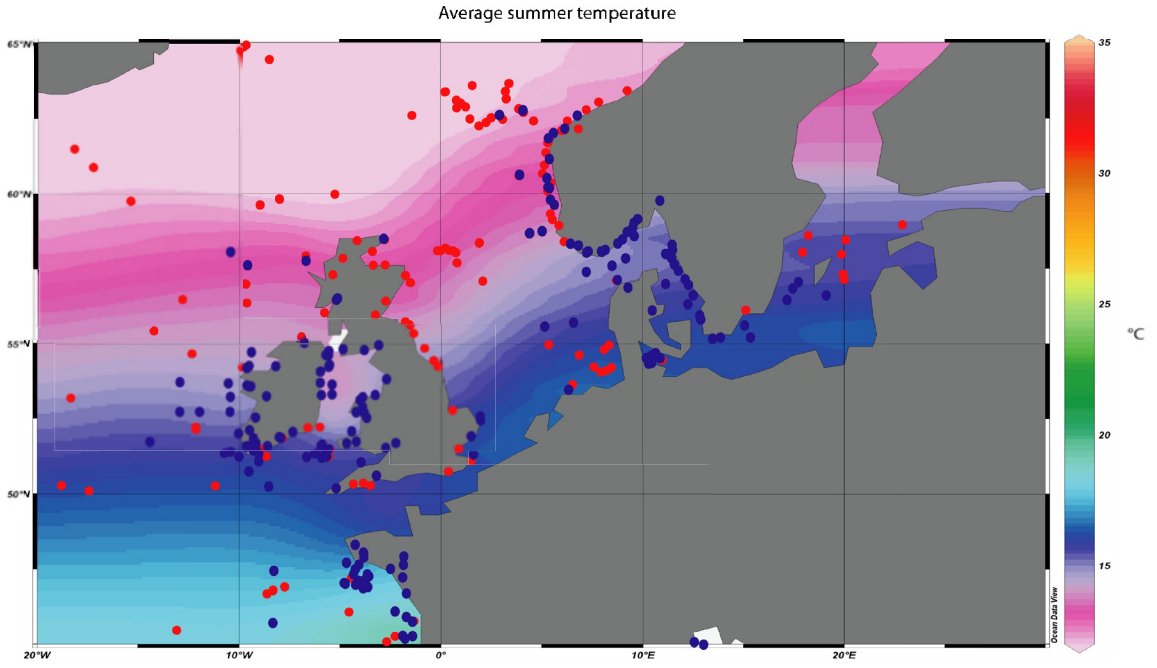

Figure 4 Presence (blue) and absence (red) of *Lingulodinium machaerophorum* in samples from a global database mapped on average summer temperatures, zoomed in on Northern Europe.

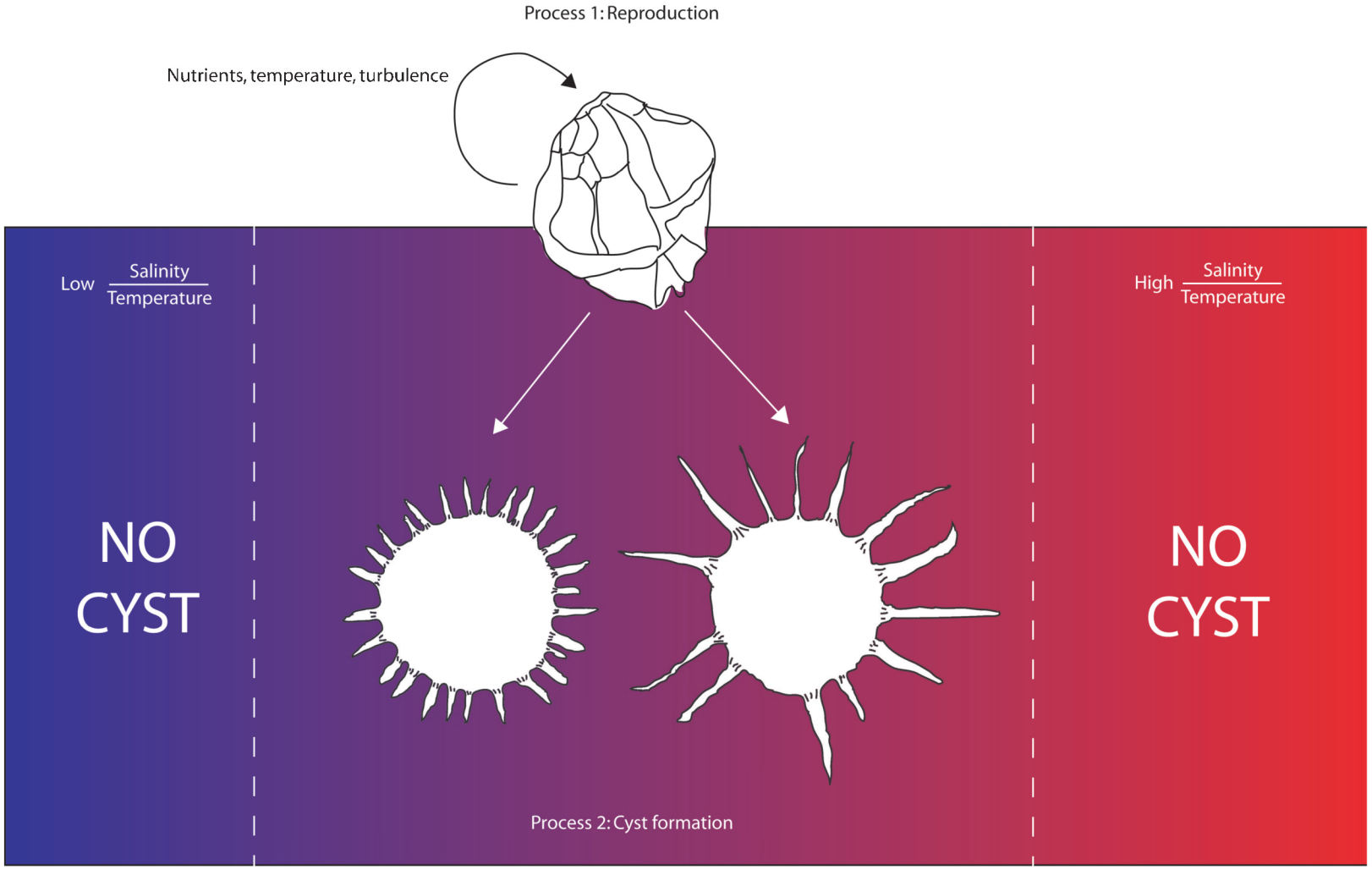

Figure 5 Two independent processes in the life cycle of *Lingulodinium polyedrum*. Process 1: Reproduction is dependent of several factors, amongst other nutrient supply, temperature and turbulence. It can be assumed that the number of cysts formed will be proportionate to the magnitude of the bloom, and it is thus dependent of these factors. Process 2: After the motile cell is triggered to start forming cysts, how the cysts are formed will be determined by the S/T ratio only. There is no formation of the cysts outside the tolerance limits (dashed lines).

Additional information

Unpublished data was provided by co-authors. Interpretations were done by Kenneth Mertens. This chapter will be submitted

CHAPTER 6

30000 years of productivity and salinity variations in the late Quaternary Cariaco Basin revealed by dinoflagellate cysts

ABSTRACT

Dinoflagellate cysts and other palynomorphs were studied from ODP Hole 1002C in the Cariaco Basin over the last 30000 years. The assemblage shifts between a dominance of heterotrophic dinoflagellate cysts (mainly *Brigantedinium* spp., *Lejeunecysta* spp., *Selenopemphix nephroides* and *Stelladinium reidii*) and autotrophic dinoflagellate cysts (mainly *Spiniferites ramosus*, *Lingulodinium machaerophorum* and *Operculodinium centrocarpum*). These assemblage shifts are associated with stronger upwelling during stadials, and stronger river influx during interstadials. Increases in productivity caused by enhanced upwelling are coupled to improved preservation and *vice versa*. More stratified water is indicated by higher abundances of *Lingulodinium machaerophorum* and succeeds Heinrich events. Average process length of *Lingulodinium machaerophorum* can be used to track changes in salinity, since it shows a similar pattern as the $\delta^{18}O_{SW}$ (paired Mg/Ca – $\delta^{18}O$) reconstruction. During the last glacial, conditions were more saline than during the current interglacial. On a millennial-scale, changes in salinity are opposite to open ocean salinities and the hydrological proxies, which can be explained by a modulation of the signal by stratification, isolation of the Basin or advection of fresh water masses. These results highlight both generalities and particularities of the paleoecological record of this tropical semi-enclosed basin.

1. Introduction

Large and rapid climate oscillations occurring at suborbital and millennial frequencies are not restricted to the northern higher latitudes but have a global signature, which is also prominent in the Caribbean Sea (Peterson et al., 2000a; Vink et al., 2001; Schmidt et al., 2004). The synchronicity of these rapid changes between Cariaco Basin, the Greenland Ice Cores and California margins show that these are likely linked through atmospheric processes (Goni et al., 2006; Dean 2006). These are expressed as hydrological variations throughout the tropics (Clement and Peterson 2008), which have the potential to amplify and perpetuate millennial-scale climate changes (Ivanochko et al., 2005).

These rapid climatic changes are well reflected in productivity records, best recorded in coastal areas. Although present-day shelf seas make up 8% of the total ocean surface area, about 10-15% of the global marine primary production takes place in these coastal seas, with 40% of it exported to the deep sea (Muller-Karger et al., 2005). The Cariaco Basin, located near to the Venezuelan margin, is characterized by high productivity, which drove the basin into anoxicity. In this respect, the basin offers an important opportunity to study productivity changes.

Planktonic organisms, such as dinoflagellates,

are regarded as very sensitive recorders of climate change (e.g. Hays et al., 2005). Dinoflagellate cysts are the hypnozygotes of unicellular planktonic algae that are considered to be useful palaeoceanographical tools to reconstruct late Quaternary palaeoproductivity (Reichart and Brinkhuis 2003; Pospelova et al., 2006; de Vernal and Marret 2007). They have also proven useful for the Cariaco Basin (González et al., 2008b). Since inferred palaeotemperature variations in the Cariaco Basin are relatively small during the last glacial - interglacial transition (max. 3-4°C, based on Mg/Ca, Lea et al., (2003) and alkenones, Herbert and Schuffert (2000)), and are of similar magnitude as salinity changes (1.2-2.4‰, based on paired Mg/Ca - $\delta^{18}O$ McConnell, 2008), changes in dinoflagellate cyst assemblages will be mainly related to changes in productivity. However, recent research showed that dinoflagellate cyst morphology changes with salinity, and more particular, process length of *Lingulodinium machaerophorum* shows a linear relationship to salinity as shown by studying cultures (Hallett 1999) and surface sediments (Mertens et al., 2009b).

Dinoflagellate cysts from the Caribbean (including the Cariaco Basin) were investigated for the first time by Wall (1967). Except for an initial study on dinoflagellate cysts in surface sediments in the close-by Amazon region by Vink et al. (2000), organic-walled microfossils have been neglected in this region. Nevertheless, González et al. (2008b) demonstrated that Cariaco dinoflagellate cysts are useful markers for reconstructing productivity during Marine Isotope stages 3 and 4. In this study the productivity record from the Cariaco Basin is extended throughout the last 30000 years and compared with other productivity proxies. Additionally, salinity variations are documented using process length variation of *Lingulodinium machaerophorum* and compared with a paired Mg/Ca-$\delta^{18}O$ record.

2. Study area and background

The Cariaco Basin is an east-west trending Quaternary pull-apart basin on the continental shelf, north of Venezuela (Figure 1). The surrounding topography prohibits inflow of deep water from the Caribbean, causing a 100 year residence time of the bottom waters (Deuser 1973). The high oxygen demands, created by upwelling-induced surface productivity, and a strong pycnocline which limits vertical exchange, leads to the present-day anoxic and sulphidic conditions below a depth of 300 m (Peterson et al., 1991). The almost complete lack of bioturbation since the start of the Bølling/Allerød implies a nearly uninterrupted sedimentary record.

Surface waters entering the Caribbean are the North Brazil Current (NBC) and the North Equatorial Current (NEC). The NBC flows via Trinidad to the west along the continental slope of the Southern Caribbean, while the NEC originates from the North Atlantic gyre. The two upper water masses are the Caribbean Surface Water (CSW) and the Subtropical UnderWater (SUW). The oligotrophic CSW (0-80 m) originates from the NEC and NBC with a substantial input of low salinity waters from the Amazon and Orinoco Rivers during October and November. The eutrophic SUW (at a depth of 80-120 m), comes from the centre of the North Atlantic, namely the surface waters of the North Atlantic Gyre, and enters the Caribbean between the Lesser Antilles and the Windward Passage between Cuba and the Jamaican Islands (Wust 1964; Nyberg et al., 2002). The SUW forms the permanent thermocline and/or nutricline of the Caribbean. The surface water of the Caribbean is generally characterized by low primary productivity except in coastal regions, such as off the Venezuelan Coast (Muller-Karger and Aparicio-Castro 1994).

The region is influenced by migrations of the Intertropical Convergence Zone (ITCZ) which causes seasonal variations in the strength of the northeast trade winds (Muller-Karger and Aparicio-Castro 1994). During winter and early spring (January to March), the ITCZ is at its southernmost position and strong trade winds blow along the coast of Venezuela, and causes upwelling of nutrient-rich waters. The phytoplankton exploits this resource and in January and February primary production rates and carbonate and opal fluxes are at a maximum (Goni et al., 2003) and diatoms dominate the phytoplankton population (Ferraz-Reyes 1983). Beginning from about June or July, when the ITCZ migrates north to a position near the Venezuelan coast, the trade winds weaken markedly and thus also the upwelling. Primary pro-

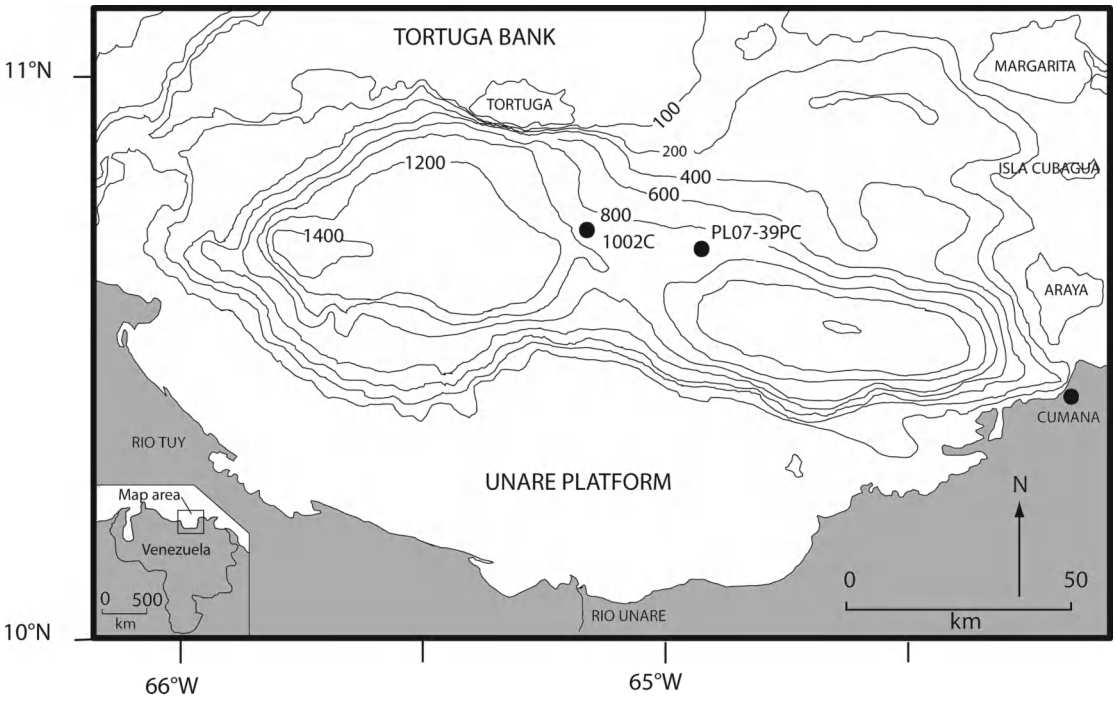

Figure 1 The Cariaco Basin, with location of ODP Site 1002 (approximately same position as core MD03-2620) and core PL07–39PC.

duction rates fall to a minimum (Muller-Karger et al., 2004). As the upwelling subsides, the northward migration of the ITCZ brings its associated rain belt above the Cariaco Basin. This rain belt triggers increased fluvial discharge from rivers, affecting the southern Caribbean, and induces a stratification of the water masses. No large rivers currently discharge into the basin, but in former times fluvial input was more important (Peterson et al., 2000b). During this season, the production is dominated by Cyanobacteria, dinoflagellates (Ferraz-Reyes 1983) and also haptophytes (Goni et al., 2003).

The interglacial basin sediments are laminated and reflect migrations of the ITCZ as the high annual sediment flux (20-100 cm/kyr) forms alternating light and dark laminae. The light laminae are mainly composed of diatoms; they reflect high winter-spring production. The micro-organisms appear grouped in aggregates, most likely faecal pellets, and are surrounded by biogenic silica (Hughen et al., 1996b). The dark laminae have a higher terrigenous content, and this reflects summer to autumn deposition during the rain season in combination with a reduced productivity. Microorganisms in these laminae are also grouped in aggregates.

As an analogue to the seasonal migrations of the ITCZ, longer term (orbital-scale, millennial-scale) changes in the mean position of the ITCZ have been proposed as a mechanism linking northern high-latitude and tropical climates (Peterson and Haug, 2006; Dean 2006).

3. Materials and methods

Ocean Drilling Program (ODP) site 1002 (10°42.37'N, 65°10.18'W, 893 m water depth) is located on the western flank of the central saddle of the Cariaco Basin (Figure 1). The saddle was chosen since varves in the subbasins tend to be disrupted by microturbidites. Shipboard Scientific Party (1997) gives a detailed description of this core. Marine Calypso core MD03-2620 (10°39.05' N; 65°10.17' W; 876 m water depth), was retrieved during the PICASSO cruise in

2003 (Laj, 2004), and is located close to the location of ODP Site 1002.

3.1 Stratigraphy

Hole 1002D is dated with 65 accelerator mass spectrometry (AMS) ^{14}C dates on planktonic Foraminifera, over the studied interval. After a constant 420-year marine reservoir correction, calendar ages were derived by transferring ages from the GISP II $\delta^{18}O$ ice core by matching inflection points and interpolation of reflection curves (Hughen et al., 2003). Hole 1002C was aligned with hole 1002D through visually matching magnetic susceptibilities provided by Shipboard Scientific Party (1997) (Figure 2). The studied core sections in Hole 1002C range in age from Late Pleistocene to late Holocene times, covering the time interval that includes Heinrich event 3 (H3), Heinrich event 2 (H2), Last Glacial Maximum (LGM), Heinrich event 1 (H1), Bølling-Allerød Warm Period (BA), Younger Dryas (YD) and the entire Holocene. Heinrich events are denoted according to their cited ages (Hemming, 2004) with respect to the Cariaco Basin age model for Hole 1002C. Sedimentation rates and accumulation rates are discussed in Mertens et al. (2009b) and range between 32 and 170 cm/kyr.

3.2 Sample preparation and light microscopy

Samples from Hole 1002C were taken at 20 cm intervals. A few samples of equal ages of core MD03-2620 were processed for comparison. Given the range of sedimentation rates, the sampling interval yields an average temporal resolution of 360 years, ranging between 10 and 1170 years. A total of 88 samples with a weight of 1.6 to 23.9 g were prepared for palynological analysis following the maceration technique described in Louwye et al. (2004). One to three *Lycopodium* tablets, containing a known number of spores, were added at the beginning of the palynological preparation. The treatment involved decalcification with cold HCl (10%) and subsequent removal of silicates with cold HF (40%). The remaining organic fraction was then sieved at 20 µm on a nylon mesh and mounted with glycerine jelly. A minimum of 300 dinoflagellate cysts were counted in each sample. In the meantime, all other palynomorphs encountered were counted. *Lycopodium* spores were counted to calculate cyst concentrations (cysts/cm^3). Accumulation rates were calculated by multiplying concentrations by sedimentation rates and dry bulk densities based on GRAPE density measurements (Shipboard Scientific Party 1997). Representative dinoflagellate cyst species are illustrated in Plate I and II, other palynomorphs are shown in Plate III. All photomicrographs are taken with a Zeiss AxioCam MRc5 camera mounted on a Zeiss Axioskop 2 Plus microscope. Taxonomy used follows Williams et al. (1998) and Rochon et al. (1999). *Spiniferites ramosus* s.l. includes *Spiniferites bulloideus* and *Spiniferites delicatus*. *Selenopemphix quanta* s.l. includes cysts of *Protoperidinium nudum*.

The morphological variation of *Lingulodinium machaerophorum* was studied by measuring the three longest processes of 50 cysts per sample, when possible. The longest processes are chosen for three reasons. Firstly, the longer processes would reflect unobstructed growth during formation of the cyst. Secondly, since only a restricted number of processes are measurable per cyst it is necessary to make a consistent approach by choosing the longest processes. Thirdly, the largest variation is obtained by choosing the longest processes, and this provides a more accurate proxy. The methodology is explained more in detail in Mertens et al. (2009b). Often less than 50 cysts were measured, when there were not enough available.

4. Results

4.1 Dinoflagellate cyst relative abundance data

A total of 47 dinoflagellate cyst taxa were identified in the studied sequence (Appendix V). Only five taxa reach relative abundances of more than 15% (Figure 3): *Brigantedinium* spp. (3-94%), *Brigantedinium cariacoense* (0-35%), *Spiniferites ramosus* (0-94%), *Selenopemphix nephroides* (0-45%) and *Lingulodinium machaerophorum* (0-63%). Other species of minor importance are *Stelladinium reidii* (0-14%),

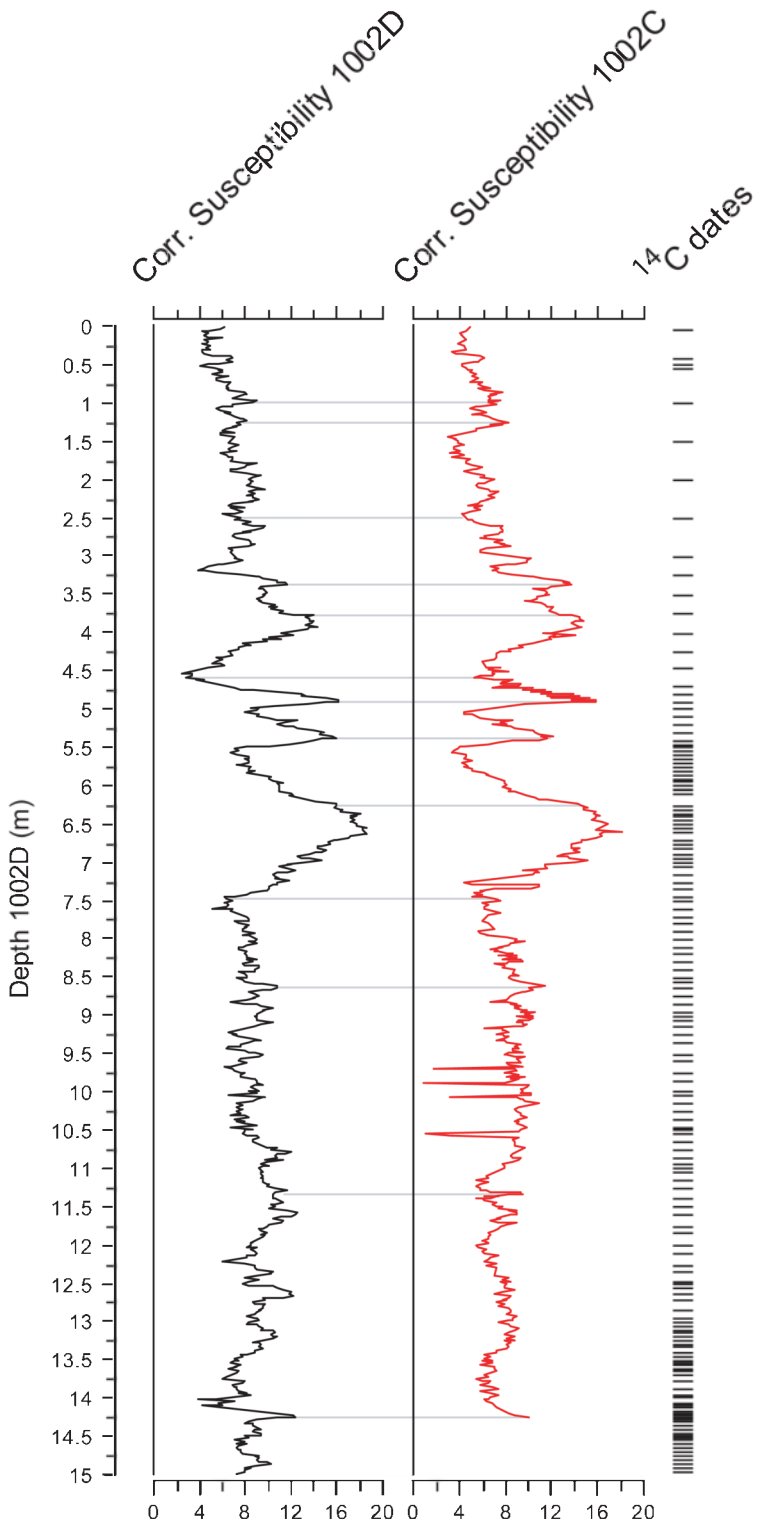

Figure 2 Alignment of magnetic susceptibilities of 1002C and 1002D using the depth scale of 1002D. Tie-points are shown by grey lines, radiocarbon dates in 1002D are shown by black horizontal lines (Hughen et al., 2004).

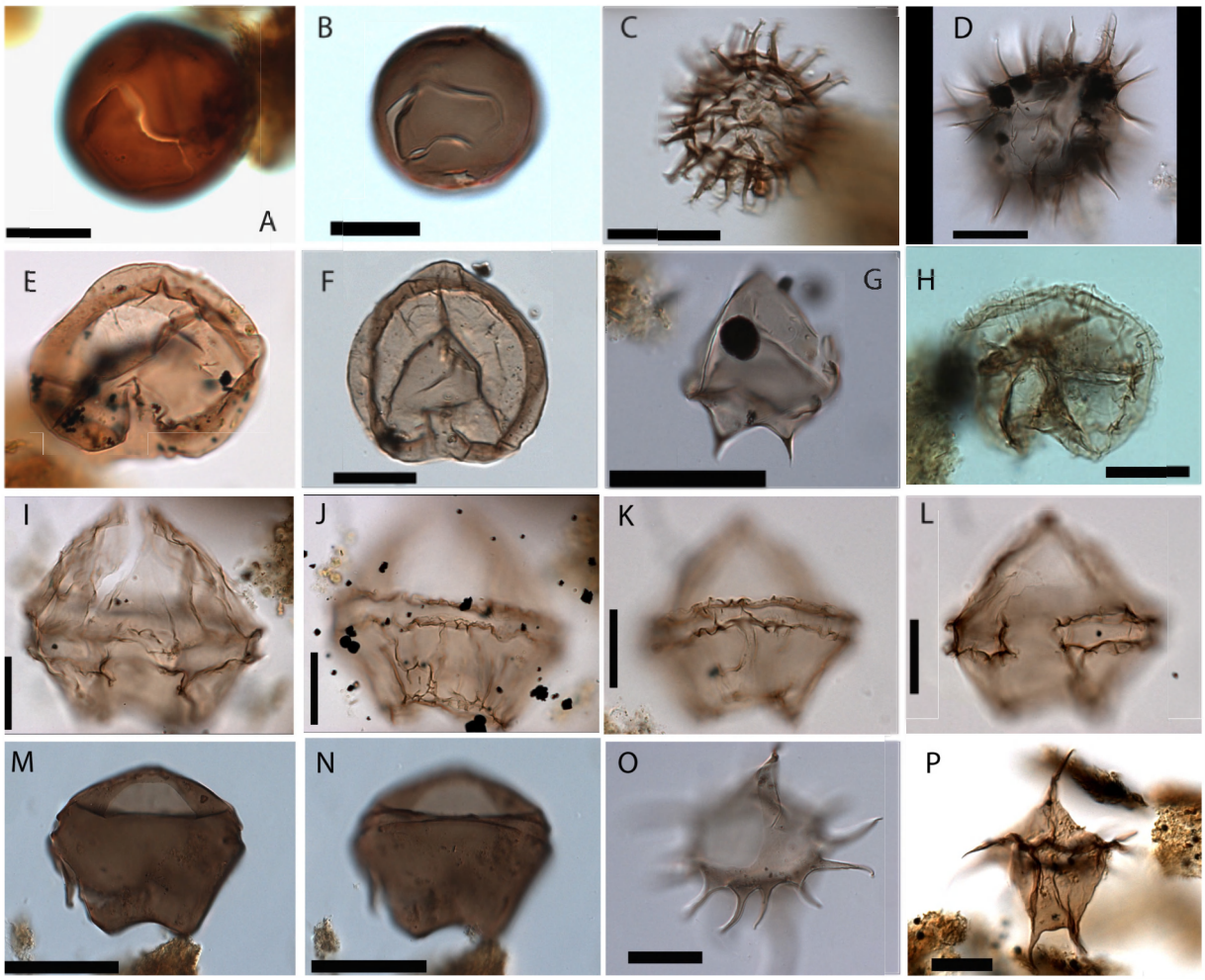

Plate I Micrographs from representative heterotrophic dinoflagellate cysts from ODP 1002C. A. 1H 2W 80-82, *Brigantedinium cariacoense*. B. 1H 4W 22-24, *Brigantedinium cariacoense*. C. 1H 4W 22-24, *Echinidinium aculeatum* with characteristic aculeate distal tips. D. 2H 1W 20-23, *Selenopemphix quanta*. E. 1H 2W141-143, *Selenopemphix nephroides*. F. 1H 5W 70-72 *Selenopemphix nephroides*. G. 2H 1W 20-23, *Lejeunecysta marieae*. H-L. 2H 4A 101-103, *Lejeunecysta* sp. A. M-N. 1H 6W 19.5-21.5, *Lejeunecysta oliva* with characteristic pronounced paracingulum. O. 2H 1W 20-23, *Stelladinium reidii*. P. 1H 5W 11-13, *Stelladinium reidii*. All scale bars are 20 µm.

Islandinium minutum (0-14%), *Selenopemphix quanta* (0-9%), *Quinquecuspis concreta* (0-9%), *Spiniferites mirabilis* (0-7%), *Brigantedinium simplex* (0-8%), *Lejeunecysta sabrina* (0-13%), *Operculodinium centrocarpum* sensu Wall and Dale (0-9%) and *Operculodinium israelianum* (0-6%). Similar species were identified as in González et al. (2008b). The cyst mentioned in González et al. (2008b) as *Selenopemphix* cf. *divaricatum* is corrected here as Lejeunecysta sp. A.

The samples are generally dominated by protoperidiniacean heterotrophic cysts (4-98%, averagely 84%), mainly *Brigantedinium* spp., *Echinidinium* spp., *Selenopemphix* spp. and *Selenopemphix quanta*. Autotrophic cysts from the Gonyaulacales occasionally dominate the assemblage during the BA and Preboreal (2-96%, averagely 16%), during which *Spiniferites* species (mainly *Spiniferites* ramosus) are accompanied by *Operculodinium centrocarpum* sensu Wall and Dale and *Lingulodinium machaerophorum*.

4.2 Dinoflagellate cysts concentrations and accumulation rates

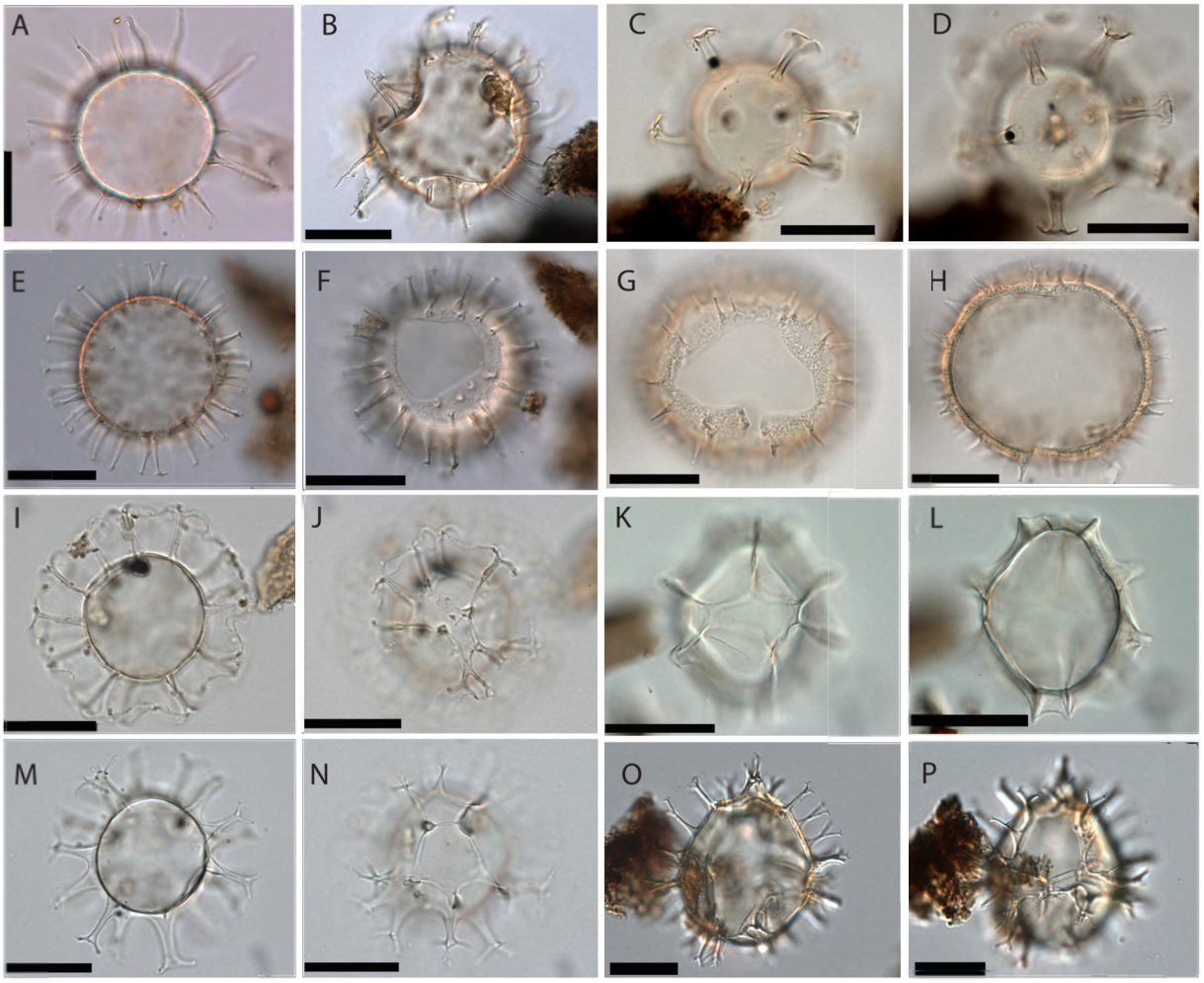

Plate II Micrographs from representative autotrophic dinoflagellate cysts from ODP 1002C. A. 1H 3W 131-133, *Lingulodinium machaerophorum*. B. 1H 2W 80-82, *Lingulodinium machaerophorum*. C-D. 1H 5W 11-13, *Melitasphaeridium choanophorum* E-F. 1H 4W 81-83, *Operculodinium centrocarpum* var. Wall & Dale, middle focus and upper focus showing archeopyle. G-H. 2H 1W 20-22, *Operulodinium israelianum*, similar views. I-J. 2H 1W 20-23, *Nematosphaeropsis labyrinthus*. K-L. 2H 1W 20-23 *Impagidinium aculeatum*. M-N. 2H 1W 20-22, *Spiniferites ramosus*. O-P. 1H 4W 22-24, *Spiniferites bentorii*. All scale bars are 20 µm.

Dinoflagellate cyst concentrations range from 180 to 79603 cysts per gram of sediment and show distinct fluctuations (Figure 4). High dinoflagellate cyst concentrations coincide with warm interstadials (BA and Preboreal) and low cyst concentrations with cold stadials (YD and H1). Highest concentrations are attained during BA and Preboreal when peaks of *Spiniferites ramosus* can be recorded. Autotrophic species reach abundances of 8 to 76247 cysts per gram sediment, whereas abundances of heterotrophic species range from 172 to 34021 cysts per gram of sediment. Autotrophic cyst concentrations show very similar fluctuations as relative abundance of autotrophic species, whereas heterotrophic cysts show distinct differences compared to relative abundance of heterotrophic species (Figure 4).

Accumulation rates range between 13 and 5135 cysts/cm^2/yr, and average 640 cyst/cm^2/yr, which are comparable to the older record from Cariaco Basin (González et al., 2008b) and the Santa Barbara basin record (Pospelova et al., 2006). All fluctuations of accumulation rates are similar to dinoflagellate cysts per gram of sediment.

It must be stressed that the residue was sieved

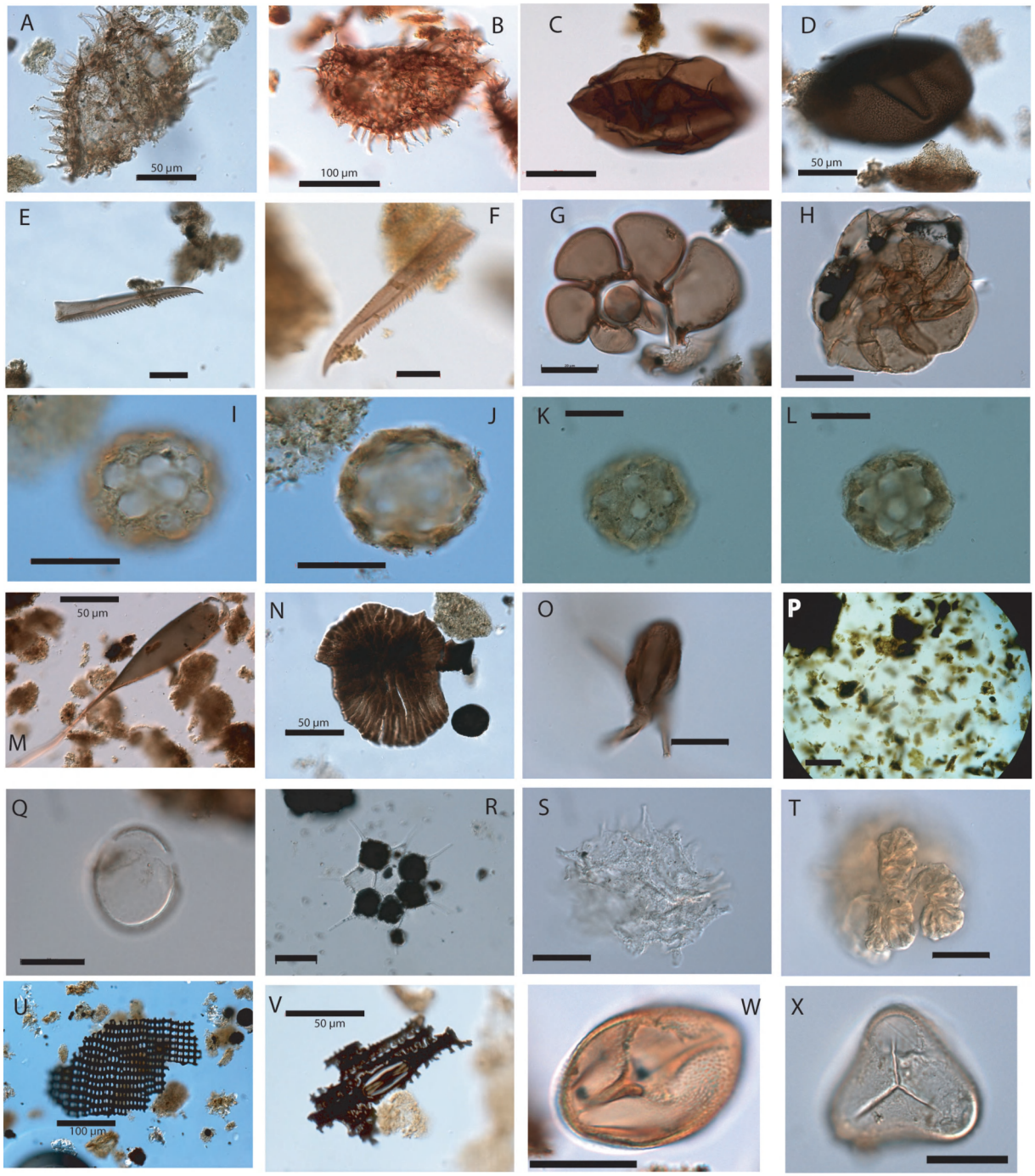

Plate III Micrographs from representative other palynomorphs from ODP 1002C. Faunal remains: A. 1H 4W 0-2, copepod egg. B. 1H 4W 22-24, copepod egg. C. 1H 5W 11-13, copepod egg. D. 1H 4W 22-24, copepod egg. E. 1H 2W 80-82, scolecodont. F. 1H 2W 141-143, scolecodont. G. 1H 2W 80-82, planispiral microforaminiferal lining. H. 2H 1W 20-23, trochospiral microforaminiferal lining. I-L. 2H 4A 101-103, organic "wrappings" of Ascidian spicule. M. 1H 2W 80-82, tintinnid lorica. Fungal remains: N. 2H 1W 20-23, fruiting body. O. 2H 1W 20-23, *Tetraploa* sp. P. 1H 1W 1.5-3.5, typical micropscopic view of anoxic Cariaco Basin palynological samples, filled with amorphous organic matter (AOM). Q. Organic lining of calcareous dinocyst. Chlororophyta: R. 2H 4W 101-103, *Pediastrum* sp. with characteristic stellate outline. S. 2H 1W20-22, less well preserved *Pediastrum* sp. T. 2H 1W 20-22, *Botryococcus* sp. Floral remains: U. 2H 1W 60-62, charcoal fragment, preservation of fine structures suggests charcoal origin V. 1H 4W 22-24, charcoal fragment. W. 1H 4W 22-24, pollen grain. X. 1H 2W 80-82, trilete spore. All scale bars are 20 µm, except where noted.

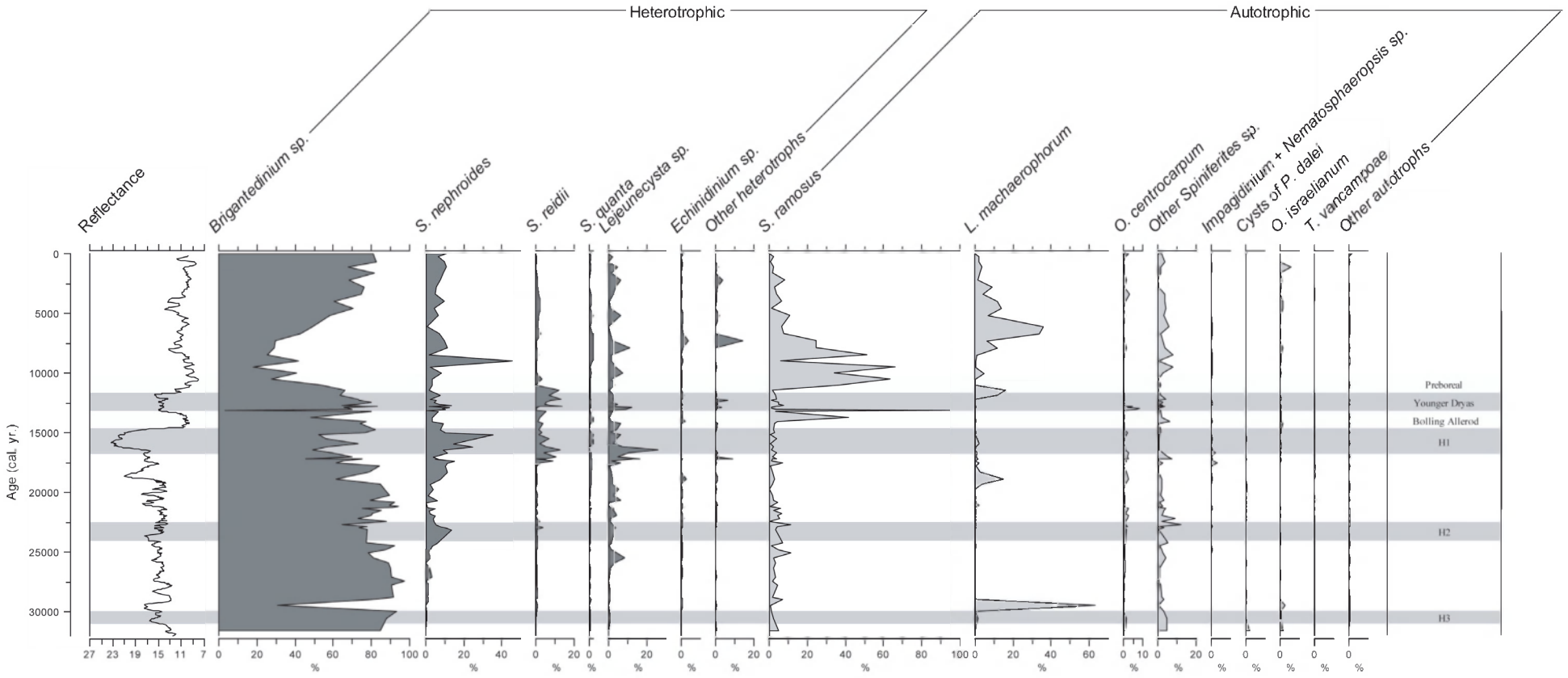

Figure 3 Relative abundances of most important dinoflagellate cyst taxa expressed in percentages of total cysts from Hole 1002C. Reflectance curve from Peterson et al. (2000a). Grey bars indicate stadials.

on a 20 µm mesh, and that part of the *Lycopodium* spores were probably lost during sieving (Lignum et al., 2008; Mertens et al., accepted). However, presumably, the large amount of amorphous organic matter in the samples will inhibit this process by quickly clogging up the filters. Also, the large fluctuations in concentrations and accumulation rates can not solely be attributed to methodological issues.

4.3 Variation of Lingulodinium machaerophorum process length

Lingulodinium machaerophorum average process length varies between 8.2 and 17.8 µm, and shows distinct fluctuations (Figure 5). It is compared to another salinity proxy, a paired Mg/Ca - $\delta^{18}O$ from *Globigerinoides ruber* (white) from the close-by Cariaco Basin core PL07-39PC constructed from Mg/Ca data from Lea et al. (2003) and $\delta^{18}O_c$ data from Lin et al. (1997). For the calculation of $\delta^{18}O_{sw}$, temperature is removed from the $\delta^{18}O_c$ record using the temperature - $\delta^{18}O_c$ equation calibrated by Thunell et al. (1999). Furthermore, *Globigerinoides ruber* (white) can be considered to be representative of annual-average conditions in the near-surface water (Lin et al., 1997).

Despite the scatter in the process length record and a possible dependence of temperature (Mertens et al., 2009b), consistencies between both independent proxies suggest that both are approximating the same environmental variable, i.e. salinity. Both short process lengths and low $\delta^{18}O_{sw}$ can be associated with lower salinities and vice versa, and thus both proxies indicate a fresher interglacial and a more saline glacial. On a millennial time-scales, H1 and YD both indicate a fresher basin, whilst the LGM, BA and Preboreal indicate a saltier environment. These trends on millennial time-scales are contrasting with these from a paired Mg/Ca - $\delta^{18}O$ by Schmidt et al. (2004) core VM28-122 from the Colombian Basin (Figure 5).

4.4 Other palynomorphs

Concentrations of all other palynomorphs show similar fluctuations as their accumulation rates, so only accumulation rates are discussed (Figure 6).

Most abundant other palynomorphs in the samples are faunal remains of zooplankton (copepod eggs, microforaminifer linings, scolecodonts and tintinnids). Tintinnids and scolecodonts show very similar fluctuations with peaks during YD and H1, whereas copepod eggs and microforaminiferal linings show a different pattern with peaks during BA and Preboreal (Figure 6). Other faunal remains are lepidopteran wing scales and organic "wrappings" of ascidian spicules. This last new faunal palynomorph has been identified, and radiating crystals are clearly visible, even after dissolution of aragonite crystals during palynological preparation (Plate III). Lepidopteran wing scales and ascidian spicules show similar patterns, with a distinct peak during the LGM. Fungal remains (fruiting bodies, ascospores, etc.) were also quantified and show a similar manifest peak during the LGM.

The most abundant floral remains are pollen and spores next to charcoal and chlorophyte algae. It has to be noted that the samples were filtered on 20 µm, so a substantial amount of pollen might have been lost, resulting in a bias towards larger pollen. Despite this, results are very similar to the results of González et al. (2008a), where sieves of 8 µm were used. Interstadials can be characterized by high pollen concentrations. Pollen grains are mainly transported into the basin by river influx (González et al., 2008a) and together with Chlorophycean algae can be used to indicate increased freshwater influx. Taxa of the class Chlorophyceae (*Pediastrum* and *Botryococcus*) show similar fluctuations as pollen and spores. Charcoal accumulations show a marked peak during the Younger Dryas, implying the occurrence of frequent fires and thus drier conditions. The charcoal peak in accumulation during the YD was presumably caused by another type of more open vegetation to dominate and would have prevented the return of preceding dense and more humid forests (Ledru et al., 2002), and can be associated with a forest-savanna turnover (Rull 2007). This peak during the YD is not surprising since frequent regional burning correlates with periods of rapid climate change (Haberle and Ledru, 2001).

Other palynomorphs include organic linings of calcareous dinocysts, *Halodinium* sp., and other ac-

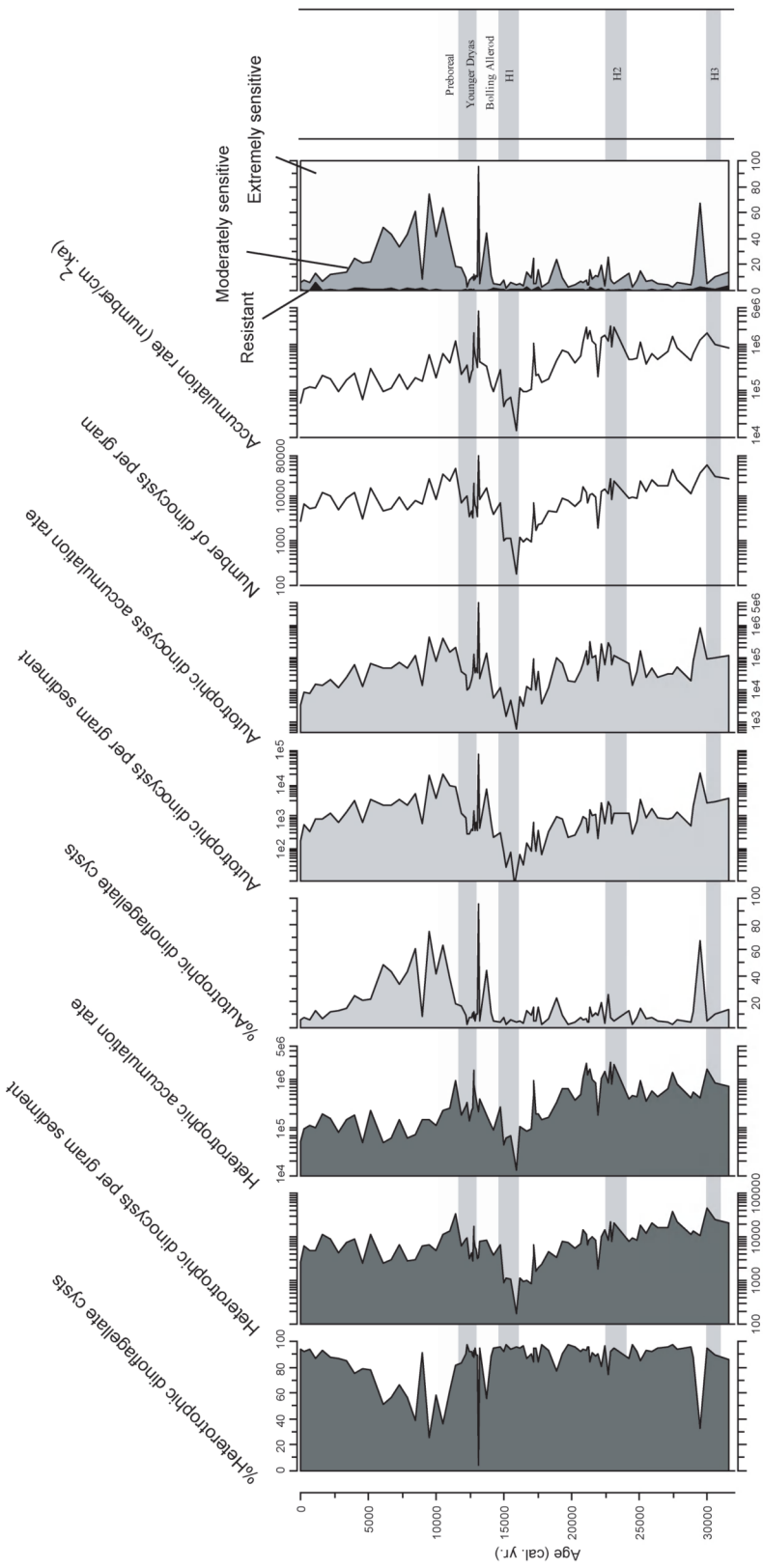

Figure 4 Relative, absolute abundances and accumulation rates of heterotrophic and autotrophic dinoflagellate cyst taxa, next to absolute and accumulation rates of total dinoflagellate cysts. The last curves show the grouping according to preservation in percentages: resistant, moderately sensitive and extremely sensitive cysts. Grey bars indicate stadials. Absolute abundances and accumulation rates are shown on a logarithmic scale.

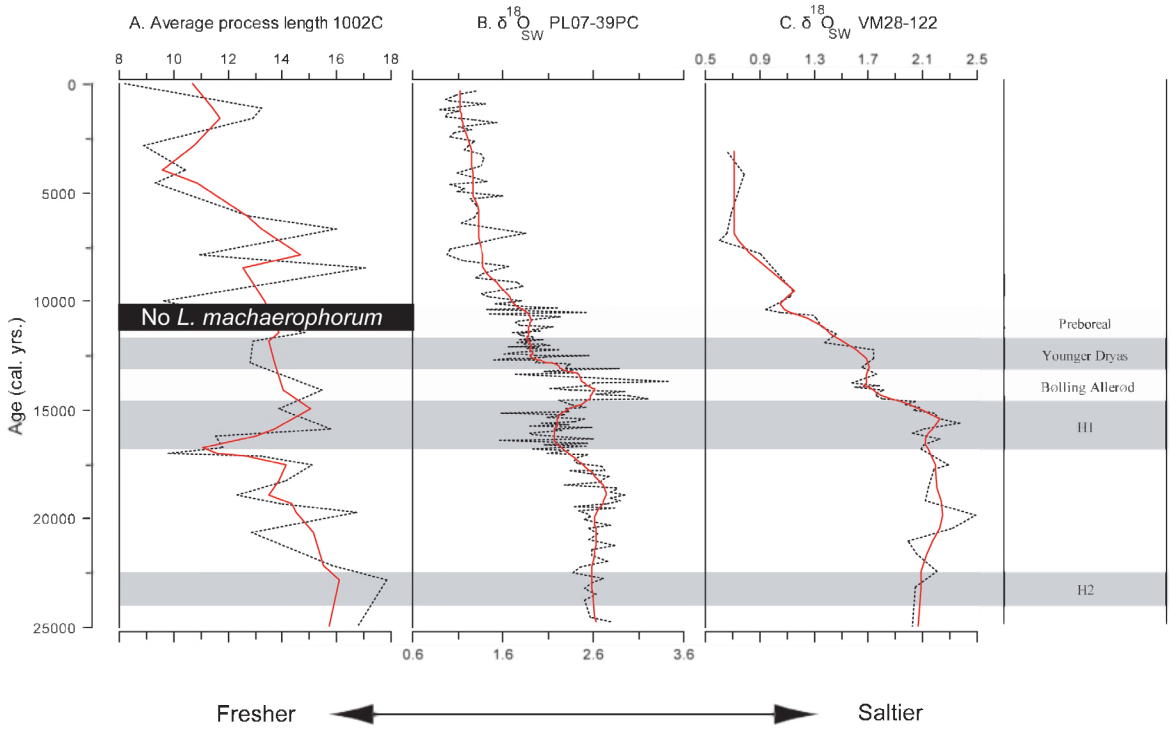

Figure 5 A. Salinity reconstruction based on *Lingulodinium machaerophorum* average process length, B. paired Mg/Ca – $\delta^{18}O$ reconstruction from core PL07-39PC from data of Lea et al. (2003) and Lin et al. (1997) and C. core VM28-122 from Schmidt et al. (2004). Grey bars indicate stadials. The Mg/Ca and $\delta^{18}O$ only extend the last 25000 years.

ritarchs. Only organic calcareous dinocysts reached high enough numbers to show reliable fluctuations, and these show a marked peak during the LGM.

5. Discussion

5.1 Transport

Pollen and spores in the Cariaco Basin are primarily transported into the basin by rivers (González et al., 2008a). Enhanced river transport is indicated by higher pollen fluxes during the interstadials (BA and Preboreal) relative to the stadials (H1 and YD) (Figure 6). The higher abundance of autotrophic dinoflagellate cysts during these periods (Figure 4) could reflect transport of these cysts from the shelf. However, this does not seem to be the case. Other palynomorphs which must be transported from the shelf, e.g. ascidian spicules and lepidopteran scales, do not show enhanced shelf transport during the BA and the Preboreal periods, but rather during the YD. Ascidians are sessile filter feeding tunicates and are important members of marine benthonic communities throughout shelf seas (Varol and Houghton 1996), and can thus be considered to be indicative of transport from the shelf. Lepidopteran wing scales must also be transported from the shelf. The only time when manifest enhanced transport from the shelf is recorded is during the LGM, since most other palynomorphs show enhanced accumulations during this period (Figure 6). This is related to the sea level lowering during the LGM exposing the shelf, which is corroborated by the observations of Piper and Dean (2002).

Another transport issue is turbidite deposition, associated with earthquake activity, which has been previously reported in the Cariaco Basin (Thunell et al., 1999; Scranton, et al., 2001). All turbidites clearly stand out in the Cariaco Basin record and all samples were carefully selected outside the turbidite layers.

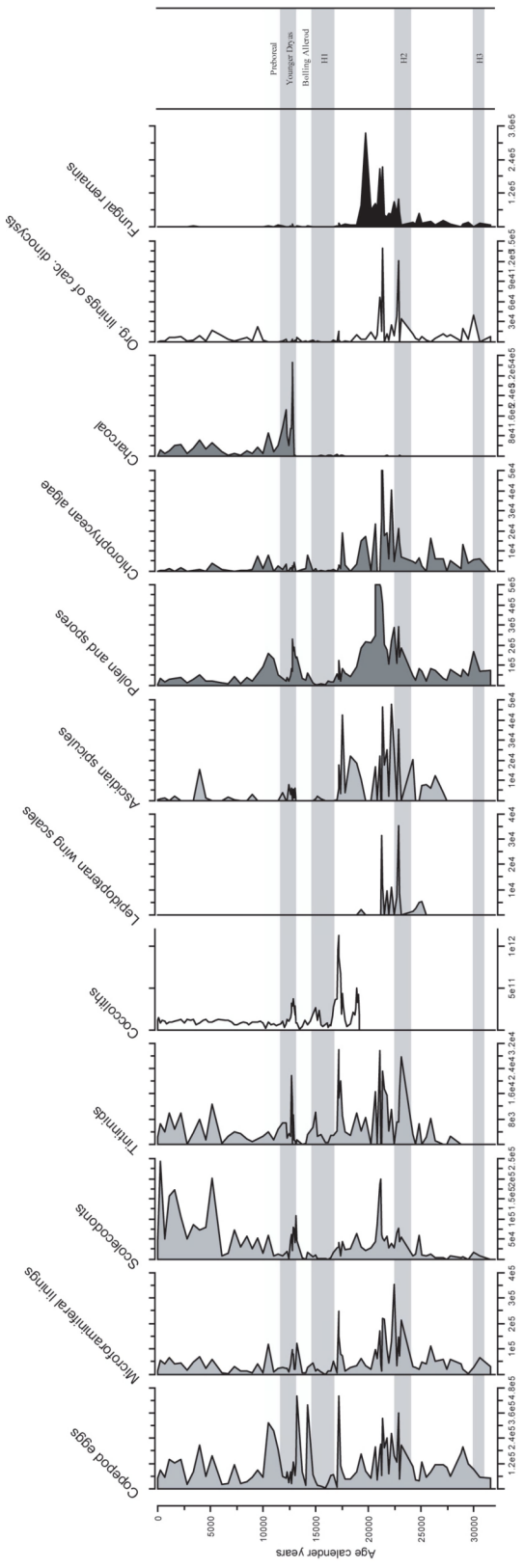

Figure 6 Accumulation rates of other palynomorphs (in number/cm^2.kyr): zooplankton (copepod eggs, microforaminiferal linings, scolecodonts and tintinnids), coccoliths (Mertens et al., 2009c), other faunal remains (Lepidopteran wing scales and Ascidian spicules), floral remains (pollen and spores, Chlorophyta, charcoal), organic linings of calcareous dinocysts and fungal remains. Grey bars indicate stadials.

5.2 Preservation

To see whether selective preservation can be an issue in the Cariaco Basin, a similar grouping as in Zonneveld et al. (2001) and Mertens et al. (accepted) was used to which we added a few species where it can be supposed that they have similar resistance to degradation:

Extremely sensitive cysts: Round brown cysts (*Brigantedinium* spp.), Spiny Brown cysts (*Echinidinium* spp. and *Islandinium minutum*), *Stelladinium* spp., *Lejeunecysta* spp., *Selenopemphix* spp., *Tuberculodinium vancampoae*.

Moderately sensitive cysts: *Lingulodinium machaerophorum*, *Melitasphaeridium choanophorum*, *Operculodinium centrocarpum* sensu Wall and Dale, *Operculodinium janduchenei*, *Spiniferites* spp., *Achomosphaera* spp, *Quinquecuspis concreta* and *Votadinium* spp.

Resistant cysts: *Nematosphaeropsis labyrinthus*, *Impagidinium* spp., *Operculodinium israelianum*, *Pentapharsodinium dalei*, *Polysphaeridium zoharyi*, *Ataxiodinium choane* and *Bitectatodinium* spp.

As fluctuations between resistant and sensitive cysts are exactly a reflection of changes between autotrophic and heterotrophic dinoflagellate cysts (Figure 4), ecological changes cannot be discarded. By studying the coccolith assemblage in the same core over the same interval, Mertens et al. (2009c) came to the conclusion that high productivity should be considered in sync with less degradation of coccoliths and *vice versa*. This seems to be similar for dinoflagellate cysts: periods of high productivity such as the YD resulted in low degradation of dinoflagellate cysts, while periods characterised by lower productivity like the BA and the Preboreal resulted in higher degradation of dinoflagellate cysts.

Pronounced disparities can be observed between fluctuations of the relative abundance record and the concentration of heterotrophic dinoflagellate cysts (Figure 4). These disparities suggests that preservation is an important factor in the interpretation of the relative abundance record of the heterotrophic dinoflagellate cysts. On the other hand, this difference between both relative abundance and concentration is not observable in the autotrophic dinoflagellate cysts (Figure 4), and could be explained by relative enrichment of resistant material causing synchronous increases in relative and absolute abundance of these species.

Degradation could have taken place in the water column, in the sediment or after coring. To assess whether selective preservation is caused by post-depositional degradation after coring, samples from Hole 1002C were compared with samples from similar intervals from MD03-2620, but we found no significant differences in assemblage composition over the selected intervals. Presumably, the degradation process can be considered to have the most important influence in the water column (Mertens et al., 2009c). Only 1.33% of the surface primary productivity is delivered to the bottom of Cariaco Basin (Muller-Karger et al., 2004). Losses of organic matter occur mostly in the watercolumn, and post-depositional losses are negligible (Wakeham and Ertel 1988). Furthermore, Thunell et al. (2007) have shown that particulate organic carbon fluxes strongly correlate with mineral fluxes in the Cariaco Basin. This mineral ballasting could potentially cause enhanced preservation of sensitive dinoflagellate cysts.

It has to be noted that the formation of a pyritized "gley" horizon has been described by Blazhchishin and Lukashina (1995), and corresponds to a zone of sulfide diffusion underlying the transition from oxic to anoxic conditions (Lyons et al., 2003), and spans H1 in Hole 1002C. This zone corresponds to a zone of low accumulations of both heterotrophic and autotrophic dinoflagellate cysts, and very likely corresponds to a zone of degradation within the sediment, possibly related to pyritization of the cysts.

To conclude, preservation is an issue in the very productive Cariaco Basin, which can be related to degradation within the water column (from BA to recent) and postdepositional degradation (during H1). However, since high productivity can be related to enhanced preservation and vice versa and since absolute abundances of heterotrophic species can be considered to reflect changes in primary productivity (Reichart and Brinkhuis, 2003), changes in productivity can still be reconstructed which will be discussed

in the next section.

5.3 Productivity

In terms of ecology, the shifts between heterotrophic and autotrophic cysts require an explanation. Dinoflagellate plankton studies are rare in the Caribbean (e.g. Marshall 1973), so it is difficult to make direct links to current dinoflagellate blooms in the Caribbean. Despite this fact, insights gained from dinoflagellate studies in other basins can be used to make inferences about paleoproductivity changes in Cariaco Basin.

Globally, heterotrophic species generally dominate areas with enhanced nutrient conditions and active upwelling (Marret and Zonneveld 2003), and absolute abundances of heterotrophic cysts reflect changes in primary productivity (Reichart and Brinkhuis 2003). Both relative and absolute abundances indeed reach higher numbers during the Younger Dryas (Figure 4), a period associated with enhanced upwelling in the Cariaco Basin (Peterson et al., 2000; Lea et al., 2003; Mertens et al., 2009c). We presume that the time interval that correlates with H1 was also a period of enhanced productivity, as noted by Mertens et al. (2009c), although the sulphidic overprint mentioned above makes it difficult to recognize it as such. The other stadials associated with Heinrich events (H2 and H3) show peaks of the accumulations of heterotrophic dinoflagellate cysts, and confirm previous observations of the older record by González et al. (2008b), although it must be stressed that other peaks of a similar amplitude can be observed in this part of the record, so that these peaks cannot serve to unambiguously identify these Heinrich events. Other heterotrophic species (*Selenopemphix nephroides*, *Stelladinium reidii*, *Lejeunecysta* spp.) show similar peaks during these HE (Figure 3). Additionally, we record an event around 8.44 kyr by a peak in *S. nephroides*, which can be related to stronger trade winds in the Cariaco Basin (Hughen et al., 1996b). This event has also been reflected as a major freshwater event in the Gulf of Mexico from 8.6 to 8.3 kyr, where it can be related to episodic megaflooding of the Mississippi river system or large scale changes in precipitation patterns over the Gulf of Mexico (LoDico et al., 2006).

The autotrophic species are to a large extent determined by relative abundances of *Spiniferites ramosus* and *Lingulodinium machaerophorum* (Figure 3). In the Amazon region, *Spiniferites ramosus* can be related to oligotrophic, shelfward conditions (Vink et al., 2000), as in British Columbia estuarine environments where autotrophic taxa, including *Spiniferites ramosus*, are related to stratified coastal waters under influence of coastal runoff (Radi et al., 2007). Also, the abundances of *Spiniferites ramosus* shows similar fluctuations as the coccolith *Gephyrocapsa oceanica*, responding to warming of the surface water and high river influx, simultaneous with weakening of upwelling rates, most pronounced during BA and Preboreal (Mertens et al., 2009c). Furthermore, the correspondence of Ti (XRF) data (Haug et al., 2001) and the relative abundance of autotrophic dinoflagellate cysts (Figure 7), suggests a rapid response of autotrophic dinoflagellate cysts to high river influx, a similar conclusion as González et al. (2008b).

Lingulodinium machaerophorum shows a very different pattern compared to *Spiniferites ramosus* (Figure 3). According to Vink et al. (2003), *Lingulodinium machaerophorum* can be related to neritic, warm, low-density, stratified environments in the Equatorial Atlantic. The stadials associated with Heinrich events are followed by short events of water column stratification. The middle Holocene also shows a similar stratification of the water column. The different pattern between *Spiniferites ramosus* and *Lingulodinium machaerophorum* suggests that high river influx inhibits *Lingulodinium machaerophorum* blooms, which could be due to a combination of a number of processes, including enhanced shelfal transports due to heavy monsoonal rainfall (Jordan and Winter 2000) and stagnation of sulphidic waters (Lyons et al., 2003) inhibiting excystment (e.g. Kremp and Anderson 2000).

The recorded shifts between an autotrophic dinoflagellate cyst dominated record, coupled to river influx, and a heterotrophic dinoflagellate cyst dominated record, coupled to higher upwelling rates, confirm the models of González et al. (2008b) and Mertens et al. (2009c) who assert that these rapid changes can be linked to migrations of the ITCZ. Again, no asynchronicity between the terrestrial and the

marine signal can be recorded, as stated in Mertens et al. (2009c).

The shifts between autotrophic and heterotrophic dinoflagellates can also explain differences between reconstructions using sterol biomarkers of Werne et al. (2000) and Dahl et al. (2004). In the first study which solely used dinosterol, little difference was found between YD and Holocene, whereas the latter authors found significant differences between both periods using a larger suite of sterols (chlorine sterol esters, CSEs). Since dinosterol is produced both by autotrophic and heterotrophic dinoflagellates, a differentiation between YD and Holocene will be less pronounced. The approach used by Dahl et al. (2004), where specific CSEs are used to track changes in dinoflagellate abundance, enables to differentiate between YD and Holocene, and can probably be attributed to these CSEs being mainly produced by autotrophic dinoflagellates. Culture studies on which dinoflagellates produce which CSEs could elucidate this further.

Similar trends in productivity are observed in the other palynomorphs (Figure 6). Copepod eggs are more abundant during the BA and the Preboreal (Figure 6). Copepods are known to prey on dinoflagellates (e.g. Huntley et al., 1986; Abrahams and Townsend 1993), which then show the highest accumulations (Figure 4). Also, the low abundance of copepod eggs during the strong upwelling during the YD, could possibly be related to aldehyde production by diatoms inducing reduced hatching success (e.g. Romano et al., 2003; Wichard et al., 2008). Tintinnids accumulations on the other hand, are similar to coccolith accumulations (Mertens et al., 2009c; Figure 6) which show their peak during H1 and YD (Mertens et al., 2009c). This suggests that coccolith accumulations are linked to tintinnid faecal pellet production, which is not surprising since tintinnids are known to feed on coccolithophores (e.g. Winter et al., 1986) and material is grouped in aggregates, most likely pellets (Hughen et al., 1996a).

5.4 Salinity reconstruction

On a glacial-interglacial scale, both the average process length of *Lingulodinium machaerophorum* and $\delta^{18}O_{sw}$ reconstruction indicate a more saline environment during the last glacial, and a fresher basin

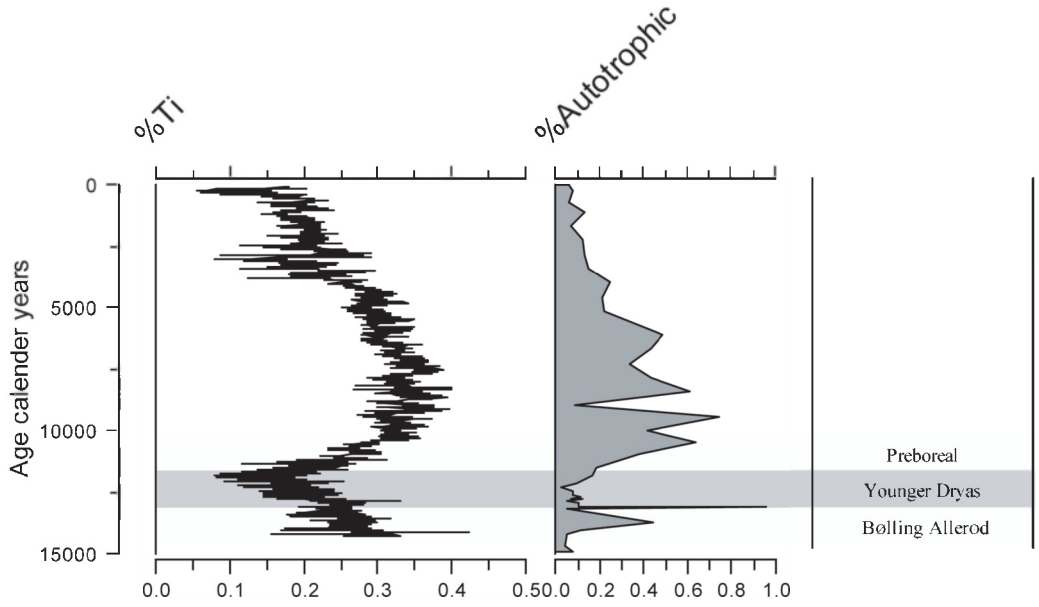

Figure 7 Comparison between two hydrological proxies, %Ti (XRF data from Haug et al., 2001) and % autotrophic dinoflagellate cysts (this study). Grey bars indicate stadials. The Ti XRF data has only been published for the last 14600 years.

during the current interglacial (Figure 5). Increased glacial high-salinity and interglacial low-salinity conditions were also suggested by Peterson et al. (1991) by studying foraminiferal assemblage changes in Cariaco Basin cores V12-104 and V12-99. Similar observations are made for Hole 1002C (Peterson et al., 2000b; Herbert and Schuffert, 2000), which can be linked to a greater aridity in the Cariaco Basin during glacial periods (Yarincik and Murray, 2000; Martinez et al., 2007). Similarly, in the Caribbean Sea, higher salinity estimates have been inferred during glacial isotope stages based on palaeoecological analyses of coccoliths (Giraudeau, 1992) and paired Mg/Ca - $\delta^{18}O$ measurements (Schmidt et al., 2004), so this is not a local phenomenon, and can belinked to shifts of the ITCZ, and can cause changes in the thermohaline circulation, (Schmidt et al., 2004).

On a millennial scale, both salinity proxies indicate a saline LGM and a fresh H1 followed by a more saline BA, and a fresh YD again followed by a more saline Preboreal. A negative excursion during H1 was previously noted by Lin et al. (1997) in the oxygen isotope records, and was considered to be related to increased rainfall or meltwater pulse. However, when compared to the salinity reconstruction from core VM28-122 located in the Colombia Basin (Schmidt et al., 2004), we observe an opposing pattern, most pronounced during LGM, H1, BA and YD (Figure 5). This millennial-scale variability is also opposite to variations in river influx in the Cariaco Basin indicated by pollen and spores, Chlorophycean algae, autotrophic dinoflagellate cysts accumulations (Figs. 7 and 9) and plant biomarkers (Hughen et al., 2004). The fresh YD contrasts also with an arid YD, which can be inferred from the upwelling record (Lea et al., 2003 and Mertens et al., 2009c), but also the charcoal accumulations (Figure 6) and continental pollen (Salgado-Labouriau, 1980; Leyden, 1985) and plant biomarker records (Xu and Jaffé 2007). Also, Amazon river discharge was 40% reduced during the YD (Maslin and Burns, 2000). Furthermore, the fresh H1 contrasts with González et al. (2008b), who suggested the development of hypersaline coastal environments during HEs. This asynchronicity between salinity records and hydrological records is enigmatic. Sea level variations do not help to explain the differences. Rapid sea-level rises during melt-water pulses can cause mobilisation of the sediment upshelf, and drops downslope during lower sea level (Summerhayes et al., 1975) and it has been shown to only change the magnitude of terrigenous pulses at the Brazil continental margin (Arz et al., 1999), although higher shelf transport during the LGM (see above) does seem to suggest this. Three possible mechanisms can be thought of. The first is an influence of stratification on the salinity records. An increased stratification during interstadials could result in higher salinities if the microfossils recording the salinities would form deeper in the water column where salinities are higher. In fact, the dinoflagellate cyst *Lingulodinium machaerophorum* has been found to occur deeper in the water column (see Mertens et al., 2009a for a review) and variants of the foraminifer *Globigerinoides ruber* (white) can also be associated with deeper depth habitats (Wang 2000; Kuroyanagi et al., 2008), resulting in different Mg/Ca temperatures (Steinke et al., 2008). Another possibility is the more isolated nature of the Cariaco Basin during these times, resulting in anomalous temperatures (Lea et al., 2003) and salinities (this study) for the Caribbean, also suggested by modelling studies (Wan et al., 2008). A last possibility is the intrusion of low salinity Antarctic Intermediate Water (AAIW) into the Caribbean during H1 and YD, evidenced by neodymium isotopic variations (Pahnke et al., 2008), which then supposedly not reached as far west as the Columbian Basin.

6. Conclusions

Assemblage changes of dinoflagellate cysts are determined by productivity changes and show rapid shifts between heterotrophic dominated assemblages and autotrophic dominated assemblages, which can be related to shifts of the ITCZ. Due to the occurrence of large losses in the water column, relative abundance records should be interpreted with care, and always compared to accumulation records. Stadials (including those associated with Heinrich events) can be characterised by higher upwelling, interstadials by higher river influx preceded by high stratification. The LGM is characterized by influx from the shelf, caused by the concurrent sea level

lowering.

The average process length of *Lingulodinium machaerophorum* shows similar fluctuations as a constructed paired Mg/Ca - $\delta^{18}O$ record and can serve as a semi-quantitative salinity proxy. These salinity proxies show a millennial-scale pattern contrasting to a salinity reconstruction from the open Caribbean Sea and to what would be expected from the hydrological proxies (autotrophic dinoflagellate cysts, Ti (XRF), pollen and spores and Chlorophyta). Changes in the stratification, isolation of the Cariaco Basin or advection of fresh water masses could explain this discrepancy.

These results confirm previous findings but also emphasize the uniqueness of this extraordinary environmental setting.

Additional information

Dinoflagellate cysts and other palynomorphs were extracted and counted by Kenneth Mertens. Interpretations were done by Kenneth Mertens. This chapter has been accepted for publication in *Boreas*.

CHAPTER 7

Reconciling dinoflagellate cyst and Mg/Ca records as tools for temperature, salinity and productivity reconstructions during the last 40000 years in the Southern Gulf of Cádiz

ABSTRACT

The southern Gulf of Cádiz is a particularly climatologically sensitive region, acting as a natural laboratory to record variations of the North Atlantic Oscillation (NAO). Past variations triggered assemblage and morphological changes of dinoflagellate cysts and other palynomorphs, analysed from core GeoB9064-1. The recovered dinoflagellate cyst assemblages are dominated by abundances of *Lingulodinium machaerophorum*, which are determined by enhanced fluvial supply during negative NAO phases, pronounced during precession minima. This enhanced fluvial supply causes transport and enhanced preservation via mineral ballasting of *Lingulodinium machaerophorum* cysts and other organic components. Positive NAO phases can be related to higher upwelling conditions during HEs, and are mirrored in cooler Mg/Ca SSTs, W/C ratios, "*Bitectatodinium tepikiense-Nematosphaeropsis labyrinthus* events" and bisaccate pollen. Despite a short lag, *Lingulodinium machaerophorum* average process lengths and paired Mg/Ca – $\delta^{18}O$ deduced salinities reflect enhanced precipitation conditions during the Bølling/Allerød and middle Holocene over the Mediterranean area. These salinity changes are in sync with temperature differences between Mg/Ca and alkenone derived SSTs, which can be related to lateral advection of alkenones, which thus exhibit a salinity influence.

1. Introduction

The Gulf of Cádiz is located between the Iberian Peninsula and Morocco, west of the Strait of Gibraltar in the East Atlantic (Figure 1). In the east, the Gulf of Cádiz is connected to the Mediterranean, and in the west to the open Atlantic Ocean. Current circulation patterns in the Gulf of Cádiz are characterised by a dynamic oceanographic setting, controlled by exchanges of water masses through the Strait of Gibraltar. The main rivers draining the Middle Atlas in the Moroccan borderlands are the Sebou River and other rivers (Figure 1) of which the plumes spread over a large coastal area (Warrick and Fong, 2004) and provide important contributions to the sediments. Trade-wind coastal upwelling occurs in a narrow 5-km band on the shelf (Mittelstaedt, 1991) and this is a much smaller zone than off the northern margin of the Gulf of Cádiz (Ruiz and Navarro, 2006) and towards the southern Canary Islands (Pelegrí et al., 2004).

The climatological regime in the Gulf of Cádiz

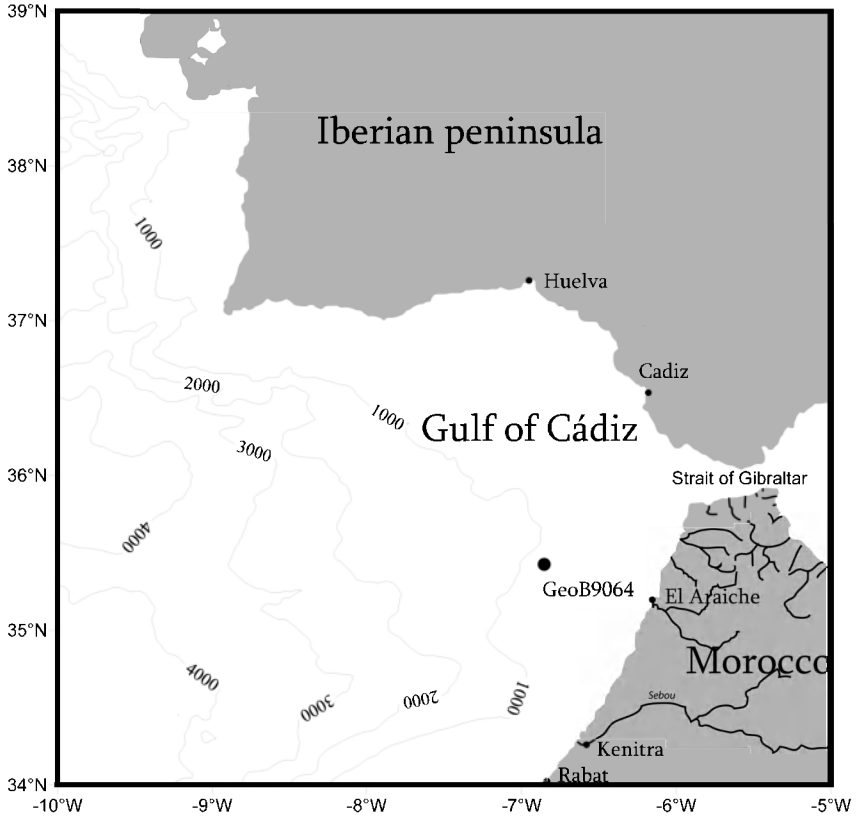

Figure 1 Map of the Gulf of Cádiz connected to the Mediterranean through the narrow Strait of Gibraltar and surrounded by Iberian Peninsula and Morocco. Depth contours are every 1000 m. In Morocco main rivers are drawn. Major coastal cities are marked, next to the location of the studied core GeoB9064-1.

extends down to 28°N and is typical for the Mediterranean region. It is called the "Mediterranean regime", and switches between a dry summer season and a rainy winter season (Hsu and Wallace, 1976). Over the past decades, changes in this climatological regime in southern Europe can be related to changes in the North Atlantic Oscillation (NAO), with negative NAO indices related to averagely higher atmospheric moisture and warmer temperatures and positive NAO indices associated with higher aridity and cooler temperatures (Hurrell, 1995). These variations are observed over longer time-scales in the Mediterranean, on centennial (Luterbacher and Xoplaki, 2003) to millennial time-scales (Moreno et al., 2004). A multi-proxy approach using coccoliths, biomarkers and grain sizes by Mertens et al. (in prep.) revealed a strong imprint of this signal in the southern Gulf of Cádiz. To complete the palaeoceanographical framework, a climatic reconstruction based on palynomorphs and Mg/Ca ratios and stable oxygen isotopes measured on the shells of the planktonic foraminifer *Globigerina bulloides* is presented here.

Dinoflagellate cysts are the hypnozygotes of unicellular, organic-walled planktonic algae, and are considered to be useful palaeoceanographical tools for the reconstruction of late Quaternary productivity (Reichart and Brinkhuis, 2003; Pospelova et al., 2006; de Vernal and Marret, 2007) and temperature and salinity (Dale and Dale, 2002; de Vernal et al., 2005). Despite possible problems with preservation (Zonneveld et al., 2007; 2008) and transport (Dale and Dale, 2002), they have proven useful for the southern Gulf of Cádiz (Marret and Turon, 1994) and the adjacent sea of Alborán (Combourieu Nebout et al., 1999). Also, recent research showed that dinoflagellate cyst morphology changes with salinity, and more particular, the process length of *Lingulodinium machaerophorum* shows a linear re-

lationship to salinity as demonstrated by studies of cultures (Hallett, 1999) and recent surface sediments (Mertens et al., 2009b).

Additionally, an inorganic geochemical method is applied based on Mg/Ca element ratios measured on shells of Foraminifera. This method relies on the thermodynamically different behaviour of trace elements during the calcification of Foraminifera, which is primarily a function of temperature. Mg/Ca palaeothermometry is applied to reconstruct sea surface temperatures (SSTs) (e.g. Mashiotta et al., 1999; Elderfield and Ganssen, 2000; Lea, 2003; Nürnberg and Groeneveld, 2006), the major advantage of this method is that oxygen isotopes ($\delta^{18}O$) can be measured on the same biotic carrier, which ensures the recording of the same seasonality and/or habitat effects. Salinity can then be reconstructed using paired Mg/Ca – $\delta^{18}O$ measurements on foraminifers (e.g. Schmidt et al., 2004; Nürnberg and Groeneveld, 2006). This method can be used as an independent control for the process length salinity proxy (Mertens et al., 2009a). The selected planktonic foraminifer was *Globigerina bulloides* which can be considered representative for relatively shallow surface waters from spring to summer in the Gulf of Cádiz (Rogerson et al., 2004).

The aim of this study in the Southern Gulf of Cádiz is to (1) document variations of marine productivity by studying relative and absolute abundances of dinoflagellate cysts, (2) record palaeotemperatures based on foraminiferal Mg/Ca palaeothermometry and dinoflagellate cyst assemblage changes, (3) record palaeosalinity variations using the paired Mg/Ca – $\delta^{18}O$ approach and morphological variations of *Lingulodinium machaerophorum,* (4) reconcile these observations with other proxies to reconstruct palaeoclimate variations in the southern Gulf of Cádiz, and explain how these are coupled to migrations of the NAO.

2. Material and methods

Gravity core GeoB9064-1 (35°24.91'N, 6°50.72'W; 702 m water depth, 544 cm recovery) was collected during RV Sonne cruise SO175 to the Gulf of Cádiz, which was organised by MARUM, Bremen, Germany (Kopf et al., 2004). The core analysed in this study is located on the Moroccan continental margin, in the El Arraiche mud volcano field (Van Rensbergen et al., 2005; Foubert et al., 2008), in the southern part of the Gulf of Cádiz. As the core lies outside the influence of the Mediterranean Outflow plume characterised by strong hydrodynamics (Rogerson et al., 2005), it has potential to contain a relatively undisturbed palaeoceanographic record compared to cores within or close to the Mediterranean Outflow plume. All data are accessible as Supplementary data.

2.1 Chronostratigraphic framework

Core GeoB9064-1 is dated with 6 accelerator mass spectrometry (AMS) ^{14}C dates on planktonic foraminifera, over the studied interval. Oxygen isotopes were measured on *Neogloboquadrina pachyderma* (dextral), and were used together with a Ti XRF record to tune to the GISP 2 isotope record using Analyseries 2.0 (Paillard et al., 1996) and is discussed elsewhere (Mertens et al., in prep.).

The record ranges from 41300 to 1600 cal. yrs BP, and span the Last Glacial Maximum, Bølling/Allerød (BA), Younger Dryas (YD) and Heinrich event (HE) 1 to 4. Sedimentation rates vary between 8 and 34 cm / kcal.yrs. Samples for Mg/Ca and palynological analysis were taken at 10 cm intervals. Given the range of sedimentation rates, the sampling interval yields an average temporal resolution of 730 years and range between 212 and 1,875 years.

2.2 Palynological preparation and light microscopy

A total of 54 samples with a dry weight of 9.5 to 13.1 g were prepared for palynological analysis following the maceration technique described in Louwye et al. (2004). Two to three *Lycopodium* tablets, containing a known number of spores were added at the beginning of the palynological preparation. The treatment involved decalcification with cold HCl (10%) and subsequent removal of silicates with cold HF (40%). The remaining organic fraction was then sieved at 20 µm on a nylon mesh and mounted with glycerine jelly. Due to the large abundance of *Lingulodinium machaerophorum* in the samples

(averagely 64% of the assemblage), it was chosen to reach a count of minimum 400 dinoflagellate cysts, excluding *Lingulodinium machaerophorum*. This meant that between 1,450 and 4,868 dinoflagellate cysts needed to be counted. All other organic-walled palynomorphs encountered were also counted per sample. *Lycopodium* spores were counted to calculate cyst concentrations (cysts/cm^3). Accumulation rates were calculated by multiplying with sedimentation rates and dry bulk densities (Mertens et al., in prep.). All micrographs are taken with a Zeiss AxioCam MRc5 camera mounted on a Zeiss Axioskop 2 Plus microscope. Taxonomy used follows Rochon et al. (1999) and Fensome and Williams (2004). *Selenopemphix quanta* s.l. includes cysts of *Protoperidinium nudum*. Tests with the "best analogue method" developed for dinoflagellate cysts by de Vernal et al. (1994, 1998) with our data were unsuccessful, due to the over-representation of *Lingulodinium machaerophorum* in the assemblages, a similar problem encountered by Eynaud et al. (2000). Chlorophyll-a concentrations in the upper water column (Y) and bottom water oxygen concentrations (O_2) are reconstructed from cysts known to be extremely sensitive to aerobic decay (S-cysts) and cysts resistant against aerobic decay (R-cysts) (Table 1) using equations from Zonneveld et al. (2007):

$$Y = 0.0002 * r + 0.2271$$

$$kt_S = \ln\left(\frac{X_i}{X_f}\right)$$

$$[O_2] = \frac{5.17}{1 + e^{-1.23*(kt-2.058)}}$$

where:

Y = Chlorophyll-a concentrations (mg/m^3)

r = accumulation rates of R-cysts (cysts/cm^2.kyr)

kt_S = the rate of decay of S-cysts

X_i = initial accumulation rate of S-cysts (cysts/cm^2.kyr)

X_f = final accumulation rate of S-cysts (cysts/cm^2.kyr)

$[O_2]$ = bottom water oxygen concentrations (ml/l)

The morphological variation of *Lingulodinium machaerophorum* was studied by measuring the 3 longest processes of 50 cysts per sample, when possible and follows (Mertens et al., 2009b). The longest processes are chosen for three reasons. Firstly, the longer processes would reflect unobstructed growth during formation of the cyst. Secondly, since only a restricted number of processes are measurable per cyst it is necessary to make a consistent approach by choosing the longest processes. Thirdly, the largest variation is obtained by choosing the longest processes, and this provides a more accurate proxy. The length of each process was measured from the middle of the process base to the process tip. Within each cyst, three processes could always be found within the focal plane of the light microscope, and for this reason this number seemed a reasonable choice. Fragments representing less than half of a cyst are not measured, as well as cysts with mostly broken processes.

Table 1 List of cyst-species included within the S-cyst and R-cyst groups.

S-cysts	R-cysts
Brigantedinium sp.	*Impagidinium* sp.
Echinidinium sp.	*Nematosphaeropsis labyrinthus*
Lejeunecysta sp.	*Operculodinium israelianium*
Quinquecuspis concreta	cyst of *Pentapharsodinium dalei*
Selenopemphix sp.	
Trinovantedinium applanatum	

2.3 Mg/Ca and $\delta^{18}O$ analysis on *Globigerina bulloides*

For stable oxygen isotope analysis, 10 specimens of *Globigerina bulloides* were picked from the >125 µm fraction for each sample. The tests were ultrasonically cleaned in distilled deionized water prior to analyses. The isotopic analyses of the planktonic foraminifers were performed with a Finnigan MAT 251 mass spectrometer equipped with an automated Kiel Carbonate Preparation line. The mass spectrometer is calibrated to NBS 19, and the isotope values are reported on the VDPB scale. The external reproducibility of in-house carbonate standards was ±0.08‰ for $\delta^{18}O$ and 0.04‰ $\delta^{18}C$ (1 σ values). All results are reported in ‰ relative to VPDB.

For Mg/Ca analysis, 20 to 50 tests of *Globigerina*

bulloides from the >125 µm fraction were picked from each sample and cleaned according to the procedure of Barker et al. (2003). These specimens originate from the same samples and size fractions as the specimens measured for stable oxygen isotope analysis. With a few exceptions, sample spacing was 10 cm between 0 and 550 cm. After dissolution the samples were centrifuged for 10 minutes at 6000 rpm and diluted for analysis on an ICP-OES (Perkin Elmer Optima 3300R, Department of Geosciences, University of Bremen). The analytical precision of the Mg/Ca analyses for *Globigerina bulloides* is 0.20%, while reproducibility based on replicate samples is ± 0.12 mmol/mol (3.8%). The validity of analyses was checked by analyzing the Mg/Ca-standard ECRM752-1 (Greaves et al., 2008), while stability of the ICP-OES was monitored via an in-house standard with a Mg/Ca ratio of 2.90 mmol/mol. The conversion of foraminiferal Mg/Ca ratios into $SST_{Mg/Ca}$ was accomplished according to the algorithm of Mashiotta et al. (1999): $Mg/Ca = 0.474\ e^{0.107}\ SST$, $R^2 = 0.98$. The error in terms of $SST_{Mg/Ca}$ is ± 0.8°C.

The calculation of $\delta^{18}O_{seawater}$ and palaeo-SSS follows Shackleton (1974), similar to Nürnberg and Groeneveld (2006):

$$\delta^{18}O_{seawater} = \delta^{18}O_{foram} - 21.9 + 0.27 + \sqrt{(310.6 + (10 * Mg/Ca_{SST}))}$$

After calculation of $\delta^{18}O_{seawater}$, the $\delta^{18}O_{foram}$ was corrected for the global ice volume signal by subtracting the Waelbroeck et al. (2002) mean-ocean $\delta^{18}O_{benthic}$ record as a reasonable approximation for variations in the global ice volume, resulting in $\delta^{18}O_{sw-ivf}$ (ivf = ice volume free), indicative for relative changes in local sea water salinity. Due to the relatively shallow location of GeoB9064-1 dissolution can be excluded from having an influence on Mg/Ca ratios.

3. Results

3.1 Dinoflagellate cyst relative abundance data

A total of 38 dinoflagellate cyst taxa were identified in the studied sequence (see species list in Appendix VI). Representative dinoflagellate cyst species are illustrated in Plates I and II (1-8). Only three taxa reach relative abundances of more than 15%: *Lingulodinium machaerophorum* (33–90%), *Spiniferites delicatus* (0–20%) and *Spiniferites* spp. (4–40%) (Figure 2). Other species of minor importance (max. 5–15%) are *Bitectatodinium tepikiense* (0–13%), *Operculodinium centrocarpum* sensu Wall and Dale (1–8%), *Spiniferites membranaceus* (0–6%), and *Impagidinium aculeatum* (0–6%). Rare species (max. 1–5%) are *Brigantedinium* spp. (0–4%), *Impagidinium patulum* (0–4%), *Spiniferites mirabilis* (0–3%), *Impagidinium* spp. (0–3%), *Nematosphaeropsis labyrinthus* (0–3%), *Operculodinium israelianum* (0–3%), *Trinovantedinium applanatum* (0–3%), *Polykrikos schwarzii* (0–3%), *Selenopemphix nephroides* (0–3%), *Spiniferites hyperacanthus* (0–2%), *Impagidinium sphaericum* (0–2%), *Selenopemphix quanta* (0–2%), *Spiniferites bentorii* (0–2%), *Spiniferites elongatus* (0–2%) and *Spiniferites ramosus* (0–1%). Very rare species (<1%) are *Ataxiodinium choane, Brigantedinium cariacoense, Echinidinium* spp., *Impagidinium pallidum, Impagidinium sphaericum, Impagidinium velorum, Islandinium minutum, Tectatodinium pellitum, Lejeunecysta* spp., cyst of *Pentapharsodinium dalei, Pyxidinopsis reticulata, Tuberculodinium vancampoae* and *Quinquecuspis concreta*. Similar assemblage was identified as in the Gulf of Cádiz by Marret and Turon (1994) and in the Alborán Sea by Combourieu Nebout et al. (1999).

The samples are dominated by autotrophic cysts (88-99%), more particularly by *Lingulodinium machaerophorum* (33-90%) and *Spiniferites* spp. (5-59%), and % *Lingulodinium machaerophorum* shows two distinct increases, during the BA and around 35 kyr, whereas % *Spiniferites* shows distinct decreases at these moments (Figure 2). Protoperidiniacean heterotrophic cysts are rather rare (0.5-13%), and are dominated by *Brigantedinium* spp., *Trinovantedinium applanatum* and *Selenopemphix* spp. There are distinct peaks in the relative abundance of heterotrophic dinoflagellate cysts, during the BA and around 35 kyr, right at the time when autotrophic cysts reach lowest values (Figure 3).

Reworked (mainly Cretaceous) dinoflagellate cysts were frequently encountered and reached relative

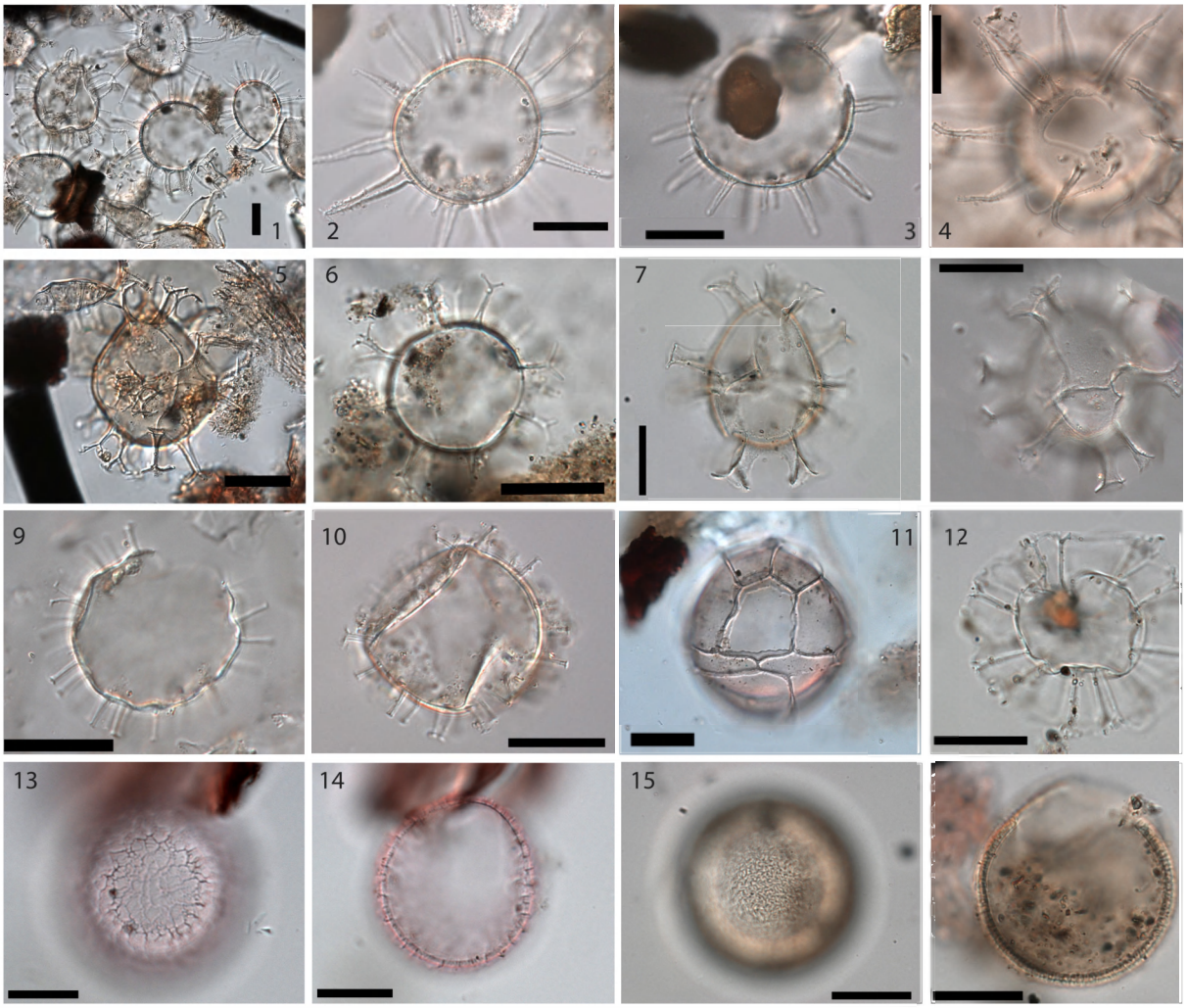

Plate 1 Micrographs from representative autotrophic dinoflagellate cysts from GeoB9064-1, Gulf of Cádiz. (1) 474 cm, typical view of GeoB9064-1 palynological samples composed of *Lingulodinium machaerophorum*. (2-3) 309 cm, *Lingulodinium machaerophorum*. Note differences in process lengths. (4) 474 cm, *Lingulodinium machaerophorum*. (5) 474 cm, *Spiniferites bentorii*. (6) 14 cm, *Spiniferites ramosus*. (7) 414 cm, *Spiniferites delicatus*, middle focus. (8) 309 cm, *Spiniferites delicatus*, upper focus. (9) 309 cm, cyst of *Pentapharsodinium dalei*. (10) 474 cm, *Operculodinium centrocarpum* sensu Wall & Dale. (11) 434 cm, *Impagidinium patulum*. (12) 14 cm, *Nematosphaeropsis labyrinthus*. (13-14) 414 cm, *Pyxidinopsis reticulata* with reticulate pattern with additional ridges. (15-16) 504 cm, *Bitectatodinium tepikiense* with microreticulate pattern. All scale bars are 20 µm.

abundances up to 4.2%.

3.2 Dinoflagellate cysts concentrations and accumulation rates

The dominant *Lingulodinium machaerophorum* concentrations range between 1,606 and 127,521 cysts per gram and show synchronous fluctuations to the relative abundances, except around 28 kyr (Figure 3). Accumulation rates of *Lingulodinium machaerophorum* range from 11,397 to 1,711,471 cysts/cm^2.ka, and are in sync with concentrations.

Autotrophic dinoflagellate cyst concentrations range from 2,904 to 145,358 cysts per gram sediment and show some opposite fluctuations to the relative abundance of autotrophic dinoflagellate cysts, related to enhanced relative abundances of heterotrophic dinoflagellate cysts (Figure 3). Accumulation rates of autotrophic dinoflagellate cysts range from 20,612

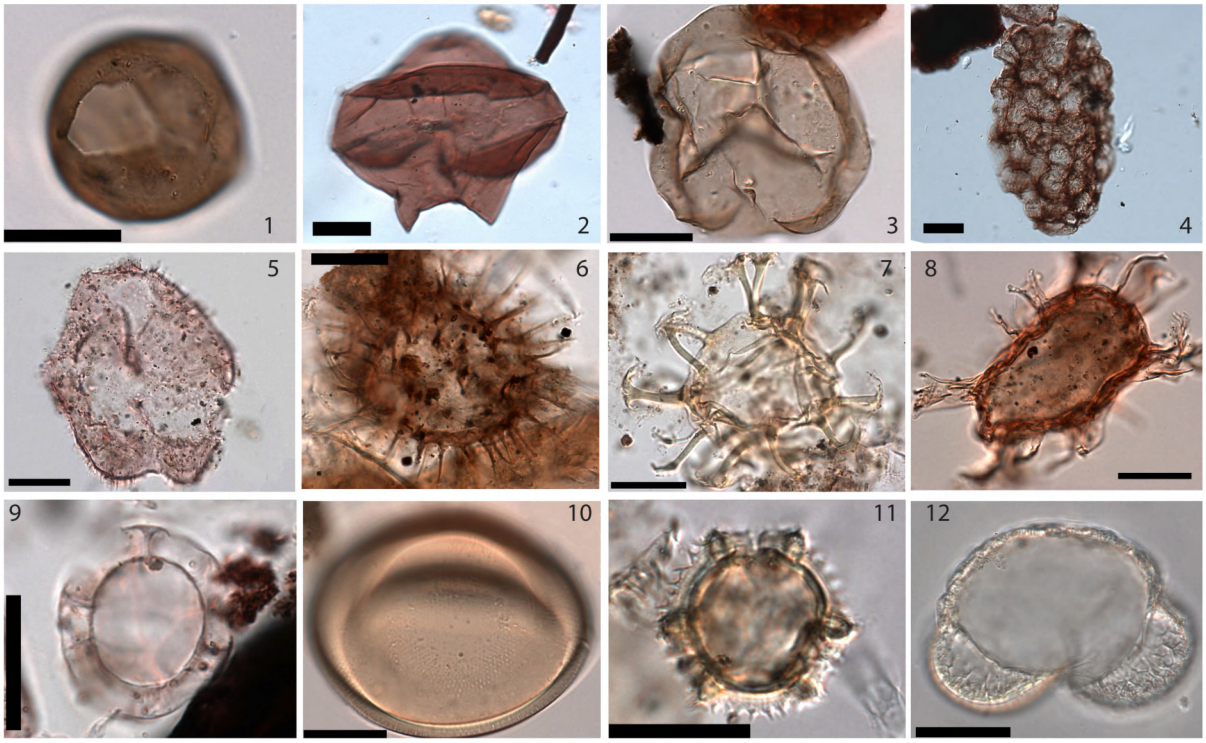

Plate 2 Micrographs from representative heterotrophic dinoflagellate cysts, reworked dinoflagellate cysts and other palynomorphs from GeoB9064, Gulf of Cádiz. (1) 309 cm, *Brigantedinium simplex*, high focus. (2) 434 cm, *Quinquecuspis concreta* with longitudinal striations. (3) 309 cm, *Selenopemphix nephroides*. (4) 434 cm, *Polykrikos schwartzii*. (5) 434 cm, *Trinovantedinium applanatum*. (6) 474 cm, *Selenopemphix quanta*. (7) 434 cm, reworked dinoflagellate cyst. (8) 474 cm, reworked dinoflagellate cyst. (9) 434 cm, *Cymatiosphaera* sp. (10) 474 cm, *Tasmanites* sp. (11) 309 cm, Asteraceae pollen grain, typical for arid, open environments. (12) 309 cm, bisaccate pollen. All scale bars are 20 µm.

to 1,927,122 cysts/cm².ka, and are in sync with autotrophic dinoflagellate cyst concentrations.

Heterotrophic dinoflagellate cyst concentrations range from 26 to 3,198 dinoflagellate cysts per gram sediment, and show synchronous fluctuations to the relative abundance of heterotrophic dinoflagellate cysts (Figure 3). Accumulation rates of heterotrophic dinoflagellate cysts range from 185 to 84,481 cysts/cm².ka, and are in sync with heterotrophic dinoflagellate cyst concentrations.

Chlorophyll-a concentrations vary between 0.35 and 2.69 mg/m³, with elevated concentrations during the BA and around 35 kyr. Bottom water oxygen concentrations fluctuate between and 2.94 and 5.16 ml/l, with lower bottom water oxygen concentrations during the BA and around 35 kyr. The average bottom water oxygen concentrations during the Holocene (5.14 ml/l) are higher than current average bottom water concentrations at 600 m water depth (4.27 ml/l) (gridded 1° World Ocean Atlas 2005, Garcia et al., 2006).

It must be stressed that the residue was sieved on a 20 µm mesh, and that part of the *Lycopodium* spores were possibly lost during sieving (Lignum et al., 2008; Mertens et al., accepted). However, the large fluctuations in concentrations and accumulation rates can not solely be attributed methodological issues.

3.3 Temperature reconstructions

Globigerina bulloides thrives in relatively shallow waters during spring and summer (Rogerson et al., 2004), and is thus representative for these environments. The Mg/Ca SST reconstruction measured on *Globigerina bulloides* yields temperatures over a range of 13.8 – 21.0°C, with minima during HEs, (Figure 4).

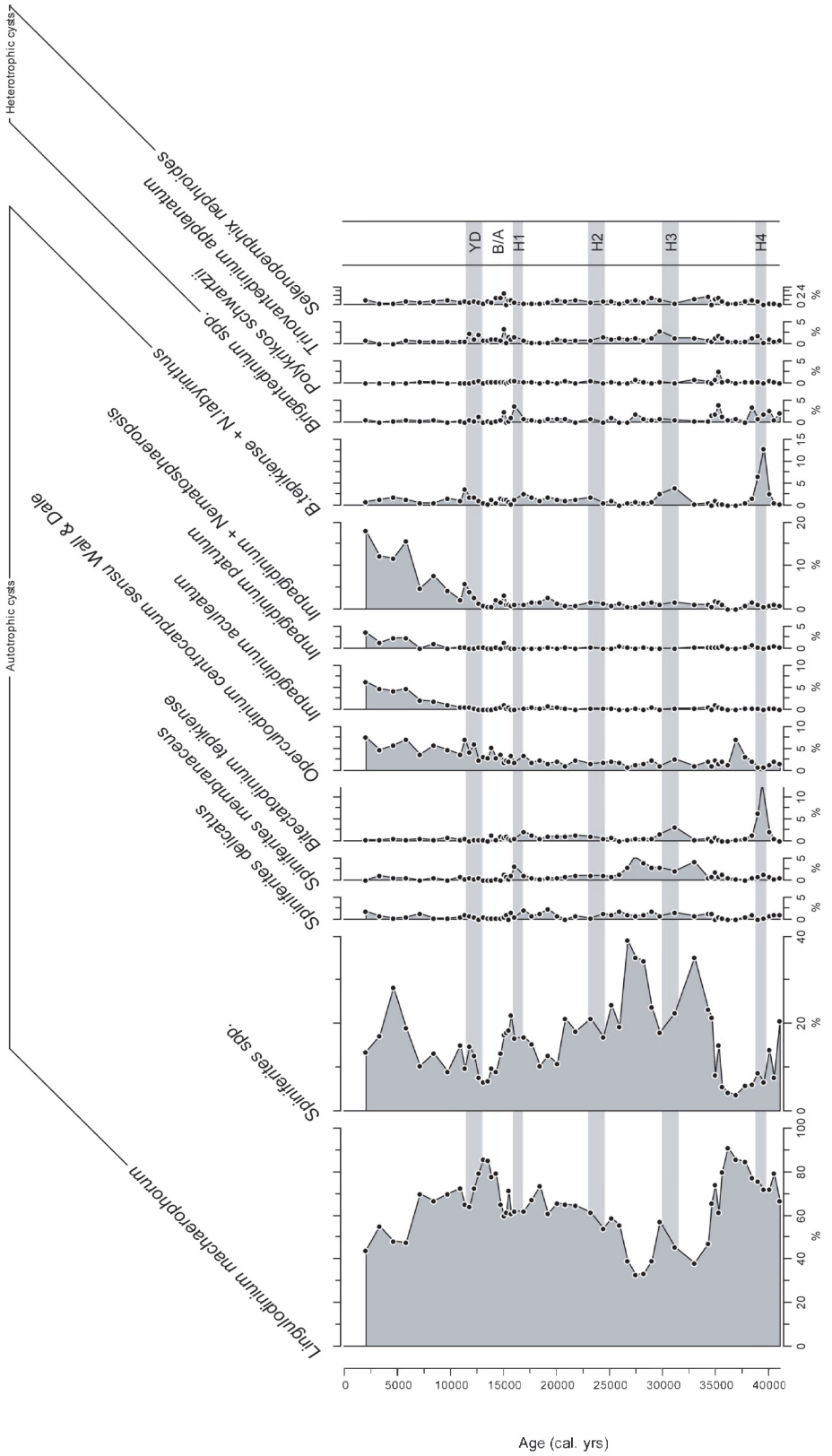

Figure 2 Relative abundances of most important dinoflagellate cyst taxa expressed in percentages of total cysts from core GeoB9064-1. bars indicate stadials.

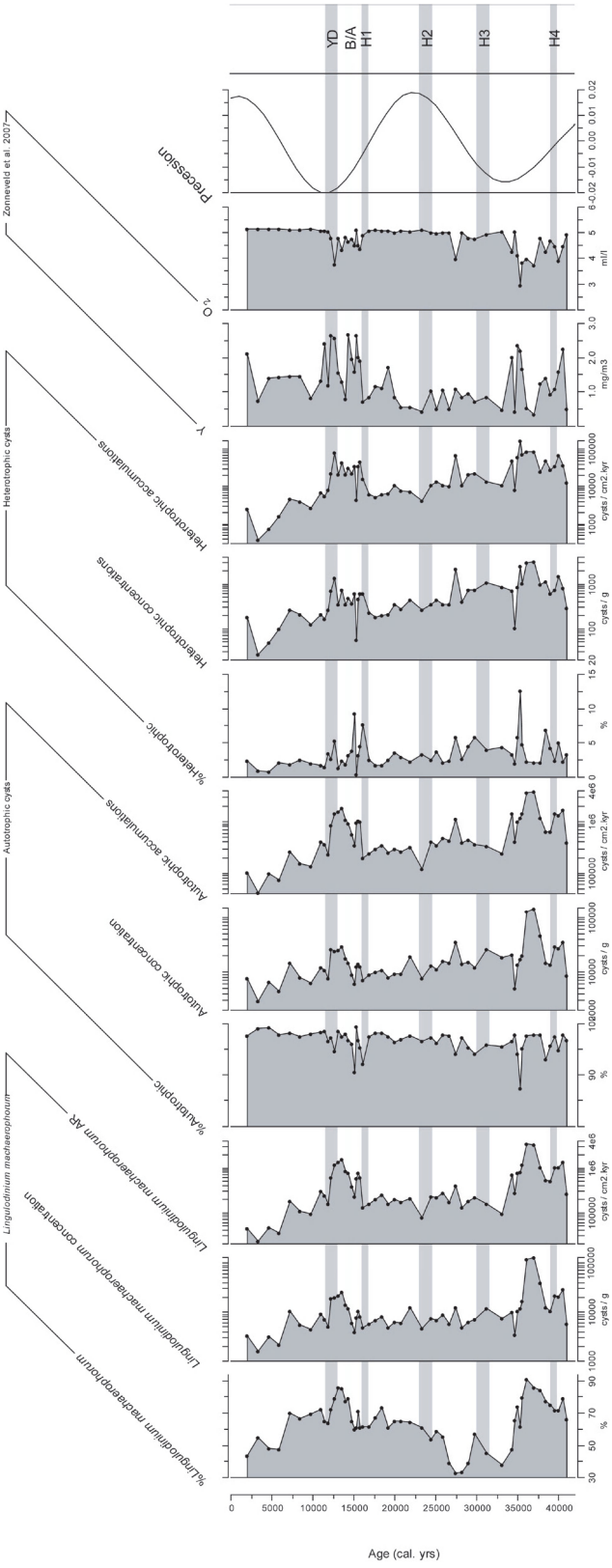

Figure 3 Relative abundances, concentrations and accumulation rates of *Lingulodinium machaerophorum*, autotrophic and heterotrophic dinoflagellate cysts. Also shown are Chlorophyll-a concentrations in the upper water column (Y) and bottom water oxygen concentrations (O_2), calculated using the equations of Zonneveld et al. (2007). bars indicate stadials.

Relatively stable temperatures are observed during the Holocene and contrasts sharply with the abrupt shifts during the glacial period. SST oscillations during the Holocene are not greater than 2°C (19-21°C) and are close to the actual annual temperature of 18.9 °C, while the SST changes of the glacial period range between 14 and 20°C. Trends are relatively similar to $U^{K'}_{37}$ SST and TEX_{86} SST curves (Mertens et al., in prep.), but are relatively warmer during interstadials.

Following Versteegh (1994) and Combourieu Nebout et al. (1999), the ratio of most thermophile dinoflagellate cyst taxa *vs.* less thermophile taxa (W/C) is used as a proxy for changes in sea-surface temperatures. In the present study, warm-water indicating species are selected following Marret and Zonneveld (2003): *Impagidinium patulum, Operculodinium israelianum, Polykrikos schwarzii, Selenopemphix nephroides, Spiniferites membranaceus, Tectatodinium pellitum, Tuberculodinium vancampooae*. Specific for this site, additional warm-water indicators are according to Turon and Londeix (1988): *Impagidinium aculeatum*, *Impagidinium strialatum, Spiniferites hyperacanthus* and *Spiniferites mirabilis,* to which *Impagidinium paradoxum* can be added, since its distribution is similar to *Impagidinium aculeatum* (Marret and Zonneveld, 2003). On the opposite side, cold-water indicators according to the latter authors are *Bitectatodinium tepikiense, Impagidinium pallidum, Islandinium minutum,* cyst of *Pentapharsodinium dalei* and *Spiniferites elongatus*, to which *Nematosphaeropsis labyrinthus* can be added (Eynaud et al., 2000). *Lingulodinium machaerophorum* can be designated as a warm-water species (Marret and Zonneveld, 2003), but here it is regarded as responding mainly to variations in productivity, being transported from the shelf (see §5.1). *Operculodinium centrocarpum* is considered to be a species too ubiquitous (e.g., Edwards and Andrle, 1992; de Vernal et al., 1994) to be used in such a ratio. The W/C value is calculated according to the following equation:

$$W/C = \frac{W}{W+C}$$

where:

W = the number of cysts of warm-water indicator taxa
C = the number of cysts of cool-water indicator taxa

The W/C ratio allows detection of most of the HEs (excluding H1) and fluctuations are similar to Mg/Ca SSTs, with relatively warm glacial temperatures (Figure 4).

3.4 Salinity reconstructions

Using the paired Mg/Ca – $\delta^{18}O$ approach, both $\delta^{18}O_{SW}$ and $\delta^{18}O_{SW-IVF}$ are calculated and show similar fluctuations (Figure 5). Lower values indicate lower salinities and *vice versa*. *Lingulodinium machaerophorum* average process length varies between 14.92 and 20.8 µm. Since process length is related both to salinity and temperature (Mertens et al., 2009b), it was attempted to calculate absolute salinity variations using the available temperature reconstructions, but this resulted in unrealistic results (changes in salinity over 12 psu). Since it can be noted that the process length record lags the $\delta^{18}O_{seawater}$ record, between ~1500 and 2000 years, this result can be attributed to transport issues (see 5.1 for further discussion). Despite this, average process length variation can be used for a semi-quantitative interpretation of salinity variations.

On a glacial-interglacial scale, both proxies show a more saline Gulf of Cádiz during the last glacial versus a fresher interglacial. On a millennial time-scale, both proxies show fresher events (pronounced during BA and early Holocene) and more saline stadials (all HE excluding H3). The freshening events would correspond to ~2 psu, calculated using the modern $\delta^{18}O_{seawater}$ versus salinity relationship for latitudes between 20°N and 50°N and longitudes between 20°W and 20°E (Schmidt et al., 1999).

Differences between Mg/Ca and alkenone based sea surface temperatures have previously been related to lower salinities in the Gulf of Guinea (Weldeab et al., 2007). In the Gulf of Cádiz the situation is reversed since higher salinities result in higher differences between $SST_{Mg/Ca}$ and $SST_{Uk'37}$ (Figure 5). This suggests that in the Gulf of Cádiz, *Globigerina bulloides* is produced *in situ* under more saline, relatively warmer conditions and alkenones are produced in and rapidly transported from areas

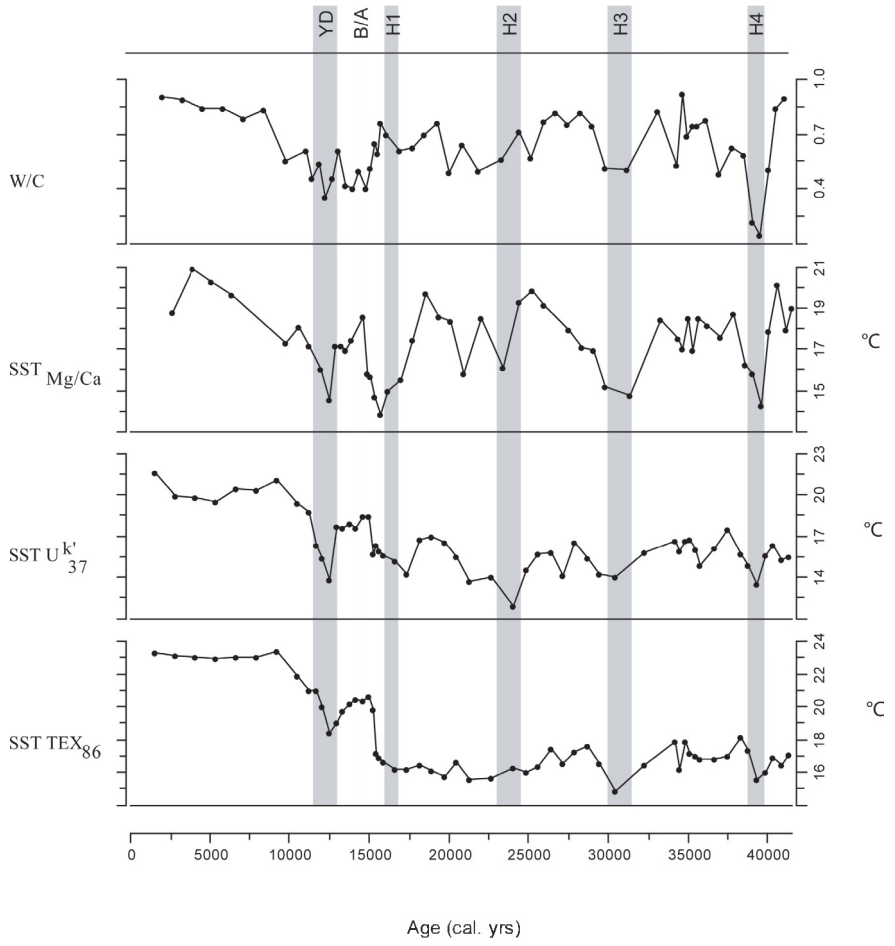

Figure 4 SST proxies measured on core GeoB9064-1: TEX_{86}, $U^{k'}_{37}$, Mg/Ca on *Globigerina bulloides* and ratio between "Warm" and "Cold" dinoflagellate cyst taxa (W/C). bars indicate stadials.

reflecting cold, fresher conditions, i.e. coastal areas with enhanced fluviatile input. This explains why alkenone SSTs correlate with $\delta^{18}O$ measured on the foraminifer *Neogloboquadrina pachyderma* (dextral), and are influenced by salinity variations (Mertens et al., in prep.).

3.5 Other palynomorphs

Concentrations of all other palynomorphs show similar fluctuations as their accumulation rates, so only accumulation rates are discussed (Figure 6). Representative other palynomorphs are illustrated in Plate II, 9-12.

Most abundant other palynomorphs in the samples are faunal remains of zooplankton (copepod eggs, microforaminiferal linings, scolecodonts and tintinnids). Accumulations of microforaminiferal linings show significant peaks succeeding H1 and preceding the YD, around 18 kyr and around 35 kyr. Accumulation rates of scolecodonts and copepod eggs show similar fluctuations, with peaks during the BA and around 35 kyr. Tintinnid loricas are present in too negligible amounts to represent reliable fluctuations.

The most abundant floral remains are pollen, mainly bisaccate and non-bisaccate pollen. Spores are present in negligible amounts. Accumulation rates of bisaccate pollen show significant peaks succeeding H1 and preceding the YD, and around 35 kyr. Accumulations of non-bisaccate pollen peak during

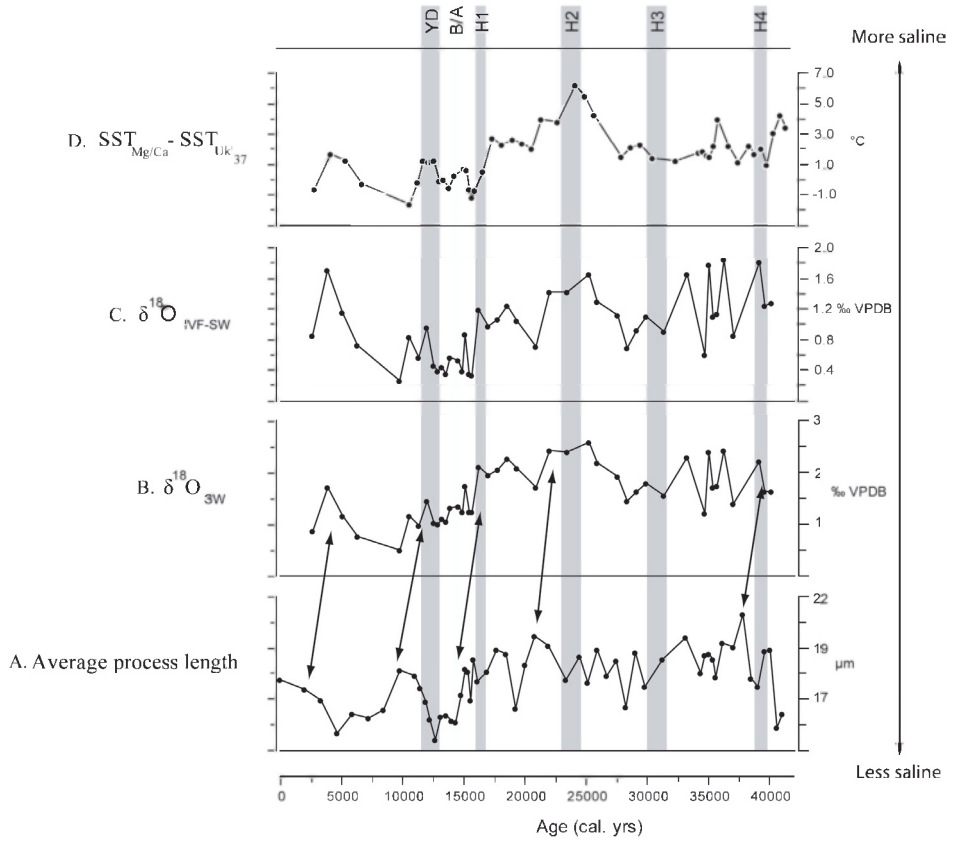

Figure 5 SSS proxies measured on core GeoB9064-1: A. *Lingulodinium machaerophorum* average process length, B. $\delta^{18}O_{SW}$ and C. $\delta^{18}O_{SW-IVF}$, D. difference between SST reconstruction based on Mg/Ca and alkenones. Grey arrows denote a lag between the average process length and $\delta^{18}O_{SW}$ record.

BA and around 35 kyr (Figure 6). Chlorophyta (*Pediastrum*) and Prasinophyta (*Cymatiosphaera*) were present, but in insignificant amounts.

Other palynomorphs that were encountered were acritarchs (a.o. *Cyclopsiella* and *Halodinium*). All these components were quite rare and did not show any clear trends.

4. Discussion

Since dinoflagellate cysts assemblages are dominated by *Lingulodinum machaerophorum*, the interpretation of the record is focused on this species. It is generally agreed that increases of the cyst of *Lingulodinium polyedrum* are related to increases in nutrient input and thus indicate higher productivity (Dale and Fjellså, 1994; Dale et al., 1999; Dale, 2008). The higher productivity of this species can be related to coastal runoff, upwelling or anthropogenic input (Lewis and Hallett, 1997). For the studied time frame anthropogenic input can be disregarded, so variations in *Lingulodinium machaerophorum* should be attributed to either increased upwelling or runoff.

Surface sediments from the Scandinavian Fjords (Persson et al., 2000), the western equatorial Atlantic (Vink et al., 2000), the North Adriatic (Sangiorgi et al., 2005), Kiel Bight (Nehring, 1994), Brittany (Morzadec-Kerfourn, 1977) and the NW Canary Basin (Holzwarth, pers. comm.) all suggest a link to fluvially deposited sediments. Also downcore, higher abundances of this species have been associated with enhanced stratification and/or more humid conditions in the Mediterranean (Giunta et al., 2006) and the Gulf of Cádiz (Marret and Turon, 1994). The similar fluctua-

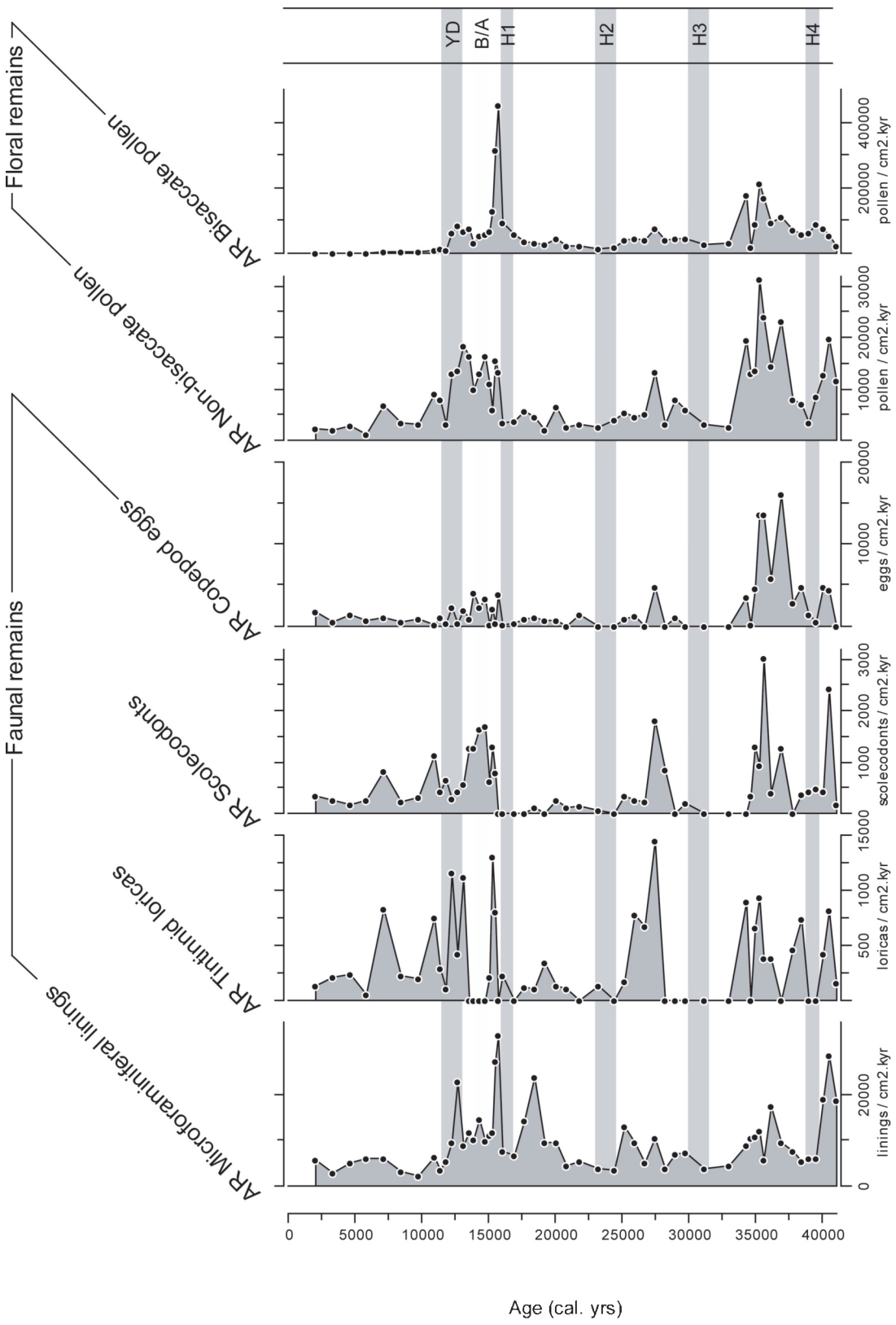

Figure 6 accumulation rates of other palynomorphs: faunal remains (microforaminiferal linings, tintinnid loricas, scolecodonts and copepods) and floral remains (non-bisaccate and bisaccate pollen).

tions of *Lingulodinium machaerophorum* abundances to non-bisaccate pollen indeed suggest river related input (compare Figure 3 and Figure 6). Furthermore, abundances of *Lingulodinium machaerophorum* in GeoB9064-1 are synchronous to accumulations of the coccolith *Gephyrocapsa muellerae*, organic carbon, carbonate and terrigenous matter, which are also associated with enhanced river influx (Mertens et al., in prep.). A link between higher abundances and increased runoff is thus evident. The cause for this relation on the other hand, can be explained by mechanisms of transport and preservation.

To understand the abundances of the cysts in this slope location, first there is need to trace them back to their source. Data from a global surface sediment study show that extremely high relative abundances of *Lingulodinium machaerophorum* (higher than 90%) are found close to river mouths (Mertens et al., 2009b). It is thus likely that this position forms the most important area of cyst production, from where the cysts are transported downslope by low-density turbidity currents and nepheloid sedimentation. This transport has been known to occur, since the cysts show a broader and deeper distribution than the corresponding motiles (Dodge and Harland, 1991) and the light but resistant *Lingulodinium machaerophorum* cysts are transported commonly in the area (Combourieu-Nebout et al., 1999). Also, the short lag between average process length and $\delta^{18}O_{sw}$ can be explained by cyst transport, which contrasts with the heavier *Globigerina bulloides* exporting the climatic signal more rapidly. A parallel can be drawn to a study by Mollenhauer et al. (2005), which shows lateral advection as an important factor to explain age offsets between co-occurring foraminifera and alkenones – which presumably have a comparable resistance as dinoflagellate cysts.

Secondly, preservation should be taken into account. The enhanced accumulations of *Lingulodinium machaerophorum* and heterotrophic dinoflagellate cysts, synchronous to reduced O_2 concentrations during the higher productivity events of the BA and around 35 kyr (Figure 3), supports enhanced organic carbon preservation through the "mineral ballast" hypothesis (Thunell et al., 2007) as suggested by Mertens et al. (in prep.). As proposed by Cacho et al. (2000) in the Alborán Sea, these events can correlate with the presence of lower oxygenated deep water masses during these interstadials, although do not support enhanced deep water ventilation during stadials.

So despite the fact that the living species react to upwelling (Blasco, 1977) or upwelling relaxation (Smayda and Reynolds, 2001), it is thus considered that higher abundances of *Lingulodinium machaerophorum* reflect enhanced river discharge over the core site and *vice versa*. *Lingulodinium machaerophorum* cysts will accumulate on the slope with increased river discharge, whilst with decreased river discharge accumulation will rather occur on the shelf. The higher amount of oligotrophic taxa such as *Impagidinium* species and *Nematosphaeropsis labyrinthus* during the Holocene reflects oligotrophic conditions and suggests significantly reduced river influx (Figure 2). The conceptual model is shown in Figure 7 and 8. The higher accumulations of *Lingulodinium machaerophorum* can be related to more negative NAO indices, enhancing fluvial supply, most pronounced during precession minima (Figure 3) and confirms results of coccoliths and biomarkers (Mertens et al., in prep.). It can also be noted that copepods, which are known to prey on dinoflagellates (e.g. Huntley et al., 1986; Abrahams and Townsend 1993), show similar accumulations as *Lingulodinium machaerophorum* accumulations (compare Figure 3 and 6).

Upwelling, active during HEs (Colmenero-Hidalgo et al., 2002; Mertens et al., in prep.), is also recorded by other components. HEs can be associated with a shift to higher upwelling during the winter season, which results in "*Bitectatodinium tepikiense – Nematosphaeropsis labyrinthus* events", also observed by Eynaud et al. (2000) (Figure 2). These HEs are also well-reflected in all SST proxies, with significant shifts in both the Mg/Ca SST and W/C ratio (Figure 4). The latter is of course determined for a large part by the cold-water "*Bitectatodinium tepikiense-Nematosphaeropsis labyrinthus* events". Bisaccate pollen can be associated with more arid events (Marret and Turon, 1994), which confirms more arid conditions during H1 and YD (Figure 6). Other HEs are less represented in this record and could be related to enhanced wind strength during these events (Mertens et al., in

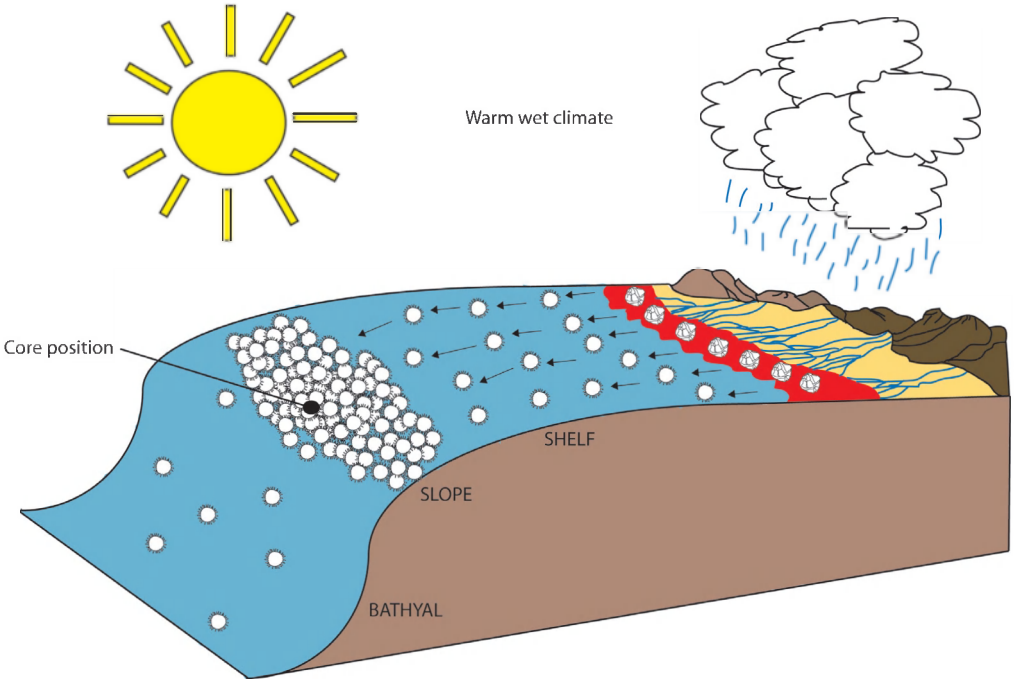

Figure 7 Model for dinoflagellate cyst deposition during warm, wet climate phases: *Lingulodinium machaerophorum* are produced and transported downslope.

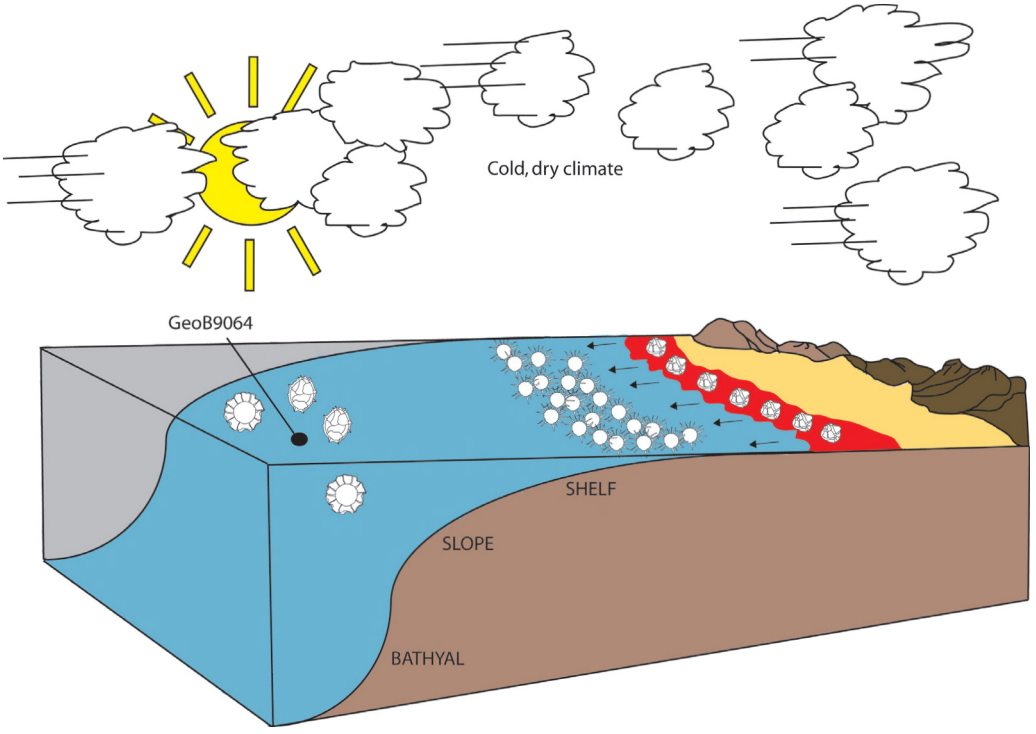

Figure 8 Model for dinoflagellate cyst deposition during cold, arid climate phases: *Lingulodinium machaerophorum* are produced but are deposited on the shelf. Oligotrophic, oceanic taxa (*Nematosphaeropsis labyrinthus* and all *Impagidinium* species) accumulate on the slope setting.

prep.), carrying this component further. These conditions can be related to positive NAO indices.

Despite the lag between both salinity proxies, both indicate lower salinities during the BA and middle Holocene, related to humid conditions in the western Mediterranean (Kallel et al., 1997; Zanchetta et al., 2007; Fletcher et al., 2009) and the low-latitude Atlantic (Wang et al., 1995). Although this relation is observed, salinity changes are not a direct reflection of local hydrological conditions, as reflected by accumulations of *Lingulodinium machaerophorum* (compare Figure 3 and 6), and are more likely the sum of hydrological and oceanographical changes. Furthermore, HEs are observed as saltier events which can be related to enhanced upwelling of saline North Atlantic Central Water (e.g. Wang et al., 1995). There is no clear indication in the southern Gulf of Cádiz of freshwater pulses during HEs as observed off the Iberian margin (Cayre et al., 1999).

5. Conclusions

The dinoflagellate cyst record of core GeoB9064-1 is dominated by abundances of *Lingulodinium machaerophorum*, which is determined by enhanced fluvial supply. This enhanced fluvial supply causes transport and enhanced preservation via mineral ballasting of *Lingulodinium machaerophorum* cysts and other organic components. The fluctuations of *Lingulodinium machaerophorum* can be related to negative NAO indices, increasing the fluvial supply, more particularly during precession minima.

Upwelling during HEs is reflected as cooler Mg/Ca SSTs, W/C ratios, "*Bitectatodinium tepikiense-Nematosphaeropsis labyrinthus* events" and bisaccate pollen and can be related to positive NAO indices.

Despite a short lag, *Lingulodinium machaerophorum* average process lengths and Mg/Ca – $\delta^{18}O$ deduced salinities reflect enhanced precipitation conditions during the BA and middle Holocene over the Mediterranean area. These salinity changes are in sync with temperature differences between Mg/Ca and alkenone derived SSTs and can be related to lateral advection of alkenones.

Additional information

Dinoflagellate cysts were extracted, measured and counted by Kenneth Mertens and Liesbeth Van Kerckhoven. Mg/Ca ratios and oxygen isotopes were measured and picked by Kenneth Mertens, Jeroen Groeneveld, Thomas Verleye and Maarten Verreth. This chapter will be submitted.

Conclusions

The present study demonstrated that coccoliths and dinoflagellate cysts are very useful as paleoclimatological indicators for the elucidation or a better understanding of the late Quaternary regional and global palaeoclimate. *Vice versa*, this study also reveals new insights in coccolithophore and dinoflagellate palaeoecology.

1. Rationale for application of dinoflagellate cysts

At the outset, two fundamental studies were undertaken to strengthen dinoflagellate cysts as a proxy for paleoecological studies. Since so-called 'standard' palynological processing methods are still very variable, and inflict damage on organic-walled microfossils to a certain extent, the effect on the determination of dinoflagellate cyst concentrations needed to be sorted out. Furthermore, since there were indications that process length variation of *Lingulodinium machaerophorum* is related to salinity, there was a need to assess its use for quantitative palaeosalinity reconstruction, which is of critical importance for better understanding of global climate change.

Firstly, the methodology for adding a *Lycopodium clavatum* spike to determine absolute abundances of dinoflagellate cysts was critically revised in an international calibration exercise with 23 participating laboratories. A new standard methodology was proposed which circumvents critical steps such as oxidation, warm acids, acetolysis, large mesh sizes (> 15 µm), decanting and long ultrasonication (> 1 min).

Secondly, a global morphological study of *Lingulodinium machaerophorum* cysts extracted from surface sediments demonstrated that the process length variation is determined by the salinity/temperature (S/T) ratio. A similar morphology of a cyst can thus be determined by different temperatures and salinities, as long as the S/T ratio remains constant. Measurements of process length on three-dimensional images, generated with confocal microscopy, revealed the existence of two end-members: one with numerous, short, close-by processes related to low S/T ratios and one with fewer and longer processes related to high S/T ratios. The tight link of morphological variations with the S/T ratio led to the observation that biogeographical zonations of *Lingulodinium machaerophorum* are delineated by the S/T ratio. This suggests that the S/T ratio can serve as a tool for prediction of the presence of cysts of *Lingulodinium polyedrum*. Furthermore, and of equal importance, this tool enables the reconstruction of the salinity when the temperature can be reconstructed with independent proxies.

2. Two study areas of millennial-scale cycles

Two locations were chosen for a high-resolution micropalaeontological study of hydrological millennial-scale cycles during Late Quaternary times: the Cariaco Basin, an anoxic basin offshore Venezuela and the Southern Gulf of Cádiz, offshore Morocco. Because of the high sedimentation rates, both sites contain a relatively undisturbed Late Quaternary climate record. Both record rapid, large climatic oscillations related to major hydrological changes caused by respectively the intertropical convergence zone (ITCZ) and the North Atlantic Oscillation (NAO). Better understanding of these phenomena through geological time is crucial in the context of global climate change.

3. Characterization of millennial-scale oscillations

The most important constructed proxies for both regions are summarized in Figure 1 and 2. The seasonal and multi-year changes between upwelling and river dominated ecosystems, related in both regions to climatological shifts of respectively the ITCZ and NAO, can be extended to millennial-scale cycles and results in specific assemblages of both dinoflagellate cysts and coccoliths.

In the Cariaco Basin, enhanced river supply causes enhanced accumulations of autotrophic dinoflagellate cysts during interstadials. Initially this process causes stratification, as indicated by *Lingulodinium machaerophorum* abundances, and evolves into *Spiniferites ramosus – Gephyrocapsa oceanica* dominated assemblage. This enhanced river supply turns the basin anoxic at the beginning of the BØlling/AllerØd. Enhanced upwelling during stadials, e.g. during the Younger Dryas, is indicated by a *Brigantedinium* spp. – *Emiliania huxleyi* dominated ecosystem. In the Gulf of Cádiz enhanced river supply during interstadials causes enhanced abundances of *Lingulodinium machaerophorum*, *Gephyrocapsa muellerae* and alkenones. Enhanced upwelling during stadials causes more outspoken abundances of large *Emiliania huxleyi* and "*Nematosphaeropsis labyrinthus - Bitectatodinium tepikiense*" events. These hydrological variations are also reflected in end-member modeled grain sizes and XRF records in the Gulf of Cádiz.

In both areas, changes in assemblages are tightly linked to changes in productivity and preservation (Table 1). Enhanced preservation of microfossils is tightly linked to higher productivity and sedimentation rates in both areas, and confirms the importance of the mineral ballast hypothesis for the interpretation of these records. Despite similar fluctuations in temperature and salinity, there is a crucial difference between both areas in terms of sedimentation rates: in the Cariaco Basin higher upwelling causes enhanced sedimentation rates, whilst in the Southern Gulf of Cádiz higher river input causes enhanced sedimentation rates and *vice versa*. This implies that both regions react contrary to climate change in terms of productivity and preservation: the Cariaco Basin enhances organic carbon and carbonate burial during stadials, whilst the Gulf of Cádiz does the opposite.

It must be stressed that the millennial-scale changes are further modulated on orbital-scale by changes in sea-level which cause pronounced changes in both areas. In the Cariaco Basin, rising sea-levels cause influx of nutrient rich subtropical underwater over the sills during interglacials, giving up its isolated nature and making it anoxic. In the Gulf of Cadiz sea-level rises causes a change in deposition of terrigenous material from slope to shelf deposition and *vice versa*.

Apart from productivity reconstruction, the focus was laid on quantitative temperature and salinity reconstructions, which are crucial for climate reconstruction. In the Gulf of Cádiz, sea surface temperatures were reconstructed using glycerol dialkyl glycerol tetraethers (GDGTs), alkenones and Mg/Ca ratios measured on *Globigerina bulloides*. Reconstructed temperatures fluctuate synchronously but differ in amplitude, which can be related to seasonality, salinity changes or lateral advection. The Warm/Cold ratio – based on dinoflagellate cyst assemblages – and morphological variations of *Emiliania huxleyi* point to similar fluctuations, and are useful for the detection of Heinrich events. The correlation between alkenone derived temperatures and the Ti XRF record suggests a temperature component in the hydrological variations caused by the NAO. In the Ti XRF record, cycles of 1000 and 585 year are recorded, which can be related to positive NAO indices. Sea surface salinity reconstructions in both regions relied on the new proxy based on process length variation of *Lingulodinium machaerophorum* and paired Mg/Ca – δ18O records and can be correlated. Differences between the salinity proxies and hydrological proxies are noted in both areas and suggest carefulness when interpreting hydrological proxies in terms of salinity variations and *vice versa*. Salinity changes reflect saline interstadials *versus* fresh stadials in both areas and are related to the combination of both global and regional hydrological and oceanographical changes.

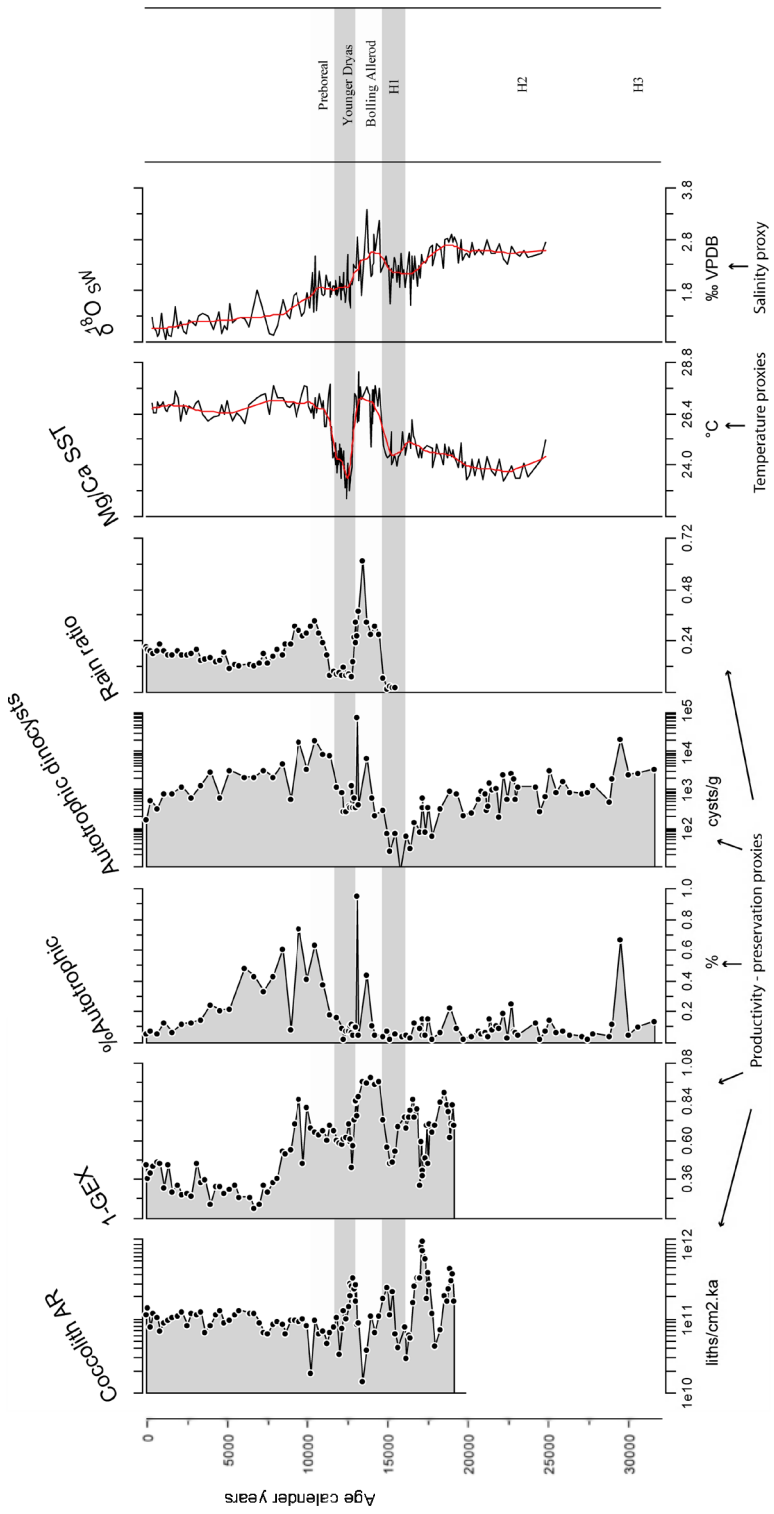

Figure 1 Most important proxies used in this study measured on cores from the Cariaco Basin (ODP 1002C and PL07-39PC). Productivity and preservation is estimated using coccoliths (coccolith accumulation rates and the GEX dissolution index), dinoflagellate cysts (relative and absolute abundances of dinoflagellate cysts) and rain ratio (ratio between TOC and Carbonate). Temperature is quantified from Mg/Ca ratios (Lea et al., 2003) and salinity is semi-quantified using the paired Mg/Ca-$\delta^{18}O$ approach (Schmidt et al., 2003).

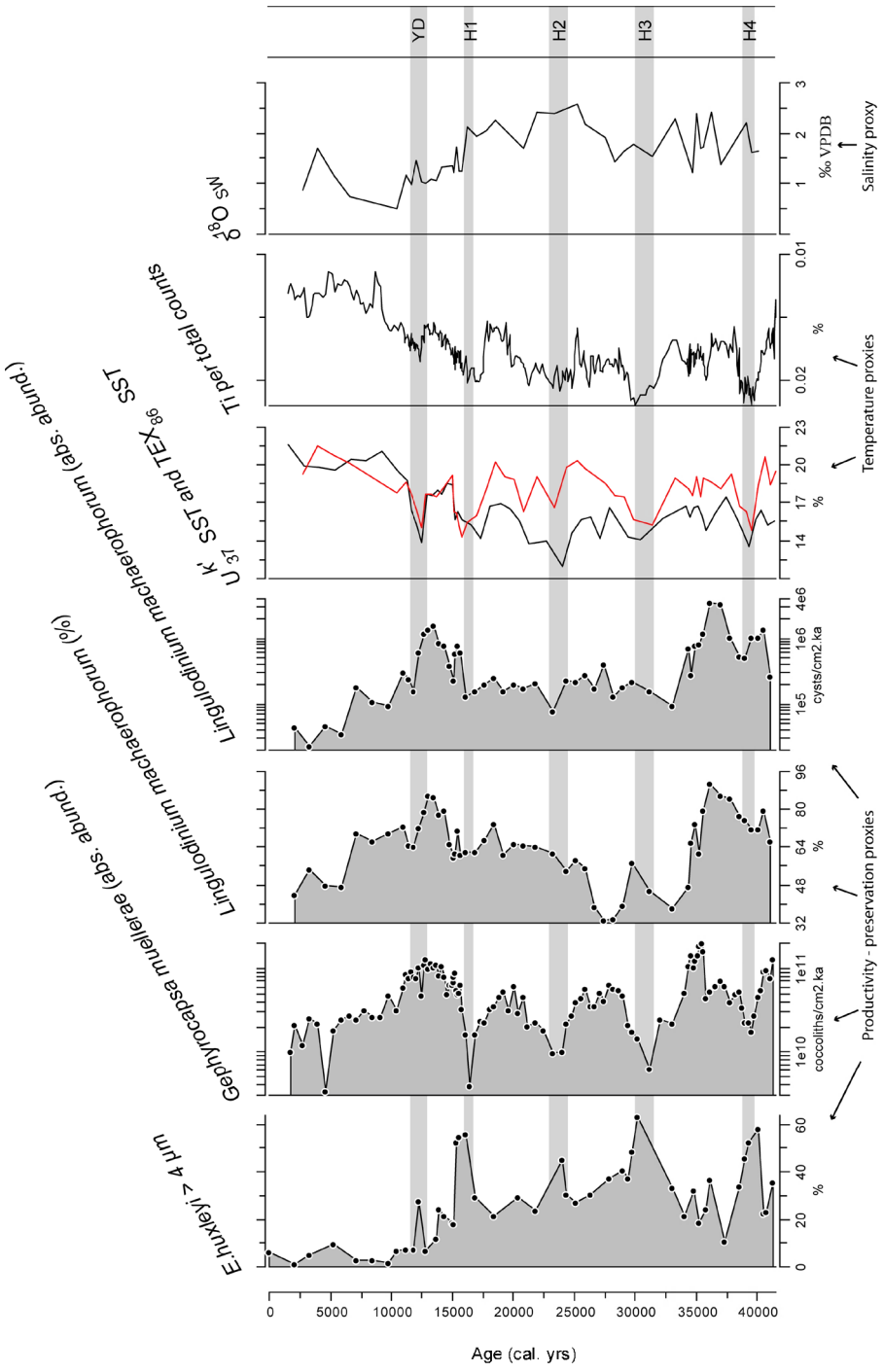

Figure 2 Most important proxies used in this study measured on core GeoB9064-1. Productivity and preservation is estimated using coccoliths (large *E. huxleyi* and *G. muellerae*) and dinoflagellate cysts (more particularly *Lingulodinium machaerophorum*). Temperature is quantified using alkenone and GDGT derived SST and Ti XRF measurements. Salinity variations are estimated using the paired Mg/Ca-$\delta^{18}O$ approach.

Table 1 Comparison of both areas in terms of microfossil assemblages, productivity vs. preservation and derived climate parameters during millennial-scale oscillations.

		Enhanced upwelling	Enhanced river supply
Cariaco Basin	Dinoflagellate cysts	Heterotrophic cysts (RBCs)	Autotrophic cysts *(L. machaerophorum + S. ramosus)*
	Coccoliths	*Emiliania huxleyi*	*Gephyrocapsa oceanica*
	Sedimentation rate	Higher	Lower
	Productivity	Higher	Lower
	Preservation	Enhanced	Worse
	Temperature	Colder	Warmer
	Salinity	Fresher	More saline
	Precipitation	Arid	Wet
	Related to	ITCZ South	ITCZ North
	Timing	Stadials	Interstadials
Gulf of Cádiz	Dinoflagellate cysts	*N. labyrinthus - B. tepikiense*	*Lingulodinium machaerophorum*
	Coccoliths	large *Emiliania huxleyi*	*Gephyrocapsa muellerae*
	Sedimentation rate	Lower	Higher
	Productivity	Lower	Higher
	Preservation	Worse	Enhanced
	Temperature	Colder	Warmer
	Sainity	Fresher	More saline
	Precipitation	Arid	Wet
	Related to	NAO+	NAO-
	Timing	Stadials	Interstadials

4. Trade-offs and questions surrounding the used proxies

Coccoliths have the advantage of being extremely abundant in the studied sediments. The very low amount of sediment needed to study the assemblages has potential to study variations on a very fine-scale (seasonal or less). Their preservation potential, however, causes difficulties with identification and over-representation of resistant high-productivity species, which often complicates interpretation of assemblage changes.

Dinoflagellate cysts on the other hand, show lower abundances in the sediments, which restricts their application on very high resolution. In terms of taphonomy, preservation of heterotrophic dinoflagellate cysts is very variable, and prone to changes in productivity and oxygenation. The preservation of autotrophic dinoflagellate cysts on the other hand is excellent in both areas, which makes them very reliable indicators for changes in productivity and salinity reconstructed from morphological variation.

This study also reveals that lateral advection of resistant components could be crucial in interpretation of the hydrological variations in both areas. The occurrence of an important amount of shelf-produced material in both sites located at slope depth suggests an important influence of transport from the shelf, possibly causing lags between pelagic and shelf components. In this respect, it remains also unknown how important turbidites or bottom currents are causing changes in the record.

Despite these taphonomical problems, this study shows that only by using a multi-proxy approach,

which takes into account necessary corrections for sedimentation rate, palaeoclimate reconstruction is still possible.

5. Comparing higher and lower latitudes

This study demonstrates that climate variations in both areas, as expressed by the studied proxies, succeed or are synchronous to changes in higher latitudes. There is no evidence to support a trigger mechanism of millennial-scale changes from lower latitudes (the so-called "tropical driver-hypothesis"). However, the expression of rapid, large shifts in productivity and assemblages of both planktonic groups linked to shifts of the ITCZ or NAO, suggests a strong sensitivity of both regions to rapid climate change, which makes these lower latitude areas extra fragile in terms of ongoing global climate change. Since these variations are inferred to be hydrological, rapid near-future changes in rainfall should be expected at both sites.

6. Future perspectives

Since millennial-scale shifts of both phenomena occur during the same periods (e.g. Younger Dryas), future work should elucidate the precise timing of both phenomena by comparing detailed multi-proxy records from north-south transects in both areas. On a finer scale, stacking of shelf to slope records could eliminate sea level effects, and extract "clean" NAO or ITCZ fluctuations. Detailed sediment-trap studies in both areas could further help to confirm the inferred interpretations of climate variations.

References

Abrahams, M.V. and Townsend, L.D. 1993. Bioluminescence in dinoflagellates: a test of the burglar alarm hypothesis. *Ecology 74*, 258-260.

Abrantes, F. 1988. Diatom productivity peak and increased circulation during Latest Quaternary: Alborán Basin (Western Mediterranean). *Marine Micropaleontology* 13, 79-96.

Alley, R.B., Anandakrishnan, S. and Jung, P., 2001. Stochastic resonance in the North Atlantic. *Paleoceanography* 16, 190-198.

Álvarez, M.C., Flores, J.A., Sierro, F.J., Diz, P., Francés, G., Pelejero, C. and Grimalt, J. 2004. Millennial surface water dynamics in the Ría de Vigo during the last 3000 years as revealed by coccoliths and molecular biomarkers. *Palaeogeography, Palaeoclimatology, Palaeoecology* 218, 1-13.

Amorim, A., Palma, A.S., Sampayo, M.A. and Moita, M.T. 2001. On a *Lingulodinium polyedrum* bloom in Setúbal bay, Portugal. In: Hallegraeff, G.M., Blackburn, S.I., Bolch, C.J. and Lewis, R.J. (Eds.), *Harmful Algal Blooms 2000*. Intergovernmental Oceanographic Commission of UNESCO, 133–136.

Anand, P., Elderfield, H. and Conte, M.H. 2003. Calibration of Mg/Ca thermometry in planktonic Foraminifera from a sediment trap time series. *Paleoceanography* 18(2), 1050, doi:10.1029/2002PA000846.

Anderson D.M. 1997. Diversity of harmful algal blooms in coastal waters. *Limnology and Oceanography* 42 (5, part 2), 1009-1022.

Anderson, D.M. and Morel, F.M.M. 1979. The seeding of two red tide blooms by the germination of benthic *Gonyaulax tamarensis* hypnocysts. *Estuarine and Coastal Marine Science* 8, 279–293.

Anderson, D.M., Taylor, C.D. and Armburst, E.V. 1987. The effects of darkness and anaerobiosis on dinoflagellate cyst germination. *Limnology and Oceanography* 32 (2), 340-351.

Andruleit, H., Lückge, A., Wiedicke, M. and Stäger, S. 2008. Late Quaternary development of the Java upwelling system (eastern Indian Ocean) as revealed by coccolithophores. *Marine Micropaleontology* 69 (1), 3-15.

Arz, H.W., Pätzold, J. and Wefer, G. 1999. Climatic changes during the last deglacation recorded in sediment cores from the northeastern Brazilian Continental Margin. *Geo-Marine Letters* 19, 209-218.

Astor, Y., Muller-Karger, F. and Scranton M. 2003. Seasonal and interannual variation in the hydrography of the Cariaco Basin: implications for basin ventilation. *Continental Shelf Research* 23, 125–144.

Aycard, M., Bout-Roumazeilles, V., Nebout-Combourieu N., Tribovillard, N., Baudin F., Derenne, S. and Largeau, C. submitted. Primary productivity and upwelling intensity since the last 16000 years in the Cariaco Basin (Venezuela). *Marine Geology*.

Bárcena, M.A., Flores, J.A., Sierro, F.J., Pérez-Folgado, M., Fabres, J., Calafat, A. and Canals, M. 2004. Planktonic response to main oceanographic changes in the Alborán Sea (Western Mediterranean) as documented in sediment traps and surface sediments. *Marine Micropaleontology* 53, 423-445.

Barker, S., Greaves, M. and Elderfield, H. 2003. A study of cleaning procedures used for foraminiferal Mg/Ca paleothermometry. *Geochemistry, Geophysics, Geosystems* 4(9), 8407, doi:10.1029/2003GC000559.

Barron, J.A., Bukry, D. and Dean, W.E. 2005. Paleoceanographic history of the Guaymas Basin, Gulf of California, during the past 15,000 years, based on diatoms, silicoflagellates, and biogenic sediments. *Marine Micropaleontology* 56, 81–102.

Baumann, K.-H. 2004. Importance of size measurements for coccolith carbonate flux measurements. *Micropaleontology* 50, 35–43.

Baumann, K.-H., Cepek, M. and Kinkel, H. 1999. Coccolithophores as indicators of ocean water masses, surface water temperatures, and paleoproductivity – examples from the South Atlantic. In: Fischer, G., Wefer, G. (Eds.), *Use of Proxies in Paleoceanography.* Springer–Verlag, Heidelberg, pp. 117–144.

Baumann, K.-H., Böckel, B. and Frenz, M. 2004. Coccolith contribution to South Atlantic carbonate sedimentation. In: Thierstein, H.R. and Young, J.R. (Eds.), *Coccolithophores – From molecular processes to global impact*. Springer, Berlin, pp. 367–402.

Baumann, K.-H., Andruleit, H., Böckel, B., Geisen, M. and Kinkel, H. 2005. The significance of extant coccolithophores as indicators of ocean water masses, surface water temperature and paleoproductivity: a review. *Paläontologische Zeitschrift* 79/1, 93-112.

Baumann, K.-H., Böckel, B., Donner, B., Gerhardt, S., Henrich, R., Vink, A., Volbers H., Willems, H. and Zonneveld, K.A.F. 2003. Contribution of calcareous plankton groups to the carbonate budget of South Atlantic surface sediments. In: Wefer, G., Mulitza, S. and Ratmeyer, V. (Eds.), *The South Atlantic in the Late Quaternary: reconstruction of material budgets and current systems.* Springer–Verlag, Heidelberg, pp. 81–99.

Belmonte, G., Miglietta, A., Rubino, F. and Boero, F. 1997. Morphological convergence of resting stages of planktonic organisms: a review. *Hydrobiologia* 355, 159-165.

Bendle J., Rosell-Melé A. and Ziveri P. 2005. Variability of unusual distributions of alkenones in the surface waters of the Nordic seas. *Paleoceanography* 20, doi:10.1029/2004PA001025.

Benninghoff, W.S. 1962. Calculation of pollen and spores density in sediments by addition of exotic pollen in known quantities. *Pollen et Spores* 6, 332–333.

Bennouna, A., Berland, B., El Attar, J. and Assobhei, O. 2002. *Lingulodinium polyedrum* (Stein) Dodge red tide in shellfish areas along Doukkala coast (Moroccan Atlantic). *Oceanologica Acta* 25(3), 159-170.

Berger, A. and Loutre, M.F. 1991. Insolation values for the climate of the last 10 million years. *Quaternary Sciences Review* 10 (4), 297-317.

Berger, W.H. 1976. Biogenous deep sea sediments: Production, preservation, and interpretation. In: Riley, J.P. and Chester, R. (Eds.), *Chemical Oceanography 5.* Academic Press, London, pp. 265-388.

Bijma, J., Altabet, M., Conte, M., Kinkel, H., Versteegh, G.J.M., Volkman, J.K., Wakeham, S.G. and Weaver, P.P.E. 2001. Primary signal: Ecological and environmental factors. Report from Working Group 2, *Geochemistry, Geophysics, Geosystems* 2, 2000GC000051.

Blackman, R.B. and Tukey, J.W. 1958. The measurement of power spectra. Dover, New York. 190 pp.

Blanco, J. 1990. Cyst germination of two dinoflagellate species from Galicia (NW Spain). *Scientia Marina* 54 (3), 287-291.

Blanco, J. 1995. Cyst production in four species of neritic dinoflagellates. *Journal of Plankton Research* 17, 165-182.

Blasco, D. 1975. Red tides in the upwelling regions. In: LoCicero, V.R. (Ed.), *Toxic dinoflagellate blooms.* Massachusetts Science and Technology Foundation, Wakefield, M.A., pp. 113-119.

Blasco, D. 1977. Red tide in the upwelling region of Baja California. *Limnology and Oceanography* 22, 255-263.

Blazhchishin, A.I. and Lukashina, N.P. 1995. Sedimentation and paleogeography of the Cariaco deep in the Upper Pleistocene and Holocene. *Oceanology* 34, 829-834.

Boeckel, B. and Baumann, K.-H. 2004. Distribution of coccoliths in surface sediments of the south–eastern South Atlantic Ocean: ecology, preservation and carbonate contribution. *Marine Micropaleontology* 51, 301–320.

Boeckel, B. and Baumann, K.-H. 2008. Vertical and lateral variations in coccolithophore community structure across the subtropical frontal zone in the South Atlantic Ocean. *Marine Micropaleontology* 67, 255-273.

Boeckel, B., Baumann, K.-H., Henrich, R. and Kinkel, H. 2006. Coccolith distribution patterns in South Atlantic and Southern Ocean surface sediments in relation to environmental gradients. *Deep-Sea Research I* 53, 1073-1099.

Bollmann, J. 1997. Morphology and biogeography of *Gephyrocapsa* coccoliths in Holocene sediments. *Marine Micropaleontology* 29, 319-350.

Bollmann, J. and Herrle, J.O. 2007. Morphological variation of *Emiliania huxleyi* and sea surface salinity. *Earth and Planetary Science Letters* 255, 273-288.

Bond, G., Showers, W., Cheseby, M., Lotti, R., Almasi, P., Demenocal, P., Priore, P., Cullen, H., Hajdas, I. and Bonani G. 1997. A pervasive millennial–scale cycle in North Atlantic Holocene and Glacial climates. *Science* 278, 1259–1266.

Bond, G., Heinrich, H., Broecker, W., Labeyrie, L., McManus, J., Andrews, J., Huon, S., Jantschik, R., Clasen, S., Simet, C., Tedesco, K., Klas, M., Bonani, G. and Ivy, S. 1992. Evidence for massive discharges of icebergs into the North Atlantic ocean during the last glacial period. *Nature* 360, 245–249.

Bonifay D. and Giresse, P. 1992. Middle to late Quaternary sediment flux and post–depositional processes between the continental slope off Gabon and the Mid–Guinean margin. *Marine Geology* 106, 107–129.

Bown, P. (Ed.), 1998. Calcareous nannofossil biostratigraphy. Kluwer Academic Publishers, Dordrecht. 314 pp.

Bown, P., Lees, J.A. and Young, J.R. 2004. Calcareous nannoplankton evolution and diversity through time. In: Thierstein, H.R. and Young, J.R. (Eds.), *Coccolithophores – From molecular processes to global impact.* Springer, Berlin, pp. 481–508.

Boyer, T. P., Stephens, C., Antonov, J. I. Conkright, M. E. Locarnini, R. A., O'Brien, T. D. and Garcia, H.E. 2002. World Ocean Atlas 2001, Volume 2: Salinity. In: S. Levitus, (Ed.), *NOAA Atlas NESDIS 50.* U.S. Government Printing Office, Washington, D.C., pp. 1-165.

Brand, L. 1984. The salinity tolerance of forty-six marine phytoplankton isolates. *Estuarine, coastal and shelf science* 18, 543-556.

Brasier, M.D. 1985. Fossil indicators of nutrient levels. 1: eutrophication and climate change. In: Bosence, D.W.J., Allison, P.A. (Eds.), *Marine Palaeoenvironmental Analysis from Fossils*. *Geological Society Special Publication* 83. Geological society, London, pp. 113–132.

Brenner, W. 2005. Holocene environmental history of the Gotland Basin (Baltic Sea) – a micropalaeontological model. *Palaeogeography, Palaeoclimatology, Palaeoecology* 220, 227-241.

Broecker, W.S., Peteet, D.M. and Rind, D., 1985. Does the ocean-atmosphere system have more than one stable mode of operation? *Nature* 315, 21-26.

Broecker, W.S., Bond, G., Klas, M., Bonani, G. and Wolfi, W. 1990. A salt oscillator in the glacial North Atlantic? 1. The concept. *Paleoceanography* 5, 469–477.

Broecker, W., Barker, S., Clark, E., Hajdas, I. and Bonani, G. 2006. Anomalous radiocarbon ages for foraminifera shells. *Paleoceanography* 21, doi:10.1029.2005PA001212.

Bukry, D. 1974. Coccoliths as Paleosalinity Indicators; evidence from Black Sea. In: Degens, E.T., and Ross, D.A. (Eds.), *The Black Sea; Geology, Chemistry, and Biology*. American Association of Petroleum Geologists, Tulsa, pp. 353-363.

Bushaw-Newton, K.L. and Sellner, K.G. 1999 (on-line). Harmful Algal Blooms. In: NOAA's State of the Coast Report. Silver Spring, MD: National Oceanic and Atmospheric Administration. http://state-of-coast.noaa.gov/bulletins/html/hab_14/hab.html

Cacho, I., Grimalt, J.O., Sierro, F.J., Shackleton, N. and Canals, M. 2000. Evidence for enhanced Mediterranean thermohaline circulation during rapid climatic coolings. *Earth and Planetary Science Letters* 183, 417-429.

Cacho, I., Grimalt, J.O., Canals, M., Sbaffi, L., Shackleton, N.J., Schönfeld, J. and Zahn, R. 2001. Variability of the western Mediterranean Sea surface temperature during the last 25,000 years and its connection with the Northern Hemisphere climatic changes. *Paleoceanography* 16 (1), 40-52.

Cagatay, M.N., Görür, N., Algan, O., Eastoe, C., Tchapalyga, A., Ongan, D., Kuhn, T. and Kuscu, I. 2000. Late Glacial-Holocene palaeoceanography of the Sea of Marmara: timing of connections with the Mediterranean and the Black Seas. *Marine Geology* 167, 191-206.

Caner, H. and Algan, O. 2002. Palynology of sapropelic layers from the Marmara Sea. *Marine Geology* 190, 35-46.

Caralp, M.-H. 1988. Late Glacial to recent deep-sea benthic foraminifera from the Northeastern Atlantic (Cádiz Gulf) and Western Mediterranean (Alborán Sea): paleoceanographic results. *Marine Micropaleontology* 13, 265-289.

Cayre, O., Lancelot, Y. and Vincent, E. 1999. Paleoceanographic reconstructions from planktonic foraminifera off the Iberian Margin: temperature, salinity, and Heinrich events. *Paleoceanography* 14 (3), 384-396.

Cembella, A.D., Quilliam, M.A., Lewis, N.I., Bauder, A.G., Dell'Aversano, C., Thomas, K., Jellett, J. and Cusack, R.R. 2002. The toxigenic marine dinoflagellate *Alexandrium tamarense* as the probable cause of mortality of caged salmon in Nova Scotia. *Harmful Algal Blooms* 1, 313–325.

Christensen, J.T., Cedhagen, T. and Hylleberg, J. 2004. Late-Holocene salinity changes in Limfjorden, Denmark. *Sarsia* 89, 379-387.

Clemens, S.C. 1998. Dust response to seasonal atmospheric forcing: proxy evaluation and calibration. *Paleoceanography* 13, 471-490.

Clement, A. and Peterson, L.C. 2008. Mechanisms of abrupt climate change of the last glacial period. *Review of Geophysics* 46, RG4002, doi:10.1029/2006RG000204.

Colmenero-Hidalgo, E., Flores, J.-A. and Sierro, F.J. 2002. Biometry of *Emiliania huxleyi* and its biostratigraphic significance in the Eastern North Atlantic Ocean and Western Mediterranean Sea in the last 20 000 years. *Marine Micropaleontology* 46, 247-263.

Colmenero-Hidalgo, E., Flores, J.-A., Sierro, F.J., Bárcena, M.A., Löwemark, L., Schönfeld, J. and Grimalt, J.O. 2004. Ocean surface water response to short-term climate changes revealed by coccolithophores from the Gulf of Cádiz (NE Atlantic) and Alborán Sea (W Mediterranean). *Palaeogeography, Palaeoclimatology, Palaeoecology* 205, 317-336.

Combourieu Nebout, N., Londeix, L., Baudin, F., Turon, J.-L., von Grafenstein, R. and Zahn, R. 1999. Quaternary marine and continental paleoenvironments in the Western Mediterranean (site 976, Alborán Sea): palynological evidence. In: Zahn, R., Comas, M.C. and Klaus, A. (Eds.), *Proceedings of the Ocean Drilling Program, Scientific Results 161*, College Station, Texas (Ocean Drilling Program), pp. 457–468.

Cane, M. A. and A. Clement, 1999. A role for the tropical Pacific coupled ocean-atmosphere system on Milankovitch and millenial timescales. Part II: Global impacts. In: Clark, P.U. and Webb, R.S. (Eds.), *Mechanisms of Millennial-Scale Global Climate Change*. American Geophysical Union, pp. 373-383.

Clement, A.C. and Cane, M.A. 1999. A role for the tropical Pacific coupled ocean-atmosphere system on Milankovich and millenial timescales. Part I: A modeling study of tropical Pacific variability. In: Clark, P.U., Webb, R.S. and Keigwin, L.D. (Eds.), *Mechanisms of Millennial-Scale Global Climate Change*. American Geophysical Union, pp. 363-371.

Cros, L., Kleijne, A., Zeltner, A., Billard, C. and Young, J.R. 2000. New examples of holococcolith–heterococcolith combination coccospheres and their implications for coccolithophorid biology. *Marine Micropaleontology* 39, 1-34.

Crudeli, D., Young, J.R., Erba, E., de Lange, G.J., Henriksen, K., Kinkel, H., Slomp, C.P. and Ziveri, P. 2004. Abnormal carbonate diagenesis in Holocene-Late Pleistocene sapropel-associated sediments from the Eastern Mediterranean; evidence from *Emiliania huxleyi* coccolith morphology. *Marine Micropaleontology* 52, 217-240.

Dahl, K.A., Repeta, D.J. and Goericke, R. 2004. Reconstructing the phytoplankton community of the Cariaco Basin during the Younger Dryas cold event using chlorine steryl esters. *Paleoceanography* 19, PA1006, doi:10.1029/2003PA000907.

Dale, B. 1976. Cyst formation, sedimentation, and preservation; factors affecting dinoflagellate assemblages in recent sediments from Trondheimsfjord, Norway. *Review of Palaeobotany and Palynology* 22, 39–60.

Dale, B. 1996. Dinoflagellate cyst ecology: modelling and geological applications. In: Jansonius, J. and McGregor, D.C. (Eds.), *Palynology: Principles and Applications, vol. 3*. American Association of Stratigraphic Palynologists, Dallas, Texas, 1249-1275.

Dale, B. 2001. The sedimentary record of dinoflagellate cysts: looking back into the future of phytoplankton blooms. *Scientia Marina* 65 (2), 257-272.

Dale, B. 2009. Eutrophication signals in the sedimentary record of dinoflagellate cysts in coastal waters. *Journal of Sea Research* 61 (1-2).

Dale, B. and Dale, A.L. 2002. Environmental applications of dinoflagellate cysts and acritarchs. In: Haslett, S.K. (Ed.), *Quaternary Environmental Micropalaeontology*. Arnold, London, pp. 207-240.

Dale, B. and Fjellså, A. 1994. Dinoflagellate cysts as paleoproductivity indicators: state of the art, potential and limits. In: Zahn, R., Pedersen, T., Kaminski, M. and Labeyrie, L. (Eds.), *Carbon Cycling in the Glacial Ocean: constraints on the ocean's role in global change*. Springer-Verlag, Berlin, pp. 521-537.

Dale, B., Dale, A.L. and Jansen, J.H.F. 2002. Dinoflagellate cysts as environmental indicators in surface sediments from the Congo deep-sea fan and adjacent regions. *Palaeogeography, Palaeoclimatology, Palaeoecology* 185, 309–338.

Dale, B., Edwards, M. and Reid, P.C. 2006. Climate change and Harmful Algal Blooms. In: Granéli, E. and Turner, J.T. (Eds.), *Ecology of Harmful Blooms*. Springer-Verlag, Berlin, pp. 367-378.

Dale, B., Thorsen, T.A. and Fjellså, A. 1999. Dinoflagellate cysts as indicators of cultural eutrophication in the Oslofjord, Norway. *Estuarine Coastal and Shelf Sciences* 48, 371-382.

Dansgaard, W., Johnsen, S.J., Clausen, H.B., Dahl–jensen, D., Gundestrup, N.S., Hammer, C.U., Hvidberg, C.S., Steffensen, J.P., Sveinbjornsdottir, A.E., Jouzel, J. and Bond, G. 1993. Evidence for general instability of past climate from a 250–kyr ice–core record. *Nature* 364, 218–220.

De Bernardi, B., Ziveri, P., Erba, E. and Thunell, R.C. 2005. Coccolithophore export production during the 1997-1998 El Niño event in Santa Barbara Basin (California). *Marine Micropaleontology* 55, 107-125.

de Leeuw, J.W., Versteegh, G.J.M. and van Bergen, P.F. 2006. Biomacromolecules of algae and plants and their fossil analogues. *Plant Ecology* 182, 209-233.

De Schepper, S. and Head, M.J. 2008. Age calibration of dinoflagellate cyst and acritarch events in the Pliocene–Pleistocene of the eastern North Atlantic (DSDP Hole 610A). *Stratigraphy* 5 (2), 137-161.

de Vernal, A. and Hillaire-Marcel, C. 2000. Sea-ice cover, sea-surface salinity and halo/thermocline structure of the northwest North Atlantic: Modern versus full glacial conditions. *Quaternary Science Reviews* 19 (5), 65-85.

de Vernal, A. and Marret, F. 2007. Organic-walled dinoflagellate cysts: tracers of sea-surface conditions. In: Hillaire-Marcel C. and de Vernal A. (Eds.), *Proxies in Late Cenozoic paleoceanography*. Elsevier, Utrecht, pp. 371-408.

de Vernal, A., Henry, M. and Bilodeau, G. 1996. Techniques de préparation et d'analyse en micropaléontologie. Les cahiers de GEOTOP, 3, Université de Québec a Montréal, unpublished report, 28 pp.

de Vernal, A., Larouche, A. and Richard, P.J.H. 1987. Evaluation of palynomorph concentrations: do the aliquot and the marker-grain methods yield comparable results? *Pollen et Spores* 19 (2-3), 291–304.

de Vernal, A., Turon, J.L. and Guiot, J. 1994. Dinoflagellate cyst distribution in high-latitude marine environments and quantitative reconstruction of sea-surface salinity, temperature, and seasonality. *Canadian Journal of Earth Sciences* 31, 48–62.

de Vernal, A., Rochon, A., Turon, J.L. and Matthiessen, J. 1998. Organic-walled dinoflagellate cysts: palynological tracers of sea-surface conditions in middle to high latitude marine environments. *Geobios* 30, 905–920.

de Vernal, A., Eynaud, F., Henry, M., Hillaire-Marcel, C., Londeix, L., Mangin, S., Matthiessen, J., Marret, F., Radi, T., Rochon, A., Solignac, S. and Turon, J.-L. 2005. Reconstruction of sea-surface conditions at middle to high latitudes of the Northern Hemisphere during the Last Glacial Maximum (LGM) based on dinoflagellate cyst assemblages. *Quaternary Science Reviews* 24, 897-924.

de Vernal, A., Henry, M., Matthiessen, J., Mudie, P.J., Rochon, A., Boessenkool, K.P., Eynaud, F., Grøsfjeld, K., Guiot, J., Hamel, D., Harland, R., Head, M.J., Kunz-Pirrung, M., Levac, E., Loucheur, V., Peyron, O., Pospelova, V., Radi, T., Turon, J.-L. and Voronina, E. 2001. Dinoflagellate cyst assemblages as tracers of sea-surface conditions in the northern North Atlantic, Arctic and sub-Arctic seas: the new 'n=677' data base and its application for quantitative palaeoceanographic reconstruction. *Journal of Quaternary Science* 16, 681–698.

de Villiers, S. 2003. Dissolution effects on foraminiferal Mg/Ca records of sea surface temperature in the western equatorial Pacific. *Paleoceanography* 18(3), 1070, doi:10.1029/2002PA000802.

Dean, W.E. 2007. Sediment geochemical records of productivity and oxygen depletion along the margin of western North America during the past 60,000 years: teleconnections with Greenland Ice and the Cariaco Basin. *Quaternary Science Reviews* 26, 98-114.

Deflandre, G. and Cookson, I.C. 1955. Fossil microplankton from Australia late Mesozoic and Tertiary sediments. *Australian journal of Marine and Freshwater Research* 6, 242-313.

Dekens, P. S., Lea, D.W., Pak, D.K. and Spero, H.J. 2002. Core top calibration of Mg/Ca in tropical Foraminifera: Refining paleotemperature estimation. *Geochemistry Geophysics Geosystems* 3(4), 1022, doi:10.1029/2001GC000200.

DeRosa, M. and Gambacorta, A. 1988. The lipids of archaeabacteria. *Progress in Lipid Research* 27, 153-175.

Desezar, Y. B. and Poulsen, N. E. 1994. On palynological preparation technique. *American Association of Stratigraphic Palynologists Newsletter* 27 (3), 12–13.

Deuser W.G. 1973. Cariaco Trench – oxidation of organic–matter and residence time of anoxic water. *Nature* 242, 601–603.

Dittert, N., Baumann, K.-H., Bickert, T., Henrich, R., Huber, R., Kinkel, H. and Meggers, H. 1999. Carbonate dissolution in the deep–sea: methods, quantification and paleoceanographic application. In: Fischer, G. and Wefer, G. (Eds.), *Use of proxies in Palaeoceanography: examples from the South Atlantic*. Springer–Verlag, Heidelberg, pp. 255–284.

Dodge, J. D. and Harland, R. 1991. The distribution of planktonic dinoflagellates and their cysts in the eastern and northeastern Atlantic Ocean. *New Phytologist* 118, 593-603.

Doose-Rolinski, H., Rogalla, U., Scheeder, G., Lückge, A. and von Rad, U. 2001. High-resolution temperature and evaporation changes during the Late Holocene in the northeastern Arabian Sea. *Paleoceanography* 16, 358–367.

Dorman, C.E., Beardsley, R.C. and Limeburner, R. 1995. Winds in the Strait of Gibraltar. *Quarterly Journal of the Royal Meteorological Society* 121, 1903-1921.

Edwards, L.E. and Andrle, V.A.S. 1992. Distribution of selected dinoflagellate cysts in modern marine sediments. In: Head, M.J. and Wrenn, J.H. (Eds.), *Neogene and Quaternary Dinoflagellate cysts and Acritarchs.* American Association of Stratigraphic Palynologists Foundation, Dallas Texas, pp. 259-288.

Edwards, M., Johns, D.G., Leterme, S.C., Svendsen, E. and Richardson, A.J. 2006. Regional climate change and harmful algal blooms in the northeast Atlantic. *Limnology and Oceanography* 51 (2), 820-829.

Elderfield H. and Ganssen, G. 2000. Past temperature and $\delta^{18}O$ of surface ocean waters inferred from foraminiferal Mg/Ca ratios. *Nature* 405, 442–445.

Ellegaard, M. 2000. Variations in dinoflagellate cyst morphology under conditions of changing salinity during the last 2000 years in the Limfjord, Denmark. *Review of Palaeobotany and Palynology* 109, 65-81.

Elliot, M., Labeyrie, L. and Duplessy, J.-.C., 2002. Changes in North Atlantic deep-water formation associated with the Dansgaard-Oeschger temperature oscillations (60-10 ka). *Quaternary Science Reviews* 21, 1153-1165.

Emerson, S. and Bender, M.L. 1981. Carbon fluxes at the sediment–water interface of the deep sea: calcium carbonate preservation. *Journal of Marine Research* 39, 139–162.

Eppley, R.W. and Harrison, W.G. 1975. Physiological ecology of *Gonyaulax polyedra* a red water dinoflagellate of southern California. In: LoCicero, V.R. (Ed.), *Proceedings of the First International Conference of Toxic Dinoflagellate Blooms.* Massachusetts Science and Technology Foundation, Wakefield, Massachusetts, pp. 11-22.

Evitt, W.R. 1985. Sporopollenin dinoflagellate cysts. Their morphology and interpretation. American Association of Stratigraphic Palynologists Foundation, Dallas, 333 pp.

Evitt, W.R. and Davidson, S.E. 1964. Dinoflagellate cysts and thecae. *Stanford University Publications Geological Sciences* 10, 1-12.

Eynaud, F., Turon, J.-L., Sánchez-Goñi, M.F. and Gendreau, S. 2000. Dinoflagellate cyst evidence of 'Heinrich-like events' off Portugal during the Marine Isotopic Stage 5. *Marine Micropaleontology* 40, 9-21.

Fairbanks, R.G. 1989. A 17,000–year glacio–eustatic sea level record – influence of glacial melting rates on the Younger Dryas event and deep–ocean circulation. *Nature* 342, 637–641.

Fensome, R.A. and Williams, G.L. 2004. The Lentin and Williams index of fossil dinoflagellates: 2004 Edition. *American Association of Stratigraphic Palynologists, Contributions Series* 42, 1–909.

Fensome, R.A., Taylor, F.J.R., Norris, G., Sarjeant, W.A.S., Wharton, D.I. and Williams, G.L. 1993. A classification of fossil and living dinoflagellates. *Micropaleontology Special Paper* 7, 1-351.

Ferraz–Reyes, E. 1983. Estudio del fitoplancton en la Cuenca Tuy–Cariaco, Venezuela, *Boletin del Instituto Oceanografico de Venezuela; Universidad de Oriente 22*, 111 – 124.

Ferreira, J., Cachao, M. and González, R. 2008. Reworked calcareous nannofossils as ocean dynamic tracers: the Guadiana shelf case study (SW Iberia). *Estuarine, Coastal and Shelf Science* 79, 59-70.

Findlay, C.S. and Flores, J.A. 2000. Subtropical fluctuations south of Australia (45°09'S, 146°17'E) for the last 130 ka years based on calcareous nannoplankton. *Marine Micropaleontology* 40, 403-416.

Fletcher, W.J., Sanchez Goñi, M.F., Peyron, O. and Dormoy, I. 2009. Abrupt climate changes of the last deglaciation detected in a western Mediterranean forest record. *Climate of the Past Discussions* 5, 203-235.

Flores, J.-A., Barcena, M.A. and Sierro, F.J. 2000. Ocean-surface and wind dynamics in the Atlantic Ocean off northwest Africa during the last 140,000 years. *Palaeogeography. Palaeoclimatololology. Palaeoecology* 161, 459– 478.

Fofonoff, P. and Millard, R.C. Jr. 1983. Algorithms for computing of fundamental properties of seawater. *Unesco Technical Papers in Marine Sciences* 44, 1-53.

Foubert, A., Depreiter, D., Beck, T., Maignien, L., Pannemans, B., Frank, N., Blamart, D. and Henriet, J.-P. 2008. Carbonate mounds in a mud volcano province off north-west Morocco: key processes and controls. *Marine Geology* 248, 74-96.

Frenz, M., Höppner, R., Stuut, J.-B.W., Wagner, T. and Henrich, R. 2003. Surface sediment bulk geochemistry and grain-size composition related to the oceanic circulation along the South American continental margin in the Southwest Atlantic. In: Mulitza, S., Ratmeyer V. and Wefer, G. (Eds.), *The South Atlantic in the Late Quaternary: Reconstruction of Material Budget and Current Systems.* Springer-Verlag, Berlin, pp. 347–373.

Fujiwara, S.M., Tsuzuki, M., Kawachi, N., Minaka, N. and Inouye, I. 2001. Molecular phylogeny of the Haptophyta based on the rbcL gene and sequence variation in the spacer region of the rubisco operon. *Journal of Phycolology* 37, 121–129.

Funkhouser, J.W. and Evitt, W.R. 1959. Preparation techniques for acid-insoluble microfossils. *Micropalaeontology* 5, 369–375.

Garcia, H. E., Locarnini, , R. A., Boyer, T. P. and Antonov, J. I. 2006. World Ocean Atlas 2005, Volume 3: Dissolved Oxygen, Apparent Oxygen Utilization, and Oxygen Saturation. In: Levitus, S. (Ed.), *NOAA Atlas NESDIS 63.* U.S. Government Printing Office, Washington, D.C., 342 pp.

Gasse, F. 2000. Hydrological changes in the African tropics since the Last Glacial Maximum. *Quaternary Science Reviews* 19, 189-211.

Geisen, M., Young, J.R., Probert, I., Sáez, A.G., Baumann, K.-H., Sprengel, C., Bollmann, J., Cros, L., De Vargas, C. and Medlin, L.K. 2004. Species level variation in coccolithophores. In: Thierstein, H.R. and Young, J.R. (Eds.), *Coccolithophores – From molecular processes to global impact*. Springer, Berlin, pp. 327-366.

Germerad, J.H., Hopping, C.A. and Muller, J. 1968. Palynology of Tertiary sediments from tropical areas. *Review of Palaeobotany and Palynology* 6, 189–348.

Giraudeau, J. 1992. Coccolith paleotemperatures and paleosalinity estimates in the Caribbean Sea for the Middle-Late Pleistocene (DSDP Leg 68 – Hole 502B). *Memorie di Scienze Geologiche* 43, 375-387.

Giunta S., Maffioli P., Negri A., Sangiorgi F., Capotondi L., Morigi C., Principato M.S. and Corselli C. 2006. The Isotopic stage 5e in the eastern Mediterranean Sea: Phytoplankton signal and its implications. *Palaeogeography, Palaeoclimatology, Palaeoecology* 235, 28-47.

Gliozzi A., Paoli G., DeRosa M. and Gambacorta A. 1983. Effect of isoprenoid cyclization on the transition temperature of lipids in thermophilic archaeabacteria. *Biochimica et Biophysica Acta* 735, 234–242.

Godhe, A. and McQuoid, M.R. 2003. Influence of benthic and pelagic environmental factors on the distribution of dinoflagellate cysts in surface sediments along the Swedish west coast. *Aquatic Microbial Ecology* 32, 185-201.

Goni, M.A.,Thunell, R.C., Woodwort, M.P. and Müller-Karger, F.E. 2006. Changes in wind-driven upwelling during the last three centuries: Interocean teleconnections. *Geophysical Research Letters* 33, L15604, doi:10.1029/2006GL026415.

Goni, M.A., Aceves, H.L., Thunell, R.C., Tappa, E., Black, D., Astor, Y., Varela, R. and Muller–Karger, F. 2003. Biogenic fluxes in the Cariaco Basin: a combined study of sinking particulates and underlying sediments. *Deep–sea Research I* 50, 781–807.

González, C., Dupont, L.M., Behling, H. and Wefer, G. 2008a. Neotropical vegetation response to rapid climate changes during the last glacial period: palynological evidence from the Cariaco Basin. *Quaternary Research* 69, 217-230.

González, C., Dupont, L.M., Mertens, K. and Wefer, G. 2008b. Reconstructing marine productivity of the Cariaco Basin during marine isotope stage 3 and 4 using organic-walled dinoflagellate cysts. *Paleoceanography* 23, PA3215, doi:10.1029/2008PA001602.

Greaves, M., Caillon, N., Rebaubier, H., Bartoli, G., Bohaty, S., Cacho, I., Clarke, L., Cooper, M., Daunt, C., Delaney, M., deMenocal, P., Dutton, A., Eggins, S., Elderfield, H., Garbe-Schoenberg, D., Goddard, E., Green, D., Groeneveld, J., Hastings, D., Hathorne, E., Kimoto, K., Klinkhammer, G., Labeyrie, L., Lea, D. W., Marchitto, T., Martínez-Botí, M. A., Mortyn, P. G., Ni, Y. Nuernberg, D., Paradis, G., Pena, L., Quinn, T., Rosenthal, Y., Russell, A., Sagawa, T., Sosdian, S., Stott, L., Tachikawa, K., Tappa, E., Thunell, R. and Wilson, P. A. 2008. Interlaboratory comparison study of calibration standards for foraminiferal Mg/Ca thermometry. *Geochemistry, Geophysics, Geosystems* 9, Q08010, doi:10.1029/2008GC001974.

Grøsfjeld, K. and Harland, R. 2001. Distribution of modern dinoflagellate cysts from inshore areas along the coast of southern Norway. *Journal of Quaternary Science* 16(7), 651-659.

Gundersen, N. 1988. En palynologisk undersøkelse av dinoflagellatcyster langs en synkende salinitetsgradient I recente sedimenter fra Østersjø-området. Unpublished candidata scientiarum thesis, University of Oslo, 96 pp.

Haberle, S.G. and Ledru, M.-P. 2001. Correlations among charcoal records of fires from the past 16,000 years in Indonesia, Papua New Guinea, and Central and South America. *Quaternary Research* 55, 97-104.

Haidar, A.T. and Thierstein, H.R. 2001. Coccolithophore dynamics off Bermuda (N. Atlantic). *Deep–Sea Research Part II* 48, 1925–1956.

Hallett, R.I. 1999. Consequences of environmental change on the growth and morphology of *Lingulodinium polyedrum* (Dinophyceae) in culture. Ph.D. thesis. University of Westminster, 109 pp.

Haug, G.H., Hughen, K.A., Sigman, D.M., Peterson, L.C. and Röhl, U. 2001. Southward migration of the intertropical convergence zone through the Holocene. *Science* 293, 1304–1308.

Haug, G.H., Pedersen, T.F., Sigman, D.M., Calvert, S.E., Nielsen, B. and Peterson, L.C. 1998. Glacial/interglacial variations in production and nitrogen fixation in the Cariaco Basin during the last 580 kyr. *Paleoceanography* 13, 427–432.

Hays, G.C., Richardson, A.J. and Robinson, C. 2005. Climate change and marine plankton. *Trends in Ecology and Evolution* 20(6), 337-344.

Head, M.J. 1996. Late Cenozoic dinoflagellates from the Royal Society borehole at Ludham, Norfolk, Eastern England, *Journal of Paleontology* 70 (4), 543-570.

Head, M.J. 2007. Last Interglacial (Eemian) hydrographic conditions in the southwestern Baltic Sea based on dinoflagellate cysts from Ristinge Klint, Denmark. *Geological Magazine* 144 (6), 987-1013.

Heilmann-Clausen, C. 1985. Dinoflagellate stratigraphy of the Uppermost Danian to Ypresian in the Viborg 1 borehole, Central Jylland, Denmark. *Serie A / Danmarks geologiske undersøgelse 7*, 1–69.

Hemming, S.R. 2004. Heinrich events: massive late Pleistocene detritus layers of the North Atlantic and their global climate imprint. *Review of Geophysics* 42, 1-43.

Hemsley, A.R., Lewis, J. and Griffiths, P.C. 2004. Soft and sticky development: some underlying reasons for microarchitectural pattern convergence. *Review of Palaeobotany and Palynology* 130, 105-119.

Hemsley, A.R., Griffiths, P.C., Lewis, J. and Hallett, R. 2000. Is self-assembled microarchitecture intrinsically robust? In: Spatz, H.-C. and Speck,, T. (Eds.), *Plant Biomechanics 2000.* Georg Thieme Verlag, Stuttgart, pp. 109-116.

Herbert, T.D. 2003. Alkenone paleotemperature determinations. In: Holland, H.D. and Turekian, K.K. (Eds.), *The Ocean and Marine Geochemistry. Treatise on Geochemistry 6*. Elsevier-Pergamon, Oxford, pp. 365–390.

Herbert, T.D. and Schuffert, J.D. 2000. Alkenone unsaturation of sea–surface temperatures at site 1002 over a full glacial cycle. In: Leckie, R.M., Sigurdsson, H., Acton, G.D. and Draper, G. (Eds.), *Proceedings of the Ocean Drilling Program, Scientific results 165*. College station (Ocean Drilling Program), Texas, pp. 239–247.

Herrle, J.O. and Bollmann, J. 2004. Accuracy and reproducibility of absolute nannoplankton abundances using the filtration technique in combination with a rotary sample splitter. *Marine Micropaleontology* 53, 389–404.

Hodgkinson, R.I. 1991. Microfossil processing: a damage report. *Micropalaeontology* 37, 320–326.

Hoefs, M.J.L., Versteegh, G.J.M., Rijpstra, W.I.C., de Leeuw, J.W. and Sinninghe Damste, J.S. 1998. Post-depositional oxic degradation of alkenones: Implications for the measurement of palaeo sea surface temperatures. *Paleoceanography* 13, 42-49.

Holz, C., Stuut, J.-B. and Henrich, R. 2004. Terrigenous sedimentation processes along the continental margin off NW Africa: implications from grain-size analysis of seabed sediments. *Sedimentology* 51, 1145-1154.

Holzwarth, U., Esper, O. and Zonneveld, K.A.F. 2007. Distribution of organic-walled dinoflagellate cysts in shelf surface sediments of the Benguela upwelling system in relationship to environmental conditions. *Marine Micropaleontology* 64, 91–119.

Honjo, S. 1996. Fluxes of particles to the interior of the open oceans. In Ittekot, V.P., Aschauffer, S., Honjo, S. and Depetreis, P. (Eds.), *Particle Flux in Open Ocean.* Wiley, New York, pp. 91–154.

Hopkins , J.A. and McCarthy, F.M.G. 2002. Postdepositional palynomorph degradation in Quaternary shelf sediments: a laboratory experiment studying the effects of progressive oxidation. *Palynology* 26, 167–184.

Hopmans, E.C., Schouten, S., Pancost, R.D., van der Meer, M.J.T. and Sinninghe Damsté, J.S. 2000. Analysis of intact tetraether lipids in archaeal cell material and sediments by high performance liquid chromatography/atmospheric pressure chemical ionization mass spectrometry. *Rapid Communications in Mass Spectrometry* 14, 585–589.

Hopmans, E.C., Weijers, J.W.H., Schefuβ, E., Herfort, L., Sinninghe Damsté, J.S. and Schouten, S. 2004. A novel proxy for terrestrial organic matter in sediments based on branched and isoprenoid tetraether lipids. *Earth and Planetary Science Letters* 224, 107-116.

Hsu, C.-P.F. and Wallace, J.M. 1976. The global distribution in annual and semiannual cycles in precipitation. *Monthly Weather Review* 104 (9), 1093-1101.

Hughen, K.A., Eglinton, T.I., Xu, L. and Makou, M. 2004. Abrupt tropical vegetation response to rapid climate changes. *Science* 304, 1955-1959.

Hughen, K.A., Overpeck, J.T., Peterson, L.C. and Anderson, R.F. 1996a. The nature of varved sedimentation in the Cariaco Basin, Venezuela, and its palaeoclimatic significance. In: Kemp, A.E.S. (Ed.), *Palaeoclimatology and Palaeoceanography from Laminated Sediments, Geological Society Special Publication 116.* Geological Society, London, pp. 171-183.

Hughen, K.A., Overpeck, J.T., Peterson, L.C. and Trumbore, S. 1996b. Rapid climate changes in the tropical Atlantic region during the last deglaciation. *Nature* 380, 51-54.

Hughen, K.A., Lehman, S., Southon, J., Overpeck, J., Marchal, O., Herring, C. and Turnbull, J. 2004. ^{14}C activity and global carbon cycle changes over the past 50,000 years. *Science* 303, 202-207.

Huguet, C., Kim, J.-H., Sinninghe Damsté, J.S. and Schouten, S. 2006a. Reconstruction of sea surface temperature variations in the Arabian Sea over the last 23 kyr using organic proxies (TEX_{86} and $U^{K'}_{37}$). *Paleoceanography* 21, doi:10.1029/2005PA001215.

Huguet, C., Hopmans, E.C., Febo-Ayala, W., Thompson, D.H., Sinninghe Damsté, J.S. and Schouten, S. 2006b. An improved method to determine the absolute abundance of glycerol dibiphytanyl glycerol tetraether lipids. *Organic Geochemistry* 37, 1036-1041.

Huguet, C., Schimmelmann, A., Thunell, R., Lourens, L.J., Sinninghe Damsté, J.S. and Schouten, S. 2007. A study of the TEX_{86} paleothermometer in the water column and sediments of the Santa Barbara Basin, California. *Paleoceanography* 22, PA3203, doi:10.1029/2006PA001310.

Huntley, M.E., Sykes, P., Rohan, S. and Marin, V. 1986. Chemically-mediated rejection of dinoflagellate prey by the copepods *Calanus pacixcus* and *Paracalanus parvus*: mechanism, occurrence and significance. *Marine Ecology Progress Series* 28, 105-120.

Hurrell, J.M. 1995. Decadal trends in the North Atlantic Oscillation: regional temperatures and precipitation. *Science* 269, 676-679.

Ivanochko, T.S., Ganeshram, R.S., Brummer, G.-J.A., Gansen, G., Jung, S.J.A., Moreton, S.G. and Kroon, D. 2005. Variations in tropical convection as an amplifier of global climate at the millennial scale. *Earth and Planetary Science Letters* 235, 302-314.

Jahnke, R.A., Craven, D.B. and Gaillard J.–F. 1994. The influence of organic matter diagenesis on $CaCO_3$ dissolution at the deep–sea floor. *Geochimica et Cosmochimica Acta* 58, 2799–2809.

Jenkyns, H., Forster, A., Schouten, S. and Damste, J. 2004. High temperatures in the Late Cretaceous Arctic Ocean. *Nature* 432, 888-891.

Jennerjahn, T.C., Ittekkot, V., Arz, H.W., Behling, H., Pätzold, J. and Wefer, G. 2004. Asynchronous Terrestrial and Marine Signals of Climate Change During Heinrich Events. *Science* 306, 2236 – 2239.

Jeong, H.J., Yoo, D.Y., Park, J.Y., Song, J.Y., Kim, S.T., Lee, S.H., Kim, K.Y. and Yih, W.H. 2005. Feeding by phototrophic red-tide dinoflagellates: five species newly revealed and six species previously known to be mixotrophic. *Aquatic Microbial Ecology* 40, 133–150.

Jordan, R.W. 2002. Environmental applications of calcareous nannofossils. In: Haslett, K. (Ed.), *Quaternary environmental micropalaeontology*. Arnold, London, pp. 185-206.

Jordan, R.W. and Chamberlain, A.H.L. 1997. Biodiversity among haptophyte algae. *Biodiversity and Conservation* 6, 131–152.

Jordan, R.W. and Winter, A. 2000. Assemblages of coccolithophorids and other living microplankton off the coast of Puerto Rico during January-May 1995. *Marine Micropaleontology* 39, 113-130.

Kallel, N., Paterne, M., Labeyrie, L., Duplessy, J.-C. and Arnold, M. 1997. Temperature and salinity records of the Tyrrenhian Sea during the last 18,000 years. *Palaeogeography, Palaeoclimatology, Palaeoecology* 135, 97-108.

Kameo, K. 2002. Late Pliocene Caribbean surface water dynamics and climatic changes based on calcareous nannofossil records. *Palaeogeography, Palaeoclimatology, Palaeoecology* 179, 211–226.

Kawamura, H., Holbourn, A. and Kuhnt, W. 2006. Climate variability and land-ocean interactions in the Indo Pacific Warm Pool: A 460-ka palynological and organic geochemical record from the Timor Sea. *Marine Micropaleontology* 59, 1-14.

Keigwin, L. D., Curry, W. B., Lehman, S. J. and Johnsen, S 1994a. The role of the deep ocean in North Atlantic climate change between 70 and 130 kyr ago. *Nature* 371, 323–326.

Keigwin, L.D. and Lehman, S.J., 1994b. Deep circulation change linked to Heinrich event 1 and Younger Dryas in a mid-depth North Atlantic core. *Paleoceanography* 9, 185-194.

Kim, J., Schouten S., Hopmans E.C., Donner B. and Sinninghe Damsté J.S. 2008. Global core-top calibration of the TEX_{86} paleothermometer in the ocean. *Geochimica et Cosmochimica Acta* 72, 1154-1173.

Kinkel, H., Baumann, K.-H. and Cepek, M. 2000. Coccolithophores in the equatorial Atlantic Ocean: response to seasonal and Late Quaternary surface water variability. *Marine Micropaleontology* 39, 87–112.

Kleijne, A., Kroon, D. and Zevenboom, W. 1989. Phytoplankton and foraminiferal frequencies in northern Indian Ocean and Red Sea surface waters. *Netherlands Journal of Sea Research* 24, 531-539.

Klöcker, R. and Henrich, R. 2006. Recent and Late Quaternary pteropod preservation on the Pakistan shelf and continental slope. *Marine Geology* 231, 103-111.

Knappertbusch, M. 1993. Geographic distribution of living and Holocene coccolithophores in the Mediterranean Sea. *Marine Micropaleontology* 21, 219–247.

Knies, 2005. Climate-induced changes in sedimentary regimes for organic matter supply on the continental shelf off Northern Norway. *Geochimica et Cosmochimica Acta* 69 (19), 4631-4647.

Kokinos, J.P. 1994. Studies on the cell wall of dinoflagellate resting cysts: morphological development, ultrastructure, and chemical composition. Ph.D. thesis, Massachusetts Institute of Technology/Woods Hole Oceanographic Institution, 224 pp.

Kokinos, J.P. and Anderson D.M. 1995. Morphological development of resting cysts in cultures of the marine dinoflagellate *Lingulodinium polyedrum* (= *L. machaerophorum*). *Palynology* 19, 143-166.

Koopmann, B. 1981. Sedimentation von Saharastaub im subtropischen Nordatlantik waehrend der letzten 25.000 Jahre. *Meteor Forschungs ergebnisse Reihe* C 35, 23-59.

Kopf, A., Bannert, B. Brückmann, W., Dorschel, B., Foubert, A.T.G., Grevemeyer, I., Gutscher, M.-A., Hebbeln, D., Heesemann, B., Hensen, C., Kaul, N., Lutz, M., Magalhaes, V.H., Marquardt, M.J., Marti, A.V., Nass, K.S., Neubert, N., Niemann, H., Nuzzo, M., Poort, J.P.D., Rosiak, U.D., Sahling, H., Schneider von Deimling, J., Somoza Losada, L., Thiebot, E. and Wilkop, T.P. 2004. Report and preliminary results of SONNE cruise SO175, Miami - Bremerhaven, 12.11. - 30.12.2003, Berichte, Fachbereich Geowissenschaften, Bremen, No. 228, 218 p.

Kotthoff, U., Pross, J., Müller, U.C., Peyron, O., Schmiedl, G., Schulz, H. and Bordon, A. 2008. Climate dynamics in the borderlands of the Aegean Sea during formation of sapropel S1 deduced from a marine pollen record. *Quaternary Science Reviews* 27, 832-845.

Krammer, R., Baumann, K.-H. and Henrich, R. 2006. Middle to late Miocene fluctuations in the incipient Bengual Upwelling System revealed by calcareous nannofossil assemblages (ODP Site 1085A). *Palaeogeography, Palaeoclimatology, Palaeoecology* 230, 319-334.

Kremp, A. and Anderson, D. 2000. Factors regulating germination of resting cysts of the spring bloom dinoflagellate *Scrippsiella hangoei* from the northern Baltic Sea. *Journal of Plankton Research* 22, 1311–1327.

Kudela, R.M. and Cochlan,W.P. 2000. Nitrogen and carbon uptake kinetics and the influence of irradiance for a red tide bloom off southern California. *Aquatic Microbial Ecology* 21, 31–47.

Kuhlmann, H., Freudenthal, T., Helmke, P. and Meggers, H. 2004. Reconstruction of paleoceanography off NW Africa during the last 40,000 years: influence of local and regional factors on sediment accumulation. *Marine Geology* 207 (1-4), 209-224.

Kuroyanagi, A., Tsuchiya, M., Kawahata, H. and Kitazato, H. 2008. The occurrence of two genotypes of the planktonic foraminifer *Globigerinoides ruber* (white) and paleo-environmental implications. *Marine Micropaleontology* 68, 236-243.

Laj, C. 2004. Cruise report: MD 132–P. I. C. A. S. S. O. images XI, Fortaleza-Baltimore-Brest, Mai Juin 2003, Institut Polaire Français Paul Emile Victor, Plouzané, France, 53 pp.

Landsberg J.H. 2002. The effects of harmful algal blooms on aquatic organisms. *Reviews in Fisheries Science* 10(2), 113–390.

Lea D.W. 2003. Elemental and isotopic proxies of past ocean temperatures. In: Holland, H.D. and Turekian, K.K. (Eds.), *The Ocean and Marine Geochemistry. Treatise on Geochemistry 6*. Elsevier-Pergamon, Oxford, pp. 365–390.

Lea, D.W., Pak, D.K., Peterson, L.C. and Hughen, K.A. 2003. Synchroneity of tropical and high–latitude Atlantic temperatures over the last glacial termination. *Science* 301, 1361–1364.

Ledru, M.-P., Mourguiart, P., Ceccantini, G., Tucq, B. and Sifeddine, A. 2002. Tropical climates in the game of two hemispheres revealed by abrupt climatic change. *Geology* 30, 275-278.

Leroy, S.A.G., Marret, F., Gibert, E., Chalie, F., Reyss, J.L. and Arpe K. 2007. River inflow and salinity changes in the Caspian Sea during the last 5500 years, *Quaternary Science Reviews* 26 (25-28), 3359-3383.

Leroy, S.A.G., Marret, F., Giralt, S. and Bulatov, S.A. 2006. Natural and anthropogenic rapid changes in the Kara-Bogaz Gol over the last two centuries reconstructed from palynological analyses and a comparison to instrumental records. *Quaternary International* 150, 52-70.

Leroy, V. 2001. Traceurs palynologiques des flux biogéniques et des conditions hydrographiques en milieu marin cotier: exemple de l'étang de Berre. DEA, Ecole doctorale Sciences de l'environment d'Aix-Marseille, 30 pp.

Lewis, J. and Hallett, R. 1997. *Lingulodinium polyedrum* (*Gonyaulax polyedra)* a blooming dinoflagellate. In: Ansell, A.D., Gibson, R.N., Barnes, M. (Eds.), *Oceanography and Marine Biology: An Annual Review 35*. UCL Press, London, pp. 97-161.

Lewis, J., Tett, P. and Dodge, J.D. 1985. The cyst-theca cycle of *Gonyaulax polyedra* (*Lingulodinium machaerophorum*) in Creran, a Scottish west coast Sea-Loch. In: Anderson, D.M., White, A.W. and Baden, D.G. (Ed.), *Toxic dinoflagellates*. Elsevier Science Publishing, pp. 85-90.

Leyden, B. 1985. Late Quaternary Aridity and Holocene Moisture Fluctuations in the Lake Valencia Basin, Venezuela. *Ecology* 66, 1279-1295.

Lignum, J., Jarvis, I. and Pearce, M.A. 2008. A critical assessment of standard processing methods for the preparation of palynological samples. *Review of Palaeobotany and Palynology* 149, 133-149.

Lin, H.-L., Peterson, L.C., Overpeck, J.T., Trumbore, S.E. and Murray, D.W. 1997. Late Quaternary climate change from $\delta^{18}O$ records of multiple species of planktonic foraminifera: high-resolution records from the anoxic Cariaco Basin, Venezuela. *Paleoceanography* 12, 415-427.

Litwin, R.J. and Traverse, A. 1989. Basic guidelines for palynomorph extraction and preparation from sedimentary rocks. In: Feldman, R.M., Chapman, R.E. and Hannibal, J.T. (Eds.), *Paleo-techniques*. Paleontological Society, Special Publication 4, pp. 87–98.

LoDico, J.M., Flower, B.P. and Quinn, T.M. 2006. Subcentennial-scale climatic and hydrologic variability in the Gulf of Mexico during the early Holocene. *Paleoceanography* 21, PA3015, doi:10.1029/2005PA001243.

Lototskaya, A. 1999. Mid–latitude North Atlantic climate between 150000 and 100000 years BP, Academisch proefschrift, Vrije Universiteit Amsterdam, 171 pp.

Louwye, S., Head, M.J. and De Schepper, S. 2004. Palaeoenvironment and dinoflagellate cyst stratigraphy of the Pliocene in northern Belgium at the southern margin of the North Sea Basin. *Geological Magazine* 141(3), 353-378.

Luterbacher, J. and Xoplaki, E. 2003. 500-year winter temperature and precipitation variability over the Mediterranean area and its connection to the large-scale atmospheric circulation. In: Bolle, H.-J. (Ed.), *Mediterranean Climate - Variability and Trends*. Springer-Verlag, Berlin, pp. 133-153.

Lynn, M.J. 1998. A high–resolution comparison of Late Quaternary upwelling records from the Cariaco Basin and Arabian Sea: coccolith paleoecology and paleoclimatic investigations. Ph.D. thesis, University of Miami, Florida.

Lyons, T.W., Werne, J.P., Hollander, D.J. and Murray, R.W. 2003. Contrasting sulfur geochemistry and Fe/Al and Mo/Al ratios across the last oxic-to-anoxic transition in the Cariaco Basin, Venezuela. *Chemical Geology* 195, 131-157.

MacRae, R.A., Fensome, R.A. and Williams, G.L. 1996. Fossil dinoflagellate diversity, originations, and extinctions and their significance. *Canadian Journal of Botany* 74, 1687– 1694.

Maher, L.J. Jr. 1981. Statistics for microfossil concentration measurements employing samples spiked with marker grains. *Review of Palaeobotany and Palynology* 32, 153–191.

Malin, G. and Steinke, M. 2004. Dimethyl sulphide production: what is the contribution of the coccolithophores? In: Thierstein, H.R. and Young, J.R. (Eds.), *Coccolithophores – from molecular processes to global impact.* Springer–Verlag, Heidelberg, pp. 127–164.

Manabe, S. and Stouffer, R.J., 1995. Simulation of abrupt climate change induced by freshwater input to the North Atlantic Ocean. *Nature* 378, 165-167.

Marceau, L. 1969. Effets, sur le pollen, des ultrasons de basse frequence. *Pollen et Spores* 11, 147–164.

Marret, F. 1993. Les effets de l'acétolyse sur les assemblages de kystes de dinoflagellés. *Palynosciences* 2, 267–272.

Marret, F. 1994. Distribution of dinoflagellate cysts in recent marine sediments from the east Equatorial Atlantic (Gulf of Guinea). *Review of Palaeobotany and Palynology* 84, 1-22.

Marret, F. and Scourse, J. 2002. Control of modern dinoflagellate cyst distribution in the Irish and Celtic seas by seasonal stratification dynamics. *Marine Micropaleontology* 47, 101–116.

Marret, F. and Turon, J.-L. 1994. Paleohydrology and paleoclimatology off Northwest Africa during the last glacial-interglacial transition and the Holocene: Palynological evidences. *Marine Geology* 118, 107-117.

Marret, F. and Zonneveld, K.A.F. 2003. Atlas of modern organic-walled dinoflagellate cyst distribution. *Review of Palaebotany and Palynology* 125, 1-200.

Marret, F., Leroy, S. A. G., Chalié, F. and Gasse, F. 2004. New organic-walled dinoflagellate cysts from recent sediments of Central Asian seas. *Review of Palaeobotany and Palynology* 129, 1-20.

Marret, F., Mudie, P., Aksu, A. and Hiscott, R.N. 2007. A Holocene dinocyst record of a two-step transformation of the Neoeuxinian brackish water lake into the Black Sea. *Quaternary International* 193, doi:10.1016/j.quaint.2007.01.010.

Marshall, H.G. 1973. Phytoplankton observations in the Eastern Caribbean Sea. *Hydrobiologia* 41, 45-55.

Martinez, N.C., Murray, R.W., Thunell, R.C., Peterson, L.C., Muller-Karger, F., Astor, Y. and Varela, R. 2007. Modern climate forcing of terrigenous deposition in the tropics (Cariaco Basin, Venezuela). *Earth and Planetary Science Letters* 264, 438-451.

Mashiotta, T.A., Lea, D.W. And Spero, H.J. 1999. Glacial-interglacial changes in Subantarctic sea surface temperature and δ^{18}O-water using foraminiferal Mg. *Earth and Planetary Science Letters* 170, 417-432.

Maslin, M.A. and Burns, S.J. 2000. Reconstruction of the Amazon Basin effective moisture availability over the past 14,000 years. *Science* 290, 2285-2287.

Matsuyama, Y., Nagai, S., Kotani, Y. and Itakura, S. 2003. Effects of water temperature on the growth of fossil-cyst producing dinoflagellates *Lingulodinium polyedrum* and *Gonyaulax* cf. *digitalis* isolated from Shioya Bay, a small inlet of Okinawa Island Japan. In: *Abstracts of the 7th International Conference on Modern and Fossil Dinoflagellates, Yataro, Nagasaki, Japan*, pp. 80.

Matthews, J. 1969. The assessment of a method for the determination of absolute pollen frequencies. *New Phytologist* 68, 161–166.

Matthiessen, J. and Brenner, W. 1996. Chlorococcalalgen und Dinoflagellaten-Zysten in rezenten Sedimenten des Greifswalder Boddens (südliche Ostsee). *Senckenbergiana Maritima* 27 (1/2), 33-48.

McCarthy, F.M.G. 1992. Quaternary climate change and the evolution of the mid-latitude western North Atlantic Ocean: palynological, foraminiferal, sedimentological, and stable isotope evidence from DSDP sites 604, 607 and 612, unpublished Ph.D. thesis. Department of Geology, Dalhousie University, Halifax, 270 p.

McClymont, E.L., Martínez-Garcia, A. and Rosell-Melé, A. 2007. Benefits of freeze-drying sediments for the analysis of total chlorins and alkenone concentrations in marine sediments. *Organic Geochemistry* 38 (6), 1002-1007, doi:10.1016/j.orggeochem.2007.01.006.

McConnell, M.C. 2008. Tropical climate variability in the Cariaco Basin, Venezuela during Marine Isotope Stage 3: a multi-proxy approach. Unpublished Ph.D. thesis. University of South Carolina, 165 p.

McConnell, M. C. and Thunell, R.C. 2005. Calibration of the planktonic foraminiferal Mg/Ca paleothermometer: Sediment trap results from the Guaymas Basin, Gulf of California. *Paleoceanography* 20, PA2016, doi:10.1029/2004PA001077.

McMinn, A. 1990. Recent dinoflagellate cyst distribution in eastern Australia. *Review of Palaeobotany and Palynology* 65, 305-310.

McMinn, A. 1991. Recent dinoflagellate cysts from estuaries on the central coast of New South Wales, Australia. *Micropaleontology* 37, 269-287.

Medlin, L.K., Barker, G.L.A., Campbell, L., Green, J.C., Hayes, P.K., Marie, D., Wrieden, S. and Vaulot, D. 1996. Genetic characterisation of *Emiliania huxleyi* (Haptophyta). *Journal of Marine Systems* 9, 13–31.

Mertens, K.N., Lynn, M., Aycard, M., Lin, H.-L. and Louwye, S. 2009c. Coccolithophores as paleoecological indicators for shift of the ITCZ in the Cariaco Basin. *Journal of Quaternary Science* 24, 159-174.

Mertens, K.N., González, C., Delusina, I. and Louwye, S. 2009a. 30000 years of productivity, temperature and salinity variations in the late Quaternary Cariaco Basin revealed by dinoflagellate cysts. *Boreas*.

Mertens, K.N., Foubert, A., Vanneste, H., Wienberg, C., Stuut, J.-B., W., Baas, M., Sinninghe Damsté, J.S., Hebbeln, D. and Louwye, S., in preparation. Tracking 40000 years of the North Atlantic Oscillation during the late Quaternary in the southern Gulf of Cádiz using coccoliths, biomarkers and sedimentological proxies.

Mertens, K. , Ribeiro, S., Bouimetarhan, I., Caner, H., Combourieu-Nebout, N., Dale, B., de Vernal, A., Ellegaard, M., Filipova, M., Godhe, A., Grøsfjeld, K., Holzwarth, U., Kotthoff, U., Leroy, S., Londeix, L., Marret, F., Matsuoka, K., Mudie, P., Naudts, L., Peña-manjarrez, J., Persson, A., Popescu, S., Sangiorgi, F., van der Meer, M., Vink, A., Zonneveld, K., Vercauteren, D., Vlassenbroeck, J. and Louwye, S. 2009b. Process length variation in cysts of a dinoflagellate, *Lingulodinium machaerophorum*, in surface sediments investigating its potential as salinity proxy. *Marine Micropaleontology* 70 (1-2), 54-69.

Mittelstaedt, E. 1991. The ocean boundary along the northwest African coast: Circulation and oceanographic properties at the sea surface. *Progress in Oceanography* 26, 307-355.

Moldowan, J.M. and Talyzina, N.M. 1998. Biogeochemical evidence for dinoflagellate ancestors in the Early Cambrian. *Science* 281, 5380, 1168-1170.

Mollenhauer, G., Eglinton, T.I., Hopmans, E.C. and Sinninghe Damsté, J.S. 2008. A radiocarbon-based assessment of the preservation characteristics of crenarchaeol and alkenones from continental margin sediments. *Organic Geochemistry* 39, 1039-1045.

Mollenhauer, G., McManus, J.F., Benthien, A., Müller, P.J. and Eglinton, T.I. 2006. Rapid lateral particle transport in the Argentine Basin: molecular ^{14}C and $^{230}Thxs$ evidence. *Deep-Sea Research I* 53, 1224-1243.

Mollenhauer, G., Kienast, M., Lamy, F., Meggers, H., Schneider, R.R., Hayes, J.M. and Eglinton, T.I. 2005. An evaluation of ^{14}C age relationships between co-occurring foraminifera, alkenones, and total organic carbon in continental margin sediments. *Paleoceanography* 20, PA1016, doi:10.1029/2004PA001103.

Moreno, A., Cacho, I., Canals, M., Grimalt, J.O. and Sanchez-Vidal, A. 2004. Millennial-scale variability in the productivity signal from the Alborán Sea record, Western Mediterranean Sea. *Palaeogeography, Palaeclimatology, Palaeoecology* 211, 205-219.

Moreno, A., Cacho, I., Canals, M., Grimalt, J.O., Sánchez-Goñi, M.F., Shackleton, N. and Sierro, F.J. 2005. Links between marine and atmospheric processes oscillating on a millennial time-scale. A multi-proxy study of the last 50,000 years from the Alborán Sea (Western Mediterranean Sea). *Quaternary Science Reviews* 24, 1623-1636.

Moreno, A., Cacho, I., Canals, M., Prins, M.A., Sanchez-Goni, M.-F., Grimalt, J.O. and Weltje, G.J. 2002. Saharan dust transport and high-latitude glacial climatic variability: the Alborán Sea record. *Quaternary Research* 58, 318–328.

Morse, J.W. and Arvidson, R.S. 2002. The dissolution kinetics of major sedimentary carbonate minerals. *Earth Science Reviews* 58, 51-84.

Morzadec-Kerfourn, M.T. 1977. Les kystes de dinoflagelleés dans les sédiments le long des cotes bretonnes. *Revue de Micropaléontologie* 20, 157–166.

Mudie, P.J., Aksu, A.E. and Yasar, D. 2001. Late Quaternary dinoflagellate cysts from the Black, Marmara and Aegean seas: variations in assemblages, morphology and paleosalinity. *Marine Micropaleontology* 43, 155-178.

Mudie, P.J., Rochon, A.E. and Levac, E. 2002. Palynological records of red tide-producing species in Canada: past trends and implications for the future. *Palaeogeography, Palaeoclimatology, Palaeoecology* 180(1), 159-186.

Mudie, P.J., Marret, F., Aksu, A.E., Hiscott, R.N. and Gillespie, H. 2007. Palynological evidence for climatic change, anthropogenic activity and outflow of Black Sea water during the Late Pleistocene and Holocene: Centennial- to decadal-scale records from the Black and Marmara Seas. *Quaternary International* 167-168, 73-90.

Mulitza, S., Prange, M., Stuut, J.-B., Zabel, M., von Dobeneck, T., Itambi, A.C., Nizou, J. and Schulz, M. 2008. Sahel megadroughts triggered by glacial slowdown of Atlantic meridional overturning. *Paleoceanography* 23, PA4206, doi:10.1029/2008PA001637.

Müller, P., Kirst, G., Ruhland, G., von Storch, I. and Rosell-Melé, A. 1998. Calibration of the alkenone paleotemperature index $U^{K'}_{37}$ based on core-tops from the eastern South Atlantic and the global ocean (60°N–60°S). *Geochimica Cosmochimica Acta* 62, 1757– 1772.

Muller–Karger, F. and Aparicio–Castro, R. 1994. Mesoscale processes affecting phytoplankton abundances in the southern Carribean Sea. *Continental Shelf Research* 14, 199–221.

Muller–Karger, F., McClain C.R., Fisher, T.R., Esaias, W.E. and Varela, R. 1989. Pigment distribution in the Caribbean Sea: observations from space. *Progress in Oceanography* 23, 23–64.

Muller–Karger, F.E., Varela, R., Thunell, R., Astor, Y., Zhang, H. and Hu, C. 2004. Processes of Coastal Upwelling and Carbon Flux in the Cariaco Basin. *Deep–Sea Research II* 51, 927–943.

Muller–Karger, F.E., Varela, R., Thunell, R., Luerssen, R., Hu, C. and Walsh, J.J. 2005. The importance of continental margins in the global carbon cycle. *Geophysical research letters* 32, L01602, doi:10.1029/2004GL021346.

Muscheler, R., Kromer, B., Björck, S., Svensson, A., Friedrich, M., Kaiser, K.F. and Southon, J. 2008. Tree rings and ice cores reveal 14C calibration uncertainties during the Younger Dryas. *Nature Geoscience* 1, 263-267.

Narciso, A., Cachao, M. and de Abreu, L. 2006. *Coccolithus pelagicus* subsp. *pelagicus* versus *Coccolithus pelagicus* subsp. *braarudii* (Coccolithophore, Haptophyta): proxy for surface subarctic Atlantic waters off Iberia during the last 200 kyr. *Marine Micropaleontology* 59, 15-34.

Nehring, S. 1994. Spatial distribution of dinoflagellate resting cysts in recent sediments of Kiel Bight, Germany (Baltic Sea). *Ophelia* 39 (2), 137-158.

Nehring, S. 1997. Dinoflagellate resting cysts from recent German coastal sediments. *Botanica Marina* 40, 307-324.

Novichkova, E.A. and Polyakova, E.I. 2007. Dinoflagellate cysts in the surface sediments of the White Sea. *Oceanology* 47 (5), 660-670.

Nürnberg, D. and Groeneveld, J. 2006. Pleistocene variability of the Subtropical Convergence at East Tasman Plateau: Evidence from planktonic foraminiferal Mg/Ca (ODP Site 1172A). *Geochemistry Geophysics Geosystems* 7 (4), Q04P11, doi:10.1029/2005GC000984.

Nürnberg, D., Bijma, J. and Hemleben, C.1996. Assessing the reliability of magnesium in foraminiferal calcite as a proxy for water mass temperatures. *Geochimica et Cosmochimica Acta,* 60 (5), 803–814.

Nyberg, J., Malmgren, B.A., Kuijpers, A. and Winter, A. 2002. A centennial–scale variability of tropical North Atlantic surface hydrography during the late Holocene. *Palaeogeography, Palaeoclimatology, Palaeoecology* 183, 25–41.

Ogden, J.G., III, 1986. An alternative to exotic spore or pollen addition in quantitative microfossil studies. *Canadian Journal of Earth Sciences* 23, 102–106.

Okada, H. 1983. Modern nannofossil assemblages in sediments of coastal and marginal seas along the western Pacific Ocean. *Utrecht Micropaleontological Bullitins* 30, 171–187.

Okada, H. 2000. An improved filtering technique for calculation of calcareous nannofossil accumulation rate. *Journal of nannoplankton research* 22, 203–204.

Okada, H. and Matsuoka, M. 1996. Lower–photic nannoflora as an indicator of the late Quaternary monsoonal paleo–record in the tropical Indian Ocean. In Whatley, R. and Moguilevsky, A. (Eds.), *Microfossils and Oceanic Environments, Proceedings of the "ODP and Marine Biosphere International Conference, Aberystwyth, April 1994".* University of Wales, Aberystwyth, pp. 231–245.

Okolodkov, Y.B. 2005. The global distributional patterns of toxic, bloom dinoflagellates recorded from the Eurasian Arctic. *Harmful Algae* 4, 351-369.

Pahnke, K., Goldstein, S.L. and Hemming, S.R. 2008. Abrupt changes in Antarctic Intermediate Water circulation over the past 25,000 years. *Nature Geoscience* 1, 871-874, doi:10.1038/ngeo360.

Paillard, D., Labeyrie, L. and Yiou, P. 1996. Macintosh program performs time-series analysis, *Eos transactions AGU* 77, 379.

Parente, A., Cachao, M., Baumann, K.-H., de Abreu, L. and Ferreira, J. 2004. Morphometry of *Coccolithus pelagicus* s.l. (Coccolithophore, Haptophyta) from offshore Portugal, during the last 200 kyr. *Micropaleontology* 50 (1), 107-120.

Pelegrí, J.L., Arístegui, J., Cana, M., González-Dávila, A., Hernández-Guerra, Hernández-León, S., Marrero-Díaz, A., Montero, M.F., Sangá, P. and Santana-Casiano, M. 2004. Coupling between the open ocean and the coastal upwelling region off northwest Africa: water recirculation and offshore pumping of organic matter. *Journal of Marine Systems* 54, 3-37.

Peña-Manjarrez, J.L., Helenes, J., Gaxiola-Castro, G. And Orellano-Cepeda, E. 2005. Dinoflagellate cysts and bloom events at Todos Santos Bay, Baja California, México, 1999-2000. *Continental Shelf Research* 25, 1375-1393.

Perch-Nielsen, K. 1985. Cenozoic calcareous nannofossils. Mesozoic calcareous nannofossils. In: Bolli, H.M., Saunders, J.B. and Perch-Nielsen, K. (Eds.). *Plankton Stratigraphy*, Cambridge University Press, Cambridge, pp. 329-554.

Persson, A. and Rosenberg, R. 2003. Impact of grazing and bioturbation of marine benthic deposit feeders on dinoflagellate cysts. *Harmful algae* 2, 43-50.

Persson, A., Godhe, A. and Karlson, B. 2000. Dinoflagellate cysts in recent sediments from the West Coast of Sweden. *Botanica Marina* 43, 69-79.

Peterson, L.C. and Haug, G.H. 2006. Variability in the mean latitude of the Atlantic Intertropical Convergence Zone as recorded by riverine input of sediments to the Cariaco Basin (Venezuela). *Palaeogeography, Palaeoclimatology, Palaeoecology* 234, 97-113.

Peterson L.C., Haug, G.H., Hughen, K.A. and Röhl, U. 2000a. Rapid changes in the hydrologic cycle of the tropical Atlantic during the last glacial. *Science* 290, 1947–1951.

Peterson, L.C., Overpeck, J.T., Kipp, N.G. and Imbrie, J. 1991. A high–resolution late Quaternary upwelling record from the anoxic Cariaco Basin, Venezuela. *Paleoceanography 6*, 99–119.

Peterson, L.C., Haug, G.H., Murray, R.W., Yarincik, K.M., King, J.W., Bralower, T.J., Kameo, K., Rutherford, S.D. and Pearce, R.B. 2000b. Late Quaternary stratigraphy and sedimentation at site 1002, Cariaco Basin (Venezuela). In: Leckie, R.M., Sigurdsson, H., Acton, G.D. and Draper, G. (Eds.), *Proceedings of the Ocean Drilling Program, Scientific results 165.* College station, Texas (Ocean Drilling Program), pp. 85–99.

Piper, D. and Dean, W.E. 2002. Trace-element deposition in the Cariaco Basin under sulfate reducing conditions—a history of the local hydrography and global climate, 20 ka to the present. *US Geological Survey Professional Paper* 1670, 41 pp.

Pospelova, V., de Vernal, A. and Pedersen, T.F. 2008. Distribution of dinoflagellate cysts in surface sediments from the northeastern Pacific Ocean (43-25°N) in relation to sea-surface temperature, productivity and coastal upwelling, *Marine Micropaleontology* 68 (1-2), 21-48.

Pospelova, V., Pedersen, T.F. and de Vernal, A. 2006. Dinoflagellate cysts as indicators of climatic and oceanographic changes during the past 40 kyr in the Santa Barbara Basin, southern California. *Paleoceanography* 21, PA2010, doi: 10.1029/2005PA001251.

Poulsen, N.E., Gudmundsson, L., Hansen, J. M. and Husfeldt, Y. 1990. Palynological preparation techniques, a new maceration tank-method and other modifications. *Geological Survey of Denmark, Series C* 10, 24 pp.

Prahl, F. G., and Wakeham, S.G. 1987. Calibration of unsaturation patterns in long-chain ketone compositions for paleotemperature assessment. *Nature* 330, 367–369.

Prins, M.A. and Weltje, G.J. 1999. End-member modelling of siliciclastic grain-size distributions: the Late Quaternary record of eolian and fluvial sediment supply to the Arabian Sea and its paleoclimatic significance. In: Harbaugh, J.W., Watney, W.L., Rankey, E.C., Slingerland, R., Goldstein, R.H. and Franseen, E.K. (Eds.), *Numerical Experiments in Stratigraphy: Recent Advances in Stratigraphic and Sedimentologic Computer Simulations. SEPM Special Publication 62.* Society for Sedimentary Geology, pp. 91-111.

Prins, M.A., Postma, G., Cleveringa, J., Cramp, A. and Kenyon, N.H. 2000. Controls on terrigenous sediment supply to the Arabian Sea during the late Quaternary: the Indus Fan. *Marine Geology* 169, 327-349.

Prins, M.A., Bouwer, L.M., Beets, C.J., Troelstra, S.R., Weltje, G.J., Kruk, R.W., Kuijpers, A. and Vroon, P.Z. 2002. Ocean circulation and iceberg discharge in the glacial North Atlantic: inferences from unmixing of sediment size distribution. *Geology* 30, 555–558.

Radi, T. and de Vernal, A. 2004. Dinocyst distribution in surface sediments from the northeastern Pacific margin (40-60°N) in relation to hydrographic conditions, productivity and upwelling. *Review of Palaeobotany and Palynology* 128, 169-193.

Radi, T., Pospelova, V., de Vernal, A. and Vaughn, B.J. 2007. Dinoflagellate cysts as indicators of water quality and productivity in British Columbia estuarine environments. *Marine Micropaleontology* 62, 269-297.

Rahmsdorf, S., 1994. Rapid climate transitions in a coupled ocean–atmosphere model. *Nature* 372, 82–85.

Rahmsdorf, S. 2002. Ocean circulation and climate during the past 120,000 years. *Nature* 419, 207-214.

Ratmeyer, V., Balzer, W., Bergametti, G., Chiapello, I., Fischer, G. and Wyputta, U. 1999. Seasonal impact of mineral dust on deep-ocean particle flux in the eastern subtropical Atlantic Ocean. *Marine Geology* 159, 241-252.

Regenberg, M., Nürnberg, D., Steph, S., Groeneveld, J., Garbe-Schönberg, D., Tiedemann, R. and Dullo, W.-C. 2006. Assessing the effect of dissolution on planktonic foraminiferal Mg/Ca ratios: Evidence from Caribbean core tops. *Geochemistry Geophysics Geosystems* 7 (7), Q07P15, doi:10.1029/2005GC001019.

Reichart, G.-J. and Brinkhuis, H. 2003. Late Quaternary *Protoperidinium* cysts as indicators of paleoproductivity in the northern Arabian Sea. *Marine Micropaleontology* 49, 303-315.

Reid, P.C. 1972. The distribution of dinoflagellate cysts, pollen and spores in recent marine sediments from the coast of the British Isles. Ph.D. thesis, University of Sheffield.

Reid, P.C. 1974. Gonyaulacean dinoflagellate cysts from the British Isles. *Nova Hedwigia* 25, 579-637.

Reid, P.C. 1977. Peridiniacean and glenodinicacean dinoflagellate cysts from the British Isles. *Nova Hedwigia* 29, 429–463.

Richards, F.A. 1975. The Cariaco Basin (Trench). *Oceanography and Marine Biology Annual Reviews* 13, 11–67.

Richter, D., Vink, A., Zonneveld, K.A.F., Kuhlmann, H. and Willems, H. 2007. Calcareous dinoflagellate cyst distributions in surface sediments from upwelling areas off NW Africa, and their relationships with environmental parameters of the upper water column. *Marine Micropaleontology* 63, 201-228.

Riding, J.B. and Kyffin-Hughes, J.E. 2004. A review of the laboratory preparation of palynomorphs with a description of an effective non-acid technique. *Revista Brasileira de Paleontologia* 7 (1), 13–44.

Riding, J.B., Kyffin-Hughes, J.E. and Owens, B. 2007. An effective palynological preparation procedure using hydrogen peroxide. *Palynology* 31, 19–36.

Robert, C., Degiovanni, C., Jaubert, R., Leroy, V., Reyss, J.L., Saliège, J.F., Thouveny, N. and de Vernal, A. 2006. Variability of sedimentation and environment in the Berre coastal lagoon (SE France) since the first millennium: Natural and anthropogenic forcings. *Journal of Geochemical Exploration* 88, 440-444.

Rochon, A., de Vernal, A., Turon, J.-L., Matthiessen, J. and Head, M. J. 1999. Distribution of recent dinoflagellate cysts in surface sediments from the North Atlantic Ocean and adjacent seas in relation to sea-surface parameters. *American Association of Stratigraphic Palynologists Foundation Contributions Series* 35, 1-152.

Rogalla, U. and Andruleit, H. 2005. Precessional forcing of coccolithophore assemblages in the northern Arabian Sea: implications for monsoonal dynamics during the last 200,000 years. *Marine Geology* 217, 31-48.

Rogerson, M., Rohling, E.J., Weaver, P.P.E. and Murray, J.W. 2004. The Azores Front since the Last Glacial Maximum. *Earth and Planetary Science Letters* 222, 779-789.

Rogerson, M., Rohling, E.J., Weaver, P.P.E. and Murray, J.W. 2005. Glacial to interglacial changes in the settling depth of the Mediterranean Outflow plume. *Paleoceanography* 20, PA3007, doi:10.1029/2004PA001106.

Rogerson, M., Weaver, P.P.E., Rohling, E.J., Lourens, L.J., Murray, J.W. and Hayes, A. 2006. Colour logging as a tool in high-resolution palaeoceanography. In: Rothwell, R.G. (Ed.), *New techniques in sediment core analysis, Geological Society Special Publication 267. Geological Society, London,* pp. 99-112.

Röhl, U. and Abrams, L.J. 2000. High-resolution, downhole, and nondestructive core measurements from Sites 999 and 1001 in the Caribbean Sea: application to the Late Paleocene Thermal Maximum. In: Leckie, R.M., Sigurdsson, H., Acton, G.D., and Draper, G. (Eds.), *Proceedings of the Ocean Drilling Program, Scientific Results 165*. College Station, Texas (Ocean Drilling Program), pp. 191–203.

Romano, G., Russo, G.L., Buttino, I., Ianora, A. and Miralto, A. 2003. A marine diatom-derived aldehyde induces apoptosis in copepod and sea urchin embryos. *The Journal of Experimental Biology* 206, 3487-3494.

Rontani, J.-F., Zabeti, N. and Wakeham, S.G. 2008. The fate of marine lipids: biotic vs. abiotic degradation of particulate sterols and alkenones in the Northwestern Mediterranean Sea. *Marine Chemistry*, doi:10.1016/j.marchem.2008.11.001.

Rosell-Melé A., Bard, E., Emeis, K.C., Grimalt, J., Muller, P., Schneider, R., Bouloubassi, I., Epstein, B., Fahl, K., Fluegge, A., Freeman, K., Goñi, M., Guntner, U., Hartz, D., Hellebust, S., Herbert, T., Ikehara, M., Ishiwatari, R., Kawamura, K., Kenig, F., de Leeuw, J., Lehman, S., Ohkouchi, N., Pancost, R.D., Prahl, F., Quinn, J., Rontani, J.F., Rostek, F.,Rullkotter, J., Sachs, J., Sanders, D., Sawada, K., Schultz-Bull, D., Sikes, E., Ternois, Y., Versteegh, G., Volkman, J. and Wakeham, S. 2001. Precision of the current methods to measure alkenone proxy $U^{K'}_{37}$ and absolute alkenone abundance in sediments: results of an inter-laboratory comparison study. *Geochemistry, Geophysics, Geosystems* 2, 2000GC00141, 1–28.

Rost, B. and Riebesell, U. 2004. Coccolithophores and the biological pump: responses to environmental changes. In: Thierstein, H.R. and Young, J.R. (Eds.), *Coccolithophores – From Molecular Processes to Global Impact*. Springer–Verlag, Heidelberg, 76–99.

Rostek F., Ruhland G., Bassinot F.C., Muller P.J., Labeyrie L.D., Lancelot Y. and Bard E. 1993. Reconstructing sea-surface temperature and salinity using $\delta^{18}O$ and alkenone records. *Nature* 364, 319-321.

Roth, P. 1983. Jurassic and Lower Cretaceous calcareous nannofossils in the western North Atlantic (Site 534): biostratigraphy, preservation, and some observations on biogeography and palaeoceanography. *Initial reports of the DSDP* 76, 587-621.

Roth, P.H. and Berger, W.H. 1975. Distribution and dissolution of coccoliths in the south and central Pacific. In: Sliter, W.V., Bé, A.W.H. and Berger, W.H. (Eds.), *Dissolution of Deep–Sea Carbonates*. *Cushman Foundation for Foraminiferal Research, Special Publication 13.* Lawrence, Kansas, pp. 87–113.

Roth, P.H. and Coulbourn, W.T. 1982. Floral and solution patterns of coccoliths in surface sediments of the North Pacific. *Marine Micropaleontology* 7, 1–52.

Ruiz, J. and Navarro, G. 2006. Upwelling spots and vertical velocities in the Gulf of Cádiz: an approach for their diagnose by combining temperature and ocean colour remote sensing. *Deep-Sea Research Part II* 53 (11-13), 1282-1293.

Rull, V. 2007. Holocene global warming and the origin of the Neotropical gran Sabana in the Venezuelan Guayana. *Journal of Biogeography 34*, 279-288.

Russell, A. D., Hönisch, B., Spero, H.J. and Lea, D.W. 2004. Effects of seawater carbonate ion concentration and temperature on shell U, Mg, and Sr in cultured planktonic Foraminifera. *Geochimica et Cosmochimica Acta* 68 (21), 4347 –4361.

Sáez, A.G., Probert, I., Geisen, M., Quinn, P., Young, J.R. and Medlin, L.K. 2003. Pseudo-cryptic speciation in coccolithophores. *Proceedings of the National Academy of Sciences* 100, 7163–7168.

Salgado-Labouriau, M. L. 1980. A pollen diagram of the Pleistocene-Holocene boundary of lake Valencia, Venezuela. *Review of Paleobotany and Palynology 30*, 297-312.

Salter, J., Murray, B.G. and Braggins, J.E. 2002. Wettable and unsinkable: the hydrodynamics of saccate pollen grains in relation to the pollination mechanism in the two New Zealand species of *Prumnopitys* Phil. (Podocarpaceae). *Annals of Botany* 89, 133–144.

Sánchez-Goni, M.F., Cacho, I., Turon, J.L., Guiot, J., Sierro, F.J., Peypouquet, J.P., Grimalt, J.O. and Shackleton, N.J. 2002. Synchroneity between marine and terrestrial responses to millennial scale climatic variability during the last glacial period in the Mediterranean region. *Climate dynamics* 19, 95-105.

Sangiorgi, F., Fabbri, D., Comandini, M., Gabbianelli, G. and Tagliavini, E. 2005. The distribution of sterols and organic-walled dinoflagellate cysts in surface sediments of the North-western Adriatic Sea (Italy). *Estuarine, Coastal and Shelf Science* 64, 395-406.

Sarnthein, M., Tetzla, G., Koopmann, B., Wolter, K. and Pflaumann, U. 1981. Glacial and interglacial wind regimes over the eastern subtropical Atlantic and North-West Africa. *Nature* 293, 193-196.

Sarnthein, M., Thiede, J., Pflaumann, U., Erlenkeuser, H., Fütterer, D., Koopmann, B., Lange, H. and Seibold, E. 1982. Atmospheric and oceanic circulation patterns off northwest Africa during the past 25 million years. In: von Rad, U., Hinz, K., Sarnthein, M. and Seibold, E. (Eds.), *Geology of the Northwest African Continental Margin.* Springer, Berlin, pp. 545–604.

Sarnthein, M., Winn, K., Jung, S.J.A., Duplessy, J.-C., Labeyrie, L., Erlenkeuser, H. and Ganssen, G. 1994. Changes in east Atlantic deepwater circulation over the last 30,000 years: eight time slice reconstructions. *Paleoceanography* 9, 209-267.

Schmidt, G.A., Bigg, G.R. and Rohling, E.J. 1999. Global Seawater Oxygen-18 Database. http://data.giss.nasa.gov/o18data/.

Schmidt, M.W., Spero, H.J. and Lea, D.W. 2004. Links between salinity variation in the Caribbean and North Atlantic thermohaline circulation. *Nature* 428, 160–163.

Schoell, M. 1974. Valdivia VA 01/03, Hydrographie II und III. Bundesanstalt für Bodenforschung, Hannover, Germany.

Schönfeld, J. 2002. A new benthic foraminiferal proxy for near-bottom current velocities in the Gulf of Cádiz, northeastern Atlantic Ocean. *Deep-Sea Research I* 49, 1853-1875.

Schouten, S., Hopmans, E.C. and Sinninghe Damsté, J.S. 2004. The effect of maturity and depositional redox conditions on archaeal tetraether lipid palaeothermometry. *Organic Geochemistry* 35, 567– 571.

Schouten, S., Hopmans, E.C., Pancost, R.D. and Sinninghe Damsté, J.S. 2000. Widespread occurrence of structurally diverse tetraether membrane lipids: Evidence for the ubiquitous presence of low-temperature relatives of hyperthermophiles. *Proceedings of the National Academy of Science* 97, 14421-14426.

Schouten, S., Hopmans, E.C., Schefuβ, E. and Sinninghe Damsté, J.S. 2002. Distributional variations in marine crenarchaeotal membrane lipids: a new tool for reconstructing ancient sea water temperatures? *Earth and Planetary Science Letters* 204, 265–274.

Schouten S., Huguet, C., Hopmans, E.C. and Sinninghe Damsté, J.S., 2007. Improved analytical methodology of the TEX_{86} paleothermometry by high performance liquid chromatography / atmospheric pressure chemical ionization-mass spectrometry. *Analytical Chemistry* 79, 2940-2944.

Schouten, S., Ossebaar, J., Schreiber, K., Kienhuis, M.V.M., Langer, G., Benthien, A. and Bijma, J. 2006. The effect of temperature, salinity and growth rate on the stable hydrogen isotopic composition of long chain alkenones produced by *Emiliania huxleyi* and *Gephyrocapsa oceanica. Biogeosciences* 3, 113-119.

Schrank, P. 1988. Effects of chemical processing on the preservation of peridinoid dinoflagellates: a case from the Late Cretaceous of NE Africa. *Review of Palaeobotany and Palynology* 56, 123–140.

Schubert, C. 1982. Origin of Cariaco Basin, southern Caribbean Sea. *Marine Geology* 47, 345–360.

Schulte, S. and Müller, P.J. 2001. Variations of sea surface temperature and primary productivity during Heinrich and Dansgaard-Oeschger events in the northeastern Arabian Sea. *Geo-Marine Letters* 21, 168-175.

Scranton, M.I., Astor, Y., Bohrer, R., Ho, T.-Y. and Muller-Karger, F. 2001. Controls on temporal variability of the geochemistry of the deep Cariaco Basin. Deep-Sea Research I 48, 1605-1625.

Sengupta, S. 1975. Experimental alterations of the spores of *Lycopodium clavatum* as related to diagenesis. *Review of Palaeobotany and Palynology* 19, 173–192.

Shackleton, N. J. 1974. Attainment of isotopic equilibrium between ocean water and the benthonic foraminifer genus *Uvigerina*: Isotopic changes in the ocean during the last glacial. In: Labeyrie, L. (Ed.), *Les Methodes Quantitative d'Etude des Variations du Climate au Cours du Pleistocene, Colloque International du Centre National de Recherche Scientifique* 219, pp. 203–210.

Shipboard Scientific Party, 1997. Site 1002. In: Sigurdsson, H., Leckie, R.M., Acton, G.D. and Draper, G. (Eds.), *Proceedings of the international Ocean Drilling Program, Initial Reports* 165. College Station, Texas (Ocean Drilling Program), pp. 359–373.

Sierro, F.J., Flores, J.A. and Baraza, J. 1999. Late glacial to recent paleoenvironmental changes in the Gulf of Cádiz and formation of sandy contourite layers. *Marine Geology* 155, 157-172.

Siesser, W.G., Bralower, T. and De Carlo, H. 1992. Mid-Tertiary *Braarudosphaera*-rich sediments on the Exmouth Plateau, In: von Rad, U., Haq, B. et al. (Eds.), *Proceedings of the Ocean Drilling Program, Scientific Results* 122. College station, Texas (Ocean Drilling Program), pp. 653-663.

Sikes, E.L. and Volkman, J.K. 1993. Calibration of alkenone unsaturation ratios $U^{k'}_{37}$ for paleotemperature estimation in cold polar waters. *Geochimica et Cosmochimica Acta* 57, 1883–1889.

Sirocko, F. 1991. Deep-sea sediments of the Arabian Sea: a paleoclimatic record of the Southwest-Asian monsoon, *Geologische Rundschau* 80, 557-566.

Smayda, T.J. 1966. A quantitative analysis of the phytoplankton of the Gulf of Panama. III. General ecological conditions, and the phytoplankton dynamics at 8,45°N, 79,23°W from November 1954 to May 1957. *Bulletin of Inter-American Tropical Tuna Commission* 11, 355–612.

Smayda, T.J. and Reynolds, C.S. 2001. Community assembly in marine phytoplankton: application of recent models to harmful dinoflagellate blooms. *Journal of Plankton Research* 23 (5), 447-461.

Smoak, J.M., Benitez-Nelson, C., Moore, W.S., Thunell, R.C., Astor, Y. and Muller-Karger F. 2004. Radionuclide fluxes and particle scavenging in Cariaco Basin. *Continental shelf research* 24, 1451–1463.

Sorrell, P., Popescu, S.-M., Head, M.J., Suc, J.-P., Klotz, S. and Oberhänsli, H. 2006. Hydrographic development of the Aral Sea during the last 2000 years based on a quantitative analysis of dinoflagellate cysts. *Palaeography, Palaeoclimatology, Palaeoecology* 234, 304-327.

Spilling, K., Kremp, A. and Tamelander, T. 2006. Vertical distribution and cyst production of *Peridiniella catenata* (Dinophyceae) during a spring bloom in the Baltic Sea. *Journal of Plankton Research* 28 (7), 659-665.

Stabell, B. and Henningsmoen, K.E. 1981. Capsules with *Lycopodium* spores for absolute diatom and pollen analysis. *Nordic Journal of Botany* 1 (5), 701–702.

Stanley, E.A. 1966. The problem of reworked pollen and spores in marine sediments. *Marine Geology* 4, 397–408.

Steinke, S., Kienast, M., Groeneveld, J., Lin, L.-C., Chen, M.-T. and Rendle-Bühring, R. 2008. Proxy dependence of the temporal pattern of deglacial warming in the tropical South China Sea: toward resolving seasonality. *Quaternary Science Reviews* 27, 688-700.

Steinmetz, J.C. 1991. Calcareous nannoplankton biocoenosis: sediment trap studies in the equatorial Atlantic, central pacific, and Panama Basin. In: Honjo, S (Ed.), *Ocean Biocoenosis Series No. 1.* Woods Hole Oceanographic Institution Press, Woods Hole, Massachusetts, pp. 1–85.

Stephens, C., Antonov, J.I., Boyer, T.P., Conkright, M.E., Locarnini, R.A., O'Brien, T.D. and Garcia, H.E. 2002. *World Ocean Atlas 2001, Volume 1: Temperature. In:* Levitus, S. (Ed.), *NOAA Atlas NESDIS 49.* U.S. Government Printing Office, Washington, D.C., 167 pp.

Stockmarr, J. 1971. Tablets with spores used in absolute pollen analysis. *Pollen et Spores* 13, 615–621.

Stoll, H.M., Arevalos, A., Burke, A., Ziveri, P., Mortyn, G., Shimizu, N. and Unger, D. 2007. Seasonal cycles in biogenic production and export in Northern Bay of Bengal sediment traps. *Deep Sea Research Part II* 54, 558-580.

Stover, L.E., Brinkhuis, H., Damassa, S.P., de Verteuil, L., Helby, R.J., Monteil, E., Partridge, A., Powell, A.J., Riding, J.B., Smelror, M. and Williams, G.L. 1996. Mesozoic–Tertiary dinoflagellates, acritarchs and prasinophytes. In: Jansonius, J., McGregor, D.C. (Eds.), *Palynology: Principles and Applications*. American Association of Stratigraphic Palynologists Foundation, Dallas, pp. 641–750.

Stuut, J.-B. and Lamy, F. 2004. Climate variability at the southern boundaries of the Namib (southwestern Africa) and Atacama (northern Chile) coastal deserts during the last 120,000 yr. *Quaternary Research* 62, 301-309.

Stuut, J.-B., Prins, M.A., Schneider, R.R., Weltje, G.J., Jansen, J.H.F. and Postma, G. 2002. A 300-kyr record of aridity and wind strength in southwestern Africa: inferences from grain-size distributions of sediments on Walvis Ridge, SE Atlantic. *Marine Geology* 180, 221-233.

Sullivan, J.M., Swift, E., Donaghay, P.L. and Rines, J.E.B. 2003. Small-scale turbulence affects the division rate and morphology of two red-tide dinoflagellates. *Harmful algae* 2, 183-199.

Summerhayes, C.P., Coutinho, P.N., Franca, A.M.C. and Ellis, J.P. 1975. Part III. Salvador to Foraleza Northeastern Brazil. In: Milliman, J.D. and Summerhayes, C.P. (Eds.), *Upper continental margin sedimentation off Brazil*. E. Schweizerbartsche Verlagsbuchhandlung, Stuttgart, pp. 45-77.

Sweeney, B.M. 1975. Red tides I have known. In: V.R. LoCicero (Ed.), *Toxic dinoflagellate blooms.* Massachusetts Science and Technology Foundation, Wakefield, Massachusetts, pp. 225-234.

Telford, R. 2006. Limitations of dinoflagellate cyst transfer functions. *Quaternary Science Reviews* 25, 1375-1382.

Thierstein, H.R. 1980. Selective dissolution of Late Cretaceous and earliest Tertiary calcareous nannofossils: experimental evidence. *Cretaceous Research* 2, 165–176.

Thomas, W.H. and Gibson, C.H. 1990. Quantified small-scale turbulence inhibits a red tide dinoflagellate, *Gonyaulax polyedra* Stein. *Deep-Sea Research* 37, 1538-1593.

Throndsen J. 1972. Coccolithophorids from the Caribbean Sea. *Norwegian Journal of Botany* 19, 51–60.

Thunell, R., Benitez-Nelson, C., Varela, R., Astor, Y. and Muller-Karger, F. 2007. Particulate organic carbon fluxes along upwelling-dominated continental margins: rates and mechanisms. *Global biogeochemical cycles* 21, GB1022, doi:1029/2006GB002793.

Thunell, R., Tappa, E., Pride, C. and Kincaid, E. 1999. Sea-surface temperature anomalies associated with the 1997-1998 El Niño recorded in the oxygen isotope composition of planktonic foraminifera. *Geology* 27, 843-846.

Thunell, R., Tappa, E., Varela, R., Llano, M., Astor, Y., Müller-Karger, F. and Bohrer, R. 1999. Increased marine sediment suspension fluxes following an earthquake. *Nature* 398, 233.

Tierney, J.E., Russell, J.M., Huang, Y., Sinninghe Damsté, J.S., Hopmans, E.C. and Cohen, A.S. 2008. Northern hemisphere controls on tropical southeast African climate during the past 60,000 years. *Science* 322, 252-255.

Tjallingii, R., Claussen, M., Stuut, J.-B., W., Fohlmeister, J., Jahn, A., Bickert, T., Lamy, F. and Röhl, U. 2008.Coherent high- and low latitude control of the northwest African hydrological balance. *Nature Geoscience* doi:10.1038/ngeo289.

Turon, J.-L. 1984. Le palynoplankton dans l'environment actuel de l'Atlantic nord-oriental. Evolution climatique et hydrologique depuis le dernier maximum glaciaire. *Mémoire de l'institut de Géologie du Bassin d'Aquitaine* 17, 1-313.

Turon, J.-L. and Londeix, L. 1988. Les assemblages de kystes de dinoflagellés en Méditerranée occidentale (Mer d'Alboran): mise en évidence de l'évolution des paléoenvironnements depuis le dernier maximum glaciaire. *Bulletin Centre Recherches Exploration-Production Elf-Aquitaine* 12, 313-344.

Tyrrell, T. 1999. The relative influence of nitrogen and phosphorus on oceanic primary production. *Nature* 400, 525-531.

Tyrrell, T. and Merico, A. 2004. *Emiliania huxleyi*: bloom observations and the conditions that induce them. In: Thierstein, H.R. and Young, J.R. (Eds.), *Coccolithophores - from molecular processes to global impact*. Springer-Verlag, Heidelberg, pp. 75-97.

Tyrrell T. and Taylor, A.H. 1995. Latitudinal and seasonal variations in carbon dioxide and oxygen in the northeast Atlantic, and the effects on *Emiliania huxleyi* and other phytoplankton. *Global Biogeochemical Cycles* 9, 585–604.

Uda I., Sugai A., Itoh Y.H. and Itoh T. 2001. Variation on molecular species of polar lipids from *Thermoplasma acidophilum* depends on growth temperature. *Lipids* 36, 103–105.

van der Meer, M.T.J., Sangiorgi, F., Baas, M., Brinkhuis, H., Sinninghe-Damsté, J.S. and Schouten, S. 2008. Molecular isotopic and dinoflagellate evidence for Late Holocene freshening of the Black Sea. *Earth and Planetary Science Letters* 267, 426-434.

van der Meer, M.T.J., Baas, M., Rijpstra, W.I.C., Marino, G., Rohling, E.J., Sinninghe Damsté, J.S. and Schouten, S. 2007. Hydrogen isotopic compositions of long-chain alkenones record freshwater flooding of the Eastern Mediterranean at the onset of sapropel deposition. *Earth and Planetary Science Letters* 262, 594-600.

van Harten, D. 2000. Variable noding in *Cyprideis torosa* (Ostracoda, Crustacea): an overview, experimental results and a model from Catastrophe Theory. *Hydrobiologia* 419 (1), 131-139.

Van Rensbergen, P., Depreiter, D., Pannemans, B. and Henriet, J.-P. 2005. Seafloor expression of sediment extrusion and intrusion at the El Arraiche mud volcano field, Gulf of Cádiz. *Journal of Geophysical Research* 110, F02010.

Vargas, J.M., García-Lafuente, J., Delgado, J. and Criado, F. 2003. Seasonal and wind-induced variability of Sea Surface Temperature patterns in the Gulf of Cádiz, *Journal of Marine Systems* 38, 205-219.

Varol, O. and Houghton, S.D. 1996. A review and classification of fossil didemnid ascidian spicules. *Journal of Micropaleontology* 15, 135-149.

Verleye, T., Mertens, K., N., Louwye, S. and Arz, H.W. 2009. Holocene Salinity changes in the southwestern Black Sea: a reconstruction based on dinoflagellate cysts. *Palynology* 32.

Versteegh, G.J.M. 1994. Recognition of cyclic and non-cyclic environmental changes in the Mediterranean Pliocene: a palynological approach. *Marine Micropaleontology* 23, 147–183.

Vidal L., Schneider, R., Marchal, O., Bickert, T., Stocker T.F. and Wefer, G. 1999. Link between the North and South Atlantic during the Heinrich events of the last glacial period. *Climate Dynamics* 15, 909–919.

Vink, A.C., Zonneveld, K.A.F. and Willems, H. 2000. Organic-walled dinoflagellate cysts in western equatorial Atlantic surface sediments: distributions and their relation to environment. *Review of Palaeobotany and Palynology* 112, 247-286.

Vink, A., Rühlemann, C., Zonneveld, K.A.F., Mulitza, S., Hüls, M. and Willems, H. 2001. Shifts in the position of the North Equatorial Current and rapid productivity changes in the western Tropical Atlantic during the last glacial. *Paleoceanography* 16 (1), 479–490.

Vink, A., Baumann, K.-H., Böckel, B., Esper, O., Kinkel, H., Volbers, A., Willems, H. and Zonneveld, K.A.F. 2003. Coccolithophorid and dinoflagellate synecology in the South and Equatorial Atlantic: improving the palaeoecological significance of phytoplanktonic microfossils. In: Wefer, G., Mulitza, S. and Ratmeyer, V. (Eds.), *The South Atlantic in the Late Quarternary: Reconstruction of Material Budget and Current Systems*. Springer-Verlag, Berlin, pp. 101-120.

Visbeck, M. 2002. The ocean's role in Atlantic climate variability. *Science* 297, 2223–2224.

Voelker, A. H. L. 2002. Global distribution of centennial-scale records for Marine Isotope Stage (MIS) 3: a database. *Quaternary Science Reviews* 21, 1185–1212.

Waelbroeck, C., Labeyrie, L., Michel, E., Duplessy, J.C., McManus, J.F., Lambeck, K., Balbon, E. and Labracherie, M. 2002. Sea-level and deep water temperature changes derived from benthic foraminifer isotopic records. *Quaternary Science Reviews* 21, 295–305.

Wakeham, S.G. and Ertel, J.R. 1988. Diagenesis of organic matter in suspended particles and sediments in the Cariaco Trench. Advances in organic geochemistry 1987. *Organic Geochemistry* 13, 815-822.

Wall, D. 1967. Fossil microplankton in deep-sea cores from the Caribbean sea. *Paleontology*, *10*, 95-123.

Wall, D. and Dale, B. 1968. Modern dinoflagellate cysts and the evolution of the Peridiniales. *Micropaleontology* 14, 265-304.

Wall, D., Dale, B. and Harada, K. 1973. Description of new fossil dinoflagellates from the Late Quaternary of the Black Sea. *Micropaleontology* 19, 18-31.

Wall, D., Dale, B., Lohman, G.P. and Smith, W.K. 1977. The environmental and climatic distribution of dinoflagellate cysts in modern marine sediments from regions in the North and South Atlantic Ocean and adjacent seas. *Marine Micropaleontology* 2, 121-200.

Wan, X., Chang, P., Saravanan, R. Zhang, R. and Schmidt, M.W. 2008. On the Interpretation of Caribbean Paleo-Temperature Reconstructions During the Younger Dryas. *Geophysical Research Letters*, doi:10.1029/2008GL035805.

Wang, L. 2000. Isotopic signals in two morphotypes of *Globigerinoides ruber* (white) from the South China Sea: implications for monsoon climate change during the last glacial cycle. *Palaeogeography, Palaeoclimatology, Palaeoecology* 161, 381-394.

Wang, L., Sarnthein, M., Duplessy, J.-C., Erlenkeuser, H., Jung, S. and Pflaumann, U. 1995. Paleo sea surface salinities in the low-latitude Atlantic: the $\delta^{18}O$ record of *Globigerinoides ruber* (white). *Paleoceanography* 10 (4), 749-761.

Warrick, J.A. and Fong, D.A. 2004. Dispersal scaling from the world's rivers. *Geophysical research letters* 31, L04301, doi:10.1029/2003GL019114.

Weaver P.P.E. and Pujol C. 1988. History of the last deglaciation in the Alborán Sea (western Mediterranean) and adjacent north Atlantic as revealed by coccolith floras. *Palaeogeography, Palaeoclimatology, Palaeoecology* 64, 35–42.

Weijers, J.W.H., Schouten, S., Spaargaren, O.C. and Sinninghe Damsté, J.S. 2006. Occurrence and distribution of tetraether membrane lipids in soils: implications for the use of the TEX_{86} proxy and the BIT index. *Organic Geochemistry* 37 (12), 1680-1693.

Weldeab, S., Schneider, R.R. and Müller, P. 2007. Comparison of Mg/Ca- and alkenone-based sea surface temperature estimates in the fresh water-influenced Gulf of Guinea, eastern equatorial Atlantic. *Geochemistry, Geophysics, Geosystems* 8 (5), Q05P22, doi:10.1029/2006GC001360.

Weltje, G.J. 1997. End-member modeling of compositional data: numerical-statistical algorithms for solving the explicit mixing problem. *Journal of Mathematical Geology* 29, 503–549.

Weninger, B., Jöris, O. and Danzeglocke, U. 2006. *Glacial radiocarbon age conversion. Cologne radiocarbon calibration and palaeoclimate research package <CALPAL> User manual*. Institut für Ur- und Frühgeschichte, Radiocarbon Laboratory, Universität zu Köln, pp. 1-29.

Werne, J.P., Hollander, D.J., Lyons, T.W. and Peterson, L.C. 2000. Climate-induced variations in productivity and planktonic ecosystem structure from the Younger Dryas to Holocene in the Cariaco Basin, Venezuela. *Paleoceanography* 15, 19-29.

Westbroek, P., Brown, C.W., Van Bleijswijk, J., Brownlee, C., Brummer, G.-J., Conte, M., Egge, J., Fernandéz, E., Jordan, R., Knappertsbusch, M., Stefels, J., Veldhuis, M., Van der Waal, P. and Young, J.R. 1993. A model system approach to biological climate forcing. The example of *Emiliania huxleyi*. *Global Planetary Change* 8, 27–46.

Wichard, T., Poulet, S.A., Boulesteix, A.-L., Ledoux, J.B., Lebreton, B., Marchetti, J. and Pohnert, G. 2008. Influence of diatoms on copepod reproduction. II. Uncorrelated effects of diatom-derived α,β,γ,δ-unsaturated aldehydes and polyunsaturated fatty acids on *Calanus helgolandicus* in the field. *Progress in Oceanography* 77, 30-44.

Winter, A. and Siesser, W.G. 1994. Coccolithophores. Cambridge, Cambridge University Press. 242 pp.

Winter, A., Jordan, R.W. and Roth, P.H. 1994. Biogeography of living coccolithophores in ocean waters. In: Winter, A. and Siesser, W.G. (Eds.), *Coccolithophores*. Cambridge University Press, Cambridge, pp. 161-177.

Winter, A., Stockwell, D. and Hargraves, P.E. 1986. Tintinnid agglutination of coccoliths: A selective or random process? *Marine Micropaleontology* 10, 375-379.

Wolfe, A.P. 1997. On diatom concentrations in lake sediments: results from an inter-laboratory comparison and other tests performed on a uniform sample. *Journal of Paleolimnology* 18, 261–268.

Wood, G.D., Gabriel, A.M. and Lawson, J.C. 1996. Palynological techniques - processing and microscopy. In: Jansonius, J. and McGregor, D.C. (Eds.), *Palynology: Principles and Applications*, *vol. 1*. American Association of Stratigraphic Palynologists Foundation, Dallas, Texas, pp. 29–50.

Wuchter, C., Schouten, S., Coolen, M. and Sinninghe Damsté, J. 2004. Temperature-dependent variation in the distribution of tetraether membrane lipids of marine Crenarchaeota: Implications for TEX_{86} paleothermometry. *Paleoceanography* 19, PA4028, doi:10.1029/2004PA001041.

Wust, G. 1964. Stratification and circulation in the Antillean–Caribbean Basins, Columbia University Press, Palisades, New York. 201 pp.

Xu, Y. and Jaffé, R. 2007. Biomarker-based paleo-record of environmental change for a eutrophic, tropical freshwater lake, lake Valencia, Venezuela. *Journal of Paleolimnology* 40 (1), 179-194.

Yarincik, K.M., Murray, R.W. and Peterson, L.C. 2000. Climatically sensitive eolian and hemipelagic deposition in the Cariaco Basin, Venezuela, over the past 578,000 years, results from Al/Ti and K/Al. *Paleoceanography* 15, 210–228.

Young, J.R. and Ziveri, P. 2000. Calculation of coccolith volume and its use in calibration of carbonate flux estimates. *Deep–Sea Research II* 47, 1679–1700.

Young J.R., Geisen M., Cros L., Kleijne A., Sprengel C., Probert I. and Oostergaard J. 2003. A Guide to Extant Coccolithophore Taxonomy. *Journal of Nannoplankton Research Special issue* 1, 125pp.

Young, J.R., Bergen, J.A., Bown, P.R., Burnett, J.A., Fiorentino, A., Jordan, R.W., Kleijne, A., van Niel, B.E., Romein, A.J.T. and von Salis, K. 1997. Guidelines for coccolith and calcareous nannofossil terminology. *Palaeontology* 40, 875-912.

Yu, E.-F., Francois, R. and Bacon, M.P., 1996. Similar rates of modern and last-glacial ocean thermohaline circulation inferred from radiochemical data. *Nature* 379, 689-694.

Zabel, M., Schneider, R.R., Wagner, T., Adegbie, A.T., de Vries, U. and Kolonic, S. 2001. Late Quaternary climate changes in Central Africa as inferred from terrigenous input to the Niger Fan. *Quaternary Research* 56, 207-217.

Zachariasse, W. J., Riedel, W. R., Sanfilippo, A., Schmidt, R. R., Brolsma, M. J., Schrader, H. J., Gersonde, R., Drooger, M. M. and Broekman, J. A. 1978. Micropaleontological counting methods and techniques; an exercise on an eight metres section of the lower Pliocene of Capo Rossello, Sicily. *Utrecht Micropaleontological Bulletins 1978*, 265 pp.

Zanchetta, G., Drysdale, R.N., Hellstrom, J.C., Fallick, A.E., Isola, I., Gagan, M.K. and Pareschi, M.T. 2007. Enhanced rainfall in the Western Mediterranean during deposition of sapropel S1: stalagmite evidence from Corchia cave (Central Italy). *Quaternary Science Reviews* 26, 279–286.

Zhang, J. and Siesser, W.G. 1986. Calcareous nannoplankton in continental-shelf sediments, East China Sea. *Micropaleontology* 32, 271-281.

Ziveri, P. and Thunell, R.C. 2000. Coccolithophore export production in Guaymas Basin, Gulf of California: response to climate forcing. *Deep-Sea Research II* 47, 2073-2100.

Ziveri, P., Rutten, A.,de Lange, G.J., Thomson, J. and Corselli, C. 2000. Present-day coccolith fluxes recorded in central eastern Mediterranean sediment traps and surface sediments. *Palaeogeography, Palaeoclimatology, Palaeoecology* 158, 175-195.

Zonneveld, K.A.F., Bockelmann, F. and Holzwarth, U. 2007. Selective preservation of organic-walled dinoflagellate cysts as a tool to quantify past net primary production and bottom water oxygen concentrations. *Marine Geology* 237, 109-126.

Zonneveld, K.A.F., Versteegh, G.J.M. and de Lange, G.J. 2001. Palaeoproductivity and post-depositional aerobic organic matter decay reflected by dinoflagellate cyst assemblages of the Eastern Mediterranean S1 sapropel. *Marine Geology* 172, 181–195.

Zonneveld, K.A.F., Versteegh, G.J.M. and Kodrans-Nsiah, M. 2008. Preservation and organic chemistry of Late Cenozoic organic-walled dinolfagellate cysts: a review. *Marine Micropaleontology* 68, 179-197.

Appendices

Appendix I

Acanthoica Lohmann, 1903 emend. Schiller 1913 and Kleijne, 1992
Acanthoica biscayensis Kleijne, 1992
Braarudosphaera bigelowii (Gran and Braarud, 1935) Deflandre 1947
Calcidiscus leptoporus (Murray and Blackman, 1898) Loeblich and Tappan, 1978
Calciosolenia brasiliensis (Lohmann, 1919) Young et al., 2003
Calciosolenia murrayi Gran, 1912
Ceratolithus cristatus Kamptner, 1950
Coccolithus pelagicus (Wallich, 1877) Schiller, 1930 ssp. pelagicus
Coccolithus pelagicus ssp. braarudii (Gaarder, 1962) Geisen et al., 2002
Coronosphaera mediterranea (Lohmann, 1902) Gaarder, in Gaarder and Heimdal, 1977
Discosphaera tubifera (Murray and Blackman, 1898) Ostenfeld, 1900
Emiliania huxleyi (Lohmann, 1902) Hay and Mohler, in Hay et al., 1967
Gephyrocapsa ericsonii McIntyre and Bé, 1967
Gephyrocapsa muellerae Bréhéret, 1978
Gephyrocapsa oceanica Kamptner, 1943
Hayaster perplexus (Bramlette and Riedel, 1954) Bukry, 1973
Helicosphaera carteri (Wallich, 1877) Kamptner, 1954
Helicosphaera pavimentum Okada and McIntyre, 1977
Helicosphaera wallichi (Lohmann, 1902) Okada and McIntyre, 1977
Oolithotus antillarum (Cohen, 1964) Reinhardt, in Cohen and Reinhardt, 1968
Ooltihotus fragilis (Lohmann, 1912) Martini and Müller, 1972
Pontosphaera Lohmann, 1902
Pontosphaera discopora Schiller, 1925
Pontosphaera multipora (Kamptner, 1948) Roth, 1970
Pontosphaera syracusana Lohmann, 1902
Reticulofenestra parvula (Okada and McIntyre, 1977) Biekart, 1989
Reticulofenestra sessilis (Lohmann, 1912) Jordan and Young, 1990
Rhabdosphaera clavigera Murray and Blackman, 1898
Scyphosphaera apsteinii Lohmann, 1902
Syracosphaera Lohmann, 1902
Syracosphaera ampliora Okada and McIntyre, 1977
Syracosphaera anthos (Lohmann) Janin, 1987
Syracosphaera lamina Lecal-Schlauder, 1951
Syracosphaera molischii Schiller, 1925
Syracosphaera pulchra Lohmann 1902
Umbellosphaera Paasche in Markali and Paasche, 1955
Umbilicosphaera foliosa (Kamptner 1963, ex Kleijne 1993) Geisen in Sáez et al., 2003
Umbilicosphaera hulburtiana Gaarder, 1970
Umbilicosphaera sibogae (Weber – van Bosse 1901) Gaarder, 1970

Appendix II

Error calculation according to Stockmarr (1971)

According to Stockmarr (1971) total error is

$$e = \sqrt{e_1{}^2 + e_2{}^2 + e_3{}^2}$$

where:

e_1 = error on number of spores in marker tablets

$$e_2 = \frac{\sqrt{cysts\ counted}}{cysts\ counted}$$ = error on dinoflagellate cysts counted

$$e_3 = \frac{\sqrt{spores\ counted}}{spores\ counted}$$ = error on the number of spores counted

Appendix III

Species name	*Grouped under*	*North Sea*	*Celtic Sea*	*NW Africa*	*Benguela*
Achomosphaera andalousiensis Jan du Chêne 1977	*Spiniferites* s.l.	x	x	x	
Cysts of *Alexandrium affine* (Ioue & Fukuyo 1985) Balech 1985	Cyst of *Alexandrium* spp.		x		x
Cysts of *Alexandrium tamarense* (Lebour 1925) Balech 1985	Cyst of *Alexandrium* spp.	x	x		
Ataxiodinium choane Reid 1974	*Ataxiodinium choane*	x	x	x	
Bitectatodinium spongium Zonneveld 1997	*Bitectatodinium* spp.		x	x	x
Bitectatodinium tepikiense Wilson 1973	*Bitectatodinium* spp.	x	x	x	x
Tectatodinium pellitum Wall, 1967 emend. Head 1994	*Tectatodinium* spp.				x
cf. Tectatodinium pellitum Wall, 1967 emend. Head 1994	*Tectatodinium* spp.	x			
Brigantedinium cariacoense (Wall 1967) Lentin and Williams 1993	Round Brown Cyst	x	x	x	x
Brigantedinium majusculum Reid 1977 ex Lentin and Williams 1993	Round Brown Cyst	x	x		
Brigantedinium simplex Wall 1965 ex Lentin and Williams 1993	Round Brown Cyst	x	x	x	x
Cyst of Protoperidinium americanum (Gran & Braarud 1935) Balech 1974	Round Brown Cyst	x	x	x	x
Dalella chathamense McMinn & Sun 1994	*Dalella chathamense*				x
Diplopelta? symmetrica Pavillard 1993 (Dale et al. 1993)	Spiny Brown Cysts			x	
Dubridinium ulsterum Reid 1977	Round Brown Cyst	x		x	x
Dubridinium caperatum Reid 1977	Round Brown Cyst	x	x	x	x
Echinidinium aculeatum Zonneveld 1997	Spiny Brown Cysts	x	x	x	x
Echinidinium bispiniformum Zonneveld 1997	Spiny Brown Cysts			x	x
Echinidinium delicatum Zonneveld 1997	Spiny Brown Cysts	x	x	x	x
Echinidinium granulatum Zonneveld 1997	Spiny Brown Cysts	x	x	x	x
Echinidinium transparantum Zonneveld 1997	Spiny Brown Cysts	x		x	x
Echinidinium cf. *transparantum* Zonneveld 1997	Spiny Brown Cysts	x	x		x
Cyst of *Gymnodinium catenatum* Graham 1943	Cyst of *Gymnodinium* spp.	x	x	x	x
Cyst of *Gymnodinium microreticulatum* Bolch et al. 1999	Cyst of *Gymnodinium* spp.	x	x		
Cyst of *Gymnodinium nolleri* Ellegaard & Moestrup 1999	Cyst of *Gymnodinium* spp.	x	x	x	x
Impagidinium aculeatum (Wall 1967) Lentin and Williams 1981	*Impagidinium* spp.		x		
Impagidinium pallidum Bujak 1984	*Impagidinium* spp.		x		
Impagidinium paradoxum (Wall 1967) Stover and Evitt 1978	*Impagidinium* spp.	x	x		x
Impagidinium patulum (Wall 1967) Stover and Evitt 1978	*Impagidinium* spp.	x	x	x	
Impagidinium sphaericum (Wall 1967) Lentin and Williams 1981	*Impagidinium* spp.	x	x		x
Impagidinium strialatum (Wall 1967) Stover and Evitt 1978	*Impagidinium* spp.				x
Impagidinium velorum Bujak 1984	*Impagidinium* spp.	x		x	
Islandinium? cezare de Vernal et al. 1989 ex de Vernal in Rochon et al. 1999	Spiny Brown Cysts	x			
Islandinium minutum Harland and Reid in Harland et al. 1980	Spiny Brown Cysts	x	x	x	x
Leipokatium invisitatum Bradford 1975	*Lejeunecysta* s.l.		x		
Lejeunecysta diversiforma (Bradford 1977) Artzner and Dörhöfer 1978	*Lejeunecysta* s.l.				x
Lejeunecysta mariae Harland in Harland et al. 1991 ex Lentin and Williams 1993	*Lejeunecysta* s.l.	x			
Lejeunecysta oliva (Reid 1977) Turon and Londeix 1988	*Lejeunecysta* s.l.	x	x	x	x
Lejeunecysta paratenella (Benedek 1972) Zonneveld & Marret xxx	*Lejeunecysta* s.l.	x	x		x
Lejeunecysta sabrina (Reid 1977) Bujak 1984	*Lejeunecysta* s.l.	x	x	x	x
Lingulodinium machaerophorum (Deflandre and Cookson 1955) Wall 1967	*Lingulodinium machaerophorum*	x	x	x	x
Nematosphaeropsis labyrinthus (Ostenfeld 1903) Reid 1974	*Nematosphaeropsis labyrinthus*	x	x	x	x
Operculodinium centrocarpum sensu Wall and Dale (1966)	*Operculodinium* s.l.	x	x	x	x
Operculodinium israelianum (Rossignol 1962) Wall 1967	*Operculodinium israelianum*	x	x	x	x
Operculodinium janduchenei Head et al. 1989	*Operculodinium* s.l.	x	x	x	x
Operculodinium sp. II? Marret, 1994	*Operculodinium* s.l.				x
Operculodinium sp. A of Vink (2000)	*Operculodinium* s.l.			x	
Cyst of *Pentapharsodinium dalei* Indelicato & Loeblich III 1986	Cyst of *Pentapharsodinium dalei*	x	x	x	x
Polykrikos kofoidii Chatton 1914	*Polykrikos* spp.	x	x	x	x
Polykrikos schwartzii Bütschli 1873	*Polykrikos* spp.	x	x	x	x
Polysphaeridium zoharyi (Rossignol 1962) Bujak et al. 1980	*Polysphaeridium zoharyi*	x	x	x	x
Pyxidinopsis reticulata (McMinn & Sun 1994) Marret & de Vernal 1997	*Pyxidinopsis reticulata*	x			
Quinquecuspis concreta (Reid, 1977) Harland, 1977	*Quinquecuspis concreta*	x	x	x	x
Selenopemphix crenata Matsuoka and Bujak, 1988	*Selenopemphix* s.l.				x
Selenopemphix nephroides Benedek 1972; emend. Bujak in Bujak et al., 1980;	*Selenopemphix* s.l.	x	x	x	x
Cyst of Protoperidinium nudum (Meunier 1919) Balech 1974	*Selenopemphix* s.l.	x	x	x	x
Selenopemphix quanta (Bradford 1975) Matsuoka 1985	*Selenopemphix* s.l.	x	x	x	
Spiniferites belerius Reid 1974	*Spiniferites* s.l.	x	x	x	x
Spiniferites bentorii (Rossignol 1964) Wall and Dale 1970	*Spiniferites* s.l.	x	x	x	x
Spiniferites bulloideus (Deflandre & Cookson 1955) Sarjeant 1970	*Spiniferites* s.l.	x	x		x
Spiniferites delicatus Reid 1974	*Spiniferites* s.l.	x	x	x	x
Spiniferites elongatus Reid 1974	*Spiniferites* s.l.	x	x		x
Spiniferites elongatus Reid 1974	*Spiniferites* s.l.	x			
Spiniferites hyperacanthus (Deflandre and Cookson 1955) Cookson and Eisenack 1974	*Spiniferites* s.l.	x	x	x	x
Spiniferites lazus Reid 1974	*Spiniferites* s.l.	x	x		x
Spiniferites membranaceus (Rossignol 1964) Sarjeant 1970	*Spiniferites* s.l.	x	x	x	x
Spiniferites mirabilis (Rossignol 1964) Sarjeant 1970	*Spiniferites* s.l.	x	x	x	x
Spiniferites pachydermus Rossignol 1964	*Spiniferites* s.l.	x	x	x	
Spiniferites ramosus (Ehrenberg 1838) Loeblich and Loeblich 1966; emend. Davey and Williams 1966	*Spiniferites* s.l.	x	x	x	x
Stelladinium reidii Bradford 1975	*Stelladinium* spp.	x	x	x	
Stelladinium stellatum (Wall and Dale 1968) Reid 1977	*Stelladinium* spp.	x	x	x	x
Trinovantedinium applanatum (Bradford 1977) Bujak and Davies 1983	*Trinovantedinium applanatum*	x	x	x	x
Tuberculodinium vancampoae (Rossignol 1962) Wall 1967	*Tuberculodinium vancampoae*	x		x	x
Votadinium calvum Reid 1977	*Votadinium* spp.	x	x	x	x
Votadinium spinosum Reid 1977	*Votadinium* spp.	x	x		x
Xandarodinium xanthum Reid 1977	*Xandarodinium xanthum*	x	x	x	x

Appendix IV

Unpublished data

Gu, Haifeng (unpublished data)
Holzwarth, Ulrike (submitted)
Kotthoff, Ullrich (in prep.)
Londeix, Laurent (unpublished)
Mertens, Kenneth (unpublished and in prep.)
Silke, Joe (unpublished data)
Turon, Jean-Louis (unpublished)
Verleye, Thomas (unpublished)
Young, Martin (unpublished)
Zonneveld, K.A.F., Chen, L. and Mahmoud, M.S., submitted. Environmental significance of dinoflagellate cysts from the proximal part of the Po-river discharge plume (off southern Italy, Eastern Mediterranean). *Journal of Sea Research.*

Published data

Abidi, N. 1997. Les kystes de dinoflagelleés marqueurs de l'environnement océanique : répartition actuelle dans l'Océan Indien occidental et application a deux séquences sédimentaires du Canal de Mozambique. Thèse de l'Université Pierre-et-Marie-Curie, Paris.

Aksu, A.E., Yasar, D. and Mudie, P.J. 1995. Paleoclimatic and paleoceanographic conditions leading to development of sapropel layer S1 in the Aegean Sea. *Palaeogeography, Palaeoclimatology, Palaeoecology* 116, 71-101.

Aksu, A.E., Yasar, D., Mudie, P.J. and Gillespie, H. 1995. Late glacial-Holocene paleoclimatic and paleoceanographic evolution of the Aegean Sea: micropaleontological and stable isotopic evidence. *Marine Micropaleontology* 25, 1-28.

Andreieff, P., Bouysse, P., Châteauneuf, J.J., L'Homer, A. and Scolari, G. 1971. La couverture sédimentaire meuble du plateau continental externe de la Bretagne méridionale (Nord du Golfe de Gascogne). *Cahiers Oceanographiques* 23, 343-381.

Azanza, R.V., Siringan, F.P., San Diego-Mcglone, M.L., Yniguez, A.T., Macalad, N.H., Zamora, P.B., Agustin, M.B. and Matsuoka, K. 2004. Horizontal dinoflagellate cyst distribution, sediment characteristics and benthic flux in Manila Bay, Philippines. *Phycological Research* 52, 376-386.

Beaudoin, C., Suc, J.-P., Escarguel, G., Arnaud, M. and Charmasson, S. 2007. The significance of pollen signal in present-day marine terrigenous sediments: the example of the Gulf of Lions (western Mediterranean Sea). *Geobios* 40, 159-172.

Beaudoin, C., Dennielou, B., Melki, T., Guichard, F., Kallel, N., Berné, S. and Huchon, A. 2004. The Late-Quaternary climatic signal recorded in a deep-sea turbiditic levee (Rhone Neofan, Gulf of Lyons, NW Mediterranean): palynological constrains. *Sedimentary Geology* 172, 85-97.

Biebow, N. 1996. Geomar Report, 57: Dinoflagellatenzysten als indikatoren der spät- und postglazialen entwicklung des auftriebgeshehens vor Peru. Geomar, Kiel, 130 pp.

Bint, A.N. 1988. Recent dinoflagellate cysts from Mermaid sound, northwestern Australia. *Memoir of the Association of Australasian Palaeontologists* 5, 329-341.

Blanco, J. 1988. Quistes de dinoflagelados de las costas de Galicia. Unpublished Ph.D. thesis.

Boessenkool, K.P., van Gelder, M.-J., Brinkhuis, H. and Troelstra, S.R. 2001. Distribution of organic-walled dinoflagellate cysts in surface sediments from transects across the Polar Front offshore southeast Greenland. Journal of Quaternary Science 16, 661-666.

Bolch, C.J. and Hallegraeff, G.M. 1990. Dinoflagellate cysts in recent marine sediments from Tasmania, Australia. *Botanica Marina* 33, 173-192.

Borel, C.M. and Gómez, E.A. 2006. Palinologiá del Holoceno del Canal del Medio, estuario de Bahiá Blanca, Buenos Aires, Argentina. *Ameghiana* 43 (2), 399-412.

Borromei, A.M. and Quattrocchio, M. 2007. Holocene sea-level change inferred from palynological data in the Beagle Channel, southern Tierra del Fuego, Argentina. *Ameginiana* 44 (1), 161-171.

Bradford, M.R. 1975. New dinoflagellate cyst genera from the recent sediments of the Persian Gulf. *Canadian Journal of Botany* 53, 3064-3074.

Bradford, M.R. and Wall, D.A. 1984. The distribution of Recent organic-walled dinoflagellate cysts in the Persian Gulf, Gulf of Oman, and northwestern Arabian Sea. *Paleontographica Abteiling B* 192, 16-84.

Brenner, W.W. 2001. Organic-walled microfossils from the central Baltic Sea, indicators of environmental change and base for ecostratigraphic correlation. *Baltica* 14, 40-51.

Brenner, W. and Meemken, H.-J. 2002. Öko- und chronostratigraphic Korrelierung der Zentralen Ostsee mit er Kieler Bucht anhand organisch-wandiger Microfossilien. *Meyniana* 54, 17-40.

Brenner, W. 2005. Holocene environmental history of the Gotland Basin (Baltic Sea) – a micropalaeontological model. *Palaeogeography, Palaeoclimatology, Palaeoecology* 220, 227-241.

Brewster-Wingard, G.I., Ishman, S.E., Edwards, L.E. and Willard, D.A. 1996. Preliminary report on the distribution of modern fauna and flora at selected sites in North-central and North-eastern Florida Bay. *USGS Open File Report 96-732*, 34 pp.

Cao, W., Lin, Y. and Fang, L. 2004. Abundance and distribution of dinoflagellate cysts in Xiamen Western Harbor. *Acta Oceanologica Sinica* 23 (2), 347-357.

Candel, M.S., Borromei, A.M., Martinez, M.A., Gordillo, S., Quattrocchio, M. and Rabassa, J. 2009. Middle-Late Holocene palynology and marine mollusks from Archipiélago Cormoranes area, Beagle Channel, southern Tierra del Fuego, Argentina. *Palaeogeography, Palaeoclimatology, Palaeoecology* 273 (1-2), 111-122.

Caratini, C., Bentaleb, I., Fontugne, M., Morzadec-Kerfourn, M.-T., Pascal, J.P. and Tissot, C. 1994. A less humid climate since 3500 yr BP from marine cores off Karwar, western India. *Palaeogeography Palaeoclimatology Palaeoecology* 109, 371-384.

Cho, H.-J. 2000. Utility of dinoflagellates in studying the marine environment: the case of the East China Sea and Adjacent Seas. Ph.D. thesis, Nagasaki University, Nagasaki, 112 p.

Cho, H.-J. and Matsuoka, K. 2001. Distribution of dinoflagellate cysts in surface sediments from the Yellow sea and East China Sea. *Marine Micropaleontology* 42, 103-123.

Churchill, D. M. and Sarjeant, W.A.S. 1962. Freshwater microplankton from Flandrian (Holocene) peats of southwestern Australia. *Grana Palynologica* 3, 29–53.

Combourieu Nebout, N., Londeix, L., Baudin, F., Turon, J.-L., von Grafenstein, R. and Zahn, R. 1999. Quaternary marine and continental paleoenvironments in the Western Mediterranean (site 976, Alborán Sea): palynological evidence. In: Zahn, R., Comas, M.C. and Klaus, A. (Eds.), *Proceedings of the Ocean Drilling Program, Scientific Results 161*, College Station, Texas (Ocean Drilling Program), pp. 457–468.

Cremer, H., Sangiorgi, F., Wagner-Cremer, F., McGee, V., Lotter, A.F. and Visscher, H. 2007. Marine littoral diatoms (Bacillariophyceae) and dinoflagellates (Dinophyceae) from Rookery Bay, Florida, U.S.A. *Caribbean Journal of Science* 43, 23-58.

Dale, B. 1985. Dinoflagellate cyst analysis of Upper Quaternary sediments in core GIK 15530-4 from the Skagerrak. *Norsk Geologirk Tidrskrift* 65, 97-102.

Dale, B. and Fjellså, A. 1994. Dinoflagellate cysts as paleoproductivity indicators: state of the art, potential, and limits. In: Zahn, R., Pedersen, T.F., et al. (Eds.), *Carbon Cycling in the Glacial Ocean: Constraints on the Ocean's Role in Global Change*. Springer, Berlin, pp. 521-537.

Dale, B., Dale, A.L. and Jansen, J.H.F. 2002. Dinoflagellate cysts as environmental indicators in surface sediments from the Congo deep-sea fan and adjacent regions. *Palaeogeography, Palaeoclimatology, Palaeoecology* 185, 309-338.

Davey, R.J. 1971. Palynology and palaeo-environmental studies, with special reference to the continental shelf sediments of South Africa. In: Farinacci, A., Matteucci, R. (Eds.), *Proceedings of the Second Planktonic Conference, Roma 1970, vol. 1*. Technoscienza, Rome, pp. 331-347.

Davey, R.J. and Rogers, J. 1975. Palynomorph distribution in Recent offshore sediments along two traverses off Southwest Africa. *Marine Geology* 18, 213-225.

Debenay, J.P., Carbonel, P., Morzadec-Kerfourn, M.-T., Cazaubon, A., Denèfle, M. and Lézine, A.-M. 2003. Multi-bioindicator study of a small estuary in Vendée (France). *Estuarine, coastal and shelf science* 58, 843-860.

Downie, C. and Singh, G. 1969. Dinoflagellate cysts from estuarine and raised beachdeposits at Woodgrange, Co. Down, N. Ireland. *Grana* 9, 1-3.

Duane, A. and Harland, R. 1990. Late Quaternary dinoflagellate cyst biostratigraphy for sediments of the Porcupine Basin, offshore western Ireland. *Review of Palaeobotany and Palynology* 63, 1–11.

Dupont, L. 1998. Pollen and dinoflagellate cysts of the upper 50 m of Site 958. In: Firth, J.V. (Ed.), *Proceedings of the Ocean Drilling Program, Scientific Results 159T.* College Station, Texas (Ocean Drilling Program), pp. 23–30.

Edwards, L.E. and Willard, D.A. 2001. Stratigraphic and Paleontologic Studies of the Neogene and Quaternary Sediments in Southern Jackson County, Mississippi. D. Dinoflagellate Cysts and Pollen from Sediment Samples, Mississippi Sound and Gulf of Mexico. *U.S. Geological Survey Open-file Report 01-415-D.*

Ellegaard, M. 2000. Variations in dinoflagellate cyst morphology under conditions of changing salinity during the last 2000 years in the Limfjord, Denmark. *Review of Palaeobotany and Palynology* 109, 65-81.

Ellegaard, M., Christensen, N.F. and Moestrup, O. 1994. Dinoflagellate cysts from Recent Danish marine sediments. *European Journal of Phycology* 29, 183-194.

Esper, O. and Zonneveld, K.A.F. 2007. The potential of organic-walled dinoflagellate cysts for the reconstruction of past sea-surface conditions in the Southern Ocean. *Marine Micropaleontology* 65, 185-212.

Eynaud, F. 1999. Dinoflagellate cyst and paleoclimatic and paleohydrologic evolution of the North Atlantic Ocean throughout the last climatic cycle, Ph.D. Thesis, University of Bordeaux, 291 pp.

Fjellså, A. and Nordberg, K. 1996. Toxic dinoflagellate “blooms” in the Kattegat, North Sea, during the Holocene. *Palaeogeography, Palaeoclimatology, Palaeoecology* 124, 87-105.

Furio, E.E., Matsuoka, K., Mizushima, K., Baula, I., Weng Chan, K., Puyong, A., Srivilai, D., Sidharta, B.R. and Fukuyo, Y. 2006. Assemblage and geographical distribution of dinoflagellate cysts in surface sediments of coastal waters of Sabah, Malaysia. *Coastal Marine Science* 30 (1), 62-73.

Giannakourou, A., Orlova, T.A., Assimakopoulou, G. and Pagou, K. 2005. Dinoflagellate cysts in recent marine sediments from Thermaikos Gulf, Greece: effects of re-suspension events on vertical cyst distribution. *Continental Shelf Research* 25(19-20), 2585-2596.

Godhe, A., Karunasagar I. and Karlson B. 2000. Dinoflagellate Cysts in Recent Marine Sediments from SW India. *Botanica Marina* 43, 39-48.

Grøsfjeld, K. and Harland, R. 2001. Distribution of modern dinoflagellate cysts from inshore areas along the coast of southern Norway. *Journal of Quaternary Science* 16(7), 651-659.

Grøsfjeld, K., Larsen, E., Sejrup, H.P., de Vernal, A., Flatebø, T., Vestbø, M., Haflidason, H. and Aarseth, I. 1999. Dinoflagellate cysts reflecting surface-water conditions in Voldafjorden, western Norway during the last 11.300 years. *Boreas* 28, 403-415.

Gu, H., Fang, Q., Sun, J., Lan, D., Cai, F. and Gao, Z. 2003. Dinoflagellate cysts in recent marine sediment from Guangxi, China. *Acta Oceanologica Sinica* 22 (3), 407-419.

Gundersen, N. 1988. En palynologisk undersøkelse av dinoflagellatcyster langs en synkende salinitetsgradient I recente sedimenter fra Østersjø-området. Unpublished candidata scientiarum thesis, University of Oslo, 96 pp.

Hald, M., Husum, K., Vorren, T.O., Grosfjeld, K., Jensen, H.B. and Sharapova, A. 2003. Holocene climate in the subarctic fjord Malangen, northern Norway: a multi-proxy study. *Boreas* 32, 543-559.

Hamel, D., de Vernal, A., Gosselin, M. and Hillaire-Marcel, C. 2002. Organic-walled microfossils and geochemical tracers: sedimentary indicators of productivity changes in the North Water and northern Baffin Bay (High Arctic) during the last centuries. *Deep-Sea Research II* 49, 5277–5295.

Harland, R. 1971. Fossil dinoflagellate cysts from Lake Gnotuk, Victoria, Australia. *Royal society of Victoria Proceedings* 84, 245-254.

Harland, R. 1973. Quaternary (Flandrian?) dinoflagellate cysts from the Grand Banks, off Newfoundland, Canada. *Review of Palaeobotany and Palynology* 16, 229-242.

Harland, R. 1983. Distribution maps of recent dinoflagellate cysts in bottom sediments from the North Atlantic Ocean and adjacent seas. *Palaeontology* 26, 321–387.

Harland, R. 1989. A dinoflagellate cyst record for the last 0.7 Ma from the Rockall Plateau, northeast Atlantic Ocean. *Journal of the Geological Society* 146, 945-951.

Harland, R. 1994. Dinoflagellate cysts from the glacial/postglacial transition in the northeast Atlantic Ocean. *Palaeontology* 37, 263-283.

Harland, R. and Howe, J.A. 1995: Dinoflagellate cysts and Holocene oceanography of the northeastern Atlantic ocean. *The Holocene* 5, 220-228.

Harland, R. and Long, D. 1996. A Holocene dinoflagellate cyst record from offshore north-east England. *Proceedings of the Yorkshire Geological Society* 51 (1), 65-74.

Harland, R. and Pudsey, C.J. 1999. Dinoflagellate cysts from sediment traps deployed in the Bellingshausen, Weddell and Scotia Seas, Antarctica. *Marine Micropaleontology* 37, 77-99.

Harland R., E.J. FitzPatrick, M. and Pudsey C.J. 1999. Latest Quaternary dinoflagellate cyst climatostratigraphy for three cores from the Falkland Trough, Scotia and Weddell seas, Southern Ocean. *Review of Palaeobotany and Palynology* 107 (3), 265-281.

Harland, R., Nordberg, K. and Filipsson, H.L. 2004. The seasonal occurrence of dinoflagellate cysts in surface sediments from Koljö Fjord, west coast of Sweden - a note. *Review of Palaeobotany and Palynology* 128, 107-117.

Harland, R., Nordberg, K. and Filipsson, H.L. 2006. Dinoflagellate cysts and hydrographical change in Gullmar Fjord, west coast of Sweden. *Science of the Total Environment* 355, 204-231.

Harland, R., Reid, J.R., Dobell, P. and Norris, G. 1980. Recent and sub-Recent dinoflagellate cysts from the Beaufort Sea, Canadian Arctic. *Grana* 19, 211-225.

Harland, R., Pudsey, C.J., Howe, J.A. and Fitzpatrick, M.E.J. 1998. Recent dinoflagellate cysts in a transect from the Falklands through to the Weddell Sea, Antarctica. *Palaeontology* 41, 1093-1131.

Herreyre, Y. 2005. Le « Déluge », mythe ou réalité ? Témoignage des dinokystes en mer de Marmara. Univ. Bordeaux1, rapport Master 2 ENVOLH, 22 pp.

Holl, C. and Kemle-von Mucke, S. 2000. Late Quaternary Upwelling Variations in the Eastern Equatorial Atlantic Ocean as Inferred from Dinoflagellate Cysts, Planktonic Foraminifera, and Organic Carbon Content. *Quaternary Research* 54 (1), 58-67.

Holzwarth, U., Esper, O. and Zonneveld, K. 2007. Distribution of organic-walled dinoflagellate cysts in shelf surface sediments of the Benguela upwelling system in relation to environmental conditions. *Marine Micropaleontology* 64, 91-119.

Howe, J.A., Harland, R. and Pudsey, C. 2002. Dinoflagellate cyst evidence for Quaternary palaeoceanographic change in the northern Scotia Sea, South Atlantic Ocean. *Marine Geology* 191, 55-69.

Ismael, A.A. and Khadr, A.M. 2003. *Alexandrium minutum* cysts in sediment cores from the Eastern Harbour of Alexandria, Egypt. *Oceanologia* 45 (4), 721-731.

Joyce, L.B. 2004. Dinoflagellate cysts in recent marine sediments from Scapa Flow, Orkney, Scotland. *Botanica Marina* 47, 173-183.

Kawamura, H. 2004. Dinoflagellate cyst distribution along a shelf to slope transect of an oligotrophic tropical sea (Sunda Shelf, South China Sea). *Phycological Research* 52, 355-375.

Kobayashi, S., Matsuoka, K. and Lizuka, S. 1986. Distribution of dinoflagellate cysts in surface sediments of Japanese coastal waters. I. Omura Bay, Kyushu (in Japanese). *Bulletin of Plankton Society of Japan* 33, 81-93.

Kojima, N., Seto, K., Takayasu, K. and Nakamura, M. 1994. Dinoflagellate cysts assemblage found in the surface sediments of Lake Nakaumi, Western Japan. *Laguna* 1, 45-51.

Kumar, A. and Patterson, T. 2002. Dinoflagellate cyst assemblages from Effingham Inlet, Vancouver Island, British Columbia, Canada. *Palaeogeography, Palaeoclimatology, Palaeoecology* 180, 187-206.

Kunz-Pirrung, M. 2001. Dinoflagellate cyst assemblages in surface sediments of the Laptev Sea region (Arctic Ocean) and their relationship to hydrographic conditions. *Journal of Quaternary Science* 16, 637-649.

Larrazabal, M.E., Lassus, P., Maggi, P. and Bardouil, M. 1990. Kystes modernes de dinoflagellés en Baie de Villaine-Bretagne sud (France). *Cryptogamie Algologie* 11, 171-185.

Laurijssen, J. 2002. Recent distribution of organic walled dinoflagellate cysts from offshore SE South America. Workshop on Middle latitude dinoflagellates and their cysts, Bedford Institute of Oceanography, Dartmouth, Canada April 29-May 2, 2002.

Lee, J.B. and Yoo, K.I. 1991. Distribution of dinoflagellate cysts in Massan Bay, Korea. *Journal of Oceanological Society of Korea* 26 (4), 304-312

Leroy, V. 2001. Traceurs palynologiques des flux biogéniques et des conditions hydrographiques en milieu marin cotier: exemple de l'étang de Berre. DEA, Ecole doctorale Sciences de l'environment d'Aix-Marseille, 30 pp.

Levac, E., de Vernal, A. and Blake, W. Jr. 2001. Sea-surface conditions in northernmost Baffin Bay during the Holocene: palynological evidence. *Journal of Quaternary Science* 16 (4), 353-363.

Lewis, J., Dodge, J.D. and Powell, A.J. 1990. Quaternary dinoflagellate cysts from the upwelling system offshore Peru, hole 686B, ODP Leg 112. In: Suess, E., von Huene, R., et al. 5eds.), *Proceedings of the Ocean Drilling Program, Scientific Results, 112.* College Station, Texas (Ocean Drilling Program), pp. 323–328.

Lewis, J., Tett, P. and Dodge, J.D. 1985. The cyst-theca cycle of *Gonyaulax polyedra* (*Lingulodinium machaerophorum*) in Creran, a Scottish west coast Sea-Loch. In: Anderson, D.M., White, A.W. and Baden, D.G. (Ed.). *Toxic dinoflagellates*. Elsevier Science Publishing, Dordrecht, pp. 85-90.

Lim, D.I. and Park, Y.A. 2003. Late Quaternary stratigraphy and evolution of a Korean tidal flat, Haenam Bay, Southeastern Yellow Sea, Korea. *Marine Geology* 193, 177-194.

Mangin, S. 2002. Distribution actuelle des kystes de dinoflagellés en Méditerranée occidentale et application aux fonctions de transfert, vol. 1. Memoir of DEA, University of Bordeaux, 34 pp.

Marret, F. 1994. Distribution of dinoflagellate cysts in recent marine sediments from the east Equatorial Atlantic (Gulf of Guinea). *Review of Palaeobotany and Palynology* 84, 1-22.

Marret, F. and de Vernal, A. 1997. Dinoflagellate cyst distribution in surface sediments of the southern Indian Ocean. *Marine Micropaleontology* 29, 367-392.

Marret, F. and Scourse, J. 2002. Control of modern dinoflagellate cyst distribution in the Irish and Celtic seas by seasonal stratification dynamics. *Marine Micropaleontology* 47, 101-116.

Marret, F. and Turon, J.-L. 1994. Paleohydrology and paleoclimatology off Northwest Africa during the last glacial-interglacial transition and the Holocene: Palynological evidences. *Marine Geology* 118, 107-117.

Marret, F., de Vernal, A., McDonald, D. and Pedersen, T. 2001. Middle Pleistocene to Holocene palynostratigraphy of ODP Site 887 in the Gulf of Alaska, northeast North Pacific. *Canadian Journal of Earth Sciences* 38, 373-386.

Marret, F., Leroy, S. A. G., Chalié, F. and Gasse, F. 2004. New organic-walled dinoflagellate cysts from recent sediments of Central Asian seas. *Review of Palaeobotany and Palynology* 129, 1-20.

Marret, F., Eiríksson, J., Knudsen, K.L., Turon, J.-L. and Scourse, J.D. 2004. Distribution of dinoflagellate cyst assemblages in surface sediments from the northern and western shelf of Iceland. *Review of Palaeobotany and Palynology* 128, 35-53.

Marret, F., Scourse, J., Kennedy, H., Ufkes, E. and Jansen, J.H.F. 2008. Marine production in the Congo-influenced SE Atlantic over the past 30,000 years: A novel dinoflagellate-cyst based transfer function approach. *Marine Micropaleontology* 68 (1-2), 198-222.

Matsuoka, K. 1976 Recent thecate and fossilized dinoflagellates off Hachinohe coast, Northeastern Japan. *Publication of the Seto Marine Biological Laboratory XXIII* (3/5), 351-369.

Matsuoka, K. 1981. Dinoflagellate cysts and pollen in pelagic sediments of the northern part of the Philippine Sea. *Bulletin of the Faculty of Liberal Arts Nagasaki University Natural Science* 21, 59-70.

Matsuoka, K. 1985. Distribution of dinoflagellate cyst in surface sediments of the Tsushima Warm Current. *Quaternary Research* 24 (1), 1-12.

Matsuoka, K. 1989. L'affluence des palynomorphes dans l'échantillon JT-02. Symposium sur la trappe sédimentaire de la fosse abyssale du Japon. *Les Océans* 21 (4), 232-238.

Matsuoka, K. 1992. Species diversity of modern dinoflagellate cysts in surface sediments around the Japanese Islands. In: Head, M.J. and Wrenn, J.H. (Eds.), *Neogene and Quaternary Dinoflagellate cysts and Acritarchs.* American Association of Stratigraphic Palynologists Foundation, Dallas, Texas, pp. 33-53.

Matsuoka, K. 1994. Holocene dinoflagellate cyst assemblages in shallow water sediments of the Tsushima Islands, west Japan. *Review of Palaeobotany and Palynology* 84, 155-168.

Matsuoka, K. 1999. Eutrophication process recorded in dinoflagellate cyst assemblages - a case of Yokohama Port, Tokyo Bay, Japan. *Science of the Total Environment* 231, 17-35.

Matsuoka, K. and Y. Fukuyo, Y. 1994. Geographical distribution of the toxic dinoflagellate *Gymnodinium catenatum* Graham in Japanese coastal waters. *Botanica Marina* 37, 495-503.

Matsuoka, K. and Lee, J.-B. 1994. Dinoflagellate cysts in surface sediments of Aso Bay and Mine Bay in Tsushima Island, West Japan. *Bulletin of the Faculty of Liberal Arts Nagasaki University Natural Science* 34, 121-132.

Matsuoka, K., Joyce, L.B., Kotani, Y. and Matsuyama, Y. 2003. Modern dinoflagellate cysts in hypertrophic coastal waters of Tokyo Bay, Japan. *Journal of Plankton Research* 25 (12), 1461-1470.

Matsuoka, K., Fukuyo, Y., Praseno, D.P., Adnan, Q. and Kodama, M. 1999. Dinoflagellate cysts in surface sediments of Jakarta Bay, off Ujung Pandang and Larantuka of Flores Islands, Indonesia with special Reference of *Pyrodinium bahamense*. *Bulletin of the Faculty of Fisheries, Nagasaki University* 80, 49-54.

Matthiessen, J. 1995. Distribution patterns of dinoflagellate cysts and other organic walled microfossils in recent Norwegian-Greenland Sea sediments. *Marine Micropaleontology* 24, 307-334.

Matthiessen, J. and Baumann, A. 1997. Dinoflagellate cyst records from the East Greenland continental margin during the last 15,000 years: implications for paleoceanographic reconstructions. In: Hass, H.C. and Kaminski, M.A. (Eds.), *Contributions to the Micropaleontology and Paleoceanography of the Northern North Atlantic*. Grzybowski Foundation Special Publication 5, pp. 149-165.

Matthiessen, J., Knies, J., Nowaczyk, N.R. and Stein, R. 2001. Late Quaternary dinoflagellate cyst stratigraphy at the Eurasian continental margin, Arctic Ocean: indications for Atlantic water inflow in the past 150,000 years. *Global and Planetary Change* 31, 65-86.

McCarthy, F.M.G., Gostlin, K.E., Mudie, P.J. and Ohlenschlager Pedersen, R. 2004. The palynological record of terrigenous flux to the deep sea: late Pliocene-Recent examples from 41°N in the abyssal Atlantic and Pacific oceans. *Review of Palaeobotany and Palynology* 128, 81-95.

McMinn, A. 1990. Distribution of dinoflagellate cysts in estuarine deposits from the east coast of Australia. *Review of Palynology and Palaeobotany* 65, 305-309.

McMinn, A. 1991a. Recent dinoflagellate cysts from estuaries on the central coast of New South Wales, Australia. *Micropaleontology* 37, 269-287.

McMinn, A. 1991b. Quaternary dinoflagellate distribution in a borehole from Lake Macquarie. *New South Wales Geological Survey Quarterly Notes* 83, 1-6.

McMinn, A. 1992. Neogene dinoflagellate distribution in the eastern Indian Ocean from Leg 123, Site 765. In: Gradstein, F.M., Ludden, J.N., et al. (Eds.), *Proceedings of the Ocean Drilling Program, Scientific Results, 123.* College Station, Texas (Ocean Drilling Program), pp. 429-441.

McMinn, A. 1992b. Recent and late Quaternary dinoflagellate cyst distribution on the continental shelf and slope of south-eastern Australia. *Palynology* 16, 13-24.

McMinn, A. 1994. Quaternary dinoflagellate distribution at Site 820, Great Barrier Reef, Australia. In: McKenzie, J.A., Davies, P.J., Palmer-Julson, A., et al. (Eds.), *Proceedings of the Ocean Drilling Program, Scientific Results* 133. College Station, Texas (Ocean Drilling Program), pp. 93-96.

McMinn, A. and Sun, X.-K. 1994. Recent dinoflagellate cysts from the Chatham Rise, Southern Ocean, east of New-Zealand. *Palynology* 18, 41-53.

McMinn, A. and Wells, P. 1997. Use of dinoflagellate cysts to determine changing Quaternary sea-surface temperature in southern Australia. *Marine Micropaleontology* 29 (3), 407-422.

McMinn, A., Heijnis, H., Murray, A. and Hallegraeff, G. 2004. Diatom and dinoflagellate assemblages of the Hawkesbury River, N.S.W., over the last two centuries: evidence for changes in hydrology. *Alcheringa: An Australasian Journal of Palaeontology* 28 (2), 505-514.

Mertens, K.N., González, C., Delusina, I. and Louwye, S. 2009a. 30000 years of productivity, temperature and salinity variations in the late Quaternary Cariaco Basin revealed by dinoflagellate cysts. *Boreas*.

Mertens, K. , Ribeiro, S., Bouimetarhan, I., Caner, H., Combourieu-Nebout, N., Dale, B., de Vernal, A., Ellegaard, M., Filipova, M., Godhe, A., Grøsfjeld, K., Holzwarth, U., Kotthoff, U., Leroy, S., Londeix, L., Marret, F., Matsuoka, K., Mudie, P., Naudts, L., Peña-manjarrez, J., Persson, A., Popescu, S., Sangiorgi, F., van der Meer, M., Vink, A., Zonneveld, K., Vercauteren, D., Vlassenbroeck, J., and Louwye, S. 2009b. Process length variation in cysts of a dinoflagellate, *Lingulodinium machaerophorum*, in surface sediments investigating its potential as salinity proxy. *Marine Micropaleontology* 70 (1-2), 54-69.

Morquecho, L. and Lechuga-Devéze, C. H. 2004. Seasonal occurrence of planktonic dinoflagellate and cyst production in relationship to environmental variables in subtropical Bahía Concepción, Gulf of California. *Botanica Marina* 47, 313-322.

Morzadec-Kerfourn, M.-T. 1976. La signification écologique des dinoflagellés et leur intérête pour l'étude des variations du niveau marin. *Revue de Micropaléontologie* 18, 229-235.

Morzadec-Kerfourn, M.-T. 1977. Les kystes de dinoflagellés dans les sediménts Récents le long des côtes Bretonnes. *Revue de Micropaléontologie* 20, 157-166.

Morzadec-Kerfourn, M.-T. 1979. Indicateurs écologiques du domaine littoral: végétation et plancton organique. *Océanis* 5, 207-213.

Morzadec-Kerfourn, M.-T. 1983. Interet de dinoflagellés pour l'établissement de reconstruction paléogéographique: exemple du Golfe de Gabes (Tunésie). *Cahiers de Micropaléontologie* 4, 15-22.

Morzadec-Kerfourn, M.-T. 1988. Paléoclimats et paléoenvironnements, du Tardiglaciaire au Récent, en Méditerranée orientale, a' l'est du Nil; l'apport des microfossiles à membrane organique. *Bulletin Centres Recherche Exploration-Production Elf-Aquitaine* 12, 268-275.

Morzadec-Kerfourn, M.-T. 1992. Upper Pleistocene and Holocene dinoflagellate cyst assemblages in marine environments of the Mediterranean Sea and the northwest Atlantic coast of France. In: Head, M.J., Wrenn, L.H. (Eds.), *Neogene and Quaternary Dinoflagellate Cysts and Acritarchs*. American Association of Stratigraphic Palynologists Foundation, Dallas, Texas, pp. 121-132.

Morzadec-Kerfourn, M.-T., Barros, A.M.A., Barros, A.B. 1990. Microfossiles à paroi organique et substances organiques des sédiments holocènes de la lagune de Guarapina (Rio de Janeiro, Brésil). *Bulletin Centres Recherche Exploration-Production Elf-Aquitaine* 14, 575-582.

Mouradian, M., A., Panetta, R.J., de Vernal, A. and Gélinas, Y., 2007. Dinosterols or dinocysts to estimate dinoflagellate contributions to marine sedimentary organic matter? *Limnology and Oceanography* 52 (6), 2569-2581.

Mudie, P.J., Rochon, A.E. and Levac, E. 2002. Palynological records of red tide-producing species in Canada: past trends and implications for the future. *Palaeogeography, Palaeoclimatology, Palaeoecology* 180 (1), 159-186.

Mudie, P.J., Rochon, A.E., Aksu, A.E. and Gillespie, H. 2004. Late glacial, Holocene and modern dinoflagellate cyst assemblages in the Aegean-Marmara-Black Sea corridor: statistical analysis and re-interpretation of the early Holocene Noah's flood hypothesis. *Review of Palaeobotany and Palynology* 128, 143-167.

Munoz-Sobrino, C., Garica-Gil, S., Diez, J.B. and Iglesias, J. 2007. Palynological characterisation of gassy sediments in the inner part of Riá de Vigo (NW Spain). New chronological and environmental data. *Geo-marine letters* 27, 289-302.

Murgese, D.S., De Deckker, P., Spooner, M.I. and Young, M. 2008. A 35,000 year record of changes in eastern Indian Ocean offshore Sumatra. *Palaeogeography, Palaeoclimatology, Palaeoecology* 265, 195-213.

Nehring, S. 1994. Spatial distribution of dinoflagellate resting cysts in recent sediments of Kiel Bight, Germany (Baltic Sea). *Ophelia* 39 (2), 137-158.

Nehring, S. 1995. Dinoflagellate resting cysts as factors in phytoplankton ecology of the North Sea. *Helgoländer meeresuntersuchungen* 49, 375-392.

Nehring, S. 1997. Dinoflagellate resting cysts from recent German coastal sediments, *Botanica Marina* 40, 307-324.

Novichkova, E.A. and Polyakova, E.I. 2007. Dinoflagellate cysts in the surface sediments of the White Sea. *Oceanology* 47 (5), 660-670.

Orlova, T., Yu, T., Morozova, K.E., Gribble, D.M., Kulis, D. and Anderson, D.M. 2004. Dinoflagellate cysts in recent marine sediments from the East Coast of Russia. *Botanica Marina* 47(3), 184-201.

Parra, I. 1994. Quantification des précipitations à partir des spectres polliniques actuels et fossiles: du Tardiglaciaire a' l'Holocène supérieur de la cote méditerranéenne espagnole, Thèse en Sciences, EPHE Univ. Montpellier II, 217 pp.

Patterson, R.T., Prokoph, A., Kumar, A., Chang, A.S. and Roe, H.M. 2005. Holocene variability in pelagic fish and phytoplankton productivity along the west coast of Vancouver Island, NE Pacific Ocean. *Marine Micropaleontology* 55, 183-204.

Peña-Manjarrez, J.L., Helenes, J., Gaxiola-Castro, G. and Orellano-Cepeda, E. 2005. Dinoflagellate cysts and bloom events at Todos Santos Bay, Baja California, México, 1999-2000. *Continental Shelf Research* 25, 1375-1393.

Persson, A., Godhe, A. and Karlson, B. 2000. Dinoflagellate cysts in recent sediments from the West coast of Sweden. *Botanica Marina* 43, 66-79.

Polyakova, Y.I., Bauch, H.A. and Klyuvitkina, T.S. 2004. Early to middle Holocene changes in Laptev Sea water masses deduced from diatom and aquatic palynomorph assemblages. *Global and Planetary Change* 48, 208-222.

Pospelova, V., Chmura, G.L. and Walker, H.A. 2004. Environmental factors influencing the spatial distribution of dinoflagellate cyst assemblages in shallow lagoons of southern New England (USA). *Review of Palaeobotany and Palynology* 128, 7-34.

Pospelova, V., de Vernal, A. and Pedersen, T.F. 2008. Distribution of dinoflagellate cysts in surface sediments from the northeastern Pacific Ocean (43-25°N) in relation to sea-surface temperature, productivity and coastal upwelling. *Marine Micropaleontology* 68 (1-2), 21-48.

Pospelova, V., Pedersen, T.F. and de Vernal, A. 2006. Dinoflagellate cysts as indicators of climatic and oceanographic changes during the past 40 kyr in the Santa Barbara Basin, southern California. *Paleoceanography* 21, PA2010, doi: 10.1029/2005PA001251.

Prauss, M. 2002. Recent global warming and its influence on marine palynology within the central Santa Barbara basin, offshore southern California, U.S.A. *Palynology* 26, 217-238.

Radi, T. and de Vernal, A. 2004. Dinocyst distribution in surface sediments from the northeastern Pacific margin (40-60°N) in relation to hydrographic conditions, productivity and upwelling. *Review of Palaeobotany and Palynology* 128, 169-193.

Radi, T. and de Vernal, A. 2008. Dinocysts as proxy of primary productivity in mid-high latitudes of the Northern Hemisphere. *Marine Micropaleontology* 68 (1-2), 84-114.

Radi, T., de Vernal, A. and Peyron, O. 2001. Relationships between dinoflagellate cyst assemblages in surface sediment and hydrographic conditions in the Bering and Chukchi seas. *Journal of Quaternary Science* 16, 667-680.

Radi, T., Pospelova, V., de Vernal, A. and Vaughn Barrie, J. 2007. Dinoflagellate cysts as indicators of water quality and productivity in British Columbia estuarine environments. *Marine Micropaleontology*, 62 (4), 269-297.

Reid, P.C. 1972. Dinoflagellate cyst distribution around the British Isles. *Journal of marine biology Association U.K.* 52, 939-944.

Ribeiro, S. and Amorim, A. 2008. Environmental drivers of temporal succession in recent dinoflagellate cyst assemblages from a coastal site in the North-East Atlantic (Lisbon Bay, Portugal). *Marine Micropaleontology* 68, 156-178.

Richerol, T., Rochon, A., Blasco, S., Scott, D.B., Schell, T.M. and Bennett, R.J. 2008. Distribution of dinoflagellate cysts in surface sediments of the Mackenzie Shelf and Amundsen Gulf, Beaufort Sea (Canada). *Journal of Marine Systems* 74, 825-839.

Rochon, A., de Vernal, A., Turon, J.-L., Matthiessen, J. and Head, M. 1999. Distribution of Recent Dinoflagellate cysts in surface sediments from the North Atlantic Ocean and adjacent seas in relation to sea-surface parameters. *American Association of Stratigraphic Palynologists Contribution Series* 35, 1-150.

Roncaglia, L. 2004. Palynofacies analysis and organic-walled dinoflagellate cysts as indicators of palaeo-hydrographic changes: an example from Holocene sediments in Skalafjord, Faroe Islands. *Marine micropaleontology* 50, 21-42.

Rossignol-Strick, M. and Duzer, D. 1979. West African vegetation and climate since 22 500 BP from deep sea cores palynology. *Pollen et Spores* 21, 105-134.

Saetre, M.M.L., Dale, B., Abdullah, M.I. and Saetre, G.-M. 1997. Dinoflagellate cysts as potential indicators of industrial pollution in a Norwegian fjord. *Marine Environmental Research* 44, 167-189.

Sangiorgi, F., Fabbri, D., Comandini, M., Gabbianelli, G. and Tagliavini, E. 2005. The distribution of sterols and organic-walled dinoflagellate cysts in surface sediments of the North-western Adriatic Sea (Italy). *Estuarine, Coastal and Shelf Science* 64, 395-406.

Seidenkrantz, M.-S., Roncaglia, L., Fischel, A., Heilmann-Clausen, C., Kuijpers, A. and Moros, M. 2008. Variable North Atlantic climate seesaw patterns documented by a late Holocene marine record from Disko Bugt, West Greenland. *Marine Micropaleontology* 68 (1-2), 66-83.

Shaozhi, M. and Harland, R. 1993. Quaternary organic-walled dinoflagellate cysts from the South China Sea and their paleoclimatic significance. *Palynology* 17, 47–65.

Shi N., Dupont L.M., Beug H.-J. and Schneider R. 2000. Correlation between Vegetation in Southwestern Africa and Oceanic Upwelling in the Past 21,000 Years. *Quaternary Research* 54 (1), 72-80.

Shimoyama S., Kosugi M., Matsuoka K., Kataoka H., Sato N., Endo K., Noi H., Takemura K., Ichihara T., Miura N. and Thono I. 1996. Integral analysis for the paleoenvironment of the coastal lowland around the innermost Ariake Bay, West Japan. *Kantô Field* 4, 53-73.

Solignac, S., Giraudeau, J. and de Vernal, A., 2006. Holocene sea surface conditions in the western North Atlantic: Spatial and temporal heterogeneities. Paleoceanography 21, PA2004, doi:10.1029/2005PA001175.

Sorrell, P., Popescu, S.-M., Head, M.J., Suc, J.-P., Klotz, S. and Oberhänsli, H. 2006. Hydrographic development of the Aral Sea during the last 2000 years based on a quantitative analysis of dinoflagellate cysts. *Palaeogeography, Palaeoclimatology, Palaeoecology* 234, 304-327.

Sprangers, M., Dammers, N., Brinkhuis, H., van Weering, T.C.E. and Lotter, A.F. 2004. Modern organic-walled dinoflagellate cyst distribution offshore NW Iberia; tracing the upwelling system. *Review of Palaeobotany and Palynology* 128, 97-106.

Stancliffe, R.P.W. and Matsuoka, K. 1991. Marine Palynomorphs found in Holocene sediments off the coast of Northwestern Kyushu, Japan. *Bulletin of the Faculty of Liberal Arts, Nagasaki University, Natural Science* 31(2), 661-681.

Stoker, M.S., Harland, R. and Graham, D.K. 1991. Glacially influenced basin plain sedimentation in the southern Faeroe-Shetland Channel, northwest United Kingdom continental margin. *Marine Geology* 100, 185-199.

Storkey, 2006. Distribution of marine palynomorphs in surface sediments, Prydz bay, Antarctica. Unpublished Ph.D. thesis. School of Earth Sciences, Victoria University of Wellington.

Targarona J. 1997. Climatic and oceanographic evolution of the Mediterranean Region over the last glacial–interglacial transition; a palynological approach. Ph.D. thesis, Utrecht University.

Targarona, J., Warnaar, J., Boessenkool, K.P., Brinkhuis, H. and Canals, M. 1999. Recent dinoflagellate cyst distribution in the North Canary Basin, NW Africa. *Grana* 38, 170-178.

Thibodeau, B., de Vernal, A. and Mucci, A., 2006. Recent eutrophication and consequent hypoxia in the bottom waters of the Lower St. Lawrence Estuary: Micropaleontological and geochemical evidence. *Marine Geology* 231, 37-50.

Thorsen, T.A., Dale, B. 1997. Dinoflagellate cysts as indicators of pollution and past climate in a Norwegian fjord. *Holocene* 7, 433-446.

Turon, J.-L. 1984. Le palynoplankton dans l'environment actuel de l'Atlantic nord-oriental. Evolution climatique et hydrologique depuis le dernier maximum glaciaire. *Mémoire de l'institut de Géologie du Bassin d'Aquitaine* 17, 1-313.

Turon, J.-L. and Londeix, L. 1988. Les asssemblages de kystes de dinoflagellés en Méditerranée occidentale (Mer d'Alboran): mise en évidence de l'évolution des paléoenvironnement depuis le dernier maximum glaciaire. *Bulletin Centres Recherche Exploration-Production Elf-Aquitaine* 12, 313-344.

Turon, J.-L., Lézine, A.-M. and Denèfle, M. 2003. Land-sea correlations for the last glaciation inferred from a pollen and dinocyst record from the Portuguese margin. *Quaternary Research* 59 (1), 88-96.

Vásquez-Bedoya, L.F., Radi, T., Ruiz-Fernández, A.C., de Vernal, A., Machain-Castillo, M.L., Kielt, J.F. and Hillaire-Marcel, C., 2008. Centennial record of organic-walled dinoflagellate cysts and benthic foraminifera in coastal sediments from the Gulf of Tehuantepec, eastern equatorial Pacific. *Marine Micropaleontology* 68, 49-65.

Maenhaut van Lemberge, V. 1986. Studie van de distributie van organische resten van recente mikroörganismen en van geremanieerd phytoplankton in waddenafzettingen. Verslag over het eerste mandaat van een specialisatiebeurs toegekend door het IWONL.

Verardo, S. 1999. Dinoflagellates. In: Cronin, T., Wagner, R. and Slattery, M. (Eds.), *Microfossils from Chesapeake Bay sediments - illustrations and species database*. United States Geological Survey Open-File Report 99-145, pp. 1-159.

Verleye, T., Mertens, K., N., Louwye, S. and Arz, H.W. 2008. Holocene Salinity changes in the southwestern Black Sea: a reconstruction based on dinoflagellate cysts. *Palynology* 32.

Vilanova, I., Guerstein, Akselman, R. and Prieto, A.R. 2008. Mid- to Late Holocene organic-walled dinoflagellate cysts from the northern Argentine shelf. *Review of Palaeobotany and Palynology* 152 (1-2), 11-20.

Vink, A., Zonneveld, K.A.F. and Willems, H. 2000. Organic-walled dinoflagellate cysts in western equatorial Atlantic surface sediments: distributions and their relation to environment. *Review of Palaeobotany and Palynology* 112, 247-286.

Vink, A., Baumann, K.-H., Boeckel, B., Esper, O., Kinkel, H., Volbers, A. N. A., Willems, H. and Zonneveld, K.A.F. 2004. Coccolithophorid and dinoflagellate synecology in the South and Equatorial Atlantic: Improving the palaeoecological significance of phytoplanktonic microfossils, In: Wefer, G., Mulitza, S. and Ratmeyer, V. (Eds.), *The South Atlantic in the Late Quaternary: Reconstruction of Material Budgets and Current Systems.* Springer, Berlin, pp. 101-120.

Voronina, E., Polyak, L., de Vernal, A. and Peyron, O. 2001. Holocene variations of sea-surface conditions in the southeastern Barents Sea, reconstructed from dinoflagellate cyst assemblages. *Journal of Quaternary Science* 16 (7), 717-726.

Wall, D. 1967. Fossil microplankton in deep-sea cores from the Caribbean Sea. *Palaeontology* 10, 95-123.

Wall, D. and Dale, B. 1970. Living Hystrichosphaerid Dinoflagellate Spores from Bermuda and Puerto Rico. *Micropaleontology* 16 (1), 47-58.

Wall, D. and Dale, B. 1973. Paleosalinity relationships of dinoflagellates in the late Quaternary of the Black Sea - a summary. *Geoscience and Man*, 7, 95-102.

Wall, D. and Dale, B. 1974. Dinoflagellates in late Quaternary deep-water sediments of the Black Sea. In: Degens, E.T. and Ross, D.A. (Eds.), *The Black Sea - geology, chemistry and biology*. American Association of Petroleum Geologists, Memoir 20, Tulsa, 364-380.

Wall, D. and Warren, J.S. 1969. Dinoflagellates in Red Sea piston cores. In: Degens, E.T. and Ross, D.A. (Eds.), *Hot Brines and Recent Heavy Metal Deposits in the Red Sea*. Springer Verlag, Berlin, pp. 317-327.

Wall, D., Dale, B. and Harada, K. 1973. Descriptions of new fossil dinoflagellates from the late Quaternary of the Black Sea. *Micropaleontology* 19, 18-31.

Wall, D., Dale, B., Lohman, G.P. and Smith, W.K. 1977. The environmental and climatic distribution of dinoflagellate cysts in modern marine sediments from regions in the North and South Atlantic Ocean and adjacent seas. *Marine Micropaleontology* 2, 121-200.

Wang, Z., Matsuoka, K., Qi, Y. and Chen, J. 2004a. Dinoflagellate cysts in recent sediments from Chinese coastal waters. *Marine ecology* 25 (4), 289-311.

Wang, Z., Matsuoka, K., Qi, Y., Chen, J. and Lu, S. 2004b. Dinoflagellate cyst records in recent sediments from Daya Bay, South China Sea. *Phycological Research* 52, 396-407.

Wang, Z., Qi, Y., Lu, S., Wang, Y. and Matsuoka, K. 2004c. Seasonal distribution of dinoflagellate cysts in surface sediments from Changjiang River Estuary. *Phycological Research* 52, 387-395.

Williams, D.B. 1971. The occurrence of dinoflagellates in marine sediments. In: B.M. Funnel and W.R. Reidel (Eds.), *The Micropalaeontology of the Oceans.* Cambridge University Press, Cambridge, pp. 231-243.

Yu, S.-Y. and Berglund, B.E. 2007. A dinoflagellate cyst record of Holocene climate and hydrological changes along the southeastern Swedish Baltic coast. *Quaternary Research* 67, 215-224.

Yu-Zao, Q., Ying, H., Lei, Z., Kulis, D.M. and Anderson, D.M. 1996. Dinoflagellate cysts from recent marine sediments of the south and east China Seas. *Asian Marine Biology* 13, 87-103.

Zhao, Y-Y. and Morzadec-Kerfourn, M-T. 1992. Kystes de dinoflagellés, pollen et spores des sédiments quaternaires du bassin abyssal de Mer de Chine sud: leur signification paléoenvironmentale. *Revue de Micropaléontologie* 35, 77-88.

Zippi, P.A. 1992. Dinoflagellate cyst stratigraphy and climate fluctuations in the eastern North Atlantic during the last 150,000 years. In: Head, M. and Wrenn, J. (Eds.), *Neogene and Quaternary Dinoflagellate Cysts and Acritarchs.* American Association of Stratigraphic Palynologists Foundation, Dallas, Texas, pp. 55-68.

Zonneveld, K.A.F. 1995. Palaeoclimatical and palaeo-ecological changes during the last deglaciation in the Eastern Mediterranean; implications for dinoflagellate ecology. *Review of Palaeobotany and Palynology* 84, 221-253.

Zonneveld, K.A.F. 1997. Dinoflagellate cyst distribution in surface sediments of the Arabian Sea (Northwestern Indian Ocean) in relation to temperature and salinity gradients in the upper water column. *Deep-Sea Research II* 44, 1411-1443.

Zonneveld, K.A.F., Hoek, R., Brinkhuis, H. and Willems, H. 2001. Lateral distribution of organic walled dinoflagellates in surface sediments of the Benguela upwelling Region. *Progress in Oceanography* 48, 25-72.

Zonneveld, K.A.F., Ganssen, G., Troelstra, S., Versteegh, G.J.M. and Visscher, H. 1997. Mechanisms forcing abrupt fluctuations of the Indian Ocean summer monsoon during the last deglaciation. *Quaternary Science Reviews* 16, 187-201.

Appendix V

Achomosphaera Evitt 1963
Ataxiodinium choane Reid 1974
Bitectatodinium spongium Zonneveld 1997
Bitectatodinium tepikiense Wilson 1973
Brigantedinium Reid, 1977 ex. Lentin and Williams 1993
Brigantedinium cariacoense (Wall 1967) Lentin and Williams 1993
Brigantedinium simplex Wall 1965 ex. Lentin and Williams 1993
Echinidinium Zonneveld 1997
Echinidinium aculeatum Zonneveld 1997
Echinidinium delicatum Zonneveld 1997
Echinidinium euaxum (Head 1993) Zonneveld 1997
Echinidinium granulatum Zonneveld 1997
Echinidinium transparantum Zonneveld 1997
Impagidinium aculeatum (Wall 1967) Lentin and Williams 1981
Impagidinium paradoxum (Wall 1967) Stover and Evitt 1978
Impagidinium patulum (Wall 1967) Stover and Evitt 1978
Impagidinium strialatum (Wall 1967) Stover and Evitt 1978
Impagidinium Stover & Evitt 1978
Islandinium minutum Harland and Reid in Harland et al. 1980
Lejeunecysta marieae Harland in Harland et al. 1991 ex. Lentin and Williams 1993
Lejeunecysta oliva (Reid 1977) Turon and Londeix 1988
Lejeunecysta sabrina (Reid 1977) Bujak 1984
Lejeunecysta sp. A
Lingulodinium machaerophorum (Deflandre and Cookson 1955) Wall 1967
Melitasphaeridium choanophorum (Deflandre and Cookson, 1955) Harland and Hill, 1979
Nematosphaeropsis labyrinthus (Ostenfeld 1903) Reid 1974
Operculodinium centrocarpum (Deflandre and Cookson 1955) Wall 1967
Operculodinium israelianum (Rossignol 1962) Wall 1967
Operculodinium janduchenei Head et al. 1989
Polysphaeridium zoharyi (Rossignol 1962) Bujak et al. 1980
Quinquecuspis concreta (Reid 1977) Harland 1977
Selenopemphix nephroides Benedek 1972; emend. Bujak in Bujak et al., 1980; emend. Benedek and Sarjeant 1981
Selenopemphix quanta (Bradford 1975) Matsuoka 1985
Selenopemphix selenoides Benedek, 1972
Spiniferites bentorii (Rossignol 1964) Wall and Dale 1970
Spiniferites elongatus Reid 1974
Spiniferites lazus Reid 1974
Spiniferites membranaceus (Rossignol 1964) Sarjeant 1970
Spiniferites mirabilis (Rossignol 1964) Sarjeant 1970
Spiniferites pachydermus (Rossignol 1964) Reid 1974
Spiniferites ramosus (Ehrenberg 1838) Loeblich and Loeblich 1966; emend. Davey and Williams 1966
Spiniferites scabratus (Wall 1967) Sarjeant 1970
Spiniferites Mantell, 1850; emend. Sarjeant 1970
Stelladinium reidii Bradford 1975
Tuberculodinium vancampoae (Rossignol 1962) Wall 1967
Votadinium calvum Reid 1977

Appendix VI

Ataxiodinium choane Reid 1974
Bitectatodinium tepikiense Wilson 1973
Brigantedinium cariacoense (Wall 1967) Lentin and Williams 1993
Brigantedinium simplex Wall 1965 ex Lentin and Williams 1993
Brigantedinium Reid 1977 ex Lentin and Williams 1993
Echinidinium Zonneveld 1997
Impagidinium aculeatum (Wall 1967) Lentin and Williams 1981
Impagidinium pallidum Bujak 1984
Impagidinium paradoxum (Wall 1967) Stover and Evitt 1978
Impagidinium patulum (Wall 1967) Stover and Evitt 1978
Impagidinium sphaericum (Wall 1967) Lentin and Williams 1981
Impagidinium strialatum (Wall 1967) Stover and Evitt 1978
Impagidinium velorum Bujak 1984
Impagidinium Stover and Evitt 1978
Islandinium minutum Harland and Reid in Harland et al. 1980
Lejeunecysta (Arztner and Dörhöher 1978) Lentin and Williams 1976
Lingulodinium machaerophorum (Deflandre and Cookson 1955) Wall 1967
Nematosphaeropsis labyrinthus (Ostenfeld 1903) Reid 1974
Operculodinium centrocarpum (Deflandre and Cookson 1955) Wall 1967
Operculodinium israelianum (Rossignol 1962) Wall 1967
Cyst of *Pentapharsodinium dalei* Indelicato & Loeblich III 1986
Polykrikos schwartzii Bütschli 1873
Pyxidinopsis reticulata (McMinn & Sun 1994) Marret & de Vernal 1997
Quinquecuspis concreta (Reid, 1977) Harland, 1977
Selenopemphix nephroides Benedek 1972; emend. Bujak in Bujak et al., 1980; emend. Benedek and Sarjeant 1981
Selenopemphix quanta (Bradford 1975) Matsuoka 1985
Spiniferites bentorii (Rossignol 1964) Wall and Dale 1970
Spiniferites delicatus Reid 1974
Spiniferites elongatus Reid 1974
Spiniferites hyperacanthus (Deflandre and Cookson 1955) Cookson and Eisenack 1974
Spiniferites lazus Reid 1974
Spiniferites membranaceus (Rossignol 1964) Sarjeant 1970
Spiniferites mirabilis (Rossignol 1964) Sarjeant 1970
Spiniferites ramosus (Ehrenberg 1838) Loeblich and Loeblich 1966; emend. Davey and Williams 1966
Spiniferites (Mantell 1850) Sarjeant 1970
Tectatodinium pellitum Wall, 1967 emend. Head 1994
Trinovantedinium applanatum (Bradford 1977) Bujak and Davies 1983
Tuberculodinium vancampoae (Rossignol 1962) Wall 1967

Glossary

A

ACETOLYSIS a decomposition of an organic molecule through the action of acetic acid or acetic anhydride.

ACRITARCH any small, non-acid soluble (i.e. non-carbonate, non-siliceous) organic structure that cannot otherwise be accounted for is classified as an acritarch.

ALKENONE long-chain (C_{37}-C_{39}) unsaturated ketones found as highly resistant organic compounds in the membranes of haptophytes.

ACCELERATOR MASS SPECTOMETRY (AMS) differs from other forms of mass spectrometry in that it accelerates ions to extraordinarily high kinetic energies before mass analysis. The special strength of AMS among the mass spectrometric methods is its power to separate a rare isotope from an abundant neighboring mass.

ANTICYCLONE a region where the surface atmospheric pressure is high, relative to its surroundings – often called 'a high'.

ACCUMULATION RATE (AR) see Mass Accumulation rate.

ARCHEOPYLE the excystment opening of dinoflagellate cysts.

ASCIDIANS (ASCIDIACEA OR SEA SQUIRTS) a class in the Urochordata subphylum of sac-like marine invertebrate filter feeders. Ascidians are characterized by a tough outer 'tunic' made of the polysaccharide tunicin, as compared to other tunicates which are less rigid.

AUTOTROPH an organism that produces complex organic compounds from simple inorganic molecules using energy from light or inorganic chemical reactions.

B

BIOMARKER can be any kind of molecule indicating the existence, past or present, of living organisms.

BRANCHED AND ISOPRENOID TETRAETHER INDEX (BIT INDEX) index based on the relative abundance of non-isoprenoidal GDGT (Glycerol Dialkyl Glycerol Tetraethers) derived from organisms living in the terrestrial environment. The BIT index can be used for the quantification of the relative fluvial input of terrestrial organic matter.

BLOCKING a phenomenon, most often associated with stationary high-pressure systems in the mid latitudes of the northern hemisphere, which produces periods of abnormal weather.

BØLLING ALLERØD (BA) a warm and moist interstadial period that occurred during the final stages of the last glacial period. This warm period ran from ca. 14700 to 12700 years before present. It began with the end of the cold period known as the Oldest Dryas, and ended abruptly with the onset of the Younger Dryas, a cold period that reduced temperatures back to near glacial levels within a decade.

BOX CORE core taken using a box corer of about 300 kg lowered to the bed by use of a cable-winch system.

BEFORE PRESENT (BP) a time scale used in archaeology, geology, and other scientific disciplines to specify when events in the past occurred. Because the 'present' time changes, standard practice is to use 1950 CE as the arbitrary origin of the age scale. For example, 1500 BP means 1500 years before 1950, that is, in the year 450 CE.

BLACKMAN-TUKEY (BT) METHOD method of spectral analysis (Blackman and Tukey 1958).

C

$CACO_3$ calcium carbonate.

CAF_2 calcium fluoride.

CALCAREOUS DINOFLAGELLATE CYST a monophyletic group of dinoflagellates that have the potential to produce cysts during their life cycle, which are characterized by the incorporation of calcite in at least one layer of the cyst wall. Calcareous dinoflagellates first appear more or less synchronously with the organic-walled dinoflagellates in the Late Triassic and represent a significant component of the marine phytoplankton at least since the Early Cretaceous documented by their often excellent fossil preservation. They are present at virtually all latitudes in all marine environments ranging from neritic to open oceanic.

CALYPSO CORE a core taken by a special kind of piston-corer which allows longer sediment recovery.

CARIBBEAN SURFACE WATER (CSW) water mass originating from the North Equatorial Current and the North Brazil Current with significant input of low salinity waters from the Amazon and Orinoco rivers in October to November.

CALCIDISCUS LEPTOPORUS – EMILIANIA HUXLEYI DISSOLUTION INDEX (CEX) dissolution index based on a ratio between the relative abundances of both taxa (Dittert et al., 1999).

CALCIDISCUS LEPTOPORUS – EMILIANIA HUXLEYI + GEPHYROCAPSA ERICSONII DISSOLUTION INDEX (CEX') dissolution index based on CEX with the addition of Gephyrocapsa ericsonii (Boeckel and Baumann 2004).

CHLOROPHYTA a division of green algae, includes about 7000 species of mostly aquatic photosynthetic eukaryotic organisms. The division contains both unicellular and multicellular species.

CHN ANALYZER a scientific instrument which can determine the elemental composition of a sample. The name derives from the three primary elements measured by the device: carbon (C), hydrogen (H) and nitrogen (N). Sulfur (S) and oxygen (O) can also be measured.

CHRYSOMONAD golden-yellow to brown freshwater algae of the class Chrysomonadales, living solitaire or in colonies. Blooms may color the water brown.

CLAVATE having one end thickened; club-shaped.

COCCOLITHS individual plates of calcium carbonate formed by coccolithophores which are arranged around them in a coccosphere.

COCCOLITHOPHORES small (2-25 µm) unicellular algae that belong to the phylum Haptophyta and the division Prymnesiophyceae. They constitute one of the major plankton groups and are preserved as coccoliths in marine sediments. They are the most important pelagic calcifying organisms in the modern ocean.

CONFOCAL LASER SCANNING MICROSCOPY (CLSM) a technique for obtaining high-resolution optical images. The key feature of confocal microscopy is its ability to produce in-focus images of thick specimens, a process known as optical sectioning. Images are acquired point-by-point and reconstructed with a computer, allowing three-dimensional reconstructions of topologically-complex objects.

COPEPODS a group of small crustaceans found in the sea and in nearly every freshwater habitat. Many species are planktonic (drifting in sea waters), but most are benthic (living on the ocean floor). Some continental species may live in limnoterrestrial habitats and other wet terrestrial places, such as swamps, bogs, springs, ephemeral ponds and puddles, damp moss, water-filled recesses (phytotelmata) of plants such as bromeliads and pitcher plants or under leaf fall in wet forests. Many live underground in marine and freshwater caves, sinkholes or stream beds. Copepods are sometimes used as bioindicators.

CPS counts per second.

CHLORIN STERYL ESTERS (CSES) are organic compounds consist of pyropheophorbide-a (a chlorophyll-a degradation product) and various sterols which can be traced back to known biological precursors, and hence can serve as biomarkers.

CRENARCHAEA (CRENARCHAEOTA OR EOCYTES) a phylum of the Archaea, which are the most abundant archaea in the marine environment.

CYANOBACTERIA (BLUE-GREEN ALGAE OR BLUE-GREEN BACTERIA OR CYANOPHYTA) a phylum of bacteria that obtains their energy through photosynthesis.

D

DANSGAARD/OESCHGER EVENTS (D/O EVENTS) are perhaps the most pronounced climate changes that have occurred during the past 120 kyr. They are not only large in amplitude, but also abrupt. In the Greenland ice cores, D/O events start with a rapid warming by 5–10 °C within at most a few decades, followed by a plateau phase with slow cooling lasting several centuries, then a more rapid drop back to cold stadial conditions. The events are not local to Greenland but are global (Voelker, 2002). Amplitudes are largest in the North Atlantic region, and many Southern Hemisphere sites, especially those in the South Atlantic, reveal a hemispheric 'see-saw'effect (cooling while the north is warming).

DRY BULK DENSITY (DBD) a measure of the weight of the soil per unit volume (g/cc), usually given on an oven-dry (110 °C) basis. Variation in bulk density is attributable to the relative proportion and specific gravity of solid organic and inorganic particles and to the porosity of the soil.

DCM dichloromethane.

DIATOMS (CLASS BACILLARIOPHYCEAE) microscopic (1-1000 µm in size) unicellular algae that inhabit almost every aquatic environment on earth. They are characterized mostly via their cell walls, which are composed of opaline silicate – being made up of two overlapping valves that together constitute the frustules. As with other siliceous microfossil groups (e.g. the silicoflagellates and radiolarians),

diatoms are often well preserved in sedimentary sequences and have become invaluable for unraveling past environmental change in both freshwater and marine systems.

DISSOLVED INORGANIC CARBON (DIC) OR TOTAL INORGANIC CARBON (TIC) the sum of inorganic carbon species in a solution. The inorganic carbon species include carbon dioxide, carbonic acid, bicarbonate anion, and carbonate anion.

DINOFLAGELLATES eukaryotic, single-celled organisms in which the motile cell possesses two flagella and a unique type of nucleus – the dinokary¬on. Based on these characteristics, they are classified in the division Dinoflagellata.

DINOFLAGELLATE CYST (DINOCYST) the hypnozygotes produced by planktonic dinoflagellates during the sexual phase of the life cycle, and are fossilizable if the wall exists of a resistant substance such as dinosporin, calcium carbonate or silica. Cysts are formed within the thecal plates of the motile stage, which sometimes results in the reflection of the morphological features of the motile form. The identification criteria of the cyst are the furrows housing the flagella (cingulum and sulcus), plate patterns, ornamentation and the excystment opening or archaeopyle. The latter is the opening through which the new motile stage exits. Most of the cysts serve as a benthic resting stage of which the cells are filled with food-storage products and are enclosed in a protective cell wall. After a mandatory resting period, motiles excyst out of the 'seed bed'.

DINOSPORIN a complex organic polymer similar to sporopollenin, which composes the walls of some fossilizable dinoflagellate cysts.

DINOSTEROL (4α,23,24-trimethylcholest-22-en-3β-ol) a biomarker almost uniquely produced by dinoflagellates, with minor quantities occurring in diatoms.

E

EL NIÑO SOUTHERN OSCILLATION (ENSO) the combined quasi-periodic oscillations of El Niño (temperature changes in the eastern Pacific) and the southern oscillation (atmospheric pressure changes in the western and south-central Pacific).

END-MEMBER (EM) MODEL a numerical-statis¬tical algorithm that can be applied to the carbonate-free grain-size distributions. The end-member algorithm attempts to explain observed variations in natural sediments as a result of mixing and has been used successfully to 'unmix' sediments produced by linear mixing. This enables a distinction between wind-blown and fluvially derived sediment fractions and use of their relative proportions as paleoclimate proxies, for the reconstruction of wind strength, aridity (or rainfall) and upwelling variations.

EOLIAN SEDIMENTS sediments deposited by the action of wind.

F

FLUVIAL SEDIMENTS sediments deposited by the action of rivers and streams.

FORAMINIFERA an order of Sarcodina, the members of which have numerous anastomosing pseudopodia and a shell that is calcareous. The shells of these organisms, when deposited in oceanic sediments, are the source of climatic information.

G

GLYCEROL DIALKYL GLYCEROL TETRAETHERS (GDGTS) membrane lipids synthesized by Crenarchaea bacteria, which occur ubiquitously and are unaffected by water redox conditions. Concentrations of these biomarkers are used for the reconstruction of productivity variations. By measuring the relative amounts of GDGTs present in marine sediments, the temperature can be determined at which Crenarchaeota produced their membranes.

GEPHYROCAPSA OCEANICA – EMILIANIA HUXLEYI DISSOLUTION INDEX (GEX) dissolution index based on a ratio between the relative abundances of both taxa (Mertens et al., 2009).

GREENLAND ICE SHEET PROJECT (GISP) a decade-long project to drill ice cores in Greenland that involved scientists and funding agencies from Denmark, Switzerland and the United States. Besides the U.S. National Science Foundation, funding was provided by the Swiss National Science Foundation and the Danish Commission for Scientific Research in Greenland. The ice cores provide a proxy archive of temperature and atmospheric constituents that help to understand past climate variations.

GLEY a type of hydric soil which exhibits a greenish-blue-grey soil color due to wetland conditions.

GAMMA RAY ATTENUATION POROSITY EVALUATION DATA (GRAPE DATA) measured gamma rays by moving a whole round core section along a horizontal Multi-Sensor Track (MST) where successive intervals are continuously bombarded by a beam of radiation. The amount of gamma radiation transmitted through the core is inversely

proportional to the bulk density of the rock or sediment.

GRAVITY CORE a core taken using a gravity corer which is allowed to fall freely through the water and is driven into the bed by its weight. A one-way valve at the top end of the tube permits the passage of water during the descent and prevents flushing of the sample during retrieval and raising of the sampler. A core-catcher generally is present at the inside of the tube just above the cutting edge. Plastic liners are used to minimize the problem of sample extrusion and storage. The core length is limited to 10 core diameters in sand and 20 core diameters in firm clay. A major disadvantage of gravity corers is the compaction of the vertical structure of the bed material during sampling.

H

H_2O_2 hydrogen peroxide

HAPTOPHYTA (PRYMNESIOPHYTA) a phylum of algae. The chloroplasts are pigmented similarly to those of the heterokonts, but the structure of the rest of the cell is different, so it may be that they are a separate line whose chloroplasts are derived from similar endosymbionts. The cells typically have two slightly unequal flagella, both of which are smooth, and a unique organelle called a haptonema, which is superficially similar to a flagellum but differs in the arrangement of microtubules and in its use. The name comes from the Greek *hapsis*, touch, and *nema*, thread. The mitochondria have tubular cristae. The best-known haptophytes are coccolithophores.

HARMFUL ALGAL BLOOM (HAB) bloom phenomenon that contain toxins or causes negative impacts.

HCL Hydrochloric acid.

HF Hydrofluoric acid.

HEINRICH EVENT (HE) an interval of rapid flow of icebergs from the margins of ice sheets into the North Atlantic, causing deposition of sediment layers rich in debris eroded from the land (Heinrich layers). Six events are distinguished which are labeled H1-H6. These icebergs caused addition of large amounts of freshwater in the North Atlantic. Such inputs of cold, fresh water may well have altered the density-driven thermohaline circulation patterns of the ocean, and often coincide with indications of global climate fluctuations. Various mechanisms have been proposed to explain the cause of Heinrich events. Most centre around the activity of the Laurentide ice sheet, but others suggest that the unstable West Antarctic Ice Sheet played a triggering role.

HEAVY LIQUIDS dense fluids or solutions used to separate materials of different density through their buoyancy. Materials with a density greater than the heavy liquid will sink, while materials with a density less than the heavy liquid will float on the liquid surface.

HEMATITE is the mineral form of iron (III) oxide (Fe2O3), one of several iron oxides. Hematite crystallizes in the rhombohedral system, and it has the same crystal structure as ilmenite and as corundum. Hematite and ilmenite form a complete solid solution at temperatures above 950°C. Hematite is colored black to steel or silver-gray, brown to reddish brown, or red. It is mined as the main ore of iron.

HEMIPELAGIC SEDIMENTS drape upper and middle continental slopes around the world. They grade from predominantly terrigenous muds into biogenic oozes. Even where biogenic constituents predominate, hemipelagic sediments typically have a dark color, which is imparted by the terrigenous component. The composition of the terrigenous muds reflects weathering intensity in the sedimentary provenance. The terrigenous muds, which were delivered to the ocean by rivers or by direct runoff from land, remained in suspension and were carried out to the continental margin by surface currents or by sediment-gravity flows.

HETEROTROPH an organism that uses organic substrates to get its chemical energy for its life cycle. This contrasts with autotrophs such as plants which are able to directly use sources of energy such as light to produce organic substrates from inorganic carbon dioxide.

HOLOCENE the relatively warm epoch, which started around 11500 years ago and runs up to present time. It is marked by several short-lived particularly warm periods, the most significant is called the Holocene optimum.

HIGH PERFORMANCE LIQUID CHROMATOGRAPHY / ATMOSPHERIC PRESSURE POSITIVE ION CHEMICAL IONIZATION MASS SPECTROMETRY (HPLC/APCI-MS) method used for GDGT (Glycerol Dialkyl Glycerol Tetraether) analysis.

HYDROLOGICAL CYCLE the movement of water and water vapor among the atmosphere, land and ocean, through evaporation, precipitation, runoff, and subsurface groundwater flow.

I

INTERGLACIAL a warmer period during glacial epochs when the major ice sheets recede to higher latitudes. The current Holocene interglacial has persisted since the Pleistocene.

INTERSTADIAL a relatively warmer stage within a glacial

phase during which the ice advance is temporarily halted.

INTERTROPICAL CONVERGENCE ZONE (ITCZ) a narrow region within the tropics where air originating in the northern and southern hemispheres converge and generally produce cloudy, showery weather. Over the Atlantic and Pacific it is the boundary between the north-east and south-east trade winds. The mean position is somewhat north of the equator but over the continents the range of motion is considerable.

K

KOH potassium hydroxide.

L

LAMINA a thin layer of sediment.

LAST GLACIAL MAXIMUM (LGM) the coldest period at the end of the last ice age between 24000 and 18000 years ago when the ice sheets over the northern hemisphere reached their greatest extent.

LOWER PHOTIC ZONE FLORA (LPZ FLORA) coccolithophore species living in deeper, well-stratified, low-temperature (<10°C) nutrient-rich sub-thermocline waters (Okada, 1983). It is generally accepted that these species have an inverse relationship to both productivity and upwelling (Okada and Matsuoka, 1996).

M

MOISTURE AND DENSITY (MAD) classical measurements for dry bulk density on discrete samples.

MAGNETIC SUSCEPTIBILITY the degree of magnetization of a material in response to an applied magnetic field.

MASS ACCUMULATION RATE (MAR) calculated from sedimentation rate by multiplying with dry bulk density.

MG/CA RATIO the ratio of the elements Mg and Ca in shells of foraminifera. The ratio can be used as index of past temperature changes.

MICROFORAMINIFERAL LINING the organic inner surfaces of microforaminifera, which resist palynological treatment.

MILLENNIAL-SCALE OSCILLATIONS fluctuations in climate lasting thousands of years wich are generally larger during glacial than interglacial intervals.

MINERAL BALLAST hypothesis the hypothesis that suggests that enhanced productivity is coupled to enhanced organic carbon preservation.

MUD VOLCANO phenomenon created by geo-excreted liquids and gases, although there are several different processes which may cause such activity. Temperatures are much cooler than igneous processes.

N

NANNOFOSSILS group of microfolssils that includes both coccoliths and nannofossils s.s., which may be unrelated but are both composed of calcite. Most Quaternary nannofossils are coccoliths.

NBS STANDARDS standards defined by the National Bureau of Standards (now NIST - National Institute of Standards and Technology).

NORTH ATLANTIC DEEP WATER (NADW) a water mass that forms in the high-latitude North Atlantic by winter chilling of salty surface water, sinks, and flows southward at depths of 2 to 4 km.

NORTH ATLANTIC OSCILLATION (NAO) an index of the circulation in the North Atlantic that is measured in terms of difference in pressure between the Azores and Iceland. In winter this index tends to switch between a strong westerly flow with pressure low to the north and high in the south and the reverse: the former tends to produce above normal temperatures over much of the northern hemisphere, the latter the reverse.

NORTH BRAZIL CURRENT (NBC) a well-established western boundary current that carries warm water of South Atlantic origin northwest along the coast of Brazil, across the equator and into the northern hemisphere.

NORTH EQUATORIAL CURRENT (NEC) a broad westward flowing current fortified by the Atlantic trade wind belt, the NEC that forms the southern limb of the North Atlantic subtropical gyre. The current originates from the northwestern coast of Africa, where it is fed mainly by the cooler waters flowing from the northeast Atlantic. As the NEC travels across the open ocean, it is joined by waters originating south of the equator thus entraining waters from the Southern Atlantic into the Northern Atlantic.

O

OCEAN DRILLING PROGRAM (ODP) a funded program by the U.S. National Science Foundation and 22 international partners (JOIDES) to conduct basic research into the history of the ocean basins and the overall nature of the crust beneath the ocean floor using the scientific drill ship JOIDES

Resolution.

P

PALYNOLOGY the science that studies contemporary and fossil palynomorphs, including pollen, spores, dinoflagellate cysts, acritarchs, chitinozoans and scolecodonts, together with particulate organic matter (POM) and kerogen found in sedimentary rocks and sediments. Palynology does not include diatoms, Foraminifera or other organisms with siliceous or calcareous exoskeletons.

PALYNOMORPH term used to describe a particle of a size between five and 500 µm composed of organic material such as chitin, pseudochitin and sporopollenin.

PISTON CORE core taken using a piston corer, used to reduce the compaction during sampling. This sampler is essentially a gravity corer, but it has an internal piston which remains at the level of the water-sediment interface when the corer penetrates into the bed. The corer is attached to a trip mechanism which is released when a counter weight hits the bed. The piston creates a slight vacuum above the sample and is supposed to reduce friction and prevent compaction.

PLANISPIRAL term applied to the condition in which a shell is coiled in a single horizontal plane and the diameter increases away from the axis of coiling.

PRASINOPHYTA a phylum that comprises an enigmatic collection of unicellular or filamentous organisms that occur in almost all aquatic environments.

PREBOREAL the first stage of the Boreal which starts at 11500 calender years, which is followed by the Boreal proper.

PRECESSION OF THE EQUINOXES the movement of the solstices and equinoxes around Earth's elliptical orbit over cycles of 23000 and 19000 years.

PROXY any source of information that contains indirect evidence of past changes in the weather.

PRACTICAL SALINITY UNITS (PSU) the practical unit of salinity defined as the conductivity ratio of a sea water sample to a standard KCl solution.

PYCNOCLINE a rapid change in water density with depth. In freshwater environments such as lakes this density change is primarily caused by water temperature (thermocline), while in seawater environments such as oceans and estuaries, the rapid density change in the water column is often caused by a combination of decreasing water temperature and increasing salinity (halocline).

PYCNOMETER a laboratory device used for measuring the density or more accurately the volume of solids, be they regularly shaped, porous or non-porous, monolithic, powdered, granular or in some way comminuted, employing some method of gas displacement and the volume: pressure relationship known as Boyle's Law.

Q

QUATERNARY the geologic time period after the Neogene Period, spanning 1.805 +/- 0.005 million years ago to the present. The Quaternary includes two geologic epochs: the Pleistocene and the Holocene Epoch.

R

RESEARCH VESSEL (RV OR R/V) a ship designed and equipped to carry out research at sea.

S

SCOLECODONTS the hard jaws of polychaete worms.

SEDIMENTATION RATE (SR) the amount of sediment accumulated in an aquatic environment over a given period of time, usually expressed as thickness of accumulation per unit time (often expressed as centimeter per thousand years (cm/ka)).

SCANNING ELECTRON MICROSCOPE (SEM) a type of electron microscope that images the sample surface by scanning it with a high-energy beam of electrons in a raster scan pattern. The electrons interact with the atoms that make up the sample producing signals that contain information about the sample's surface topography, composition and other properties such as electrical conductivity.

SHANNON-WIENER INDEX (SHANNON INDEX) index used to measure diversity in categorical data. It is simply the Information entropy of the distribution, treating species as symbols and their relative population sizes as the probability.

SHELF the extended perimeter of each continent and associated coastal plain, that was part of the continent during the glacial periods, but undersea during interglacial periods.

SLOPE a ramplike structural edge of a continent that slopes into the ocean.

SPT Sodium polytungstate.

SEA SURFACE SALINITY (SSS) the salinity measured at sea surface.

SEA SURFACE TEMPERATURE (SST) the temperature measured at sea surface.

STADIAL a period during glacial epochs when the ice sheets

advanced to lower latitudes.

STRATIFICATION Phenomenon that occurs when water of high and low salinity (halocline), as well as cold and warm water (thermocline), forms layers that act as barriers to water mixing.

SUBTROPICAL UNDERWATER (SUW OR STUW) watermass characterized by a salinity maximum typical of every subtropical gyre. Surface waters of the central subtropical gyre are very salty as a result of evaporation under the atmospheric high pressure region. As this salty water subducts southward beneath water that is not quite as saline, it forms a salinity maximum in the vertical column, which is called Subtropical Underwater. In the Caribbean it forms the permanent thermocline and/or nutricline.

T

TAPHONOMY the study of decaying organisms over time and how they become fossilized.

TERRIGENOUS SEDIMENTS sediments derived from continental erosion; that is, that are derived from terrestrial environments. Consisting of sand, mud, and silt carried to sea by rivers, their composition is usually related to their source rocks; deposition of these sediments is largely limited to the continental shelf.

TETRAETHER INDEX OF TETRAETHERS (TEX_{86}) index determined by the temperature at which Crenarchaeota produced their membranes by measuring the relative amounts of GDGTs (Glycerol Dialkyl Glycerol Tetraethers) present in marine sediments.

THECAMOEBIAN (ARCELLACEANS) clonal, predominantly freshwater protozoans, although they can also occur in brackish water environments and moist soils. They can be found in a wide range of geographic settings, ranging from tropical to arctic latitudes. These organisms have an amoebid sarcodine cell with pseudopods and a simple sac-like test, either flattened or rounded with an aperture located on or near the tapered end, or a beret-shaped test with an invaginated aperture on the ventral side which is more or less flattened. A substantial amount of morphological variability has been observed among these two broad groups.

THERMOCLINE a region in the ocean of rapidly changing temperature between the warm upper layer (the epilimnion) and the colder deeper water (the hypolimnion).

TINTINNID ciliates of the choreotrich taxon *Tintinnida*, distinguished by vase-shaped shells called loricae, which are mostly protein but may incorporate minute pieces of minerals.

TOTAL ORGANIC CARBON (TOC) the amount of carbon present in a sample. A typical analysis for TOC measures both the total carbon (TC) present as well as the total inorganic carbon (TIC). Subtracting the inorganic carbon from the total carbon yields TOC.

TRILETE SPORE spore showing a triradiate mark formed by the dissociation of a spore tetrad.

TROCHOSPIRAL helical.

TURBIDITES sediments which are transported and deposited by density flow, not by tractional or frictional flow.

U

UPWELLING an oceanographic phenomenon that involves wind-driven motion of dense, cooler, and usually nutrient-rich water towards the ocean surface, replacing the warmer, usually nutrient-depleted surface water. There are at least five types of upwelling: coastal upwelling, large-scale wind-driven upwelling in the ocean interior, upwelling associated with eddies, topographically-associated upwelling, and broad-diffusive upwelling in the ocean interior.

V

VARVE an annual layer of sediment or sedimentary rock. When these stratifications are of seasonal origin they can be used to study climate change.

VIENNA-PEEDEE BELEMNITE (VPDB) STANDARD the primary reference for carbon and oxygen isotopes and refers to the Cretaceous belemnite formation at Peedee in South Carolina, USA. The PDB formation is exhausted but still acts as a reference.

X

X-RAY FLUORESCENCE (XRF) the emission of characteristic 'secondary' (or fluorescent) X-rays from a material that has been excited by bombarding with high-energy X-rays or gamma rays.

Y

YOUNGER DRYAS (YD) a sudden, abrupt cold episode which interrupted the sustained warming trend between the Last Glacial Maximum and the Holocene (12900 – 11600 years ago).

Samenvatting (Summary in Dutch)

Klimaatschommelingen in tropische tot subtropische gebieden zijn gekoppeld aan hydrologische veranderingen. De reconstructie van deze hydrologische veranderingen tijdens de snelle klimaatsfluctuaties tijdens het late Quartair is van cruciaal belang voor de studie van globale klimaatsverandering. Deze studie toont aan dat coccolieten en cysten van dinoflagellaten bruikbare klimaatsindicatoren zijn voor de reconstructie van deze hydrologische cycli tijdens het late Quartair, op zowel regionale als globale schaal. *Vice versa* brengt deze studie nieuwe paleoecologische inzichten aan het licht betreffende coccolithoforen en dinoflagellaten.

1. Rationale voor de toepassing van dinoflagellatencysten

Ter ondersteuning van het gebruik van dinoflagellatencysten als klimaatsindicatoren werden twee fundamentele studies verricht. Doordat zogenaamde "standaard"-maceratiemethodes op alle vlakken zeer variabel zijn en schade kunnen toebrengen aan microfossielen met organische wanden, diende onderzocht te worden wat de gevolgen zijn voor de concentratiebepaling van dinoflagellatencysten. Aangezien er aanwijzingen zijn dat de uitsteeksellengte van *Lingulodinium machaerophorum* gerelateerd is aan saliniteitsvariatie, werd getracht deze relatie kwantitatief te bepalen en zodoende bij te dragen tot reconstructie van saliniteit, van belang voor beter begrip van globale klimaatsverandering.

Eerst werd de methode om concentraties van dinoflagellatencysten te bepalen door toevoeging van sporen van *Lycopodium clavatum* gekalibreerd door een samenwerking van 23 internationale laboratoria. Een nieuwe standaardmethodologie werd voorgesteld die kritische stappen overslaat, meer bepaald oxidatie, gebruik van warme zuren, acetolyse, te grote maaswijdte (> 15 µm), decanteren en te lange ultrasonicatie (> 1 min).

De tweede studie omvatte een morfologische studie van cysten van *Lingulodinium machaerophorum* afkomstig uit recente oppervlaktesedimenten. De studie toonde aan dat de variatie van de uitsteeksellengte bepaald wordt door de verhouding tussen saliniteit en temperatuur (S/T). Eenzelfde morfologie kan dus resulteren uit verschillende temperaturen en saliniteiten, zolang dat de verhouding tussen beide constant blijft. Metingen van driedimensionale beelden gegenereerd met confocale microscopie, tonen het bestaan aan van twee morfologische uitersten: één met vele, korte, dicht opeengepakte uitsteeksels gevormd bij lage S/T verhoudingen en één met lange, ver uiteen staande uitsteeksels gevormd bij hoge S/T verhoudingen. Het verband tussen de S/T verhoudingen en de morfologie leidde tot de observatie dat de biogeografie van *Lingulodinium machaerophorum* afgelijnd is door de S/T verhouding. Dit suggereert dat de S/T ratio het voorkomen van cysten van *Lingulodinium polyedrum* kan voorspellen. Belangrijk is dat het vroegere zoutgehalte kan gereconstrueerd worden indien de temperatuur door onafhankelijke proxies kan bepaald worden.

2. Twee studiegebieden voor cycli op millenium-schaal

Twee locaties werden uitgepikt om hydrologische cycli op millenniumschaal op hoge resolutie te bestuderen tijdens het late Quartair: het Cariaco Bekken, een anoxisch bekken ter hoogte van Venezuela, en de zuidelijke Golf van Cádiz. Door hoge sedimentatiesnelheden, beschikken beide sites over een relatief onverstoord laat Quartair klimaatslogboek. In beide bekkens komen verder snelle, uitgesproken fluctuaties voor, veroorzaakt door veranderingen

van de intertropische convergentiezone (ITCZ) en de Noord-Atlantische Oscillatie (NAO). Een beter begrip van beide fenomenen is cruciaal in de context van globale klimaatsverandering.

3. Karakterisering van cycli op millenium-schaal

De seizoenale en meerjaarlijkse veranderingen tussen opwellingsgedomineerde en riviergedomineerde ecosystemen, in beide regio's gerelateerd aan klimatologische veranderingen van respectievelijk de ITCZ en de NAO, kan naar millenniumschaal geëxtrapoleerd in resulteert in specifieke assemblages van dinoflagellatencysten en coccolieten. In het Cariaco bekken zorgt verhoogde rivierinput initieel voor een verhoogde stratificatie, aangeduid door abundanties van *Lingulodinium machaerophorum*. Toegenomen rivierinput zorgt voor *Spiniferites ramosus – Gephyrocapsa oceanica* gedomineerde assemblages. Het is precies deze toevoer die het bekken anoxisch maakt aan het begin van het Bølling/Allerød. Verhoogde opwelling, o.a. gedurende het Younger Dryas, bewerkstelligd een *Brigantedinium* spp. – *Emiliania huxleyi* gedomineerd ecosysteem. In de Golf van Cádiz zorgt verhoogde riviertoevoer voor verhoogde abundanties van *Lingulodinium machaerophorum, Gephyrocapsa muellerae* en alkenonen. Verhoogde opwelling veroorzaakt hier een toename in abundantie van grote *Emiliania huxleyi* morfotypes, naast pieken van *"Nematosphaeropsis labyrinthus - Bitectatodinium tepikiense"*. Deze hydrologische variaties worden ook weerspiegeld in korrelgroottes en XRF opnames in de Golf van Cádiz.

In beide gebieden zijn veranderingen in assemblage sterk gekoppeld aan veranderingen in productiviteit en bewaring, wat wijst op het belang van de "mineralen-als-ballast hypothese". Desondanks gelijkaardige veranderingen in temperatuur en saliniteit is er een cruciaal verschil in beide gebieden in sedimentatiesnelheid: in het Cariaco Bekken zorgt verhoogde opwelling voor verhoogde sedimentatiesnelheid, terwijl in de zuidelijke Golf van Cádiz verhoogde rivierinput verhoogde sedimentatiesnelheid veroorzaakt. Dit heeft tot gevolg dat beide regio's verschillend reageren op klimaatsverandering in termen van productiviteit en bewaring: in het Cariaco Bekken is er verhoogde koolstofbewaring gedurende stadialen, terwijl in de Golf van Cádiz het omgekeerde plaatsvindt.

Er moet benadrukt worden dat verandering op milleniumschaal verder gemoduleerd worden door zeespiegelveranderingen op orbitale schaal. In het Cariaco Bekken zorgt een stijgende zeespiegel voor influx van nutrientrijk subtropisch water over sills gedurende interglacialen, hetgeen het bekken anoxisch maakt. In de Golf van Cádiz zorgt een zeespiegelstijging voor een verplaatsing van afzetting van terrigeen materiaal van de helling naar shelf en *vice versa*.

Naast productiviteit werd de kwantitatieve reconstructie van de temperatuur en het zoutgehalte beklemtoond. Dit zijn cruciale parameters voor klimaatsreconstructie. In de Golf van Cádiz werden zeeoppervlaktetemperaturen gereconstrueerd met behulp van glycerol dialkyl glycerol tetraethers (GDGTs), alkenonen en Mg/Ca ratios gemeten op *Globigerina bulloides*. De gereconstrueerde temperaturen vertonen gelijkaardige schommelingen. Ze verschillen echter in grootte, hetgeen te wijten is aan seizoenaliteit, saliniteitswijzigingen of laterale advectie. De verhouding tussen thermofiele en niet-thermofiel dinoflagellatencysten en de morfologische veranderingen van *Emiliania huxleyi* en zijn bruikbaar voor de detectie van Heinrich events. De correlatie tussen alkenonenafgeleide temperaturen en Ti XRF opnames wijst op een belangrijke invloed van temperatuur in hydrologische variaties veroorzaakt door de NAO. In de Ti XRF opname kunnen cycli van 1000 en 585 jaar vastgesteld worden, gerelateerd aan positieve NAO indices. Het zoutgehalte in beide regio's werd behulp van de uitsteeksellengte van *Lingulodinium machaerophorum* en gepaarde Mg/Ca – $\delta^{18}O$ metingen gereconstrueerd en gecorreleerd. Verschillen tussen de saliniteitsproxies en de hydrologische proxies kunnen aangetoond worden en suggereren dat veranderingen in het zoutgehalte het resultaat zijn van globale en regionale hydrologische en oceanografische veranderingen.

4. Voor- en nadelen van de aangewende proxies

Coccolieten hebben het voordeel om extreem abundant aanwezig te zijn in de onderzochte sedimenten. De zeer kleine hoeveelheid sediment nodig om de assemblages te bestuderen maakt dit mogelijk op zeer fijne resolutie (seizoenaal op minder). Het bewaringspotentiaal veroorzaakt echter problemen met identificatie en overrepresentatie van resistente, hoge-productiviteitsspecies, die vaak de interpretatie van assemblageveranderingen compliceren.

Cysten van dinoflagellaten hebben echter lagere abundanties in de sedimenten, hetgeen de toepassing op zeer hoge resolutie bemoeilijkt. Vanuit tafonomisch standpunt is de bewaring van heterotrofe dinoflagellatencysten zeer variabel, en zeer gevoelig aan veranderingen in productiviteit en zuurstofgehalte. De bewaring van autotrofe dinoflagellatencysten is echter uitstekend in beide gebieden, hetgeen ze zeer betrouwbare indicators maakt voor veranderingen in productiviteit en saliniteit (gereconstrueerd door morfologische studie).

Deze studie toont ook aan dat laterale advectie van resistente componenten mogelijks cruciaal is in de interpretatie van de hydrologische variaties in deze gebieden. De aanwezigheid van een belangrijke hoeveelheid shelf-materiaal in beide gebieden toont een belangrijk transport aan vanuit de shelf, hetgeen mogelijks 'lags' veroorzaakt tussen pelagische en shelfcomponenten. In deze optiek is het tevens onduidelijk hoe turbidieten of bodemstromingen het logboek verstoren.

Desondanks deze tafonomische problemen, toont deze studie aan dat enkel door het gebruik van een multi-proxy aanpak, die de nodige correcties voor sedimentatiesnelheid in rekening brengt, klimaatsreconstructie mogelijk blijft.

5. Verband tussen hoge en lage breedtegraden

Deze studie toont aan dat klimaatsveranderingen in beide gebieden, zoals uitgedrukt door de bestudeerde proxies, synchroon zijn met klimaatsveranderingen in hogere breedtegraden of ze opvolgen. Er is geen bewijs voor een "trigger" voor millenium-schaalveranderingen vanuit lagere breedtegraden (de zogenaamde "tropical-driver hypothesis"). Desondanks wijst de uitdrukking van snelle, grote veranderingen in productiviteit en assemblage gekoppeld aan verschuivingen van de ITCZ of NAO, op een uitgesproken gevoeligheid van deze gebieden aan klimaatsverandering. Dit maakt deze gebieden extra kwetsbaar voor de huidige globale klimaatsverandering. Doordat deze verandering hydrologisch van aard zijn, kan verandering in precipitatiepatronen voor beide regio's verwacht worden.

6. Toekomstperspectieven

Doordat millenium-schaal veranderingen van beide fenomenen synchroon plaatsvinden, dient toekomstig werk de precieze timing van beide fenomenen te verhelderen door gedetailleerde multi-proxy benaderingen in noord-zuid transecten te verrichten. Op een fijnere resolutie, zou "stacking" van shelf tot slope kernen zeespiegeleffecten uitfilteren, en zuivere NAO of ITCZ veranderingen kunnen weergeven. Tevens kunnen gedetailleerde sedimenttrap studies in beide gebieden er toe bijdragen de interpretaties te bevestigen.